

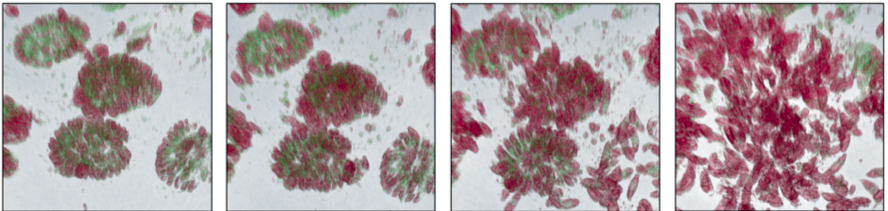
Camilo Sebastián Larrazabal Reyes

New insights into the role of cholesterol-related pathways in apicomplexan parasite infections

Inaugural-Dissertation zur Erlangung des Grades eines

Dr. med. vet.

beim Fachbereich Veterinärmedizin der Justus-Liebig-Universität Gießen



Das Werk ist in allen seinen Teilen urheberrechtlich geschützt.

Die rechtliche Verantwortung für den gesamten Inhalt dieses Buches liegt ausschließlich bei dem Autoren dieses Werkes.

Jede Verwertung ist ohne schriftliche Zustimmung der Autoren oder des Verlages unzulässig. Das gilt insbesondere für Vervielfältigungen, Übersetzungen, Mikroverfilmungen und die Einspeicherung in und Verarbeitung durch elektronische Systeme.

1. Auflage 2022

All rights reserved. No part of this publication may be reproduced, stored in a retrieval system, or transmitted, in any form or by any means, electronic, mechanical, photocopying, recording, or otherwise, without the prior written permission of the Author or the Publisher.

1st Edition 2022

© 2022 by VVB LAUFERSWEILER VERLAG, Giessen
Printed in Germany



edition scientifique
VVB LAUFERSWEILER VERLAG

STAUFENBERGRING 15, 35396 GIESSEN, GERMANY
Tel: 0641-5599888 Fax: 0641-5599890
email: redaktion@doktorverlag.de

www.doktorverlag.de

Aus dem Institut für Parasitologie, Justus-Liebig-Universität Gießen

New insights into the role of cholesterol-related pathways in apicomplexan parasite infections

Inaugural-Dissertation zur Erlangung des Grades eines

Dr. med. vet.

beim Fachbereich Veterinärmedizin der

Justus-Liebig-Universität Gießen

eingereicht von

Camilo Sebastián Larrazabal Reyes

Tierarzt aus Temuco, Chile

Gießen 2022

Mit Genehmigung des Fachbereichs Veterinärmedizin
der Justus-Liebig-Universität Gießen

Dekan:

Prof. Dr. Dr. Stefan Arnhold

Gutachter:

Prof. Dr. Anja Taubert

Prof. Dr. Sybille Mazurek

Prüfer:

Prof. Dr. Joachim Roth

Tag der Disputation: 28.11.2022

In the memory of my loved grandmother, Lidia Herrera Rodríguez

(08.05.1929 - 01.11.2021)

LIST OF PUBLICATIONS AND CONFERENCE CONTRIBUTIONS

Several data of this dissertation have already been published or presented at conferences:

Original papers

1. **Larrazabal, C.**, Silva, L.M.R., Hermosilla, C., and Taubert, A. (2021). Ezetimibe blocks *Toxoplasma gondii*-, *Neospora caninum*- and *Besnoitia besnoiti*-tachyzoite infectivity and replication in primary bovine endothelial host cells. *Parasitology* 148, 1107–1115.
2. **Larrazabal, C.**, Silva, L.M.R., Pervizaj-Oruqaj, L., Herold, S., Hermosilla, C., and Taubert, A. (2021). P-Glycoprotein Inhibitors Differently Affect *Toxoplasma gondii*, *Neospora caninum* and *Besnoitia besnoiti* Proliferation in Bovine Primary Endothelial Cells. *Pathogens* 10.
3. **Larrazabal, C.**, Hermosilla, C., Taubert, A. and Conejeros, I. (2021). 3D holotomographic monitoring of Ca^{++} dynamics during ionophor-induced *Neospora caninum* tachyzoite egress from primary bovine host endothelial cells. *Parasitol Res* 121 1169-1177.
4. **Larrazabal, C.**, Lopez-Osorio, S., Velásquez, ZD., Hermosilla, C., Taubert, A., Silva, LMR. (2021). Thiosemicarbazone copper chelator BLT-1 blocks apicomplexan parasite replication by selective inhibition of the scavenger receptor b type I (SR-BI). *Microorganisms* 9 (11).
5. Silva, L.M.R., Lütjohann, D., Hamid, P., Velasquez, Z.D., Kerner, K., **Larrazabal, C.**, Failing, K., Hermosilla, C., and Taubert, A. (2019). *Besnoitia besnoiti* infection alters both endogenous cholesterol *de novo* synthesis and exogenous LDL uptake in host endothelial cells. *Sci Rep* 9, 6650.
6. Taubert, A., Silva, L.M.R., Velásquez, Z.D., **Larrazabal, C.**, Lütjohann, D., and Hermosilla, C. (2018). Modulation of cholesterol-related sterols during *Eimeria bovis* macromeront formation and impact of selected oxysterols on parasite development. *Mol Biochem Parasitol* 223, 1–12.

Conference contributions

1. **C. Larrazabal**, Z. D. Velásquez, L. M. R Silva, C. Hermosilla, A. Taubert. Effect of cholesterol uptake and transport inhibition on coccidian parasite replication in primary bovine endothelial cells. Meeting of the German Veterinary Society (DVG), specialist group of parasitology, 17-19 June 2019, Leipzig, Germany.
2. N. H. Anschütz, S. Gerbig, **C. Larrazabal**, J. D. Velez, L. Silva, C. Hermosilla, A. Taubert, B. Spengler. AP-SMALDI MSI of *Cryptosporidium parvum* and *Neospora caninum*-infected cells and tissues. 53rd Annual conference of the DGMS including 27th ICP-MS User's Meeting 1, 4 March 2020, Münster, Germany.
3. **C. Larrazabal**, L. M. R Silva, C. Hermosilla, A. Taubert. Role of cholesterol uptake and transport in apicomplexan parasite replication in primary bovine endothelial cells. Meeting of the German Parasitology Society (DGP), 15-17 March 2021, Bonn, Germany (online).
4. **C. Larrazabal**, D. Grob, Z. D. Velásquez, C. Hermosilla, A. Taubert, I. Conejeros. Analysis of Ca⁺⁺ signaling and dynamics during *Besnoitia besnoiti* tachyzoite invasion and intracellular development in bovine endothelial host cells. Meeting of the German Veterinary Society (DVG), specialist group of parasitology, 28-30 June 2021 (online).
5. **C. Larrazabal**, L. M. R. Silva, C. Hermosilla, A. Taubert. Comparative analyses on P-glycoprotein inhibitor-mediated effects on apicomplexan parasite replication in primary bovine endothelial cells. Meeting of the German Veterinary Society (DVG), specialist group of parasitology, 28-30 June 2021 (online).
6. **C. Larrazabal**, Silva L.M.R, Hermosilla C. Taubert A. Ezetimibe blocks coccidian parasite replication in primary bovine endothelial cells. Meeting of the German Veterinary Society (DVG), specialist group of parasitology, 28-30 June 2021 (online).
7. **C. Larrazabal**, L. M. R. Silva, C. Hermosilla, A. Taubert. P-glycoprotein inhibitors differentially modulates fast replicating coccidian replication in primary bovine endothelial cells. Meeting of the world association for the advancement of veterinary parasitology (WAAVP), 19-22 July 2021, Dublin, Ireland (online).

8. **C. Larrazabal**, D. Grob, Z. D. Velásquez, C. Hermosilla, A. Taubert, I. Conejeros. Ca^{++} signaling in *Besnoitia besnoiti* tachyzoite invasion and development in primary bovine host endothelial cells. Meeting of the world association for the advancement of veterinary parasitology (WAAVP), 19-22 July 2021, Dublin, Ireland (online).

TABLE OF CONTENTS

1. INTRODUCTION	1
1.1. Apicomplexan parasites	1
1.1.1. Family Eimeriidae	2
1.1.2. Family Sarcocystidae	3
1.2. Coccidian parasites and host cell interactions	8
1.2.1. Intracellular biology of coccidia	8
1.2.2. Host cell modulation by coccidian parasites	11
1.3. Cholesterol metabolism in animal cells	13
1.4. Modulation of host cellular cholesterol metabolism by coccidian parasites	17
2. ORIGINAL PUBLICATIONS	22
2.1. <i>Besnoitia besnoiti</i> infection alters both endogenous cholesterol de novo synthesis and exogenous LDL uptake in host endothelial cells	22
2.2. Modulation of cholesterol-related sterols during <i>Eimeria bovis</i> macromeront formation and impact of selected oxysterols on parasite development	41
2.3. Ezetimibe blocks <i>Toxoplasma gondii</i>-, <i>Neospora caninum</i>- and <i>Besnoitia besnoiti</i>-tachyzoite infectivity and replication in primary bovine endothelial host cells	54
2.4. P-glycoprotein inhibitors differently affect <i>Toxoplasma gondii</i>, <i>Neospora caninum</i> and <i>Besnoitia besnoiti</i> proliferation in bovine primary endothelial cells	64
2.5. The thiosemicarbazone copper chelator BLT-1 blocks apicomplexan parasite replication by selective inhibition of the scavenger receptor B type I (SR-BI)	81
2.6. 3D holotomographic monitoring of Ca⁺⁺ dynamics during ionophor-induced <i>Neospora caninum</i> tachyzoite egress from primary bovine host endothelial cells	99
3. RESULTS AND DISCUSSION	109
3.1. <i>B. besnoiti</i> relies on different strategies of cholesterol scavenging	109
3.2. <i>E. bovis</i> drives changes in host cellular sterol composition during first merogony	111

3.3. NPC1L1 blockage as potential anti-coccidian strategy	114
3.4. Chemical blockage of P-gp activity affects proliferation of fast replicating coccidia in an inhibitor generation-dependent manner	115
3.5. Blockage of neutral lipid efflux impairs coccidian intracellular replication....	117
3.6. Changes in Ca⁺⁺ dynamics as pivotal early signal in coccidian parasite stages	118
3.7. Intracellular Ca⁺⁺ signals are relocated during parasite egress	120
4. ZUSAMMENFASSUNG.....	122
5. SUMMARY	124
6. REFERENCES	126
7. ACKNOWLEDGMENTS.....	144
8. DECLARATION	145
9. FUNDING	146

ABBREVIATIONS

ABC	ATP binding cassette
ACAT 2	acyl-CoA-Cholesterol-acyltransferase 2
acLDL	acetylated LDL
AUC	area under the curve
BAEC	bovine aortic endothelial cells
BUVEC	bovine umbilical vein endothelial cells
CHO	chinese hamster ovary cells
E.R.	endoplasmic reticulum
FCS	fetal calf serum
HCT-8	human colorectal tumor cells 8
HDL	high density lipoproteins
HFF	human foreskin fibroblast
HMG-CoA	hydroxymethylglutaryl-CoA
HUVEC	human umbilical vein endothelial cells
InsP₃/Ca⁺⁺	inositol-triphosphate/calcium
LDL	low density lipoproteins
LDLR	LDL receptor
NPC1	Niemann-Pick C1
NPC1L1	Niemann-Pick C1-Like
P.V.	parasitophorous vacuole
P-gp	P-glycoprotein
PLC	phospholipase C
SERCA	sarco/endoplasmic reticulum Ca ⁺⁺ ATPase
SR-BI	scavenger receptor BI
VLDL	very low density lipoproteins

1. INTRODUCTION

1.1. Apicomplexan parasites

Apicomplexa represent a phylum of obligate intracellular protozoan parasites, characterized by the presence of a unique apical complex that defines the phylum name (Votýpka et al., 2017). They are composed of a unique cytoskeleton, secretory organelles (rhoptries, micronemes and dense granules) endosymbiotic-derived organelles (mitochondria and apicoplast), specific structures (acidocalcisomes and plant-like vacuoles), and universal eukaryotic structures (nucleus, endoplasmic reticulum, Golgi apparatus and ribosomes), surrounded by a membranous structure named pellicle forming characteristic banana-shaped stages (Ferguson and Dubremetz, 2014; Votýpka et al., 2017). From a biological perspective, these parasites operate complex life cycles, alternating in sexual and asexual multiplication, and developing a parasitic relationship with a broad range of suitable host species, including not only vertebrates, such as mammals, birds, reptiles or amphibians, but also insects and mollusks, in an extensive ecological distribution (Votýpka et al., 2017). Nevertheless, the importance of apicomplexa is driven by a distinct group of parasites capable of infecting both humans and domestic animals, exerting a significant impact on human and animal health.

The taxonomic assignment of apicomplexa is still ongoing. Currently, three major parasitic classes are defined: hematozoa, gregarina and coccidia (See **Fig 1.1**) (Votýpka et al., 2017). In specific, the hematozoa class is relevant for human and veterinary medicine and includes remarkable genera, such as *Plasmodium*, *Babesia* or *Theileria*, while the gregarine class contains *Cryptosporidium*, a parasite species responsible for occasionally fatal diarrhoea in infants and neonate animals (Ryan et al., 2014; Sow et al., 2016). Additionally, the coccidian class comprises two important parasite families: Eimeriidae and Sarcocystidae. Both families show marked biological differences but also share common characteristics, such as asexual merogonic proliferation cycles occurring in the intermediate and/or definitive hosts, followed by a sexual gametogonic proliferation phase that exclusively takes place in definitive hosts. During the latter stage, the parasite will develop into micro- (male) and macro (female)-gamonts, perform syngamy finally resulting in infective offspring termed sporozoites, within an enveloped structure named oocyst (Dauguschies and Najdrowski, 2005; Lindsay and Dubey, 2020; Martorelli Di Genova and Knoll, 2020; Votýpka et al., 2017).

Introduction

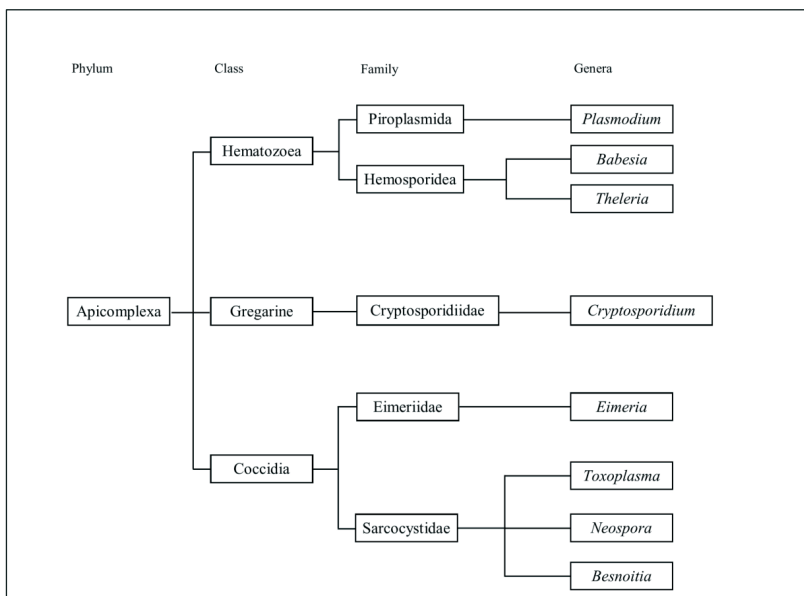


Fig 1.1. Taxonomic classification of the main apicomplexan species here presented. Adapted from Votýpka et al., 2017

1.1.1.1. Family Eimeriidae

This family contains monoxenous species-specific parasites with a wide host range (Daugšies and Najdrowski, 2005; Keeton and Navarre, 2018). Several genera are included in this family, such as *Caryospora*, *Cyclospora*, *Eimeria*, *Goussia*, *Isospora*, *Tyzzeria*, and *Wenyonella*, which infect different hosts (Deplazes 2021).

Over one thousand *Eimeria* species are known to cause coccidiosis in different host species. In cattle, several *Eimeria* spp. have been described, including globally occurring species, such as *E. subspherica*, *E. ellipsoidalis*, *E. pellita*, *E. cylindrica*, *E. alabamensis*, *E. zuernii* and *E. bovis* (Keeton and Navarre, 2018). The last three species are the most pathogenic representatives of this family causing “pasture” (*E. alabamensis*) and “stable” (*E. bovis*, *E. zuernii*) coccidiosis in young cattle (Deplazes et al., 2021). Overall, bovine coccidiosis can be highly prevalent in cattle farms, thereby causing significant economic losses not only as

consequence of clinical disease and treatment, but also by delayed weight gain during subclinical episodes (Dauguschies and Najdrowski, 2005).

The life cycle of *Eimeria* spp. includes endogenous (parasitic) and exogenous (environmental) phases. When describing *E. bovis* as an example, host infection occurs after oral intake of sporulated oocysts, containing four sporocysts with two sporozoites, each. Sporozoites are released into the duodenal lumen, penetrating the epithelial barrier and invading endothelial cells of the villous lymphatic vessels (Friend and Stockdale, 1980). This particular host cell tropism is also shared by other pathogenic *Eimeria* species, such as *E. zuernii* (López-Osorio et al., 2018), and is followed by a massive intracellular schizogonical division during the long lasting first merogony leading to macromeront (> 300 µm) formation and the release of thousands of merozoites I (Hermosilla et al., 2002). Second merogony then occurs in the colon, leading to the formation of smaller meronts in epithelial cells (Hermosilla et al., 2002). In general, the total number of merogonies within the host differs between *Eimeria* species (Dauguschies and Najdrowski, 2005; Keeton and Navarre, 2018), nevertheless the cycle is continued by sexual stage formation [macro- (female) and micro- (male) gametes], generating afterwards a sporont within an oocyst that will be shed into the environment (Martorelli Di Genova and Knoll, 2020). Since all these stages are obligate intracellular, consecutive division cycles along intestinal structures will cause significant harm to the intestinal mucosa. Clinically, in case of *E. bovis* this is mirrored by a typhlocolitis accompanied by a profuse catarrhal or hemorrhagic diarrhoea, potentially leading to life-threatening dehydration and a long-standing impairment of food absorption in convalescent animals (Dauguschies and Najdrowski, 2005; Keeton and Navarre, 2018).

1.1.2. Family Sarcocystidae

The Sarcocystidae family contains several species that share a facultative or obligate indirect life cycle (Votýpka et al., 2017). As in other coccidian relatives, gamogony exclusively occurs in definitive hosts, while merogonies occur in both definitive and intermediary hosts (Lindsay and Dubey, 2020; Martorelli Di Genova and Knoll, 2020; Votýpka et al., 2017). Sexual stages mainly are formed in epithelial cells of definitive hosts, leading to the formation of unsporulated oocysts that either undergo sporogony in definite hosts (*Sarcocystis* spp.) or are shed and sporulate in the environment, typically containing 2

sporocysts with 4 sporozoites, each (Dubey et al., 1998). One remarkable feature of this family is the presence of extra-intestinal merogonies that mainly mediate parasite spread and pathophysiological consequences, and are characterized by cyst formation, thereby facilitating horizontal transmission through predator-prey-relationships (Votýpka et al., 2017).

1.1.2.1. *Toxoplasma gondii*

T. gondii is a globally spread cyst-forming coccidian parasite with a facultative indirect life cycle that involves cats (*Felis catus*) and other felids as definitive hosts (Dubey, 2008; Innes, 2010). The capacity of this parasite to persist in different ecosystems is mostly associated with an enormous wide range of intermediate host species, including mammals and birds (Shapiro et al., 2019). Almost 30% of the global human population is infected with *T. gondii*, infections are often asymptomatic or associated with a non-specific (i. e. lymphadenopathy and mild fever) and self-limited illness during its acute stage, and a persistent asymptomatic infection during its chronic stage (Montoya and Liesenfeld, 2004). Contrastingly, major complications can occur in immunocompromised patients and pregnant woman (Milne et al., 2020). In specific, acute human toxoplasmosis in immunocompromised individuals is often consequence of chronic infection reactivation, characterized not only by encephalitis-driven neurological signs (mental status changes, seizures and neuropsychiatric findings), but also other consequences, such as chorioretinitis, pneumonia, or multi-organ involvement (Montoya and Liesenfeld, 2004). Likewise, pregnant women, who are primary infected with *T. gondii*, can suffer a vertical dissemination of parasite infection, provoking in some cases spontaneous abortion, prematurity or stillbirth, while CNS (central nervous system) foetal infection is largely characterized by chorioretinitis, intracranial calcifications and hydrocephaly (McAuley, 2014). Furthermore, the importance of *T. gondii* in domestic animals is mostly based on abortive infections in ovine productive systems, representing the second most common abortive pathogen in sheep flocks (Benavides et al., 2017; Innes et al., 2009).

In general, *T. gondii* life cycle follows the same scheme as other relatives from the Sarcocystidae family. Hosts become infected after ingestion of environmental oocysts or meat/intermediate hosts harboring cyst stages (Innes, 2010; Shapiro et al., 2019). Infectious

stages (sporozoites, bradyzoites) invade host cells and perform merogonies where fast proliferating offspring termed tachyzoites develop by endodyogeny within any nucleated host cell type, a phenomenon that permits *T. gondii* to invade different tissues and cells (Black and Boothroyd, 2000; Votýpka et al., 2017). Over time, tachyzoite dissemination is mainly limited by host immune reactions, simultaneously promoting the conversion of intracellular *T. gondii* tachyzoites into bradyzoites which develop inside cysts. These are characterized by a thin cyst wall of approximately 0.5 μm and are preferentially located in the CNS and muscle tissues (Benavides et al., 2011; Dubey and Sharma, 1980; Dubey et al., 1998). The cyst stage represents an alternative source of infection besides oocysts, permitting the ecological expansion of the parasite independent of definitive hosts (Shapiro et al., 2019; Tenter et al., 2000). Epidemiological studies documented a global seroprevalence of 30% in domestic cats (ranging from 16%-80% in the USA), which contrasts with a prevalence of oocyst shedding below 1% (Elmore et al., 2010). The latter evidences that oocyst shedding represents only a transient event in feline toxoplasmosis mainly occurring in young animals, thereby highlighting the relevance of cyst formation for *T. gondii* spreading in larger populations (Elmore et al., 2010).

1.1.2.2. *Neospora caninum*

N. caninum is a cyst-forming coccidian parasite first identified as a *T. gondii*-like protozoan in neurologically compromised young dogs, being nowadays accepted as a major abortive pathogen in bovines (Lindsay and Dubey, 2020; Reichel et al., 2013). During its indirect life cycle, gamogony occurs in dogs (*Canis lupus familiaris*) and coyotes (*Canis latrans*), nevertheless other canids like dingoes (*Canis lupus dingo*) and wolves (*Canis lupus*) have been proposed as definitive hosts (Rosypal and Lindsay, 2005). *N. caninum* is not a zoonotic parasite, but its DNA was detected in several animal species including not only domestic ruminants like bovines, ovines and caprines, but also wild animals, such as white-tailed deer, rabbits, rodents and diverse bird species (Rosypal and Lindsay, 2005).

Shortly after infection, *N. caninum* undergoes a fast replicating phase characterized by tachyzoite proliferation in nucleated host cells, later on followed by a slow replicative phase where bradyzoites will develop in rather thick-walled (0.5-4 μm) cysts (Speer et al., 1999). Similar to *T. gondii*, bradyzoite-containing cysts are located mainly in the CNS and muscular

Introduction

tissues of the hosts, thereby representing infection sources for intermediate and definitive hosts (Lindsay and Dubey, 2020). Regardless of parasite transmission via oocyst shedding - which seems of minor importance - *N. caninum* owns a remarkable capacity to invade foetal tissue in pregnant animals (Anderson et al., 2000; Dubey, 2003). This vertical or transplacental infection route was consistently reported in bitches and different species of domestic ruminants (i.e. cow, sheep or goat) (Lindsay and Dubey, 2020; Speer et al., 1999). Importantly, prenatal infections may occur without any clinical consequence for progeny, thereby boosting horizontal spreading of the parasite in animal populations over time. Even though bovines can also become infected after the uptake of sporulated oocysts from pastures, the vertical infection route is of major relevance in cattle production systems and leads to persistently infected animals within herds suffering from an enhanced chance of abortion (Reichel et al., 2013).

Overall, *N. caninum*-induced reproductive losses in bovines can occur at any gestational stage, causing embryonic resorption, foetal mummification or clinically ill newborn calves besides clinically healthy ones (Lindsay and Dubey, 2020). Epidemic abortive neosporosis in bovines (>10% of abortion risk in cows) mainly occurs in immunological naïve cows being primary infected with *N. caninum* sporulated oocysts and subsequent tachyzoite invasion into the foetus. In contrast, endemic bovine neosporosis is consequence of constant vertical transmission within herds leading to consecutive infections over several breeding generations (Anderson et al., 2000; Reichel et al., 2013). In bovines, this transmission route can affect 70-100% of infected animals (Reichel et al., 2013). In that context, it was suggested that some *N. caninum*-infected cows might experience infection recurrence, leading to a more aggressive foetal infection (Anderson et al., 2000). The reason of this recrudescence is still under debate, but it seems accepted that it is preceded by both an increase in *N. caninum*-specific antibody levels in plasma and an enhanced abortion risk over subsequent pregnancies. Overall, *N. caninum* infections induce significant economic losses in cattle production industry by both health compromise and early culling (Lindsay and Dubey, 2020; Reichel et al., 2013).

1.1.2.3. *Besnoitia besnoiti*

B. besnoiti is a cyst-forming coccidian parasite and the causal agent of bovine besnoitiosis, a cattle disease that is re-emerging in Europe (Alvarez-García et al., 2013). *B. besnoiti* possesses an indirect life cycle, alternating between tachyzoites and bradyzoites stages within intermediate hosts, however, the full life cycle of this parasite has not been elucidated yet (Cortes et al., 2014). Thus, sexual stages of *B. besnoiti* could not be demonstrated in any experimentally infected animal. Bovines are the most important intermediate hosts described so far (Alvarez-García et al., 2013; Cortes et al., 2014). Likewise, the low serological *Besnoitia* spp. prevalence in wild ruminants in endemic areas suggests that *B. besnoiti* infection is mainly limited to bovine populations (Gutiérrez-Expósito et al., 2016). In cattle, infections include acute and chronic phases. The acute stage is mainly consequence of tachyzoite replication within host cells, and it is clinically characterized by fever-driven signs (i. e. hyperthermia, tachypnoea, tachycardia, anorexia) in addition to vasculitis/necrosis of venules or arterioles in different organs as result of endothelial cell lysis (Alvarez-García et al., 2014; Langenmayer et al., 2015). The course of the disease leads to a chronic phase, with bradyzoite-containing cyst accumulating in skin and mucosa (vagina, preputium and sclera) causing vast skin alterations and infertility of bulls (Alvarez-García et al., 2014).

So far, the actual geographic extension of *B. besnoiti* infections in cattle systems was not thoroughly monitored in the last years. Nevertheless, epidemiological studies showed seroprevalences of 1-10% in endemic areas (Alvarez-García et al., 2013). Overall, animal movements seem to be an important driving factor of herd infections. However, considering that major gaps of knowledge still exist on *B. besnoiti* biology, the underlying cause of infection transmission within herds is still unknown. In this context, mechanical transmission by cyst rupture during mating or direct mucosal contacts have been suggested. Moreover, blood sucking insects, such as tabanids (*Atylotus nigromaculatus*, *Tabanocella denticornis* and *Haematopota albihirta*) and stable flies (*Stomoxys calcitrans*) were already proven to contribute to horizontal dissemination in cattle herds (Alvarez-García et al., 2013; Baldacchino et al., 2014; Liénard et al., 2013).

1.2. Coccidian parasites and host cell interactions

1.2.1. Intracellular biology of coccidia

Due to their obligate intracellular life style, coccidian parasites must invade and replicate within a suitable host cell. *In vitro*, the process of coccidian infection comprises five main steps that include attachment, invasion, parasitophorous vacuole (P.V.) formation, intracellular replication and egress of offspring (See Fig 1.2) (Black and Boothroyd, 2000).

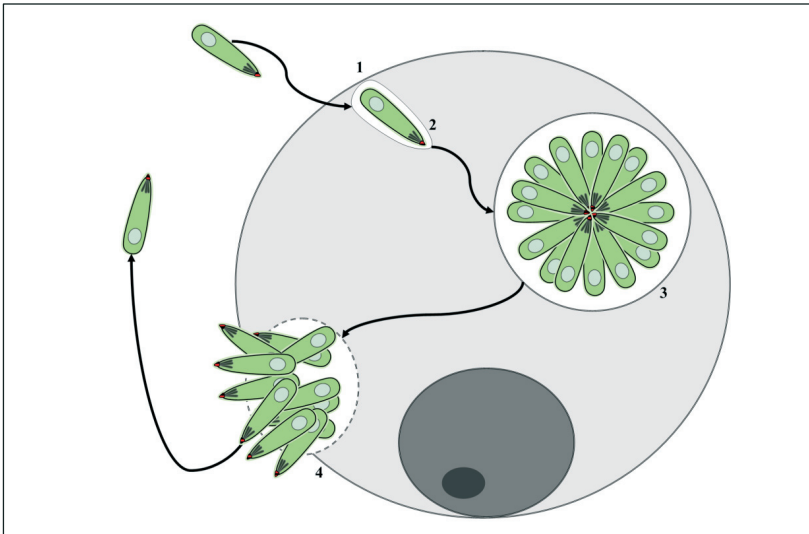


Fig 1.2. The lytic cycle of coccidian parasites. The scheme represents the main steps of coccidian parasites intracellular cycle, which are invasion (1), P.V. formation (2), intracellular replication (3) and cell lysis-mediated egress (4). Adapted from Black and Boothroyd, 2000.

Differing from other intracellular pathogens, such as viruses or bacteria, coccidian invasion is an active process initiated by host cell contact and attachment (Black and Boothroyd, 2000). Before invasion, a protein complex, composed by microneme- and rophtry-derived molecules, defines the penetration site on the host cell surface (Black and Boothroyd, 2000; Dubey et al., 1998; Votýpka et al., 2017). The precise signals that initiate this event cascade are unclear, but it has been shown that interactions of free coccidian stages with host cells

Introduction

trigger both a rise in cytoplasmic Ca^{++} levels via phospholipase C (PLC) activation and downstream signaling by inositol-triphosphate/calcium ($\text{InsP}_3/\text{Ca}^{++}$) pathway (See **Fig 1.3**) (Hortua Triana et al., 2018; Lourido and Moreno, 2015). Overall, this conserved signaling route seems pivotal for coccidian intracellular signaling, since it proved necessary for *T. gondii* motility, host cell attachment and microneme secretion (Carruthers et al., 1999; Garcia et al., 2017; Lovett and Sibley, 2003).

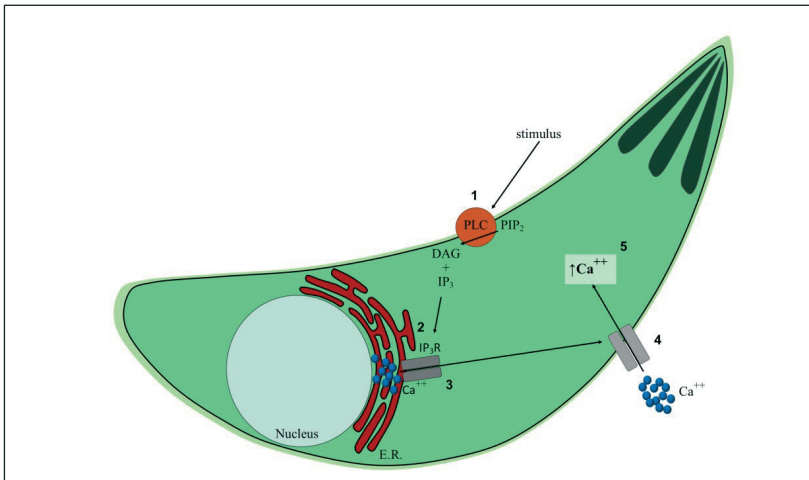


Fig 1.3. Ca^{++} signaling in coccidian parasites. Schematic illustration of resting tachyzoite activation by the $\text{InsP}_3/\text{Ca}^{++}$ pathway. The steps here illustrated are: Stimulus-dependent PLC activation (1), IP_3 - IP_3R interaction (2), release of intracellular Ca^{++} (3), extracellular Ca^{++} entry (4) and increase of cytoplasmic Ca^{++} levels (5). Adapted from Lourido and Moreno, 2015.

Furthermore, during host cell invasion, a cytoplasmic membrane invagination is induced, which together with parasite-derived proteins later generates the P.V. (Black and Boothroyd, 2000). This unique membranous non-fusogenic vacuole is largely composed by host cell membrane (>85%) and modified by proteins originating from rhoptry and dense granule secretions. It creates a unique niche for parasite survival and replication (Black and Boothroyd, 2000). Interestingly, soon after invasion, the early P.V. attracts host cell

Introduction

structures, such as mitochondria, Golgi and endoplasmic reticulum (E.R.), most probably to facilitate host cellular nutrient delivery by proximity (Black and Boothroyd, 2000; Nolan et al., 2015; Romano et al., 2013; Shunmugam et al., 2022; Sinai et al., 1997). Physiologically, the P.V. ensures intracellular parasitism by permitting both small molecule (<1300 Da) diffusion and active import of larger molecules by selective transport thereby representing a key requirement for intracellular development of apicomplexan parasites (Black and Boothroyd, 2000).

In most cases, the replication process is initiated after full formation of the P.V. In general, division of coccidian parasites differs in several aspects from the respective process in classical animal cells. Overall, coccidia show different types of asexual division, i. e. by endodyogeny, schizogony and endopolygeny (Francia and Striepen, 2014). These different division strategies are defined by the mode of nuclear division before cytokinesis (Francia and Striepen, 2014). In addition, coccidian parasites show different proliferation speeds, characterizing them as fast- or slow-replicating species. Species of the family *Eimeriidae*, such as *E. bovis*, are representatives of slow proliferating species, fulfilling first merogony after 18 days p. i. *in vitro* (Hermosilla et al., 2002). In contrast, fast replicating species, such as *T. gondii*, *N. caninum* and *B. besnoiti*, already release new offspring after 24-72 hours p. i. during acute replication (Taubert et al., 2006a, 2016). Obviously, this divergence in replication speed ultimately influences the final number of merogonic progeny being released: while *T. gondii* produces 32 to 64 tachyzoites within each round of merogony, during *E. bovis* first merogony >120,000 merozoite I can be produced following single sporozoite infection (Hermosilla et al., 2002; Taubert et al., 2006a).

Regardless of the coccidian species, the asexual replication cycle will end with progeny egress from infected host cells. This process permits the spread of newly released parasites into different tissues *in vivo*, thereby influencing the outcome of disease (Black and Boothroyd, 2000). In most coccidian species, egress represents a quite fast event that results in the lysis of the host cell and the release of motile parasites. In contrast to host cell invasion, far less is known on cellular egress, nonetheless, it is accepted that Ca⁺⁺-driven signals precede parasite exit from cells in a similar fashion as invasion (Hoff and Carruthers, 2002). Remarkably, in *T. gondii* tachyzoites both processes share a dependency on motility and

microneme secretion, thereby suggesting that they are governed by similar signaling routes (Arrizabalaga and Boothroyd, 2004). Overall, the pivotal role of Ca^{++} fluxes has been demonstrated in different coccidian species, such as *T. gondii*, *N. caninum* and *E. bovis*, by Ca^{++} ionophore treatments (Behrendt et al., 2008). However, since ionophores act in a receptor-independent manner, interpretations regarding signaling pathways (i. e. via PLC) should be carefully taken (Caldas and de Souza, 2018). In this context, so far, no specific physiological signals were identified as reliable egress inducers in coccidian parasites. Despite that, studies on *T. gondii* tachyzoites showed that immunomodulatory molecules, such as nitric oxide and TNF- α , can provoke an early egress from infected host cells (Tomita et al., 2009; Yan et al., 2015; Yao et al., 2017).

1.2.2. Host cell modulation by coccidian parasites

Since coccidian parasites are obligate intracellular parasites, successful intracellular development highly depends on effective modulation of host cellular functional categories. However, host cells themselves may sense parasite infection and activate pathogen defense mechanisms. Thus, studies in bovine umbilical vein endothelial cells (BUVEC) showed that coccidian infection triggered a pro-inflammatory and leukocyte-recruiting response by adhesion molecule, chemoattractant and other mediator upregulation (Taubert et al., 2006a, 2006b). This conserved immune response is not only linked to fast replicating coccidian species like *T. gondii*, *N. caninum* and *B. besnoiti*, but also to the slow replicating parasite *E. bovis*, promoting leukocyte migration and ultimately an antimicrobial response (Maksimov et al., 2016; Taubert et al., 2006a, 2006b). The latter response has special relevance since cell death itself represents an (ultimate) defense mechanism against intracellular pathogens, often orchestrated by T CD8^{+} cytotoxic lymphocytes and NK cells (Gigley, 2016). Given that, the parasite must overcome apoptotic signals of infected cells to fulfil its intracellular cycle. In line, *T. gondii* blocks host cell apoptosis by interfering with pro-apoptotic signals, such as caspases, or up-regulating anti-apoptotic mediators like Bcl-2 proteins (Mammari et al., 2019). Likewise, *E. bovis* modulates enhances the expression of anti-apoptotic mediators such c-IAP1 and c-FLIP during first merogony (Lang et al., 2009). Meanwhile, it is largely accepted that coccidian parasites are capable of modulating the host cellular phenotype to satisfy parasitic needs, thereby implicating complex interactions with infected host cells.

Introduction

In that context, a multitude of transcriptomic analyses proved that coccidian infections considerably affect host cellular gene transcription. In the case of *T. gondii*, RNA-seq of pigs fed with *T. gondii* oocysts, showed up regulation of 217, 223, 347, 119, and 161 genes in brain, liver, lung, mesenteric lymph nodules and spleen, respectively, at 18 days p. i. (He et al., 2019). Likewise, intraperitoneal inoculation of *T. gondii* tachyzoites in mice up-regulated approximately 935 genes in brain tissue at 32 days p. i. (Tanaka et al., 2013), and approximately 2997 genes in uterine tissue in 8 days-pregnant mice (Zhou et al., 2020). Similarly, host cell transcriptome modulation driven by *T. gondii* infection has been explored *in vitro*, permitting to understand the modulatory capacity of this coccidian parasite at cellular level. In this context it was reported that *T. gondii* infection modulates the expression of 214 gene-encoding RNAs in human umbilical vein endothelial cells (HUVEC) at 18 h p. i. (Franklin-Murray et al., 2020). Interestingly, *T. gondii*-driven gene modulation seems to be influenced by time and cell line type, since 1266, 2303, 3022, 1757, 3088, and 2531 genes were differentially expressed at 3, 9, 12, 24, 36 and 48 h p. i., respectively, in human foreskin fibroblast (HFF) cells (Wang et al., 2022). Noteworthy, transcriptomic-based evidence is mirrored at protein level by proteomic-based studies. In specific, murine intraperitoneal infections with *T. gondii* induced changes in expression of 38 proteins in macrophages (Zhou et al., 2011), 58 proteins in placenta (Jiao et al., 2017) and approximately 301 proteins in liver tissue (He et al., 2016), indicating an overall modulation of host phenotypes by parasite infection. Contrastingly, transcriptomic-based evidence is limited in the case of other coccidian parasites, however, RNA-seq analysis showed that more than 446 genes are differentially transcribed in bovine aortic endothelial cells (BAEC) infected with *B. besnoiti* at 32 h p.i. (Jiménez-Meléndez et al., 2020), and *N. caninum*-infected bovine trophoblasts revealed 207 differentially expressed genes (Horcajo et al., 2018). During *E. bovis* long-lasting merogony I in BUVEC, more than 1184 RNA sequences were modulated at 14 days p. i. (Taubert et al., 2010), confirming the broad modulation of different cell routes driven by coccidian infections.

The implications of this wide transcription reprogramming driven by coccidian parasite infection were addressed by gene ontology enrichment analyses, suggesting that a considerable proportion of transcriptomic effects were linked to host immune responses (Franklin-Murray et al., 2020; Horcajo et al., 2018; Jiménez-Meléndez et al., 2020; Regidor-

Cerrillo et al., 2020; Wang et al., 2022). Nonetheless, once the parasites start growing and dividing in its host cell, massive amounts of nutrients must be acquired from the infected host cell (Black and Boothroyd, 2000). In this context, transcriptomic and proteomic analyses consistently demonstrated a significant induction of nutrient acquirement-related pathways during coccidian parasite development *in vitro* in different cell lines (Franklin-Murray et al., 2020; Horcajo et al., 2018; Jiménez-Meléndez et al., 2020; Regidor-Cerrillo et al., 2020; Sun et al., 2021; Wang et al., 2022). Specifically, in *T. gondii*-infected HFF cells, reprogramming of cell metabolism was evident by differential expression levels of proteins involved in key metabolic pathways, such as glycolysis, lipid/sterol metabolism and purine metabolism (Nelson et al., 2008; Sun et al., 2021). In the case of *B. besnoiti*, a modulation of genes related to carbohydrates metabolism were reported in BAEC (Jiménez-Meléndez et al., 2020). Similarly, *N. caninum* infection drove an enhancement in expression of carbohydrate-, amino acid- and fatty acid-related genes in infected trophoblasts, showing specifically higher levels of expression profiles in more virulent *N. caninum* strains, which exhibits superior growth rates *in vitro* (Regidor-Cerrillo et al., 2020) thereby delivering a link between effective host cell modulation and virulence.

Interestingly, when developing an obligatory intracellular lifestyle during evolution, apicomplexan parasite genomes experienced a massive loss of genes that encode for more complex metabolic pathways. Thus, these parasites now rely on host cellular metabolic pathways for survival, and indeed are auxotrophic for several basic metabolites (Coppens, 2014), rendering them vulnerable for new promising pharmacological targets. In the case of *T. gondii*, it is widely accepted that this species is auxotrophic for key molecules like purines, aromatic amino acids, and cholesterol (Coppens, 2014). In this context, cholesterol auxotrophy seems to be shared throughout the apicomplexan phylum, all scavenging this molecule from infected host cells (Coppens, 2013).

1.3. General cholesterol metabolism in animal cells

In animals, cholesterol is obtained by two main routes: intracellular *de novo* biosynthesis and extracellular uptake via dietary sources (Simons and Ikonen, 2000). *De novo* biosynthesis via the mevalonate pathway is an anabolic synthetic route occurring in the E.R. of almost all cells, but mainly being executed in hepatic tissue (See **Fig 1.4**) (Buhaescu and Izzedine, 2007;

Introduction

Simons and Ikonen, 2000). This synthesis pathway involves more than 20 enzymes beginning with the generation of mevalonate from acetyl-CoA (Goldstein and Brown, 1990). This conversion depends on the activity of hydroxymethylglutaryl-CoA (HMG-CoA) reductase, a highly regulated enzyme that represents the rate-limiting enzyme of this pathway. Following mevalonate synthesis, farnesyl PP, squalene and lanosterol are the three most relevant cholesterol intermediates (Buhaescu and Izzedine, 2007; Goldstein and Brown, 1990). Of note, free cholesterol is a hydrophobic metabolite that is cytotoxic, consequently it is detoxified via metabolic conversion (esterification) by acyl-CoA-Cholesterol-acyltransferase 2 (ACAT2), thereby allowing for cellular cholesterol accumulation as cholesteryl esters (Olzmann and Carvalho, 2019).

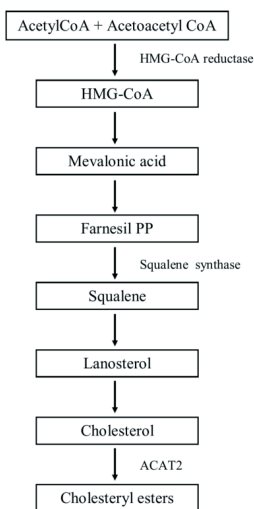


Fig 1.4. Cholesterol *de novo* biosynthesis via mevalonate pathway. Schematic illustration of the main enzymes and intermediate cholesterol metabolites. Adapted from Buhaescu and Izzedine, 2007; Goldstein and Brown, 1990.

Given that cholesterol biosynthesis represents a complex metabolic and energetic-costly process, cholesterol is additionally obtained via dietary acquisition. In mammals, this

Introduction

process occurs by incorporation of cholesterol in micellar complexes in the small intestine (Betteres and Yu, 2010). Mechanistically, cholesterol absorption through the enterocyte barrier is mainly mediated by the Niemann-Pick C1-Like (NPC1L1) protein. This transmembrane protein is highly expressed in the apical membrane of enterocytes and hepatocytes. It interacts with extracellular micellar cholesterol by a sterol sensing domain (SSD); incorporation then occurs by a clathrin-mediated endocytosis (Betteres and Yu, 2010; Davis et al., 2004). In analogy to free cholesterol, dietary cholesterol is mostly esterified by ACAT2 into cholesteryl esters within the E.R. and then released into lymphatic circulation within nascent chylomicrons and very low density lipoproteins (VLDL) along with triglycerides and free cholesterol (Luo et al., 2020). Over time, the lipid composition of VLDL will be affected by removal of some of its content in peripheral tissue, thereby generating cholesterol-rich low density lipoproteins (LDL), which represent the most significant cholesterol transport mechanisms in animals (Luo et al., 2020; Simons and Ikonen, 2000). At cellular level, LDL uptake represents the most important cholesterol source (Simons and Ikonen, 2000). Incorporation of this lipoprotein type relies on its interaction with the LDL receptor (LDLR), and the concomitant endocytosis of this ligand-receptor complex (See **Fig 1.5**) (Ikonen, 2008; Simons and Ikonen, 2000). This endocytic complex undergoes hydrolysis in early endosomes, which are enriched in acid-containing vesicles mediating LDLR recycling into the cytoplasmic membrane, while LDL-derived cholesterol is cleaved by acid lipase and incorporated as free cholesterol into the E.R. (Luo et al., 2020). The mechanism of LDL-derived cholesterol exit from late endosomes is largely dependent on the Niemann-Pick C1 (NPC1) molecule. NPC1 is a transmembrane protein localized at the membrane of late endosomes (Meng et al., 2020). Mechanistically, this protein acts as a free cholesterol carrier, mediating cholesterol transport to other membranes (i. e. cytoplasmic, endosomal, mitochondrial) and the E.R., where it is then esterified by ACAT 2 (Ikonen, 2008; Meng et al., 2020).

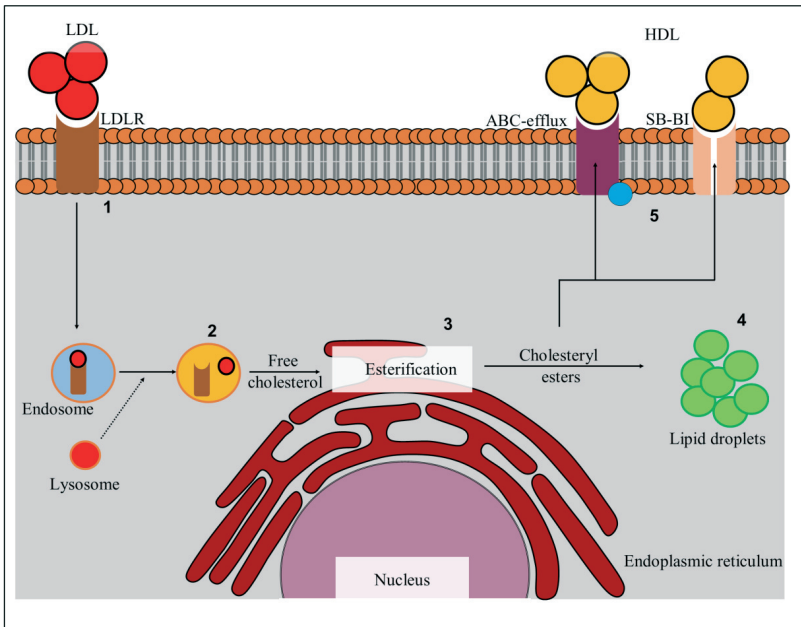


Fig 1.5. Main mechanisms of cellular cholesterol uptake and intracellular transport.

Steps here illustrated are: Endocytosis of LDL-LDLR complex (1), lysosome-driven endosomal acidification and free cholesterol release (2), cholesterol re-esterification within the E.R. (3), cholesteryl ester storage within lipid droplets (4) and removal of excess cellular cholesterol by transfer into HDL particles by ABC-transporters and SR-BI (5). Adapted from Ikonen, 2008; Simons and Ikonen, 2000.

Irrespective of the cholesterol source (*de novo* or acquired), excess free cholesterol as well as some other lipids are cytotoxic. To avoid imbalance-driven toxicity, different strategies of free cholesterol detoxification or efflux exist at cellular level. Overall, cells that rely on LDL uptake, can simply down-regulate LDLR abundance in the membrane (Luo et al., 2020). However, down-regulation by itself may not be sufficient to prevent cholesterol imbalances. In this context, cholesteryl esters are largely stored in cytoplasmic structures named lipid droplets (Olzmann and Carvalho, 2019). Lipid droplets are dynamic organelles originating from the E.R. They are composed by a core of neutral lipids, such as triacylglycerol and

cholesteryl esters, and enclosed by a phospholipid monolayer (Olzmann and Carvalho, 2019). Physiologically, lipid droplet numbers are in a constant balance being regulated by actual metabolic requirements of a cell. Thereby, a ready-to-use cholesterol source for cellular needs is generated in addition to a buffering compartment for more toxic liposoluble molecules (Olzmann and Carvalho, 2019). Additionally, cholesterol imbalances are prevented by efflux of this metabolite. However, since it is a lipophilic metabolite, cholesterol efflux through cytoplasmic membranes is an energy-dependent mechanism. In this context, key molecules of active cholesterol efflux are ATP binding cassette (ABC) transporters (Dean et al., 2001; Phillips, 2014). Overall, the first and best understood ABC transporter for cholesterol efflux is ABCA1, mediating cholesterol efflux by triggering its incorporation into high density lipoproteins (HDL) particles as extracellular acceptors (Betters and Yu, 2010; Dean et al., 2001; Simons and Ikonen, 2000). HDL particles are the most abundant cholesterol acceptor molecules for cellular efflux and HDL-driven cholesterol reverse transport represents a main route for avoiding cholesterol imbalances in cells. Likewise, this lipoprotein enhances the hepatic clearance of cholesterol (Phillips, 2014). From a mechanistic perspective, cholesterol uptake from HDL particles into hepatic tissue is driven the scavenger receptor BI (SR-BI) of hepatocytes (Linton et al., 2017; Phillips, 2014). SR-BI is a transmembrane receptor firstly described as HDL receptor and abundantly expressed in hepatic tissue. The unique capacity to incorporate free cholesterol and cholesteryl esters from HDL particles by a non-endocytic mechanism allows for direct cholesterol transport into hepatocytes for further disposal and into steroidogenic tissue for hormone biosynthesis (Phillips, 2014). Interestingly, this receptor can also interact with other lipoproteins like LDL, mediating cholesteryl ester incorporation into cells by an LDLR-independent pathway (Vishnyakova et al., 2020), thereby suggesting an alternative route for cholesterol uptake.

1.4. Modulation of host cellular cholesterol metabolism by coccidian parasites

Given that apicomplexa are auxotrophic for cholesterol, they need to obtain this molecule from their host cell (Coppens, 2013). In that context, coccidian parasites developed several strategies to fulfil cholesterol requirements during asexual replication. At transcriptomic level, an upregulation of mRNAs for HMG-CoA (synthase 1 and reductase) and ACAT 2 was reported in *E. bovis*-infected BUVEC at 17 d p. i. (Hamid et al., 2015). This finding was

Introduction

functionally mirrored by the blockage of the respective biosynthesis route by statins, which dramatically affected *E. bovis* macromeront development in BUVEC (Hamid et al., 2014). However, the relevance of this biosynthesis pathway in other parasite species remains unclear: while *T. gondii* proliferation in macrophages was reduced by statins treatments (Nishikawa et al., 2011), it seemed to play a minor role in *T. gondii*-infected CHO cells and in *C. parvum*-infected epithelial cells (Coppens et al., 2000; Ehrenman et al., 2013), suggesting parasite species- and host cell type-dependent mechanisms. Interestingly, the involvement of downstream enzymes of the mevalonate pathway like ACAT 2 is highlighted, since pharmacological inhibition of cholesterol esterification reduced *T. gondii* and *E. bovis* replication in fibroblastic cells and BUVEC, respectively (Hamid et al., 2014; Sonda et al., 2001).

Overall, despite the potential importance of *de novo* biosynthesis during coccidian replication, it is generally accepted that cholesterol from other sources can also ensure the parasite's needs during asexual replication. Nevertheless, different strategies among coccidian parasites are reported. For example, *C. parvum* is capable of incorporating micellar cholesterol by NPC1L1-mediated uptake in colorectal tumor cells (HCT-8) (Ehrenman et al., 2013), while *T. gondii* tachyzoite replication within fibroblasts does not seem to exploit this route (Coppens et al., 2000). Despite that, LDL-mediated cholesterol uptake is the most important source to fulfil cholesterol requirements in coccidia-infected host cells. Specifically, *T. gondii* replication in Chinese hamster ovary (CHO) cells largely relies on exogenous LDL (Coppens et al., 2000). Likewise, *N. caninum* and *C. parvum* replication is diminished by LDL-deprivation (Ehrenman et al., 2013; Nolan et al., 2015), showing that LDL-mediated uptake is pivotal for parasite replication *in vitro*. In addition, downstream mediators of the LDL endocytic pathway, such NPC1, are required for cholesterol trafficking during coccidian infections. Thus, proteomic analysis shows an enhanced expression of NPC1 over time driven by *N. caninum* infection in trophoblasts (Regidor-Cerrillo et al., 2020). Moreover, *N. caninum* shows a functional dependency on host cellular NPC1 expression for successful replication in infected HHF cells (Nolan et al., 2015). Similar findings are reported for *T. gondii*-infected CHO cells, where the pharmacological blockage of NPC1 by U18666A treatments reduces parasite proliferation by lysosomal cholesterol sequestering (Coppens et al., 2000). Taken together, it may be concluded that LDL-driven

Introduction

cholesterol is only available for coccidia after its re-esterification in the E.R. Alternatively, novel data propose an unconventional non-endocytic route for cholesterol acquisition from LDL particles by the participation of SR-BI (Vishnyakova et al., 2020). Nevertheless, the implication of this route in coccidian parasites infection remains unknown, so far. Interestingly, this receptor seems to be required for invasion and replication of *Plasmodium berghei* and *P. falciparum* in the hepatic stage (Rodrigues et al., 2008; Yalaoui et al., 2008).

As described above and irrespective of its source, free cholesterol accumulation within host cells is cytotoxic. Given that, coccidian parasites must master a delicate balance of cholesterol incorporation and utilization during replication within the P.V. (Ehrenman et al., 2010). Overall, availability of cholesterol in the coccidian P.V. seems largely linked to lipid droplet incorporation (Hu et al., 2017; Nolan et al., 2017). Independent studies have shown that *E. bovis*, *T. gondii* and *N. caninum* infections induce an increase in lipid droplet numbers within the infected host cell over time (Hamid et al., 2015; Hu et al., 2017). Moreover, in *T. gondii*-infected host cells, lipid droplets are assimilated by the P.V., building up a source of neutral lipids, including cholesteryl esters, for parasite requirements (Hu et al., 2017; Nolan et al., 2017). *T. gondii* recruits lipid droplets to the P.V. as demonstrated by increasing lipid droplet numbers during the first 8 h of infection (Hu et al., 2017). Mechanistically, an up-regulation of RNAs encoding for proteins required for lipid droplet synthesis and transport, such as AGPTA2, DGAT2 and FABP5 is registered in *T. gondii*-infected host cells (Hu et al., 2017). Interestingly, artificial enhancement of neutral lipid content by oleic acid supplementation leads to an increase of lipid droplet numbers within *T. gondii*-infected host cells, suggesting an enhancement of the lipogenic capacity (Hu et al., 2017; Nolan et al., 2017). In line, oleic acid treatments of *E. bovis*-infected host cells boost offspring production (Hamid et al., 2015). Besides lipid droplet formation, cholesterol imbalances are also controlled by ABC transporter-mediated active efflux of this metabolite from infected host cells (Ehrenman et al., 2010). Moreover, ABC transporters were also found involved in drug resistance-related phenomena in other protozoan parasites, such as *Plasmodium* spp., *Leishmania* spp. and *Trypanosoma* spp. (Leprohon et al., 2011). However, the role of this transporter family in cholesterol physiology during coccidian infection is yet not fully understood. In this context, *T. gondii* relies on ABC transporters from the G subfamily (ABCG), not only for sterol efflux from the P.V., but also for its incorporation (Ehrenman et

Introduction

al., 2010). Likewise, host cellular ABCB1 (syn. MDR1, P-gp) is required for successful *T. gondii*- and *N. caninum*-intracellular proliferation, since P-gp inhibitor treatments resulted in impaired lipid transport into the P.V. and in a diminishment cholesterol incorporation into host cells (Bottova et al., 2009). The latter is of special relevance since pharmacological blockage of P-gp diminishes intracellular replication of several coccidian species like *T. gondii*, *N. caninum* and *C. parvum* (Bottova et al., 2010; Perkins et al., 1998), suggesting a pivotal role of this protein during coccidian proliferation.

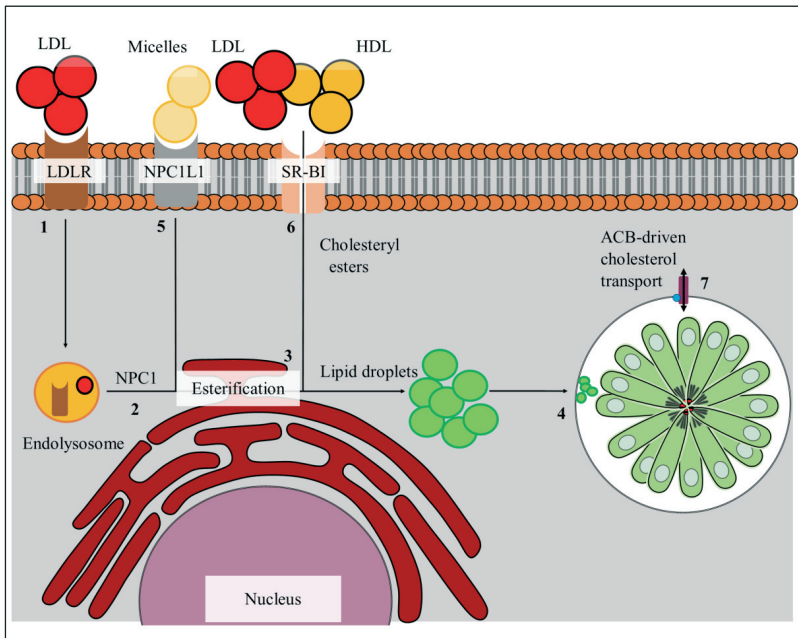


Fig 1.6. Schematic illustration of the main cholesterol-related metabolic routes during apicomplexan parasite infection. Steps here illustrated are: endocytosis of LDL-LDLR complex (1), NPC1-mediated free cholesterol transport (2), cholesterol re-esterification within the E.R. (3), acquisition of lipid droplet-derived cholesteryl esters in the P.V. (4), NPC1L1-driven incorporation of micellar cholesterol (5), cholesteryl ester uptake from extracellular lipoproteins via SR-BI (6) and modulation of cholesterol imbalances in the P.V.

Introduction

by ABC transporter activity (7). Adapted from Coppens, 2013; Coppens et al., 2000; Ehrenman et al., 2010; Nolan et al., 2017; Rodrigues et al., 2008; Yalaoui et al., 2008.

Overall, the main objective of this doctoral thesis is to analyze the relevance of distinct cholesterol-related pathways involving NPC1L1, P-gp and SR-BI for successful asexual proliferation of three different coccidian species (*T. gondii*, *N. caninum* and *B. besnoiti*). Moreover, novel aspects of parasite-host cell-interactions and coccidian physiology will be addressed.

2. ORIGINAL PUBLICATIONS

2.1. *BESNOITIA BESNOITI* INFECTION ALTERS BOTH ENDOGENOUS CHOLESTEROL DE NOVO SYNTHESIS AND EXOGENOUS LDL UPTAKE IN HOST ENDOTHELIAL CELLS

Silva, L.M.R., Lütjohann, D., Hamid, P., Velasquez, Z.D., Kerner, K., Larrazabal, C., Failing, K., Hermosilla, C., and Taubert, A. (2019).

Sci Rep 9, 6650; doi: 10.1038/s41598-019-43153-2

Own part in the publication:

- Project planning: 30 %, Together with co-authors and supervisors
- Development of experiments: 30 %, Together with co-authors
- Evaluation of experiments: 30 %, Together with co-authors
- Writing of the manuscript: 10 %, Together with co-authors

SCIENTIFIC REPORTS

OPEN

Besnoitia besnoiti infection alters both endogenous cholesterol *de novo* synthesis and exogenous LDL uptake in host endothelial cells

Received: 8 November 2018
Accepted: 12 April 2019
Published online: 30 April 2019

Liliana M. R. Silva¹, Dieter Lütjohann², Penny Hamid^{1,3}, Zahady D. Velasquez^{1,4}, Katharina Kerner⁵, Camilo Larrazabal¹, Klaus Failing⁶, Carlos Hermosilla² & Anja Taubert¹

Besnoitia besnoiti, an apicomplexan parasite of cattle being considered as emergent in Europe, replicates fast in host endothelial cells during acute infection and is in considerable need for energy, lipids and other building blocks for offspring formation. Apicomplexa are generally considered as defective in cholesterol synthesis and have to scavenge cholesterol from their host cells for successful replication. Therefore, we here analysed the influence of *B. besnoiti* on host cellular endogenous cholesterol synthesis and on sterol uptake from exogenous sources. GC-MS-based profiling of cholesterol-related sterols revealed enhanced cholesterol synthesis rates in *B. besnoiti*-infected cells. Accordingly, lovastatin and zaragozic acid treatments diminished tachyzoite production. Moreover, increased lipid droplet contents and enhanced cholesterol esterification was detected and inhibition of the latter significantly blocked parasite proliferation. Furthermore, artificial increase of host cellular lipid droplet disposability boosted parasite proliferation. Interestingly, lectin-like oxidized low density lipoprotein receptor 1 expression was upregulated in infected endothelial host cells, whilst low density lipoproteins (LDL) receptor was not affected by parasite infection. However, exogenous supplementations with non-modified and acetylated LDL both boosted *B. besnoiti* proliferation. Overall, current data show that *B. besnoiti* simultaneously exploits both, endogenous cholesterol biosynthesis and cholesterol uptake from exogenous sources, during asexual replication.

Besnoitia besnoiti is an obligate intracellular apicomplexan parasite which causes bovine besnoitiosis and has a significant economic impact on cattle industry in endemic areas¹. Clinical bovine besnoitiosis includes rather general signs during the acute febrile phase of infection (e.g. lethargy, tachycardia, tachypnoea, congestive mucosae, oedema, anorexia, weight loss) whilst massive skin alterations or bull infertility are characteristic for the chronic phase². Successive reports on *B. besnoiti* infections in several European countries in the recent years^{3–11} revealed this disease as emerging in Europe^{11,12}. During the febrile acute stage of besnoitiosis, tachyzoites mainly proliferate in bovine host endothelial cells of different organs and vessels causing vasculitis, thrombosis, and necrosis of venules and arterioles¹. *In vitro* experiments proved a series of cell types besides endothelial cells as permissive for parasite replication and *B. besnoiti* showed fast proliferative qualities, which are alike to those of *Toxoplasma gondii* or *Neospora caninum*^{4,13–16}. During acute proliferation, the parasite is in a significant need for energy and cell building blocks, which may either be scavenged from the host cell or be synthesized by the parasite itself, depending on its synthetic capacities. Especially for offspring production, the parasite needs vast amounts of cholesterol. Cholesterol was shown to be sequestered in cholesterol-rich organelles and to be inserted

¹Institute of Parasitology, Biomedical Research Center Seltersberg, Justus Liebig University Giessen, Schubertstr. 81, D-35392, Giessen, Germany. ²Institute for Clinical Chemistry and Clinical Pharmacology, University Clinics Bonn, Laboratory for Special Lipid Diagnostics/Center Internal Medicine/Building 26/UG 68, Sigmund-Freud-Str. 25, D-53127, Bonn, Germany. ³Department of Parasitology, Faculty of Veterinary Medicine, Universitas Gadjah Mada, Jl. Fauna No. 2 Karangmalang, 55281, Yogyakarta, Indonesia. ⁴Institute for Hygiene and Infectious Diseases of Animals, Justus-Liebig-University, Giessen, Frankfurter Str. 85-89, D-35392, Germany. ⁵Unit for Biomathematics and Data Processing, Faculty of Veterinary Medicine, Justus Liebig University Giessen, Frankfurter Str. 95, D-35392, Giessen, Germany. Correspondence and requests for materials should be addressed to L.M.R.S. (email: Liliana.Silva@vetmed.uni-giessen.de)

Besnoitia besnoiti infection alters both endogenous cholesterol *de novo* synthesis and exogenous LDL uptake in host endothelial cells

www.nature.com/scientificreports/

into the parasite plasma membrane and the parasitophorous vacuole membrane in the case of the closely related parasite *T. gondii*²⁷. Furthermore, cholesterol is esterified for storage in lipid droplets, which were consistently found enhanced in apicomplexan parasites-infected host cells^{17–18}. However, apicomplexan parasites are generally considered as defective in cholesterol synthesis^{17,29–31}. For compensation, they need to scavenge cholesterol from their host cells thereby following different strategies of cholesterol acquisition. In general, two main routes of cholesterol disposal are provided by potential host cells: endogenous cholesterol *de novo* synthesis and sterol uptake from extracellular sources via specific receptors. These scavenging pathways are differentially exploited by different apicomplexan species. While several species, such as *T. gondii* (in Chinese hamster ovary cells - CHO), *Cryptosporidium parvum* or *N. caninum* mainly rely on host cellular LDL-mediated sterol uptake^{17,33,34}, others mainly utilize host cellular *de novo* synthesis for cholesterol acquisition (e. g. *T. gondii* in macrophages)¹⁵. In contrast, hepatic *Plasmodium* spp. salvage cholesterol from both pathways but do not strictly depend on cholesterol acquisition for optimal proliferation³². Interestingly, the actual need of cholesterol of different apicomplexan species obviously depends on their mode of proliferation. Thus, for the slow but massively proliferating parasite *Eimeria bovis*, the simultaneous induction of both pathways was described^{17,29–31} whilst fast proliferating apicomplexan rather seem to utilize one single route of cholesterol acquisition. The fact that *T. gondii* triggers LDL-mediated sterol uptake in CHO cells but not in macrophages, where endogenous *de novo* synthesis represents the main source of cholesterol^{17,35}, additionally strengthens the assumption that the mode of cholesterol acquisition may also depend on the host cell type.

To date, no data exist on the mode of cholesterol salvage being utilized by *B. besnoiti*. Therefore, the aim of the study was to analyse whether *B. besnoiti* infection of primary bovine endothelial host cells, i. e. the cell type that is mainly infected in the *in vivo* situation, influences the host cellular cholesterol *de novo* synthesis and exogenous sterol uptake, cholesterol conversion and esterification, as well as neutral lipid and lipid droplet formation during active intracellular proliferation. To provide actual data on the true cellular situation, we here analysed the content of several cholesterol-related sterols in *B. besnoiti*-infected endothelial host cells via a biochemical approach. Overall, the data show that *B. besnoiti* infections induce endogenous cholesterol synthesis rates in primary endothelial host cells and additionally profits from enhanced exogenous LDL levels for optimal parasite proliferation.

Results

***B. besnoiti* infections enhance total cholesterol contents in endothelial host cells.** *B. besnoiti*-infected BUVEC (bovine umbilical vein endothelial cells) showed a stronger filipin staining (Fig. 1A1,A2) than non-infected controls (Fig. 1A3,A4) thereby suggesting a higher cholesterol content. Freshly released tachyzoites (Fig. 1A5,A6) were stained by filipin. Within tachyzoites, the strongest reactions were found in the posterior region of these stages. Single cell measurements of fluorescence intensity of filipin in *B. besnoiti*-infected (white arrows) and non-infected (orange arrows) host cells (Fig. 1A7, zoom of Supplementary Fig. 1) confirmed significantly enhanced levels of cholesterol in infected cells ($p = 0.0024$, Fig. 1A8). Amplex Red-based measurements of the total cholesterol contents (Fig. 1B1) confirmed a significantly increase of total cholesterol in *B. besnoiti*-infected endothelial host cells (effect of time: $p = 0.033$, infection: $p = 0.0002$ and interaction: $p = 0.0014$), as well as by GC-SM analyses ($p = 0.0429$; Fig. 1B2). Overall, kinetic analyses indicated increasing effects on cholesterol content with ongoing duration of infection leading to an enhancement of 1.8-fold, 2.2-fold and 2.4-fold at 12, 24 and 48 h p. i. (*t*-test with Bonferroni-Holm adjustment, $p < 0.0001$), respectively.

Exogenous cholesterol and desmosterol supplementation boosts parasite proliferation. To control the role of exogenous cholesterol sources for parasite proliferation, we supplemented cholesterol and its precursor desmosterol by direct addition of the cell culture medium. As previously shown³⁶, ethanol-dissolved cholesterol or desmosterol indeed directly acts on cells despite the hydrophobic characteristics of these molecules. In fact, supplementation with both desmosterol and cholesterol significantly enhanced *B. besnoiti* tachyzoite production in infected host cells (cholesterol $p < 0.01$; desmosterol $p < 0.05$; Fig. 1C). When comparing desmosterol and cholesterol for their effects, supplementation with cholesterol boosted parasite proliferation stronger than with desmosterol ($p < 0.01$). In addition, we supplied these molecules via M3CD complexes, in order to generate inclusion complexes that are able to donate these molecules to the host cell³⁶. However, treating BUVEC with such complexes did not improve parasite proliferation (data not shown). In addition, treatments of tachyzoites with cholesterol-M3CD-complexes prior to infection also failed to influence parasite proliferation (data not shown).

Neutral lipids and lipid droplet formation are enhanced in *B. besnoiti*-infected host cells. Neutral lipids and lipid droplets could be visualized via Bodipy 493/503 and Nile Red staining in *B. besnoiti*-infected BUVEC as well as in free tachyzoite stages. As estimated by fluorescence microscopy, infected cells showed increased numbers of lipid droplets in the cytoplasm of the host cell (Fig. 2A1–4). These findings were verified on a quantitative level via a FACS-based approach. By applying two different MOIs (3:1 and 4:1) we could show that lipid droplets are significantly enhanced in *B. besnoiti*-infected endothelial host cells when compared to non-infected controls (all $p < 0.01$, Fig. 2B). However, comparing the different MOIs or time points of infection, no significant differences were detected.

Microscopic analyses showed a stronger Nile Red staining in *B. besnoiti*-infected host cells (Supplementary Fig. 2; white arrows) when compared to non-infected cells within the same cell layer (Supplementary Fig. 2; orange arrows). Single cell measurements (from 3 different BUVEC isolates) confirmed significantly enhanced levels of neutral lipids in *B. besnoiti*-infected host cells ($p = 0.0181$, Fig. 2C). Tachyzoite stages also showed strong reactions after Nile Red staining indicating the presence of neutral lipids. As also shown for filipin staining, the strongest reactions were apparent in the posterior part of the tachyzoites (Fig. 2D1–2, arrows).

Besnoitia besnoiti infection alters both endogenous cholesterol *de novo* synthesis and exogenous LDL uptake in host endothelial cells

www.nature.com/scientificreports/

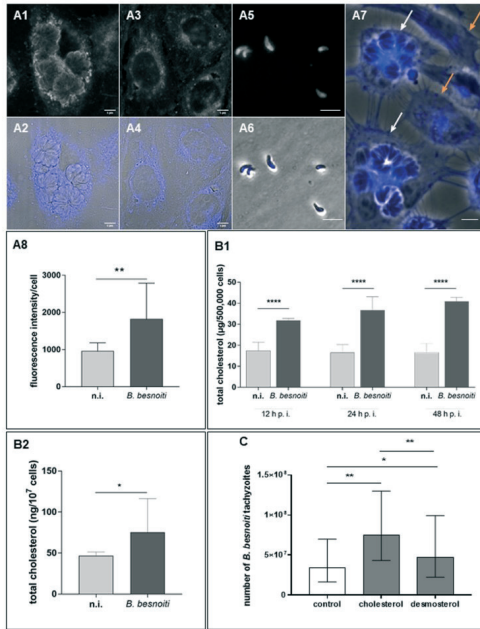


Figure 1. Cholesterol content in *B. besnoiti*-infected endothelial host cells and effects of cholesterol/desmosterol supplementation on parasite proliferation: (A) For cholesterol visualization, *B. besnoiti*-infected BUVEC and tachyzoite stages (24 h p. i.; A1–2, infected cell; A3–4, non-infected BUVEC; A5–6, *B. besnoiti* tachyzoites) were stained with filipin III (A1, A3 and A5); filipin + phase contrast (A2, A4, A6, A7). Single cell fluorescence intensity measurements were performed (A7; infected cells - white arrows; non-infected cells - orange arrows), and significantly increased amounts of cholesterol were observed in *B. besnoiti* infected cells (A8). (B) For analysis of total cholesterol content in *B. besnoiti*-infected host cells, BUVEC ($n = 6$) were infected with *B. besnoiti* tachyzoites and subjected to total cholesterol extraction using the Amplex Red test kit at different time points of infection (B1) or determined by GC-MS-based analyses (B2). Non-infected BUVEC were equally processed and served as negative controls. (C) To analyse the effect of exogenous cholesterol and desmosterol supplementation on tachyzoite production, *B. besnoiti*-infected BUVEC were either cultivated in non-supplemented (control) or cholesterol/desmosterol-enriched medium. 48 h after infection, the number of tachyzoites present in cell culture supernatants was determined. Geometric means of three biological replicates, geometric standard deviation, * $p < 0.05$, ** $p < 0.01$, *** $p < 0.001$. Error bar 20 µm.

Artificially enhanced lipid droplet disposability improves parasite proliferation. To estimate whether an increase of lipid droplet formation is beneficial for optimal parasite proliferation, we here artificially enhanced host cellular lipid droplet numbers by oleic acid treatments prior to infection. As depicted in Fig. 2E, the artificial enhancement of lipid droplet disposability indeed significantly boosted *B. besnoiti* tachyzoite

Besnoitia besnoiti infection alters both endogenous cholesterol *de novo* synthesis and exogenous LDL uptake in host endothelial cells

www.nature.com/scientificreports/

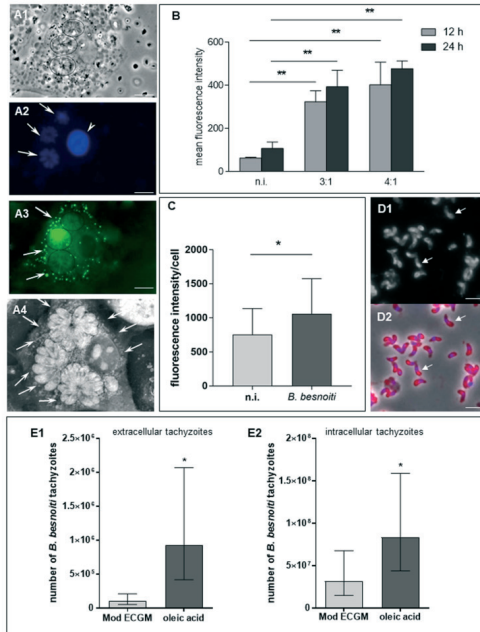


Figure 2. Neutral lipids and lipid droplet contents in *B. besnoiti*-infected endothelial host cells and effects of oleic acid treatments on parasite proliferation. (A) For lipid droplet visualization, *B. besnoiti*-infected endothelial host cells were stained by Bodipy 493/503 (A3) or directly analysed by tomographic microscopy (A4). Host cell nuclei were stained by DAPI (A2, arrowhead). A1–3: illustration of a single infected cell showing three typical *B. besnoiti* rosettes (24 h p. i., arrows) and a high abundance of cytoplasmic lipid droplets (A3, arrows). A4: 3D tomographic image of a *B. besnoiti* infected cell showing several cytoplasmic lipid droplets (arrows). (B) For lipid droplet quantification, *B. besnoiti*-infected BUVEC (MOI 3:1 and 4:1) were stained with Bodipy 493/503 at 12 (grey columns) and 24 h (black columns) p. i. and processed for flow cytometric analyses. Non-infected BUVEC were equally processed and served as negative controls. Arithmetic means of three BUVEC isolates, standard deviation (***p* < 0.01). (C) For neutral lipid quantification, Nile Red-stained *B. besnoiti*-infected BUVEC (MOI: 3:1, 24 h p. i.) were analysed for fluorescence intensities on single cell level [single infected and non-infected single cells were estimated within the same cell layers under identical experimental conditions using the ImageJ software]. Data were calculated as arithmetic means ± standard deviation (**p* = 0.0181). (D) Tachyzoite stages also showed strong reactions after Nile Red staining indicating the presence of neutral lipids. The strongest reactions were apparent in the posterior part of the tachyzoites (D1–2, arrows). (E) Effect of artificially enhanced lipid droplet disposability on *B. besnoiti* proliferation: to enhance lipid droplet formation in BUVEC, cells were treated with oleic acid in BSA-M3CD formulation prior to *B. besnoiti* tachyzoite infection. Non-treated BUVEC served as negative controls. Two days p. i. the number of tachyzoites being present in cell culture supernatants (E1) or still intracellular (E2) was estimated via PCR. Geometric means of three biological replicates, geometric standard deviation (**p* < 0.05). Error bar 20 μm.

Besnoitia besnoiti infection alters both endogenous cholesterol *de novo* synthesis and exogenous LDL uptake in host endothelial cells

www.nature.com/scientificreports/

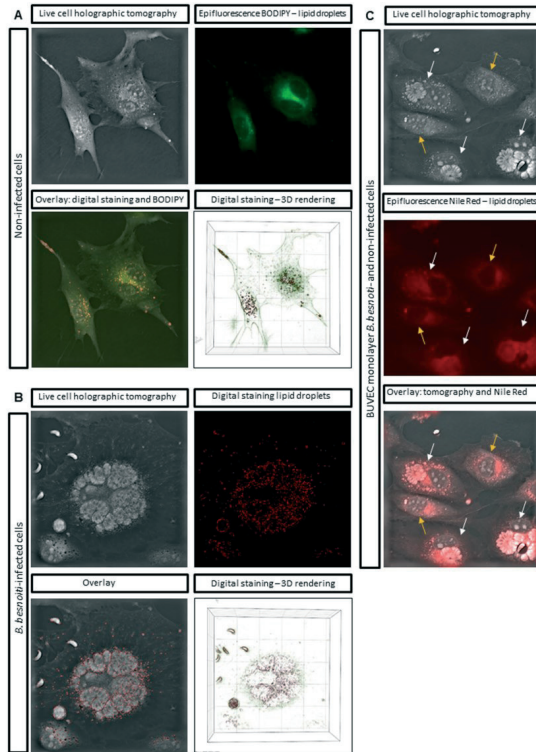


Figure 3. Live cell holographic tomography-based illustration of lipid droplets in non-infected and *B. besnoiti*-infected BUVEC. (A) Non-infected BUVEC were analysed for lipid droplet content via both, Bodipy 493/503-based staining (as visualized by epifluorescence) and live cell holographic tomography. 3D holotomographic images were obtained by using 3D cell-explorer microscope (Nanolive 3D Explorer) at 60X magnification ($\lambda = 520$ nm, sample exposure 0.2 mW/mm²) and a depth of field of 30 μ m. Lipid droplets were stained via digital staining (STEVE software, Nanolive) according to the refractive index of the intracellular structures. Overlays from both detection techniques proved the applicability of tomographic microscopy via matching of the signals. (B) Holographic tomography of live *B. besnoiti*-infected BUVEC at 24 h p. i. and detection of lipid droplets via digital staining. (C) Holographic tomography of live *B. besnoiti*-infected (white arrows) and non-infected (orange arrows) BUVEC at 24 h p. i. and detection of lipid droplets via Nile Red staining.

Besnoitia besnoiti infection alters both endogenous cholesterol *de novo* synthesis and exogenous LDL uptake in host endothelial cells

www.nature.com/scientificreports/

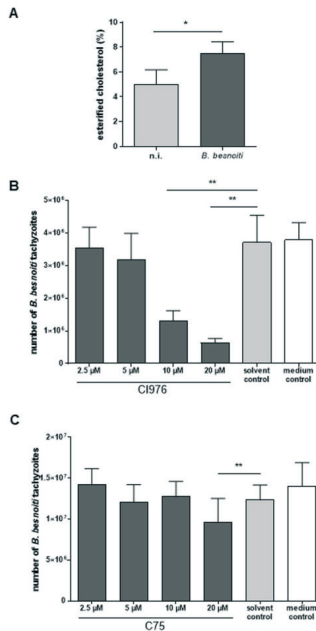


Figure 4. Cholesterol esterification in *B. besnoiti*-infected endothelial host cells and effects of CI976 and C75 treatments on parasite proliferation. (A) For estimation of the cholesterol esterification degree, *B. besnoiti*-infected BUVEC ($n = 3$) were subjected to GC-MS-based analyses of total and esterified cholesterol contents. Arithmetic mean of three biological with three technical replicates each, standard deviation; * $p < 0.05$. (B) Effects of CI976 (inhibitor of cholesterol esterification) treatment on tachyzoites proliferation: BUVEC were treated with CI976 (2.5, 5, 10 and 20 μ M) 24 h before *B. besnoiti* infection. Non-treated host cells served as controls. 48 h after infection, the number of tachyzoites present in cell culture supernatants were measured. Bars represent arithmetic means of three biological replicates, standard deviation (** $p < 0.01$). (C) Effects of C75 (inhibitor of fatty acids synthesis) treatment on *B. besnoiti* replication. BUVEC were treated with C75 (2.5, 5, 10 and 20 μ M) 24 h before *B. besnoiti* infection. Non-treated host cells served as controls. 48 h after infection, the number of tachyzoites present in cell culture supernatants was measured. Bars represent arithmetic means of three biological replicates, standard deviation (** $p < 0.01$).

production. Thus both, the number of freshly released (=extracellular, Fig. 2E1, $p = 0.0109$) and still intracellular (Fig. 2E2, $p = 0.0259$) tachyzoites (both log-transformed in the comparison) was found upregulated in oleic acid-treated BUVEC resulting in a 9-fold and 2.5-fold increase of parasite proliferation within 48 h, respectively.

Live cell 3D holotomographic microscopy. 3D holotomographic microscopy confirmed the presence of numerous lipid droplet-like structures in *B. besnoiti*-infected cells (Fig. 2A4, arrows). To prove the lipid

Besnoitia besnoiti infection alters both endogenous cholesterol *de novo* synthesis and exogenous LDL uptake in host endothelial cells

www.nature.com/scientificreports/

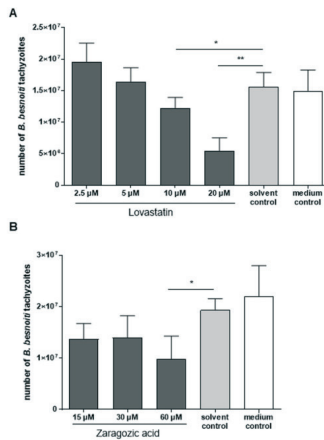


Figure 5. Effects of lovastatin (A) and zaragozic acid (B) treatments on *B. besnoiti* tachyzoite production. BUVEC were treated with lovastatin (A) or zaragozic acid (B) 24 h before *B. besnoiti* infection. Non-treated host cells served as controls. 48 h after infection, the number of tachyzoites present in cell culture supernatants was measured. Bars represent arithmetic means of three biological replicates, standard deviation (* $p < 0.05$; ** $p < 0.01$).

droplet-nature of these structures, holographic tomography and epifluorescence analyses (Bodipy 493/503 staining) were performed in parallel on BUVEC which proved the precise matching of these two independent techniques (Fig. 3A). The mean refractive index (RI) of Bodipy stained lipid droplets was estimated ($n = 50$) and was 1.355 ± 0.00333 . These parameters ($RI > 1.355$) were then applied to *B. besnoiti*-infected BUVEC (24 h p. i.) in 3D holotomographic microscopy and confirmed the presence of a high number of lipid droplets in infected cells (Fig. 3B). Moreover, Nile Red stained BUVEC also presented the same features (Fig. 3C).

Cholesterol esterification is essential for optimal parasite proliferation. Lipid droplets represent the main storage organelles for esterified cholesterol. Given that lipid droplets were found enhanced in *B. besnoiti*-infected BUVEC, we here analysed by biochemical means whether esterified cholesterol content was upregulated by *B. besnoiti* infection. Referring to total cholesterol content, *B. besnoiti*-infected BUVEC indeed showed a 1.5-fold, significant increase of esterified cholesterol levels when compared to non-infected controls (Fig. 4A, $p = 0.045$), thereby indicating infection-induced enhancement of free cholesterol conversion via esterification. To analyse further the role of cholesterol esterification for parasite proliferation we additionally performed functional inhibition experiments by the use of CI976, an inhibitor of the cholesterol-esterifying enzyme, sterol O-acyltransferase. Overall, CI976 treatments effectively inhibited *B. besnoiti* proliferation in a dose-dependent ($p = 0.0038$) manner (10 µM and 20 µM treatments: both $p < 0.01$; Fig. 4B). Thus, CI976 treatments led to a reduction of tachyzoite production of 4.6%, 14.1%, 64.7% and 82.9% when the cells were treated with 2.5, 5, 10 and 20 µM CI976 (Fig. 4B). Based on the inhibition of tachyzoite production, an IC_{50} of 7.56 µM was calculated for CI976 treatments. Microscopic control revealed that the host cells themselves were not altered in their morphology by CI976 treatments.

For cholesteryl ester formation, the hydroxyl group of cholesterol is linked to the carboxylate group of a fatty acid. Therefore, we additionally tested whether the blockage of fatty acid synthesis by the compound C75 would also impair *B. besnoiti* proliferation. C75 treatments of *B. besnoiti*-infected host cells moderately inhibited tachyzoite formation in dose dependent reduction ($p = 0.049$). However, only at 20 µM concentration a significant reduction of the number of parasites was observed when compared to solvent control (DMSO 0.1%; $p = 0.0032$; Fig. 4C).

Besnoitia besnoiti infection *B.* alters both endogenous cholesterol *de novo* synthesis and exogenous LDL uptake in host endothelial cells

www.nature.com/scientificreports/

Molecule	sterol:cholesterol ratio in control cells	sterol:cholesterol ratio in infected cells	n-fold	t-test p-value
Lanosterol	0.323±0.133	0.863±0.158	2.67	<0.0001
Dihydrolanosterol	0.035±0.014	0.049±0.009	1.41	0.0071
Lathosterol	7.718±3.517	14.710±3.867	1.91	0.0007
7-Dehydrocholesterol	3.263±0.416	5.765±1.661	1.77	0.0008
Desmosterol	3.383±2.179	3.861±1.069	1.14	n.s.
Cholestanol	2.680±0.312	2.626±0.363	0.98	n.s.
7 α -OH Cholesterol	0.124±0.055	0.129±0.020	1.04	n.s.
24-OH Cholesterol	0.131±0.065	0.104±0.029	0.79	n.s.
25-OH Cholesterol	0.094±0.105	0.054±0.025	0.57	n.s.
27-OH Cholesterol	0.077±0.041	0.048±0.006	0.62	0.0368
4 β -OH Cholesterol	0.086±0.051	0.064±0.013	0.75	n.s.
7 β -OH Cholesterol	0.239±0.089	0.257±0.059	1.07	n.s.
7-keto Cholesterol	2.021±1.352	1.655±0.539	0.82	n.s.
Campesterol	0.195±0.024	0.173±0.046	0.89	n.s.
Stigmasterol	0.101±0.034	0.075±0.017	0.73	0.0105
Sitosterol	0.254±0.058	0.189±0.047	0.74	0.0118

Table 1. Ratios of sterol/oxysterol to cholesterol (GC-MS-based analyses) in *Besnoitia*-infected and non-infected BUEC ($n = 3$). n.s. not significant.

Endogenous cholesterol synthesis is enhanced in endothelial host cells and appears essential for optimal *B. besnoiti* proliferation. Endogenous *de novo* cholesterol synthesis is performed by a multi-step biochemical pathway being supported by numerous enzymatic reactions. Given that analyses on gene transcription or protein expression of certain involved molecules may not precisely reflect their true enzymatic activity, we here analysed the actual content of cholesterol-related sterols (e. g. cholesterol precursors, metabolites) via biochemical means in *B. besnoiti*-infected BUEC and control cells. Therefore, the content of three groups of cholesterol-related sterols were measured: *i*) biosynthetic precursors of cholesterol in the endogenous synthesis pathway serving as indicators of cellular cholesterol *de novo* synthesis (lanosterol, dihydrolanosterol, lathosterol 7-dehydrocholesterol desmosterol); *ii*) downstream metabolites of *de novo* synthesis and indicators of cholesterol conversion [cholestanol, 24-hydroxycholesterol (24-OHC), 25-hydroxycholesterol (25-OHC), 27-hydroxycholesterol (27-OHC), 7 α -hydroxycholesterol (7 α -OHC), 7-ketocholesterol (7-ketoC), 4 β -hydroxycholesterol (4 β -OHC) and 7 β -hydroxycholesterol (7 β -OHC)] with some of these molecules (e. g. 7-ketoC, 7 α -OHC and 7 β -OHC) being recognized as indices of cellular oxidative stress; *iii*) phytosterols as indicators of cholesterol-uptake from the extracellular environment (campesterol, stigmasterol and sitosterol). We here calculated sterol:cholesterol ratios (Table 1) which are generally accepted as indicative for endogenous cholesterol synthesis rates. Notably, the individual BUEC isolates differed considerably in their basic absolute levels of sterols as indicated by rather high standard deviations already present in non-infected samples.

Overall, concerning indicators of endogenous cholesterol synthesis, *B. besnoiti* infections indeed led to a shift of sterol:cholesterol ratios by that way that several cholesterol precursors were found at enhanced contents in parasite-infected BUEC. Overall these reactions proved significant for lanosterol ($p < 0.0001$), dihydrolanosterol ($p = 0.0071$), lathosterol ($p = 0.0007$) and 7-dehydrocholesterol ($p = 0.0008$) and indicated that host cellular *de novo* synthesis of cholesterol is upregulated by *B. besnoiti* infection (Table 1). In contrast to indicators of endogenous cholesterol synthesis, most oxysterols representing downstream metabolites were not found changed in their sterol:cholesterol ratios. Thus, oxysterol:cholesterol ratios denied any positive shift of these ratios in infected cells, but even confirmed a slight decrease of the 27-OHC:cholesterol ratio ($p = 0.037$) in infected cells (Table 1). Given that especially 7 β -OHC, 7-ketoC, and 7 α -OHC upregulation may indicate oxidative cell stress reactions since these molecules represent antioxidants that are mainly formed by radical oxidative species, *B. besnoiti* infections do not appear to cause considerable oxidative stress in bovine endothelial host cells. Along with enhanced endogenous cholesterol *de novo* synthesis, cholesterol-related needs can also be satisfied via an enhanced sterol uptake from the extracellular environment. Since phytosterols exclusively are of plant origin and are submitted to the cells via the FCS fraction, intracellular phytosterols levels are often used as indices of sterol uptake. Although the overall absolute levels of sitosterol, stigmasterol and campesterol were found slightly increased in *B. besnoiti*-infected host cells (sitosterol: 1.2-fold, stigmasterol: 1.4-fold and campesterol: 1.5-fold), phytosterol:cholesterol ratios did not confirm enhanced levels and even showed slightly reduced values for stigmasterol ($p = 0.0105$) and sitosterol ($p = 0.0118$) (Table 1) in *B. besnoiti*-infected cells.

Given that cholesterol-related sterol profiling indicated enhanced endogenous cholesterol synthesis rates, we here additionally performed functional inhibition experiments using blockers of the mevalonate biosynthesis pathway. Therefore, statin treatments were here applied. Statins represent a class of drugs widely used to lower plasma cholesterol levels⁴⁶. We used lovastatin, which affects the total cellular isoprenoid/sterol synthesis and thus interferes at a very early step of *de novo* synthesis by blocking HMG-CoA-reductase (HMGCR). Overall, lovastatin treatments exhibited dose-dependent significant effects on parasite proliferation ($p = 0.02$). Thus, tachyzoite production was reduced for 21% and 66% when infected cells were treated with 10 μ M ($p < 0.05$) and

Besnoitia besnoiti infection alters both endogenous cholesterol *de novo* synthesis and exogenous LDL uptake in host endothelial cells

www.nature.com/scientificreports/

20 μM ($p < 0.01$) lovastatin, respectively (Fig. 5A). Based on the inhibition of tachyzoite production an IC_{50} of 11.31 μM was calculated for lovastatin treatments.

Besides lovastatin, we also used zarogazole acid (syn. squalenstatin) for treatments of *B. besnoiti*-infected BUEVC. Zarogazole acid is a squalene synthase inhibitor, which directly targets sterol synthesis. Zarogazole acid treatments resulted in a reduction of parasite replication (Fig. 5B), but effects were less prominent than those observed with lovastatin and required higher inhibitor concentrations. However, 60 μM zarogazole acid treatment induced a significant reduction of *B. besnoiti* replication (48.8%, $p < 0.05$). These data underline the key role of cellular *de novo* synthesis for successful parasite replication.

***B. besnoiti* infections induce LOX-1 but not LDLR expression and profit from exogenous sterol uptake.** Besides being synthesized endogenously, cholesterol may also be taken-up from extracellular sources via receptor-mediated LDL incorporation. The endothelial cell type is well-known to internalize different LDL species, such as non-modified LDL (LDL), acetylated LDL (acLDL) or oxidized LDL (oxLDL). LDL uptake is preferentially mediated by the classical LDL receptor (LDLR) whilst a series of non-classical, so-called scavenger receptors (e. g. LOX-1, SRB1) preferentially promote modified LDL incorporation. In this study we focused on two key receptors, LDLR and LOX-1, and analysed whether the gene transcription and protein expression of these receptor was influenced by *B. besnoiti* infections in BUEVC. Gene transcriptional profiling revealed that LDLR and LOX-1 were differentially altered by parasite infection. Whilst LDLR gene transcription and protein expression was not altered in *B. besnoiti*-infected BUEVC (Fig. 6A,C), LOX-1 gene transcripts were found upregulated throughout *B. besnoiti* *in vitro* infection peaking at 12 h p. i. (Fig. 6B). In agreement, LOX-1 protein expression was also found upregulated in infected cells: this was confirmed by two methods, a commercial LOX-1-specific ELISA (Fig. 5D), *B. besnoiti* infection vs. controls at 24 h p. i.: $p = 0.0025$) and by the FACS-based measurement of LOX-1 surface expression (Fig. 5E, *B. besnoiti* infection vs. controls 6 h p. i.: $p = 0.0167$, 24 h p. i.: $p = 0.0243$).

Given that LDLR and LOX-1 differentially promotes LDL species uptake, we here analysed whether supplementation of different LDL species (LDL, acLDL, oxLDL) is beneficial for parasite proliferation. Thus, LDL and acLDL was supplemented to *B. besnoiti*-infected BUEVC cultures at 10 μM final concentration. In case of oxLDL, the final concentration had to be reduced to 2.5 μM since this LDL variant revealed as toxic for BUEVC at higher concentrations. As depicted in Fig. 5F, both LDL and acLDL significantly boosted *B. besnoiti* tachyzoite production when compared to non-supplemented controls (LDL: $p < 0.01$; acLDL: $p < 0.001$). Moreover, acLDL induced a significantly stronger parasite proliferation than LDL supplementation ($p < 0.05$). In contrast, oxLDL failed to improve parasite replication at 2.5 μM supplementation. These data revealed that optimal *B. besnoiti* proliferation depends on the supply of exogenous cholesterol or other lipids and additionally proves that infected host cells may profit from different LDL variants, i. e. from modified and non-modified LDL.

Discussion

Apicomplexan parasites are generally considered as defective in cholesterol synthesis. Given that apicomplexan species are obligate intracellular parasites with highly proliferative capacities, this metabolic characteristic renders these pathogens as highly dependent on their respective host cells in terms of cholesterol supply. In principle, host cells support two major pathways of cholesterol resourcing: endogenous *de novo* synthesis and exogenous sterol uptake. Most reports indicate that different apicomplexan species may utilize diverse pathways of cholesterol acquisition in a species- or even host cell type-dependent manner.

The current data demonstrate that *B. besnoiti* uses both pathways of cholesterol acquisition when infecting bovine endothelial cells, which correspond to host cells to be infected during the acute phase of cattle besnoitiosis⁴⁵. This is in agreement to recent data on a slow proliferating apicomplexan species, *Eimeria bovis*^{37,38,39} but differs from findings on *T. gondii*³⁵. Since we here measured the cellular content of cholesterol biosynthetic precursors and metabolites via GC-MS-based approaches, the current data should directly reflect the actual biochemical situation in *B. besnoiti*-infected endothelial host cells. Sterol:cholesterol ratios of cholesterol biosynthetic precursors, which are generally accepted as reflecting the activity of the endogenous cholesterol biosynthetic pathway⁴⁶, showed a significant enhancement in *B. besnoiti*-infected host cells. Accordingly, an infection-driven increase of lanosterol-, dihydrolanosterol-, 7-dehydrocholesterol- and lanosterol-related ratios was detected. In line, a pivotal role of cholesterol *de novo* synthesis was also suggested for *E. bovis* or *T. gondii* infections^{37,38,40,41} and in case of *E. bovis* these data also relied on GC-MS-based analyses³⁷. These biochemical data were furthermore supported by a significant reduction of *B. besnoiti* proliferation triggered by statin treatments, which interfere with endogenous cholesterol synthesis. Statins represent a class of drugs widely used to lower plasma cholesterol levels⁴⁰. Statin treatments also proved effective in other apicomplexan-related infection systems, such as *T. gondii*-infected macrophages^{28,42}, *Plasmodium*- and *Babesia*-infected erythrocytes⁴³, *C. parvum*-infected epithelial cells³ or *E. bovis*-infected BUEVC³⁹. The current data revealed a higher efficacy of lovastatin, which interferes with the total cellular isoprenoid/sterol synthesis, when compared to zarogazole acid that directly targets sterol synthesis. Noteworthy, the blockage of merozoite production in other apicomplexan also depends on the choice of statin. As such, treatments with rosuvastatin and atorvastatin failed to influence parasite proliferation, whilst the application of lovastatin in higher concentrations (~72–96 μM) reduced tachyzoite production for more than 50% in *T. gondii*-infected macrophages⁴². Zarogazole acid is an inhibitor of squalene synthase and for this reason considered as more specific for cholesterol blockage than other statin treatments⁴⁴. In *B. besnoiti*-infected host cells, 60 μM zarogazole acid treatments resulted in a significant blockage of tachyzoites production (reduction of 48.8%) confirming that *B. besnoiti* replication depends on host cell *de novo* synthesis. In contrast to *E. bovis* with 70.2% reduction rate at 5 μM treatment³⁶, 15 μM zarogazole acid treatments in *C. parvum*-infected epithelial cells only induced moderate effects, as indicated by 25% growth delay³³. Comparable rates of reduction were described in *T. gondii*-infected macrophages with 1–10 μM zarogazole acid⁴². Squalene synthase-defective CHO cells revealed no significant anti-proliferative effects on *T. gondii* development compared to non-defective controls⁴⁷. However,

Besnoitia besnoiti infection alters both endogenous cholesterol *de novo* synthesis and exogenous LDL uptake in host endothelial cells

www.nature.com/scientificreports/

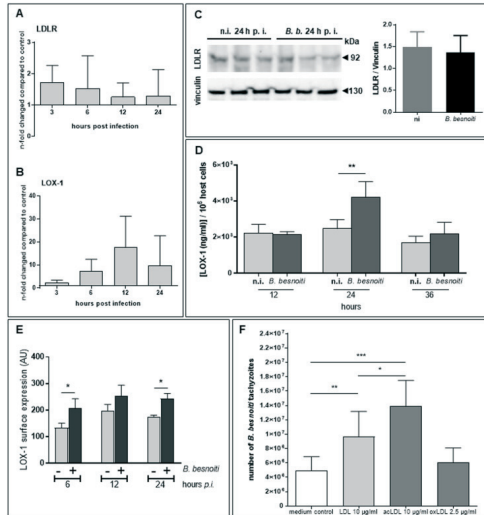


Figure 6. LDLR and LOX-1 gene transcription and protein expression in *B. besnoiti*-infected endothelial host cells and effects of LDL supplementation on parasite proliferation. (A, B) For estimation of LDLR and LOX-1 gene transcription during *B. besnoiti* replication *in vitro*, total RNA of infected and non-infected BUEC ($n = 3$) was extracted at different time points p. i., reverse transcribed and submitted to LDLR- and LOX-1-specific real-time qPCR. Data represent arithmetic means \pm standard deviation. (C) For analyses on protein expression of LDLR, *B. besnoiti*-infected and non-infected BUEC soluble protein fractions were isolated from cell pellets at 24 h p. i. and submitted to immunoblotting using LDLR-specific antibodies. The expression of vinculin in each sample was used for protein content normalization. Two different gels/blots from the same samples. (D, E) For analyses on protein expression of LOX-1, *B. besnoiti*-infected BUEC and non-infected controls were either analysed by a commercial test kit (LOX-1 bovine ELISA kit, DL Develop) (D) or subjected to flow cytometric analyses on LOX-1-related surface expression (E) by using LOX-specific antibodies. Bars represent arithmetic mean of three biological replicates \pm standard deviation ($*p < 0.05$; $**p < 0.01$; $***p < 0.001$). (F) For LDL supplementation experiments, non-modified LDL (LDL), acetylated LDL (acLDL) or oxidised LDL (oxLDL) were supplemented at indicated concentrations to *B. besnoiti*-infected and non-infected host cell cultures. The total number of *B. besnoiti* tachyzoites was determined at 48 h p. i. Arithmetic mean \pm standard deviation of three biological replicates ($*p < 0.05$, $**p < 0.01$, $***p < 0.001$).

other authors applied two quinacidine-based inhibitors of squalene synthase in *T. gondii*-infected epithelial cells and described anti-proliferative effects of both compounds achieving a similar percentage of reduction of tachyzoite replication as in *B. besnoiti*-infections (48–58% reduction) but with much lower doses of zaragozic acid (3 μ M)⁴⁶. Overall, the data on cholesterol biosynthetic precursors and inhibitor treatments indicate that successful *B. besnoiti* replication depends on the host cell cholesterol *de novo* synthesis. Nevertheless, the fact that replication is not entirely blocked by zaragozic acid treatment may argue for additional sources of cholesterol besides *de novo* synthesis.

As a general feature, sterol up-take from the extracellular compartment seems to be exploited by apicomplexan parasites in a species-specific and host cell-specific manner. Whilst this pathway appeared of major importance in the case of *T. gondii* in CHO cells¹⁷, *C. parvum* in epithelial cells¹³, *N. caninum* infections¹⁵ or *E. bovis*-infected endothelial cells²⁵, a minor or even absent role of LDL-mediated cholesterol supply was reported

Besnoitia besnoiti infection alters both endogenous cholesterol *de novo* synthesis and exogenous LDL uptake in host endothelial cells

www.nature.com/scientificreports/

for *T. gondii* infections in macrophages³⁵ or for *Plasmodium* spp. infections in hepatocytes³². In the case of *B. besnoiti* infections, the current data on LDL supplementation confirm a pivotal role of exogenous sterol uptake for parasite proliferation. For the first time, we here applied different LDL species (LDL, acLDL, oxLDL), which are present in blood or lymph and may therefore all serve as exogenous sources *in vivo*. Interestingly, the supplementation with both, acLDL and LDL, revealed as beneficial for *B. besnoiti* proliferation and boosted tachyzoite production. LDL supplementation was also beneficial for *T. gondii* proliferation in CHO cells¹⁷ whilst such a treatment had no stimulatory effects on hepatic *Plasmodium* spp. and *C. parvum* proliferation^{32,33} or on *T. gondii* growth in macrophages³⁵ indicating parasite- and cell type-specific mechanisms. However, to our best knowledge this signifies the first report on acLDL-mediated effects on intracellular apicomplexan proliferation.

In addition to LDL-related data, the direct exogenous supply of excess cholesterol or desmosterol also boosted *B. besnoiti* proliferation. This is in line with other data that proved this method of cholesterol supplementation as effective in the case of *T. gondii* in CHO cells¹⁷ or endothelial *E. bovis* infections²⁷. So far, it remains unclear why the supplementation of cholesterol via M3CD complexes failed to influence parasite proliferation which contrasts data of other studies⁶⁷. Referring to exogenous sterol supplementation, the current data on phytosterols measurements appear somewhat conflicting. Phytosterols signify cholesterol analogues that exclusively originate from plant dietary intake⁶⁸. In cell cultures, these molecules are derived from PCS present in the cell medium and an enhanced cellular content of plant sterols is commonly accepted as an indicator of cellular sterol uptake from the extracellular environment^{43,49}. However, current biochemical measurements data failed to show enhanced phytosterol:cholesterol ratios in *B. besnoiti*-infected BUVEC but even revealed slightly reduced values for stigmasterol and sitosterol. So far, we have no plausible explanation for these findings. While cell type-specific differences in individual phytosterol species uptake were reported, the capacity of BUVEC to incorporate all three phytosterols here detected was previously proven since a significant enhancement of sitosterol, stigmasterol and campesterol contents was reported in *E. bovis*-infected endothelial cells¹⁷.

Given that LDL species are internalized via a receptor-mediated uptake, we here furthermore analysed whether *B. besnoiti* infections influence the gene transcription and protein expression of two classical endothelial LDL-related receptors. In contrast to reports on *T. gondii* infections in CHO cells¹⁷ and *E. bovis* infections in BUVEC²⁷, LDLR expression was not altered by *B. besnoiti* infections. These data were in accordance to the fact that reduced LDLR expression did not affect the liver stage burden in the case of *Plasmodium* spp.³⁴. Contrary to LDLR, an infection-driven upregulation of the scavenger receptor LOX-1 was here found in *B. besnoiti*-infected BUVEC on both, gene transcriptional and protein expression level. Recent microarray data on *B. besnoiti*-infected BUVEC confirmed a significant upregulation of LOX-1 (Silva L.M.R., unpublished data). LOX-1 is considered as an important receptor for ox-LDL internalization in vascular endothelial cells⁴⁹⁻⁵¹ but is also able to bind acLDL at a comparable affinity⁵². This receptor was recently also reported to be upregulated in *E. bovis* infections of bovine endothelial cells^{27,53}. Given that in both cases of LOX-1 induction, endothelial host cells served as host cells may indicate a cell type-specific mechanism.

Excess cellular levels of free cholesterol demand for cholesterol efflux or conversion since too high concentrations are toxic for cells. Two main conversion routes in endothelial cells involve cholesterol esterification and oxidation. In the current study, a significantly enhanced level of esterified cholesterol was detected in *B. besnoiti*-infected cells when compared with non-infected controls. This corresponds to recent findings in *E. bovis*-infected BUVEC²⁷. In line, the key role of cholesterol esterification was here additionally confirmed by its chemical blockage via C1976 treatments leading to a significant inhibition of *B. besnoiti* replication. Thus, tachyzoite production was reduced by 64.7 and 82.9%, at 10- and 20- μ M treatments, respectively. These data are in agreement with reports on *T. gondii* and *E. bovis* documenting the essential role of cholesterol esterification for optimal parasite proliferation^{54,55}. Concerning relevant inhibitor concentrations, it has to be noted that antiproliferative effects occurred at a comparable level in *T. gondii* (merozoite reduction rates of approximately 60 and 70% induced by 4- and 10- μ M C1976 treatments) and *B. besnoiti* infections. Even stronger effects were reported for *E. bovis* infections since 5 μ M treatments almost entirely inhibited merozoite I production (99.6% reduction) as mirrored by a low IC₅₀ of 0.34 μ M⁵⁶. The higher sensitivity of *E. bovis* to C1976 treatments may be due to a stronger need for cholesteryl ester formation during macromeront formation (>120,000 merozoites I) when compared to non-macromeront-forming parasites. Interestingly, *T. gondii* appears to be able to synthesize and store cholesteryl esters by itself, if host cell cholesterol is available^{57,58}. In fact, two SOAT-like molecules were identified in *T. gondii* stages and proved sensitive to SOAT inhibitor treatments^{58,59}. So far, no data are available with this respect for *B. besnoiti*. Nevertheless, it remains to be elucidated whether C1976-driven, detrimental effects on *B. besnoiti* proliferation accounted only to the host cell compartment or were also brought about by direct antiparasitic effects, as in the case of *T. gondii*.

Cholesteryl esters play a pivotal role in the development of several apicomplexan parasites and cholesterol and fatty acids are needed for cholesteryl ester formation, though the effects of fatty acid synthase blockage was additionally here investigated. The synthetic α -methylene- γ -butyrolactone compound C75 inhibits fatty acid synthase activity and has been studied for its anti-inflammatory and anti-tumoral activities⁶⁰⁻⁶². C75 treatments induced a significant reduction of *B. besnoiti* replication at 20 μ M concentration. However, in the case of *E. bovis*, lower concentrations of C75 were needed for anti-proliferative effects indicating a high relevance of fatty acids for this parasite⁶⁰. Moreover, C75 inhibition was ineffective on *Trypanosoma cruzi* growth in infected macrophages⁶⁰.

The main storage organelles of cholesteryl esters are represented by lipid droplets. The key role of enhanced lipid droplet formation in infected host cells was reported for several protozoan parasites, such as *T. cruzi*, *T. gondii*, *P. berghei*, *P. falciparum* or *E. bovis*^{17,33,25-28} and was here confirmed for *B. besnoiti* infections. Thus, a significantly enhanced abundance of lipid droplets was found in *B. besnoiti*-infected BUVEC. The pivotal role of these organelles was additionally confirmed by the fact that an artificial increase of lipid droplet disposability via oleic acid treatments significantly boosted tachyzoite formation. Likewise, an oleic acid-driven boost of offspring

Besnoitia besnoiti infection alters both endogenous cholesterol *de novo* synthesis and exogenous LDL uptake in host endothelial cells

www.nature.com/scientificreports/

production was also observed in case of *E. bovis*, corroborating the assumption of lipid droplets mainly functioning as lipid storage and “feeder” organelles in *E. bovis* macronutrient formation⁷⁷.

Overall, *B. besnoiti* infections failed to trigger the synthesis of oxysterols in host endothelial cells. Interestingly, enzymatically synthesized side-chain oxysterols (e. g. 24-OHC, 25-OHC, 27-OHC), which are known as key regulators of cholesterol homeostasis and as effector molecules of cellular innate immunity^{59–63} were not affected by *B. besnoiti* infections. In contrast, *E. bovis* infections were recently proven to selectively upregulate the synthesis of 25-OHC, a molecule that was proven to bear antiparasitic properties⁶⁷. Moreover, a lack of 7 α -OHC, 7-keto-C and 7 α -OHC upregulation, which is generally mediated via autoxidative processes, revealed that BUVEC do not experience considerable oxidative cell stress triggered by *B. besnoiti* infections.

In summary, this investigation adds further data on the modulatory capacity of the fast proliferating apicomplexan parasite *B. besnoiti*. The current data strengthen the assumption that the modulation of distinct pathways of cholesterol acquisition is dependent on both, the parasite species and the host cell type. Thus, we here show that successful *B. besnoiti* infections in primary bovine endothelial host cells rely on both, endogenous cholesterol synthesis and on sterol uptake from exogenous sources by using different LDL species leading to selective LOX-1 upregulation.

Materials and Methods

Host cell culture. Primary bovine umbilical vein endothelial cells (BUVEC) were isolated from bovine umbilical cords as recently described⁶⁴. For cell cultures, BUVEC were resuspended in complete ECGM (PromoCell) in 75 cm² plastic tissue culture flasks (Greiner BioOne). After confluency, cells were split, plated in 25 cm² plastic tissue culture flasks (Greiner BioOne) and incubated at 37 °C and 5% CO₂ atmosphere. Medium was changed every 2–3 days using ECGM-medium supplemented with 70% medium 199 (ModECGM); 500 IU/ml penicillin (Sigma-Aldrich) and 50 µg/ml streptomycin (Sigma-Aldrich) and 10% FCS (Biocrom)⁶⁵. Only cells of low passages (1–3) were used for this study.

Parasites. *Besnoitia besnoiti* (strain Bb1Evora04) tachyzoites were maintained by serial passages in *Mycoplasma*-free BUVEC according to previous reports⁶¹. Confluent BUVEC monolayers in 25 cm² flasks were infected with freshly isolated *B. besnoiti* tachyzoites (MOI = 5:1). Free-released tachyzoites were collected from BUVEC culture supernatants, washed in ModECGM and pelleted (400 × g, 12 min). *B. besnoiti* tachyzoites were counted in a Neubauer chamber and used for BUVEC infection.

Cholesterol visualization and quantification. For staining intracellular stages for cholesterol, BUVEC were grown on coverslips ($n = 3$) and infected with *B. besnoiti* tachyzoites (MOI = 5:1). At 24 h p.i. (hours post infection), the samples were washed with PBS, fixed in 4% paraformaldehyde (10 min), washed three times with PBS. To detect free cholesterol, the samples were stained by filipin III (35 µg/ml in PBS, 15 min, in the dark, RT; Sigma-Aldrich). All samples were washed with PBS, mounted in Fluoromount-G mounting medium (Invitrogen). Cells were analysed using an inverted fluorescence microscope (IX81, Olympus) applying the UV filter set (340–380 nm excitation, 430 nm pass filter) and/or by using confocal microscopy analysis (Confocal LSM 710; Zeiss; 63X magnification, numerical aperture 1.2 µm). Single cells ($n = 20$) fluorescence intensity measurements were performed using ImageJ⁶⁶ (mean grey value) and expressed as mean ± standard deviation. Image processing was carried out with ImageJ using merged channels plugins and restricted to minor adjustment of brightness and contrast.

Total cholesterol quantification was performed according to previous studies⁶⁷. Therefore, total lipid extractions from *B. besnoiti*-infected (12, 24 and 48 h p.i.) and control BUVEC ($n = 6$) were executed in hexaneisopropanol⁶⁸. The cells were washed twice with ice-cold PBS, trypsinized, washed again (400 × g, 10 min) and total cell numbers were counted using a Neubauer chamber. Hexaneisopropanol (3:2, v/v) was added to the cell pellet. Cells were disrupted for 10 min in Tissue Lyser (Qiagen) using stainless steel beads. After centrifugation (8,000 × g, 1 min) the supernatants were collected. The extraction was repeated once for each sample. Combined supernatants were dried manually under liquid nitrogen stream. The total lipid extracts were reconstituted in 500 µL isopropanol:NP40 (9:1; all Roth) and sonicated in a water bath (RT, 30 min). 5 µL of each sample were pre-treated with catalase (5 µL of 0.5 mg/mL; Sigma-Aldrich) in 40 µL of 1X reaction buffer (37 °C, 15 min) in 96-well black clear-bottom plates (Greiner Bio-One) to reduce background fluorescence of peroxides in the solvents⁶⁷, before the enzyme cocktail of the Amplex Red Cholesterol Assay Kit (Life Technologies) was added. 50 µL of enzyme mixture (0.1 M potassium phosphate buffer, pH 7.4; 0.25 M NaCl, 5 mM cholic acid, 0.1% Triton X-100, 0.3 U/mL cholesterol oxidase, cholesterol esterase, 1.3 U/mL HRP, and 0.4 mM ADHP) were added and incubated at 37 °C for 15 min. Cholesterol standard (10, 5, 2.5, 1.25, 0.625 and 0.325 µM; Sigma-Aldrich) and blanks (solvent only) were included in every experiment. Resorufin formation was measured by fluorescence intensities (excitation wavelength of 530 nm, emission wavelength of 580 nm) in the Varioskan Flash Multimode Reader (Thermo Scientific). Total cholesterol of the samples was extrapolated to the values of the cholesterol standard and the total cholesterol content of each sample was normalized to its total cell number counts.

Lipid droplet and neutral lipid staining and quantification. For staining of intracellular stages (24 h p.i.), BUVEC were grown on coverslips and infected, whilst tachyzoite stages were directly dropped onto poly-L-lysine-coated coverslips. Specimens were washed in PBS, fixed in 4% paraformaldehyde (10 min, RT), washed three times in PBS and incubated in 1% glycine PBS (10 min, RT) to quench non-specific signals, followed by three washes in PBS. For neutral lipid and lipid droplet visualization, cells were stained with Nile Red (10 µg/ml; Sigma-Aldrich, 10 min, 37 °C, in the dark) or with Bodipy 493/503 (1 µg/ml; Life Technologies; 10 min, RT, in the dark), respectively. All samples were washed with PBS, mounted in Fluoromount-G mounting medium (Invitrogen) and analysed using an inverted fluorescence microscope (IX81, Olympus). Single cell ($n = 20$)

Besnoitia besnoiti infection alters both endogenous cholesterol *de novo* synthesis and exogenous LDL uptake in host endothelial cells

www.nature.com/scientificreports/

fluorescence intensity measurements were performed using ImageJ¹⁷ (mean grey value) and expressed as mean \pm standard deviation. Image processing was carried out with ImageJ using merged channels plugins and restricted to minor adjustment of brightness and contrast.

For neutral lipid quantification, infected BUVEC layers (MOI = 3:1) were stained with Nile Red. The mean fluorescence intensities per area of single infected ($n = 20$) and non-infected single cells ($n = 20$) were estimated applying identical experimental conditions using an inverted fluorescence microscope (IX81, Olympus). Fluorescence intensity measurements were performed using ImageJ¹⁷ (mean grey value) and expressed as mean \pm standard deviation. For lipid droplet quantification, *B. besnoiti*-infected (MOI = 3:1 and 4:1) and control BUVEC ($n = 3$) were trypsinized at 12 and 24 h p. i. and pelleted ($400 \times g$, 3 min, 4°C). Resuspended cells were stained with Bodipy 493/503 (10 min, on ice) and washed twice with 1 ml PBS ($400 \times g$, 3 min, 4°C). The cells were transferred to 5-ml FACS tubes (BD Biosciences) containing 200 μ l PBS and were processed in a FACS Calibur flow cytometer (BD Biosciences) by laser excitation at 488 nm (FL1-H channel). Flow cytometry data were acquired by the BD Cell Quest Pro software as previously reported (Hamid *et al.*²³).

Cholesterol and LDL supplementation experiments. For exogenous cholesterol supplementation, cholesterol and desmosterol (both Sigma-Aldrich) dissolved in ethanol¹⁸ were added to BUVEC cultures ($n = 3$) at 5 μ M final concentration at the time point of *B. besnoiti* infection. Additionally, cholesterol enrichment was performed by supplementation of cholesterol-M β CD (Chol-M β CD; Sigma-Aldrich)-complexes in basal medium (PromoCell) lacking FCS (Chol-M β CD; 0.3 mM, 30 min, 24 h and 60 min prior infection). For the preparation of Chol-M β CD complexes (stock solution 10 mM), cholesterol was dissolved in M β CD water solution (40 mg/ml) at 30°C, overnight, with constant agitation.

For LDL enrichment, non-modified LDL (Sigma-Aldrich, 10 mg/ml final concentration), acetylated LDL (acLDL; Life Technologies, 10 mg/ml final concentration) and oxidized LDL (oxLDL; Life Technologies, 2.5 mg/ml final concentration) were supplemented 24 h before *B. besnoiti* infection and ongoing until the end of the experiments.

To estimate the effect of supplementations on parasite proliferation, tachyzoite numbers were estimated 48 h p. i. by quantitative PCR.

Lipid droplet enrichment. To artificially enhance lipid droplet formation in host cells, oleic acid (OA; Sigma-Aldrich) was supplemented in BSA formulation complexes to the cell culture medium according to Martin and Parton⁶⁸. Direct conjugation was performed by mixing oleic acid-free BSA (fraction V, Roth) with oleic acid at the molar ratio of 6:1 (oleic acid:BSA). Prior to infection, an induction step was performed with culture medium supplemented with 50 μ M OA (1 h, 37°C, 5% CO₂). Parasites were allowed to infect BUVEC in non-supplemented cell culture medium for 4 h. Then, medium was changed and OA was supplemented in a final concentration of 2.5 μ M.

PCR-based quantification of *B. besnoiti* tachyzoites. Tachyzoite numbers were estimated via a quantitative PCR according to Cortes, *et al.*⁶⁹. Therefore, biological triplicates with technical duplicates were processed. Firstly, cell culture supernatants containing free-released tachyzoites (= extracellular tachyzoites) were collected at 48 h p. i. and pelleted ($600 \times g$, 15 min). In addition, the remaining host cells carrying not yet released tachyzoites (= intracellular tachyzoites) were trypsinized and pelleted ($600 \times g$, 15 min). All cell/parasite pellets were treated with 200 μ l of cell lysis buffer containing 0.32 M sucrose, 1% Triton X-100, 0.01 M Tris-HCl (pH 7.5), 5 mM MgCl₂ and incubated in 100 μ l IX PCR buffer (Quanta) containing 20 μ l proteinase K (20 mg/ml; Qiagen) at 56°C for 1 h. Proteinase K was heat-inactivated by heating the samples (95°C, 10 min) and the DNA-containing samples were frozen at -20°C until further use. Real-time PCR was performed in a total volume of 20 μ l containing 2 μ l DNA of test samples, 400 nM of each primer, 200 nM probe and 10 μ l Perfecta MasterMix (Quanta) at the following cycling conditions: 95°C for 10 min; 40 cycles at 95°C for 10 s, 60°C for 15 s and 72°C for 30 s.

Biochemical estimation of cholesterol esterification and of cholesterol-related sterols. Pellets of *B. besnoiti*-infected BUVEC and of non-infected control cells were dried in a Savant SpeedVac concentrator (Thermo Fisher Scientific) for 24 h. Cholesterol, non-cholesterol sterols and oxysterols were extracted from dry weight aliquots using Folch reagent (chloroform/methanol; 2:1 (v/v)); with 0.25 mg BHT added per ml solvent) per 10 mg dried cell pellets. Extraction was performed for 12 h at 4°C in a dark cold room. The extracts were kept at -20°C until further use. One mL of the Folch was submitted to alkaline hydrolysis, extraction of the free sterols and oxysterols, silylation to their corresponding (di)trimethylsilyl ethers prior to gas chromatographic separation and detection by mass selective detection (for non-cholesterol sterols or oxysterols using epicoprostanol and the corresponding deuterium labelled oxysterols as internal standards, respectively) as described in detail previously^{70,71}. The degree of esterification of cholesterol was calculated from total (alkaline hydrolysis) and free cholesterol (without alkaline hydrolysis) concentrations using D6-cholesterol as internal standard.

Inhibitor treatments. For inhibitor treatments, blockers of cholesterol esterification (CI976, Sigma-Aldrich), of fatty acid synthase (C75, Sigma-Aldrich) and of HMC-CoA reductase (lovastatin, Sigma-Aldrich) were used at concentrations of 2.5, 5, 10 and 20 μ M⁷². Additionally, zaragozic acid (inhibitor of squalene synthase) was used at 15, 30 and 60 μ M concentration. Viability assays were performed with non-infected BUVEC ($n = 3$) for all inhibitors in all mentioned concentrations for 72 h (CYQUANT XTT Cell Viability Assay, Invitrogen; Supplementary Fig. 3), according to manufacture instructions. For blocking experiments, BUVEC ($n = 3$) were grown to 80% confluency. Inhibitors were supplemented to the cell culture medium 24 h prior to parasite infection and from 4 h p. i. ongoing. For *B. besnoiti* infections, the medium was removed, BUVEC were washed once with PBS and tachyzoites were added to the cells (MOI = 4:1) in inhibitor-free medium. Four h p. i. the medium was removed and replaced by inhibitor-supplemented medium. 48 h after

Besnoitia besnoiti infection alters both endogenous cholesterol de novo synthesis and exogenous LDL uptake in host endothelial cells

www.nature.com/scientificreports/

Symbol	Name	Accession number	Amplifem length	Forward (5'→3')	Reverse (3'→5')	Probe (reporter 5'-3'quencher)
ACAT1	Acetyl-CoA acetyl-transferase 1	NM_001046075.1	102	TCATATGGGCACTGTGCTGA	CTGCTTACTCTTGGTATAG	FAM-AGCATAAATGATCTGTCTCTCTGGT-BHQ1
ACAT2	Acetyl-CoA acetyl-transferase 2	NM_001075484.1	194	AGCAGTGGTCTTATGAA	AGGCTCATTTGATTTCAAA	FAM-ATCAAGATCTCCAGGAGCA-BHQ1
CH25H	Cholesterol 25-hydroxylase	NM_001075243.1	87	TTGGGTGTCTTTGACATG	CAGCAGATGTTGACAAC	FAM-GGTCTTGGCTCCAGTGTG-BHQ1
HMGCS	3-hydroxy-3-methylglutaryl-CoA synthase 1	NM_001006578	197	CTACTCAAGTCATTAGA	CTCTGTCTGTGGTATTAA	HEX-AMGATTCACAGCAACCCAGGAC-BHQ1
HMGCR	3-hydroxy-3-methylglutaryl-CoA reductase	NM_001105613.1	109	GGCATCAACTGGATGAG	CCTCAATCATGGCTCTG	FAM-TCTTGGACAACTTGGCTGGAAT-BHQ1
LDLR	Low density lipoprotein receptor	NM_001166550.1	96	CGCTACCTCTCTCTTAC	ACCACGTTCTTAAGGTG	FAM-TGGCTTGGCTCCAGTGTG-BHQ1
OLR1	Oxidized low density lipoprotein (lectin like) receptor 1	NM_1174133.2	102	CGCTACCTCTCTCTTAC	ACCACGTTCTTAAGGTG	TEF-TGGCTTGGCTCCAGTGTG-BHQ1
SQLE	Squalene epoxidase	NM_001098061.1	132	CCCTTCTTCAACAGTAA	CCCTTCAGCAATTTCTG	HEX-AMGACAGTATCTTCCAGCAGATA-BHQ1
GAPDH	Glyceraldehyde-3-phosphate dehydrogenase	AF_022183	82	GGGACACTCACTCTACCTTGA	TGTATACAGGAAATGAGCTTAC	FAM-CTGGCATTGGCTCAACGACACTT-BHQ1

Table 2. Sequences of primers and probes used in real-time qPCR.

infection, the numbers of tachyzoites being present in cell culture supernatants were counted in a Neubauer counting chamber. Non-treated (medium only) and solvent (DMSO, acetone or ethanol)-treated, *B. besnoiti*-infected BUVEC were equally processed and served as negative controls.

RT-qPCR for the relative quantification of LDLR and LOX-1 mRNAs. BUVEC ($n = 3$) grown in 25 cm² culture tissue flasks were infected with freshly isolated *B. besnoiti* tachyzoites (MOI = 5:1). *B. besnoiti*-infected and control BUVEC were equally processed for total RNA isolation at different time points of parasite proliferation (3, 6, 12, 24 h p. i.). For total RNA isolation, the RNeasy kit (Qiagen) was used according to manufacturer's instructions. Therefore, BUVEC were lysed within the cell culture flasks with RLT lysis buffer (600 μ l/25 cm² flask) and processed as proposed by the manufacturer including an on-column DNase treatment. Total RNAs were stored at -20°C until further use. The quality of total RNA samples was controlled on 1% agarose gels. In order to remove any genomic DNA leftover, a second DNA digestion step was performed. Therefore, 1 μ g of total RNA was treated with 10 U DNase I (Thermo Scientific) in 1x DNase reaction buffer (37 $^{\circ}\text{C}$, 1 h). DNase was inactivated by heating the samples (65 $^{\circ}\text{C}$, 10 min). The efficiency of genomic DNA digestion was verified by including no-RT-controls in each RT-qPCR experiment. cDNA synthesis was performed using the SuperScript III First-Strand Synthesis System (Thermo Fisher Scientific) according to manufacturer's instructions with slight modifications. 1 μ g of DNase-treated total RNA was added to 0.5 μ l of 50 μM oligo d(T), 1 μ l of 50 ng/ μ l random hexamer primer, 1 μ l of 10 mM dNTP mix and DEPC-treated water was adjusted to 10 μ l total volume. The samples were incubated at 65 $^{\circ}\text{C}$ for 5 min and then immediately cooled on ice. For first strand cDNA synthesis, 2 μ l of 10x RT buffer, 4 μ l 25 mM MgCl₂, 2 μ l 0.1 M DTT, 1 μ l RNaseOUT (40 U/ μ l, Thermo Fisher Scientific), 0.5 μ l SuperScript III enzyme (200 U/ μ l) and 0.5 μ l DEPC-treated water were added and the samples were incubated at 25 $^{\circ}\text{C}$ for 10 min followed by 50 $^{\circ}\text{C}$ for 60 min and a 85 $^{\circ}\text{C}$ -inactivation step for 15 min.

Primers (MWG Biotech) and probes used for qPCR are shown in Table 2³⁷. Probes were labelled at the 5'-end with a reporter dye FAM (6-carboxyfluorescein) and at the 3'-end with the quencher dye TAMRA (6-carboxytetramethyl-rhodamine). qPCR amplification was performed on a Rotor-Gene Q Thermocycler (Qiagen) in duplicates in a 10 μ l total volume containing 400 nM forward and reverse primers, 200 nM probe, 10 ng cDNA and 5 μ l 2x PerfeCTa qPCR FastMix (Quanta Biosciences). The reaction conditions for all systems were as follows: 95 $^{\circ}\text{C}$ for 10 min, 40 cycles at 95 $^{\circ}\text{C}$ for 10 s, 60 $^{\circ}\text{C}$ for 15 s and 72 $^{\circ}\text{C}$ for 30 s. No-template controls (NTC) and no-RT reactions were included in each experiment. As reference gene GAPDH was used as previously reported^{27,65,71}. Analyses of the qPCR data used the comparative $\Delta\Delta C_T$ method⁴³ and reported as n-fold differences comparing *B. besnoiti*-infected BUVEC with non-infected controls after normalizing the samples by the GAPDH reference gene.

Protein extraction. For protein extraction, *B. besnoiti*-infected and non-infected BUVEC isolates ($n = 3$) were washed in PBS to remove any medium traces, trypsinized and pelleted (600 \times g, 10 min). Proteins were extracted by homogenizing the cell pellets in RIPA buffer [50 mM Tris-HCl, pH 7.4; 1% NP-40; 0.5% Na-deoxycholate; 0.1% SDS; 150 mM NaCl; 2 mM EDTA; 50 mM NaF (all Roth)] in the presence of a protease inhibitor cocktail (Sigma-Aldrich). The homogenates were centrifuged at 10,000 \times g for 10 min at 4 $^{\circ}\text{C}$ to sediment intact cells and nuclei. The supernatants were stored at -80°C until further use. The protein content was quantified via Coomassie Plus (Bradford) Assay Kit (Thermo Scientific) following the manufacturer instructions.

SDS-PAGE and Western Blotting. The samples were denatured using 6 M urea loading buffer and heated for 5 min at 95 $^{\circ}\text{C}$. Fifty μ g of total protein were loaded per slot and run in 12% polyacrylamide gels (120 V, 1.5 h)⁷². After electrophoretic separation, the proteins were transferred to a polyvinylidene difluoride (PVDF) membrane (Millipore) (200 mA, 2 h). Blots were blocked with 3% BSA in TBS containing 0.1% Tween (Sigma) for 1 h at RT and then incubated overnight in primary antibody solutions (see Table 3). Vinculin expression was used as a reference for the normalization of the samples. After washing in TBS containing 0.1% Tween (thrice,

Besnoitia besnoiti infection alters both endogenous cholesterol *de novo* synthesis and exogenous LDL uptake in host endothelial cells

www.nature.com/scientificreports/

	Antibody	Company	Cat number	Isotype	Dilution
Primary antibodies	Vinculin	Santa Cruz	sc-73614	Mouse	1:1,000
	ACAT-1	Sigma-Aldrich	AV54278	Rabbit	1:100
	ACAT-2	Abcam	ab66259	Rabbit	1:250
	CH25H	Abcam	ab133933	Rabbit	1:250
	LDLR	Santa Cruz	Sc-18823	Mouse	1:500
Secondary antibodies	Goat anti-mouse IgG Peroxidase conjugated	Pierce	31430	Mouse	1:40,000
	Goat anti-rabbit IgG Peroxidase conjugated	Pierce	31460	Rabbit	1:40,000

Table 3. List of antibodies used for Western blot and surface expression assays.

5 min), blots were incubated in secondary antibody solutions (30 min, RT). Signal development was accomplished with an enhanced chemiluminescence detection system (ECL plus kit, GE Healthcare) and signal strength was determined in a ChemoCam Imager (Intas Science Imaging). Protein sizes were controlled by a protein ladder (PageRuler Plus Prestained Protein Ladder ~10–250 kDa, Thermo Fisher Scientific).

Quantification of LDLR and LOX-1 expression. The surface expression of LDLR and LOX-1 was estimated in infected and non-infected BUVEC applying a flow cytometry-based technique according to Hamid *et al.*²⁷. Therefore, BUVEC were infected with *B. besnoiti* tachyzoites (MOI 5:1). One day before infection, the cells were cultured in medium with lipoprotein-deficient serum (LPDS, 10%, Sigma-Aldrich). For measurements, medium was removed and cells were detached using accutase (Sigma-Aldrich) treatment (37°C, 5 min) after a washing with PBS. Cells were pelleted (400 × g, 5 min, 4°C) and incubated in anti-LDLR monoclonal (1:25, RT, 1 h; Antibody Online, ABIN235770) or anti-LOX-1 polyclonal (1:500, RT, 1 h Bioss Antibodies, bs-2044R) antibody solutions. After centrifugation (400 × g, 5 min, 4°C), the cells were washed twice in PBS/0.01% NaN₃ and incubated in secondary antibody solutions (1:40,000, 30 min, in the dark; Table 2). Secondary antibody controls were included in each experiment for signal normalization. After incubation, cells were washed thrice (400 × g, 5 min, 4°C), resuspended in 100 μL PBS, transferred to 5 mL-FACS tubes (Greiner Bio-One) containing 200 μL of 1× PBS and processed in a FACSCallibur™ flow cytometer (Becton-Dickinson, Heidelberg, Germany; FL1-H channel [red]). Data were acquired using the Cell Quest Pro (Becton-Dickinson) software.

Additionally, the expression of LOX-1 in *B. besnoiti*-infected BUVEC and non-infected control cells was determined by a commercially available bovine ELISA kit (DL-Develop). Therefore, BUVEC ($n = 3$) were grown to subconfluency in 75 cm² cell culture flasks (Greiner) and infected at an MOI of 5:1 with freshly collected *B. besnoiti* tachyzoites. Cells were harvested at different time points *p. i.* (12, 24, 36 h *p. i.*) according to manufacturer's instructions. Briefly, after washing with PBS, the cells were trypsinized and pelleted (400 × g, 12 min). Cell pellets were washed thrice with PBS and the number of cells per sample was determined microscopically before ultrasonication treatment (3 times for 20 s, on ice). Samples were centrifuged at 1,000 × g (15 min, 2–8°C) to remove cell debris and the supernatants were stored at –20°C until being processed by the ELISA kit.

Live cell 3D holotomographic microscopy. BUVEC ($n = 3$) were seeded into 35 mm tissue culture μ-dishes (Ibidi®), grown overnight and infected with freshly released *B. besnoiti* tachyzoites (MOI 3:1). At 24 h *p. i.*, holotomographic images were obtained by using 3D cell-explorer microscope (Nanolive 3D) equipped with a 60× magnification ($\lambda = 520$ nm, sample exposure 0.2 mW/mm²) and a depth of field of 30 μm³. For lipid droplet visualization, cells were stained with Bodipy 493/503 (1 μg/mL, Life Technologies; 3h, 37°C, in the dark). After incubation, medium was changed. Live cell 3D holotomographic microscopy and analysis of Bodipy 493/503-based fluorescence was performed in parallel to prove the identity of lipid droplets. A total of 50 lipid droplets were measured for their refractive index to obtain marker values for these organelles in BUVEC. Images were analysed using STEVE software (Nanolive) to obtain a refractive index-based z-stack²⁷ and digital staining was applied according to the refractive index of the lipid droplets.

Statistical analysis. Statistical analyses were performed with the statistical program package BMDP[®] or with GraphPad Prism. In all cases, data revealed as normally or log-normally distributed (verified by residual analysis) and parametric statistical methods could be applied. Data description was performed by presenting arithmetic mean ± standard deviation for not log-transformed data, by geometric mean and standard deviation for log-transformed data or as *n*-fold changes relative to the controls. Depending on the design of the experiment, some data were analysed by one- or two-way analysis of variance (ANOVA) with repeated measures (program BMDP2V) to test the effects of infection and/or incubation time, dose of the inhibitor or cell ratio. If only one time point was considered, the analysis could be reduced to a *t*-test for dependent samples (program BMDP3D). In the case of a hierarchical design of the experiments incorporating more than one random factor (e. g. BUVEC and replication) a general mixed model analysis (glmM) with equal sample size (program BMDP8V) was applied. Occasionally, post hoc pairwise comparison tests succeeded the global comparison by ANOVA, being performed either by Student-Newman-Keuls method (SNK-test) or by Bonferroni-Holm method controlling the family-wise error rate, or even by *t*-test. The outcomes of the statistical tests were considered to indicate significant differences when $p \leq 0.05$ (significance level).

Besnoitia besnoiti infection alters both endogenous cholesterol *de novo* synthesis and exogenous LDL uptake in host endothelial cells

www.nature.com/scientificreports/

Data Availability

All data generated or analysed during this study are included in this published article (and its Supplementary Information Files).

References

1. Cortes, H., Letao, A., Gottstein, B. & Hemphill, A. A review on bovine besnoitiosis: a disease with economic impact in herd health management, caused by *Besnoitia besnoiti* (Franco and Borges). *Parasitology* **141**, 1406–1417, <https://doi.org/10.1017/S002185961000262> (2014).
2. Alvarez-Garcia, G., Frey, C. F., Mora, L. M. & Schares, G. A century of bovine besnoitiosis: an unknown disease re-emerging in Europe. *Trends Parasitol.* **29**, 407–415, <https://doi.org/10.1016/j.pt.2013.06.002> (2013).
3. Cortes, H. *et al.* Besnoitiosis in bulls in Portugal. *Vet. Rec.* **157**, 262–264 (2005).
4. Fernandez-Garcia, A. *et al.* First isolation of *Besnoitia besnoiti* from a chronically infected cow in Spain. *J. Parasitol.* **95**, 474–476, <https://doi.org/10.1645/GE-1772.1> (2009).
5. Schares, G. *et al.* First *in vitro* isolation of *Besnoitia besnoiti* from chronically infected cattle in Germany. *Vet. Parasitol.* **163**, 315–322, <https://doi.org/10.1016/j.vepar.2009.04.009> (2009).
6. Golnick, N. S., Gentile, A. & Schares, G. Diagnosis of bovine besnoitiosis in a bull born in Italy. *Vet. Rec.* **166**, 599, <https://doi.org/10.1136/vr.e2314> (2010).
7. Gentile, A. *et al.* Evidence for bovine besnoitiosis being endemic in Italy—first *in vitro* isolation of *Besnoitia besnoiti* from cattle born in Italy. *Vet. Parasitol.* **184**, 108–115, <https://doi.org/10.1016/j.vepar.2011.09.014> (2012).
8. Basso, W. *et al.* Bovine besnoitiosis in Switzerland: imported cases and local transmission. *Vet. Parasitol.* **198**, 265–273, <https://doi.org/10.1016/j.vepar.2013.09.013> (2013).
9. Hornok, S., Fedak, A., Baska, F., Hofmann-Lehmann, R. & Basso, W. Bovine besnoitiosis emerging in Central-Eastern Europe, Hungary. *Parasit. Vectors* **7**, 20, <https://doi.org/10.1186/1756-3305-7-20> (2014).
10. Ryan, E. G. *et al.* Bovine besnoitiosis (*Besnoitia besnoiti*) in an Irish dairy herd. *Vet. Rec.* **178**, 608, <https://doi.org/10.1136/vr.103683> (2016).
11. Vanhoult, A. *et al.* First confirmed case of bovine besnoitiosis in an imported bull in Belgium. *Vlaams Diergen. Tijds.* **84**, 205–211 (2015).
12. EFSA. Bovine Besnoitiosis: An emerging disease in Europe. *EFSA J.* **8** (2010).
13. Shkap, V., Bin, H., Lebovich, B. & Pipano, E. *Besnoitia besnoiti*: quantitative *in vitro* studies. *Vet. Parasitol.* **39**, 207–213 (1991).
14. Cortes, H. *et al.* Isolation of *Besnoitia besnoiti* from infected cattle in Portugal. *Vet. Parasitol.* **141**, 226–233, <https://doi.org/10.1016/j.vepar.2006.05.022> (2006).
15. Muñoz-Caro, T., Hermosilla, C., Silva, L. M. R., Cortes, H. & Taubert, A. Neutrophil extracellular traps as innate immune reaction against the emerging apicomplexan parasite *Besnoitia besnoiti*. *PLoS One* **9**, e91415, <https://doi.org/10.1371/journal.pone.0091415> (2014).
16. Samish, M., Shkap, V., Bin, H. & Pipano, E. M. Cultivation of *Besnoitia besnoiti* in four tick cell lines. *Int. J. Parasitol.* **18**, 291–296 (1988).
17. Coppens, I., Sinal, A. P. & Joiner, K. A. *Toxoplasma gondii* exploits host low-density lipoprotein receptor-mediated endocytosis for cholesterol acquisition. *J. Cell Biol.* **149**, 167–180 (2000).
18. Rodriguez-Acosta, A. *et al.* Liver ultrastructural pathology in mice infected with *Plasmodium berghei*. *J. Submicrosc. Cytol. Pathol.* **30**, 299–307 (1998).
19. Sonda, S. *et al.* Cholesterol esterification by host and parasite is essential for optimal proliferation of *Toxoplasma gondii*. *J. Biol. Chem.* **276**, 34434–34440, <https://doi.org/10.1074/jbc.M10525200> (2001).
20. Melo, R. C., Pávoia, H., Fabrino, D. L., Almeida, P. E. & Bozza, P. T. Macrophage lipid body induction by Chagas disease *in vivo*: putative intracellular domains for eicosanoid formation during infection. *Tissue Cell* **35**, 59–67 (2003).
21. Jackson, K. E. *et al.* Food vacuole-associated lipid bodies and heterogeneous lipid environments in the malaria parasite, *Plasmodium falciparum*. *Mol. Microbiol.* **54**, 109–122, <https://doi.org/10.1111/j.1365-2958.2004.04284.x> (2004).
22. Vielmeyer, C., McIntosh, M. T., Joiner, K. A. & Coppens, I. Neutral lipid synthesis and storage in the intraerythrocytic stages of *Plasmodium falciparum*. *Mol. Biochem. Parasitol.* **135**, 197–209, <https://doi.org/10.1016/j.molbiopara.2003.08.017> (2004).
23. Coppens, I. Contribution of host lipids to *Toxoplasma* pathogenesis. *Cell Microbiol.* **8**, 1–9, <https://doi.org/10.1111/1462-5822.2005.00647.x> (2006).
24. Coppens, I. *et al.* *Toxoplasma gondii* sequesters lysosomes from mammalian hosts in the vacuolar space. *Cell* **125**, 261–274, <https://doi.org/10.1016/j.cell.2006.01.056> (2006).
25. Coppens, I. & Vielmeyer, C. Insights into unique physiological features of neutral lipids in Apicomplexa: from storage to potential mediation in parasite metabolic activities. *Int. J. Parasitol.* **35**, 597–615, <https://doi.org/10.1016/j.ijpara.2005.01.009> (2005).
26. Gomes, A. F. *et al.* *Toxoplasma gondii*-skeletal muscle cells interaction increases lipid droplet biogenesis and positively modulates the production of IL-12, IFN- γ and PGE2. *Parasit. Vectors* **7**, 47, <https://doi.org/10.1186/1756-3305-7-47> (2014).
27. Hamid, P. H. *et al.* *Eimeria bovis* infection modulates endothelial host cell cholesterol metabolism for successful replication. *Vet. Res.* **46**, 100, <https://doi.org/10.1186/s13567-015-0239-z> (2015).
28. Nishikawa, Y. *et al.* Host cell lipids control cholesteryl ester synthesis and storage in intracellular *Toxoplasma*. *Cell Microbiol.* **7**, 849–867, <https://doi.org/10.1111/j.1462-5822.2005.00518.x> (2005).
29. Furlong, S. T. Sterols of parasite protozoa and helminths. *Exp. Parasitol.* **68**, 482–485 (1989).
30. Banal, D., Bhatti, H. S. & Sehgal, R. Role of cholesterol in parasitic infections. *Lipids Health Dis.* **4**, 10, <https://doi.org/10.1186/1476-511x-4-10> (2005).
31. Bano, N., Romano, J. D., Jayabalasingham, B. & Coppens, I. Cellular interactions of *Toxoplasma* liver stage with its host mammalian cell. *Int. J. Parasitol.* **37**, 1329–1341, <https://doi.org/10.1016/j.ijpara.2007.04.005> (2007).
32. Labatied, M. *et al.* *Plasmodium* salvages cholesterol internalized by LDL and synthesized *de novo* in the liver. *Cell Microbiol.* **13**, 569–586, <https://doi.org/10.1111/j.1462-5822.2010.01555.x> (2011).
33. Ehrenman, K., Wanyiri, J. W., Bhat, N., Ward, H. D. & Coppens, I. *Cryptosporidium parvum* scavenges LDL-derived cholesterol and micellar cholesterol internalized into enterocytes. *Cell Microbiol.* **15**, 1182–1197, <https://doi.org/10.1111/cmi.12107> (2013).
34. Nolan, S. J., Romano, J. D., Luechtefeld, T. & Coppens, I. *Neospora caninum* recruits host cell structures to its parasitophorous vacuole and salvages lipids from organelles. *Eukaryot. Cell* **14**, 454–473, <https://doi.org/10.1128/ec.00262-14> (2015).
35. Nishikawa, Y. *et al.* Host cholesterol synthesis contributes to growth of intracellular *Toxoplasma gondii* in macrophages. *J. Vet. Med. Sci.* **73**, 633–639 (2011).
36. Hamid, P. H., Hirschmann, J., Hermosilla, C. & Taubert, A. Differential inhibition of host cell cholesterol *de novo* biosynthesis and processing abrogates *Eimeria bovis* intracellular development. *Parasitol. Res.* **113**, 4165–4176, <https://doi.org/10.1007/s00436-014-0992-5> (2014).
37. Schneider, C. A., Rasband, W. S. & Eliceiri, K. W. NIH Image to ImageJ: 25 years of image analysis. *Nat. Methods* **9**, 671–675, <https://doi.org/10.1038/nmeth.2089> (2012).
38. Xu, F. *et al.* Dual roles for cholesterol in mammalian cells. *Proc. Natl. Acad. Sci. USA* **102**, 14551–14556, <https://doi.org/10.1073/pnas.0503390102> (2005).
39. Zidovetki, R. & Levitan, I. Use of cyclodextrins to manipulate plasma membrane cholesterol content: evidence, misconceptions and control strategies. *Biochim. Biophys. Acta* **1768**, 1311–1324, <https://doi.org/10.1016/j.bbamem.2007.03.026> (2007).

Besnoitia besnoiti infection alters both endogenous cholesterol *de novo* synthesis and exogenous LDL uptake in host endothelial cells

www.nature.com/scientificreports/

40. Braubauer, A. & Ballantyne, C. M. Pharmacological strategies for lowering LDL cholesterol: statins and beyond. *Nat. Rev. Cardiol.* **8**, 253–265, <https://doi.org/10.1038/nrcardio.2011.2> (2011).
41. Muñoz-Caro, T., Silva, L. M., Ritter, C., Taubert, A. & Hermosilla, C. *Besnoitia besnoiti* tachyzoites induce monocyte extracellular trap formation. *Parasitol. Res.* **113**, 4189–4197, <https://doi.org/10.1007/s00436-014-4094-3> (2014).
42. Ökölönen, V. M., Gylling, H. & Kesäniemi, E. Plant sterols, cholesterol precursors and oxysterols: Minute concentrations—Major physiological effects. *J. Steroid Biochem. Mol. Biol.* **169**, 4–9, <https://doi.org/10.1016/j.jsbmb.2015.12.026> (2017).
43. Cortez, E., Stumbo, A. C., Oliveira, M., Barbosa, H. S. & Carvalho, L. Statins inhibit *Toxoplasma gondii* multiplication in macrophages *in vitro*. *Int. J. Antimicrob. Agents* **33**, 185–186, <https://doi.org/10.1016/j.ijantimicag.2008.07.036> (2009).
44. Grellet, P., Valentin, A., Milleroux, V., Schrevel, J. & Rigomer, D. 3-Hydroxy-3-methylglutaryl coenzyme A reductase inhibitors lovastatin and simvastatin inhibit *in vitro* development of *Plasmodium falciparum* and *Babesia divergens* in human erythrocytes. *Antimicrob. Agents Chemother.* **38**, 1144–1148 (1994).
45. Lindsey, S. & Harwood, H. J. Jr. Inhibition of mammalian squalene synthetase activity by zaragoic acid A is a result of competitive inhibition followed by mechanism-based irreversible inactivation. *J. Biol. Chem.* **270**, 9083–9096 (1995).
46. Martins-Duarte, E. S., Urbina, J. A., de Souza, W. & Vommaro, R. C. Antiproliferative activities of two novel quinacridine inhibitors against *Toxoplasma gondii* tachyzoites *in vitro*. *J. Antimicrob. Chemother.* **58**, 59–65, <https://doi.org/10.1093/jac/dk1180> (2006).
47. Pucadyil, T. J., Tewary, P., Madhubala, R. & Chatteropadhyay, A. Cholesterol is required for *Leishmania donovani* infection: implications in leishmaniasis. *Mol. Biochem. Parasitol.* **133**, 145–152 (2004).
48. Lütjohann, D. Methodological aspects of plant sterol and stanol measurement. *J. AOAC Int.* **98**, 674–676, <https://doi.org/10.1093/jaoac/98.3.674> (2015).
49. Sawamura, T. et al. An endothelial receptor for oxidized low-density lipoprotein. *Nature* **386**, 73–77, <https://doi.org/10.1038/386073a0> (1997).
50. Moriawaki, H. et al. Ligand specificity of LOX-1, a novel endothelial receptor for oxidized low density lipoprotein. *Arterioscler. Thromb. Vasc. Biol.* **18**, 1541–1547 (1998).
51. Kume, N. et al. Inducible expression of lectin-like oxidized LDL receptor-1 in vascular endothelial cells. *Circ. Res.* **83**, 322–327 (1998).
52. Kumano-Kuramochi, M. et al. Identification of 4-hydroxy-2-nonenal-histidine adducts that serve as ligands for human lectin-like oxidized LDL receptor-1. *Biochem. J.* **442**, 171–180, <https://doi.org/10.1042/bj011029> (2012).
53. Taubert, A. et al. Microarray-based transcriptional profiling of *Eimeria bovis*-infected bovine endothelial host cells. *Vet. Res.* **41**, 70, <https://doi.org/10.1051/veter/2010041> (2010).
54. Lige, B., Sampedro, V. & Coppens, J. Characterization of a second sterol-esterifying enzyme in *Toxoplasma* highlights the importance of cholesterol storage pathways for the parasite. *Mol. Microbiol.* **87**, 951–967, <https://doi.org/10.1111/mmi.12142> (2013).
55. Kuhajda, F. P. et al. Synthesis and antitumor activity of an inhibitor of fatty acid synthase. *Proc. Natl. Acad. Sci. USA* **97**, 3450–3454, <https://doi.org/10.1073/pnas.05082897> (2000).
56. Flavin, R., Pelluso, S., Nguyen, P. L. & Loda, M. Fatty acid synthase as a potential therapeutic target in cancer. *Future Oncol.* **6**, 551–562, <https://doi.org/10.2217/foc.10.11> (2010).
57. Matsuo, S., Yang, W. L., Aziz, M., Kameoka, S. & Wang, P. Fatty acid synthase inhibitor c75 ameliorates experimental colitis. *Mol. Med.* **20**, 1–9, <https://doi.org/10.2119/molmed.2013.00113> (2014).
58. D'Avella, H. et al. Host cell lipid bodies triggered by *Trypanosoma cruzi* infection and enhanced by the uptake of apoptotic cells are associated with prostaglandin E2 generation and increased parasite growth. *J. Infect. Dis.* **204**, 951–961, <https://doi.org/10.1093/infdis/jir432> (2011).
59. Gill, S., Chow, R. & Brown, A. J. Sterol regulators of cholesterol homeostasis and beyond: the oxysterol hypothesis revisited and revised. *Prog. Lipid Res.* **47**, 391–404, <https://doi.org/10.1016/j.plipres.2008.04.002> (2008).
60. Olsen, B. N., Schlesinger, P. H., Ory, D. S. & Baker, N. A. 25-Hydroxycholesterol increases the availability of cholesterol in phospholipid membranes. *Biophys. J.* **100**, 948–956, <https://doi.org/10.1016/j.bpj.2010.12.3728> (2011).
61. Olsen, B. N., Schlesinger, P. H., Ory, D. S. & Baker, N. A. Side-chain oxysterols from cells to membranes to molecules. *Biochim. Biophys. Acta* **1818**, 330–336, <https://doi.org/10.1016/j.bbamem.2011.06.014> (2012).
62. Belska, A. A., Schlesinger, P., Covey, D. F. & Ory, D. S. Oxysterols as non-genomic regulators of cholesterol homeostasis. *Trends Endocrinol. Metab.* **23**, 99–106, <https://doi.org/10.1016/j.tem.2011.12.002> (2012).
63. Lembo, D., Cagno, V., Cirra, A. & Pali, G. Oxysterols: An emerging class of broad spectrum antiviral effectors. *Mol. Aspects Med.* **49**, 23–30, <https://doi.org/10.1016/j.mam.2016.04.003> (2016).
64. Taubert, A. et al. Metabolic signatures of *Besnoitia besnoiti*-infected endothelial host cells and blockage of key metabolic pathways indicate high glycolytic and glutamolytic needs of the parasite. *Parasitol. Res.* **115**, 2023–2034, <https://doi.org/10.1007/s00436-016-4948-0> (2016).
65. Taubert, A., Zahner, H. & Hermosilla, C. Dynamics of transcription of immunomodulatory genes in endothelial cells infected with different coccidian parasites. *Vet. Parasitol.* **142**, 214–222, <https://doi.org/10.1016/j.vetpar.2006.07.021> (2006).
66. Hara, A. & Radin, N. S. Lipid extraction of tissues with a low-toxicity solvent. *Anal. Biochem.* **90**, 420–426 (1978).
67. Robinet, P., Wang, Z., Hazen, S. L. & Smith, J. D. A simple and sensitive enzymatic method for cholesterol quantification in macrophages and foam cells. *J. Lipid Res.* **51**, 3364–3369, <https://doi.org/10.1194/jlr.D007336> (2010).
68. Martin, S. & Parton, R. G. Characterization of Rab18, a lipid droplet-associated small GTPase. *Methods Enzymol.* **438**, 109–129, [https://doi.org/10.1016/B0076-6879\(07\)38008-7](https://doi.org/10.1016/B0076-6879(07)38008-7) (2008).
69. Cortes, H. C. et al. Application of conventional and real-time fluorescent ITS1 rDNA PCR for detection of *Besnoitia besnoiti* infections in bovine skin biopsies. *Vet. Parasitol.* **146**, 352–356, <https://doi.org/10.1016/j.vetpar.2007.03.003> (2007).
70. Lütjohann, D. et al. Profile of cholesterol-related sterols in aged amyloid precursor protein transgenic mouse brain. *J. Lipid Res.* **43**, 1078–1085 (2002).
71. Mackay, D. S., Jones, P. J., Myrrie, S. B., Plat, J. & Lütjohann, D. Methodological considerations for the harmonization of non-cholesterol sterol bio-analysis. *J. Chromatogr. B Analyt. Technol. Biomed. Life Sci.* **957**, 116–122, <https://doi.org/10.1016/j.jchromb.2014.02.052> (2014).
72. Nübel, T., Damm, J., Roos, W. P., Kaina, B. & Fritz, G. Lovastatin protects human endothelial cells from killing by ionizing radiation without impairing induction and repair of DNA double-strand breaks. *Clin. Cancer Res.* **12**, 933–939, <https://doi.org/10.1158/1078-0432.ccr-05-1903> (2006).
73. Hermosilla, C., Zahner, H. & Taubert, A. *Eimeria bovis* modulates adhesion molecule gene transcription in and PMN adhesion to infected bovine endothelial cells. *Int. J. Parasitol.* **36**, 423–431, <https://doi.org/10.1016/j.ijpara.2006.01.003> (2006).
74. Livak, K. J. & Schmittgen, T. D. Analysis of relative gene expression data using real-time quantitative PCR and the 2⁻(Delta Delta C_T) Method. *Methods* **25**, 402–408, <https://doi.org/10.1006/meth.2001.1262> (2001).
75. Nagel, K. et al. The development of an off-therapy breast cancer questionnaire and protocol for survivors of childhood cancer. *J. Pediatr. Oncol. Nurs.* **19**, 22–23, <https://doi.org/10.1053/j.pon.2002.12.076> (2002).
76. Gattfield, J. et al. The selective active metabolite ACT-333679 displays strong anti-contraction and anti-remodeling effects, but low β-arrestin recruitment and desensitization potential. *J. Pharmacol. Exp. Ther.* <https://doi.org/10.1124/jpet.116.239665> (2017).
77. Sandoz, P. A. et al. Label free 3D analysis of organelles in living cells by refractive index shows pre-mitotic organelle spinning in mammalian stem cells. *BioRxiv*, <https://doi.org/10.1101/407239> (2018).
78. Dixon, W. J. *BMDP Statistical Software Manual*. Vol. 1 and 2 (University of California Press, 1993).

Besnoitia besnoiti infection alters both endogenous cholesterol *de novo* synthesis and exogenous LDL uptake in host endothelial cells

www.nature.com/scientificreports/

Acknowledgements

The authors thank the outstanding work of B. Hofmann and Dr. C. Ritter in all cell culture experiments, C. Henrich for technical support and G. Lochnit (Institute of Biochemistry, Faculty of Medicine, Justus Liebig University) for his help in Amplex Red-based total cholesterol measurements. We also acknowledge A. Wehrend (Clinic for Obstetrics, Gynecology and Andrology of Large and Small Animals, Justus Liebig University, Giessen, Germany) for the continuous supply of bovine umbilical cords.

Author Contributions


A.T., D.L., L.S. and P.H. conceived and designed the experiments. L.S., D.L., P.H., Z.D.V., C.L., K.K. and A.T. performed the experiments. L.S., D.L., K.F., Z.D.V., C.H. and A.T. performed analyses and interpretation of the data. L.S., A.T., C.H. and Z.D.V. prepared the manuscript. All authors revised and approved the final version of the manuscript.

Additional Information

Supplementary information accompanies this paper at <https://doi.org/10.1038/s41598-019-43153-2>.

Competing Interests: The authors declare no competing interests.

Publisher's note: Springer Nature remains neutral with regard to jurisdictional claims in published maps and institutional affiliations.

 **Open Access** This article is licensed under a Creative Commons Attribution 4.0 International License, which permits use, sharing, adaptation, distribution and reproduction in any medium or format, as long as you give appropriate credit to the original author(s) and the source, provide a link to the Creative Commons license, and indicate if changes were made. The images or other third party material in this article are included in the article's Creative Commons license, unless indicated otherwise in a credit line to the material. If material is not included in the article's Creative Commons license and your intended use is not permitted by statutory regulation or exceeds the permitted use, you will need to obtain permission directly from the copyright holder. To view a copy of this license, visit <http://creativecommons.org/licenses/by/4.0/>.

© The Author(s) 2019

2.2. MODULATION OF CHOLESTEROL-RELATED STEROLS DURING EIMERIA BOVIS MACROMERONT FORMATION AND IMPACT OF SELECTED OXYSTEROLS ON PARASITE DEVELOPMENT

Taubert, A., Silva, L.M.R., Velásquez, Z.D., Larrazabal, C., Lütjohann, D., and Hermosilla, C. (2018).

Mol Biochem Parasitol 223, 1–12; doi: 10.1016/j.molbiopara.2018.06.002

Own part in the publication:

- Project planning: 30 %, Together with co-authors and supervisors
- Development of experiments: 40 %, Together with co-authors
- Evaluation of experiments: 20 %, Together with co-authors
- Writing of the manuscript: 10 %, Together with co-authors

Modulation of cholesterol-related sterols during *Eimeria bovis* macromeront formation and impact of selected oxysterols on parasite development

Molecular & Biochemical Parasitology 223 (2018) 1–12



Contents lists available at ScienceDirect

Molecular & Biochemical Parasitology

journal homepage: www.elsevier.com/locate/molbiopara



Modulation of cholesterol-related sterols during *Eimeria bovis* macromeront formation and impact of selected oxysterols on parasite development



A. Taubert^{a,*}, L.M.R. Silva^a, Z.D. Velásquez^a, C. Larrazabal^a, D. Lütjohann^b, C. Hermosilla^b

^a Institute of Parasitology, Biomedical Research Center Selmersberg, Justus Liebig University Giessen, Schubertstr. 81, 35392 Giessen, Germany

^b Institute of Clinical Chemistry and Clinical Pharmacology, University Clinics of Bonn, Sigmund-Freud-Str. 25, 53127 Bonn, Germany

ARTICLE INFO

Keywords:

Cholesterol metabolism
Apicomplexan parasites
Coccidia
Endogenous cholesterol biosynthesis
Oxysterols
Phytosterols

ABSTRACT

Obligate intracellular apicomplexan parasites are considered as deficient in cholesterol biosynthesis and scavenge cholesterol from their host cell in a parasite-specific manner. Compared to fast proliferating apicomplexan species producing low numbers of merozoites per host cell, (e.g. *Toxoplasma gondii*), the macromeront-forming protozoa *Eimeria bovis* is in extraordinary need for cholesterol for offspring production ($\geq 170,000$ merozoites / macromeront). Interestingly, optimized *in vitro E. bovis* merozoite I production occurs under low foetal calf serum (FCS, 1.2%) supplementation. To analyze the impact of extensive *E. bovis* proliferation on host cellular sterol metabolism we here compared the sterol profiles of *E. bovis*-infected primary endothelial host cells grown under optimized (1.2% FCS) and non-optimized (10% FCS) cell culture conditions. Therefore, several sterols indicating endogenous *de novo* cholesterol synthesis, cholesterol conversion and sterol uptake (phytosterols) were analyzed via GC-MS-based approaches. Overall, significantly enhanced levels of phytosterols were detected in both FCS conditions indicating infection-triggered sterol uptake from extracellular sources as a major pathway of sterol acquisition. Interestingly, a simultaneous induction of endogenous cholesterol synthesis based on increased levels of distinct cholesterol precursors was only observed in case of optimized parasite proliferation indicating a parasite proliferation-dependent effect. Considering side-chain oxysterols, 25 hydroxycholesterol levels were selectively found increased in *E. bovis*-infected host cells, while 24 hydroxycholesterol and 27 hydroxycholesterol contents were not significantly altered by infection. Exogenous treatments with 25 hydroxycholesterol, 27 hydroxycholesterol, and 7 ketocholesterol revealed significant adverse effects on *E. bovis* intracellular development. Thus, the number and size of developing macromeronts and merozoite I production was significantly reduced indicating that these oxysterols bear direct or indirect antiparasitic properties. Overall, the current data indicate parasite-driven changes in the host cellular sterol profile reflecting the huge demand of *E. bovis* for cholesterol during macromeront formation and its versatility in the acquisition of cholesterol sources.

1. Introduction

Apicomplexan parasites represent an important group of protozoan pathogens that strictly develop and proliferate intracellularly and affect both, humans and animals. During specific phases of their asexual replication, apicomplexan species differ significantly in their developmental behavior, since some replicate fast (mainly within 24–48 h) and produce rather low numbers of merozoites (e.g. *Toxoplasma gondii*: 32–64 tachyzoites) whilst others undergo a slow proliferation process over several weeks but end up with the production of > 1000-fold offspring specimen compared to fast proliferative species. In this context, the pathogenic species *Eimeria bovis*, which causes cattle coccidiosis worldwide, represents one of the most prolific apicomplexan

parasites since it may produce more than 170,000 merozoites I per macromeront during first merogony. Corresponding life cycles with macromeront formation in host endothelial cells are also known for other pathogenic ruminant *Eimeria* species, such as *E. zuernii*, *E. ninkokohyakimovae*, *E. arloingi*, *E. christensenii*, *E. camelii*, *E. dromedarii* and *E. bakuensis*.

Considering the broad spectrum of apicomplexan parasites, transitional characteristics apply for several species. For their intracellular replication, these parasites are in need for energy and building blocks and, especially during multiplication process, they have a high demand for cholesterol for offspring membrane synthesis. Correspondingly, enhanced total cholesterol contents were demonstrated for *E. bovis*-infected endothelial host cells [1]. However, apicomplexan parasites are

* Corresponding author.

E-mail addresses: Anja.Taubert@vetmed.uni-giessen.de (A. Taubert), Liliana.Silva@vetmed.uni-giessen.de (L.M.R. Silva), Zahady.Velasquez@vetmed.uni-giessen.de (Z.D. Velásquez), Camilo.Larrazabal@vetmed.uni-giessen.de (C. Larrazabal), Dieter.Luetjohann@ukbonn.de (D. Lütjohann), Carlos.R.Hermosilla@vetmed.uni-giessen.de (C. Hermosilla).

<https://doi.org/10.1016/j.molbiopara.2018.06.002>

Received 29 March 2018; Received in revised form 12 June 2018; Accepted 12 June 2018
Available online 15 June 2018
0166-6851/ © 2018 Elsevier B.V. All rights reserved.

Modulation of cholesterol-related sterols during *Eimeria bovis* macromeront formation and impact of selected oxysterols on parasite development

A. Tauber et al.

Molecular & Biochemical Parasitology 223 (2018) 1–12

generally considered as defective for *de novo* cholesterol synthesis and need to scavenge cholesterol from their host cells as already shown for several species, such as *T. gondii*, *Neospora caninum*, *Cryptosporidium parvum*, *E. bovis* or *Plasmodium* spp. [1–6]. To provide intracellular parasites with sufficient cholesterol, the host cell may either enhance its endogenous *de novo* synthesis or upregulate LDL-mediated cholesterol uptake from extracellular sources. So far, several reports indicate that cholesterol acquisition occurs in a parasite-specific or even host cell type-specific manner. Thus, *T. gondii* scavenges cholesterol via enhanced LDL-uptake but not via induction of *de novo* synthesis in CHO cells [2] whilst the LDL trafficking pathway was not subverted in *T. gondii*-infected macrophages [7]. The closely related parasite *N. caninum* mainly relies on lipoprotein uptake [5] and in *C. parvum*-infected intestinal epithelial cells cholesterol requirements were mainly fulfilled via infection-induced LDL uptake but an additional, although modest, contribution of endogenous cholesterol synthesis was also observed since treatments with squalenstatin diminished parasite proliferation [3]. *Plasmodium* spp. in principle utilizes both pathways of cholesterol acquisition in hepatic stages, but none of these appeared essential for successful parasite replication [5]. So far, only a few data are available on slowly developing but highly proliferative apicomplexan species. In this context, *E. bovis* is one of the top candidates since it exhibits an enormous replicative capacity during first merogony and resides for up to a month within its endothelial host cell for development *in vivo*. In contrast to *T. gondii* as fast proliferating parasite triggering either pathway [2,7], *E. bovis* appears to exploit both cellular pathways of cholesterol acquisition at a time, since several molecules being associated with the endogenous *de novo* biosynthesis pathway and of LDL-mediated cholesterol uptake were simultaneously found upregulated on a transcriptional level in infected endothelial host cells [1,8]. In addition, inhibitor treatments interfering with key molecules of endogenous cholesterol synthesis confirmed the pivotal role of this acquisition mode in *E. bovis*-infected cells and significantly blocked parasite proliferation [9]. Simultaneously, an enhanced LDL uptake via increased LDL receptor surface abundance was shown for *E. bovis*-infected endothelial host cells and excess LDL supply boosted parasite proliferation [1].

Since too high free cholesterol concentrations are toxic for mammalian cells [10], excess cholesterol entails an enhanced need for biochemical conversion of these molecules in apicomplexan-infected host cells. Consequently, cholesterol molecules are either recycled to the membranes or converted, e. g. by oxysterol formation or cholesterol esterification. Consequently, increased cholesterol esterification activities were detected in *T. gondii*-infected cells [11] and gene transcripts of sterol O-acyltransferase 1 (SOAT1) promoting cholesterol esterification were found significantly enhanced in *E. bovis*-infected host cells [1]. Furthermore, biochemical blockage of cholesterol esterification or the absence of cholesterol esterifying enzymes led to diminished parasite proliferation proving the pivotal role of cholesterol conversion for optimal apicomplexan parasite development [9,11]. Since cholesteryl esters are generally stored in cellular lipid droplets, enhanced levels of these organelles were consistently reported in different apicomplexan-infected host cells [1,2,11–18]. Referring to oxysterol formation, first indications on enhanced activities were given on a transcriptional level in *E. bovis*-infected endothelial cells since the mRNA abundance of cholesterol 25 hydroxylase promoting 25 hydroxycholesterol synthesis was found increased in infected host cells [1,8]. Interestingly, 25 hydroxycholesterol is considered as a major antiviral molecule in several virus infections [19], but also has cholesterol-homeostatic and cell signaling properties [20,21]. However, no detailed 25 hydroxycholesterol-related data are available on apicomplexan infections, so far.

The aim of the current study was to analyze the host cellular profile of diverse cholesterol-related sterols in *E. bovis*-infected primary bovine endothelial host cells at both, parasite proliferation-boosting conditions and suboptimal conditions to directly mirror the actual metabolic situation. Current data confirm an infection-triggered enhancement of

cholesterol conversion and of host cellular sterol uptake from exogenous sources. Additionally, a proliferation-dependent effect of *E. bovis* infections on endogenous host cellular cholesterol synthesis was observed. These data strengthen the hypothesis that *E. bovis* has an extraordinary need for cholesterol for successful parasite replication and that this parasite indeed differs significantly in its metabolic actions and requirements from fast proliferating apicomplexan parasites.

2. Material and methods

2.1. Parasites

Current *E. bovis* strain H was initially isolated from the field in Northern Germany and since then maintained by passages in parasite-free male Holstein Friesian calves. All animal procedures were performed according to the Justus Liebig University (JLU) Giessen Animal Care Committee guidelines, approved by the Ethic Commission for Experimental Animal Studies of the State of Hesse (Regierungspräsidium Giessen, GI 18/10 No A37/2011, JLU-No. 494) and are in accordance to the current German Animal Protection Laws.

For oocysts production, calves were orally infected at an age of 8 weeks with 3×10^4 sporulated *E. bovis* oocysts. The oocysts were isolated from the faeces beginning 18 days p. i. according to Jackson [22]. Oocyst sporulation was achieved by incubation in a 2% (w/v) potassium dichromate (Merck) solution at room temperature (RT) with a constant influx of O_2 via an aquarium pumping system. Sporulated oocysts were stored in 2% (w/v) potassium dichromate solution at 4 °C until further use (but for a maximum of 12 months). For sporozoite excystation, the oocysts were suspended in sterile 0.02 M L-cysteine HCl/0.2 M NaHCO₃ solution and incubated for 20 h in a 100% CO₂ atmosphere at 37 °C. Then oocysts were pelleted (600 x g, 15 min, 20 °C) and resuspended in Hank's balanced salt solution (HBSS; Gibco) containing 0.04% (w/v) trypsin (Sigma-Aldrich) and 8% (v/v) sterile filtered (0.2 µm filter; Sarstedt) bovine bile obtained from the local abattoir. The oocysts were incubated for up to 4 h (37 °C, 5% CO₂ atmosphere) under microscopic control. Free sporozoites were washed twice in cell culture medium, (M199; Sigma-Aldrich), passed through a 10 µm pore-size filter (pluriStrainer, PluriSelect, Life Science) and counted in a Neubauer chamber. For primary bovine umbilical vein endothelial cell (BUVEC) infection, the sporozoites were resuspended in cell culture medium. For sterol analyses sporozoites were pelleted (10×10^6 /per sample, 850 x g, 5 min), frozen in liquid nitrogen and stored at -80 °C until further use.

2.2. Host cells and *E. bovis* host cell infections

Primary bovine endothelial cells (BUVEC) were isolated according to Jaffe et al. [23]. Therefore, umbilical cords were collected under aseptic conditions from animals born by *sectio caesaria* and kept at 4 °C in 0.9% HBSS-HEPES buffer (pH 7.4, Gibco) supplemented with 1% penicillin (500 U/ml, Sigma-Aldrich) and streptomycin (50 µg/ml, Sigma-Aldrich) until use. For the isolation of endothelial cells, 0.025% collagenase type II (Worthington Biochemical Corporation) suspended in Pucks solution (Gibco) was infused into the lumen of the ligated umbilical vein and incubated for 20 min at 37 °C in 5% CO₂ atmosphere. After gently massaging the umbilical vein, the cell suspension was collected in cell culture medium and supplemented with 1 ml fetal calf serum (FCS, Gibco) in order to inactivate the collagenase type II. After two washings (350 x g, 12 min, 20 °C), cells were resuspended in complete endothelial cell growth medium (EGCM, PromoCell, supplemented with 10% FCS), plated in 25 cm² tissue plastic culture flasks (Greiner) and kept at 37 °C in 5% CO₂ atmosphere. BUVEC were cultured in modified EGCM medium (EGCM, PromoCell, diluted at 30% in M199 medium and supplemented with 10% FCS, 1% penicillin and streptomycin (both Sigma-Aldrich) with medium changes every 2–3 days. BUVEC cell layers were used for infection after 1–2 passages in

Modulation of cholesterol-related sterols during *Eimeria bovis* macromeront formation and impact of selected oxysterols on parasite development

A. Taubert et al.

Molecular & Biochemical Parasitology 223 (2018) 1–12

in vitro. In case of reduced FCS conditions, the cells were cultured in modified ECGM medium being supplemented with 1.2% FCS from days -2 p. i. onwards.

For comparative analyses on merozoite I production, BUVEC were cultured in 25 cm²-flask formats under 1.2, 1.8 and 10% FCS conditions, infected by 5×10^9 *E. bovis* sporozoites/flask and analyzed for merozoite I production at day 20 p. i. by counting the parasite stages present in the supernatants using a Neubauer chamber.

For comparative GC-MS-based sterol analyses, BUVEC layers (three biological replicates with four technical replicates, each) were grown in 75 cm²-flask formats, supplemented with either 10% or 1.2% FCS and infected at 80–90% confluency with 1.5×10^9 *E. bovis* sporozoites/flask. The culture medium was changed 24 h after parasite infection and thereafter every third day. For cell harvesting at day 14 p. i., the monolayers were treated with trypsin (Serva) buffer for cell detachment. Then, the cells were washed twice in PBS (350 × g, 12 min, 20 °C), resuspended in PBS, counted in a Neubauer chamber and aliquoted (10⁷ cells/sample). The cell pellets were immediately frozen in liquid nitrogen and thereafter stored at -80 °C until further use.

2.3. Oxysterol treatments of *E. bovis* sporozoites and *E. bovis*-infected host cells

In preliminary experiments, adverse effects of 25 hydroxycholesterol, 27 hydroxycholesterol or 7 ketocholesterol on BUVEC proliferation or vitality were controlled via XTT tests. Overall, 5 μM concentration of all three oxysterols revealed as non-cytotoxic and was chosen for exogenous BUVEC treatments. Thus, 25 hydroxycholesterol, 27 hydroxycholesterol or 7 ketocholesterol (all Cayman Chemical Company) were exogenously supplied to *E. bovis*-infected BUVEC cultures (12-well formats; biological triplicates, technical duplicates) in two experimental settings: i) beginning with one day p. i. (= soon after sporozoite invasion) or ii) beginning with 10 days p. i. (= onset of parasite proliferation). Solvent (ethanol)-treated cultures served as controls. In general, BUVEC monolayers were always controlled microscopically during inhibition experiments for adverse effects and only confluent monolayers were included in the experiments. As read-out parameters for oxysterol effects on parasite development, the number and size of macromeronts were estimated microscopically using the CellSens software (Olympus) at days 15 and 19 p. i., respectively. Additionally, merozoite I production was quantified at 24 days p. i. via MIC-4-based qPCR. Therefore, the BUVEC layer was detached via trypsin treatment and pelleted together with the respective supernatant (12 min, 350 × g). After washing twice with PBS (850 × g, 5 min), DNA from cell pellets was isolated by a commercial kit (DNeasy Blood and Tissue kit, Qiagen) and subjected to MIC-4-based qPCR.

In addition, freshly excysted sporozoites were pre-treated with 25 hydroxycholesterol, 27 hydroxycholesterol, 7 ketocholesterol (all 5 μM) or solvent (ethanol) for 60 min at 37 °C and thereafter used for BUVEC infection. In the case of 25 hydroxycholesterol, time- (pre-incubation for 1, 2 and 3 h) and concentration-dependent (5 and 10 μM) pre-treatments were performed as mentioned above.

2.4. *E. bovis* microneme protein 4 (MIC-4)-based qPCR for merozoite I quantification

DNA from *E. bovis*-infected cell cultures (24 days p. i.) was subjected to *E. bovis*-specific MIC-4-based qPCR for merozoite I quantification. Real-time PCR was performed in a 20 μl total volume containing 0.8 μl (10 μM) Eb-MIC4 forward (5'-3' CACAGAAAGCAAAAAGACA) and reverse (5'-3' GACCATTCTCCAAATTC) primers each, 0.4 μl (10 μM) probe (reporter 5'-3' quencher: FAM-CGCACTCAGTCTTCCTCC-BHQ1), 5 μl DNA, 3 μl H₂O dest. and 10 μl 2x PerfeCTa qPCR FastMix (Quanta Biosciences, USA). The reaction conditions were as follows: 95 °C for 10 min, 40 cycles at 95 °C for 10 s, 60 °C for 15 s and 72 °C for 30 s. PCRs were performed on a Rotor-Gene Q cycler (Qiagen, Hilden,

Germany). The PCR data were extrapolated to standard curves using DNA from known numbers of merozoites I.

2.5. SDS-PAGE and immunoblotting

For protein extraction, *E. bovis*-infected and non-infected BUVEC isolates ($n = 3$) were washed in PBS to remove any medium traces, trypsinized and pelleted (350 × g, 12 min). Proteins were extracted by homogenizing the cell pellets in RIPA buffer (50 mM Tris-HCl, pH 7.4; 1% NP-40; 0.5% Na-deoxycholate; 0.1% SDS; 150 mM NaCl; 2 mM EDTA; 50 mM NaF, all Roth) in the presence of a protease inhibitor cocktail (Sigma-Aldrich). The homogenates were centrifuged at 10,000 × g for 10 min at 4 °C to sediment intact cells and nuclei. The protein content was quantified via Coomassie Plus (Bradford) Assay Kit (Thermo Scientific) following the manufacturer's instructions. For immunoblotting, samples were supplemented with 6 M urea. After boiling (95 °C) for 5 min, 50 μg of total protein were loaded per slot on 12% polyacrylamide gels (120 V, 1.5 h). The proteins were then transferred to polyvinylidene difluoride (PVDF) membranes (Millipore). Blots were blocked with 3% BSA in TBS containing 0.1% Tween (blocking solution; Sigma-Aldrich) for 1 h at RT and then incubated (overnight at 4 °C) in the primary antibodies diluted in blocking solution. The detection of vinculin was used as a loading control for the normalization of the samples (sc-73614). For cholesterol 25 hydroxylase detection, we used a specific rabbit polyclonal antibody raised against an internal region of the CH25H protein (sc-135228). As secondary antibodies, goat anti-mouse IgG and goat anti-rabbit IgG (both peroxidase-conjugated, Pierce, order No. 31,430 and 31460, respectively) were used and incubated for 30 min at RT. Detection was accomplished with an enhanced chemiluminescence detection system (ECL plus kit, GE Healthcare) and signal development was determined in a ChemoCam Imager (Intas Science Imaging). Protein sizes were controlled by a protein ladder (PageRuler[®] Plus Prestained Protein Ladder - 10–250 kDa, Thermo Fisher Scientific). Band intensity quantification was analyzed using Fiji Gel Analyzer plugin.

2.6. Quantification of cholesterol-related sterols and of cholesterol esterification in *E. bovis*-infected BUVEC

At day 14 p. i., *E. bovis*-infected and non-infected control cells (three biological replicates and four technical replicates, each) were analyzed for the absolute content of plant sterols (campesterol, stigmasterol and sitosterol), cholesterol precursors (lathosterol, lanosterol, dihydrolanosterol, desmosterol, and 7-dehydrocholesterol) and oxidative metabolites, i.e. oxysterols (24-, 25-, 27-, 7α-, 7β- and 4β-hydroxycholesterol and 7 ketocholesterol). Therefore, cell pellets were dried in a SavantTM SpeedVacTM concentrator (Thermo Fisher Scientific, Schwerte, Germany) for 24 h. All lipids containing free and esterified cholesterol, non-cholesterol sterols (plant sterols and cholesterol precursors) and oxysterols were extracted from dry weight aliquots using Folch reagent (chloroform/methanol; 2:1 (v/v); with 0.25 mg BHT added per ml. solvent) per 10 mg dried cell pellets. Extraction was performed for 12 h at 4 °C in a dark cold room. The extracts were kept at -20 °C until analysis. One ml of the Folch extract was subjected to alkaline hydrolysis in order to deconjugate esterified non-cholesterol sterols and oxysterols. As described in detail previously [24,25], free sterols and oxysterols were then extracted and silylation to their corresponding (di)trimethylsilyl ethers was performed. Thereafter, gas chromatographic separation and detection by mass selective detection (for non-cholesterol sterols or oxysterols using epicoprostanol and the corresponding deuterium labelled oxysterols as internal standards, respectively) was conducted. The degree of esterification of cholesterol was calculated from total (after alkaline hydrolysis) and free cholesterol (without alkaline hydrolysis) concentrations using D6-cholesterol as internal standard.

Modulation of cholesterol-related sterols during *Eimeria bovis* macromeront formation and impact of selected oxysterols on parasite development

A. Taubert et al.

Molecular & Biochemical Parasitology 223 (2018) 1–12

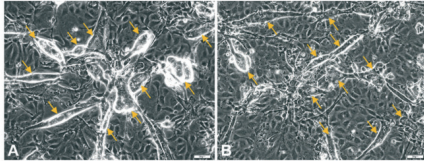
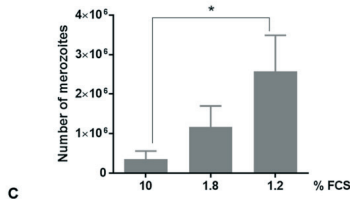


Fig. 1. FCS-dependent *E. bovis* merozoite I production in bovine host endothelial cells.

Bovine umbilical vein endothelial cells (BUVEC, $n = 3$) were cultured in cell culture medium containing 1.2%, 1.8% or 10% FCS and infected with vital *E. bovis* sporozoites [exemplary illustrations of infected BUVEC layers at day 17 p. i., cultured under 1.2% (A) or 10% FCS (B); macromeronts are indicated by arrows]. At 20 days p. i., the number of merozoite I was estimated in each culture condition (C). * = $p \leq 0.05$.



2.7. Statistics

The results are illustrated as mean \pm STD for at least three independent experiments. One-way analyses of variance (ANOVA) with Bartlett's or Tukey's test were performed using GraphPad Prism 7 software with a significance level of 5%. For the analysis of cholesterol precursors, oxysterols and esterified cholesterol data, two-tailed *t*-test were used comparing the control vs. infected cells. The following indications of significance were used in the figures: **** = $p \leq 0.0001$, *** = $p \leq 0.001$, ** = $p \leq 0.01$, * = $p \leq 0.05$.

3. Results

3.1. FCS-dependent *E. bovis* proliferation and infection-induced alteration of extracellular sterol-uptake, endogenous cholesterol synthesis and cholesterol conversion

FCS-dependent *E. bovis* culture confirmed that low FCS conditions were beneficial for *E. bovis* development and boosted merozoite I production without affecting cell layer integrity (Fig. 1A, B). Thus, only confluent BUVEC layers were included in the current experiments. Overall, macromeronts being cultured at low (1.2%) FCS conditions had a slightly larger and especially thicker appearance (Fig. 1A) than the more flat ones present at high (10%) FCS conditions (Fig. 1B). Consistently, a significantly higher number of *E. bovis* merozoites I were produced when using 1.2% FCS-supplemented cell culture medium compared to 10% FCS (1.2% vs. 10%: 7.4-fold enhancement; $p = 0.0111$) (Fig. 1C). Consequently, analyses on *E. bovis*-related sterol profiles were conducted under these two different FCS conditions to shed light on actual *E. bovis* requirements in the case of optimal growth conditions. It has to be stated that this study does not aim to distinguish between parasite- and host cell-derived metabolic actions but to consider the infected host cell as a biological unit. It seems obvious that the newly formed, intracellular merozoite I stages contain sterols. However, since apicomplexan parasites are generally considered as defective in cholesterol synthesis, these sterols have to be provided by the host cells and infection-induced alterations of cholesterol-related sterol contents will primarily rely on host cell-driven reactions.

Overall, cholesterol-related sterols were grouped as follows: (i) phytosterols (campesterol, sitosterol and stigmasterol) that were taken up from FCS-derived medium fractions and therefore served as indicators of sterol uptake from exogenous sources; (ii) molecules acting as cholesterol precursors thereby serving as indicators of endogenous cellular cholesterol synthesis (lathosterol, lanosterol, dihydrolanosterol, desmosterol, 7 dehydrocholesterol); (iii) downstream metabolites representing indicators of cholesterol conversion and oxidative cell stress (24 hydroxycholesterol, 25 hydroxycholesterol, 27 hydroxycholesterol, 7 α hydroxycholesterol, 7 ketocholesterol, 7 β cholesterol, 4 β cholesterol). In general, it has to be noted that different primary BUVEC isolates showed varying qualitative and quantitative infection-triggered alterations of the cholesterol metabolism. When considering the mean of all BUVEC isolates the resulting high standard deviation sometimes concealed significant reactions that were present on the single isolate level.

All parasite cultures were analyzed at 14 days p. i., i. e. at a time point when intracellular *E. bovis* macromeronts had already grown considerably but merozoites I were not fully formed yet. As expected, the number of macromeront-carrying cells was relatively low (1.2% FCS: $12.1 \pm 1.4\%$; 10% FCS: $11.5 \pm 1.5\%$) reflecting the typical *in vitro* developmental characteristics of *E. bovis*. However, it has to be kept in mind that all effects measured here resulted from such a low number of infected host cells.

The current sterol profile indicated an infection-triggered increase of cellular sterol uptake from extracellular sources that occurred irrespective of FCS conditions (Fig. 2). Thus, all three phytosterols were found significantly increased in their cellular content in *E. bovis*-infected cell layers being cultured under 1.2% and 10% FCS (campesterol: *E. bovis*/10% vs. control: $p = 0.0187$; *E. bovis*/1.2% vs. control: $p = 0.0285$; sitosterol: *E. bovis*/10% vs. control: $p = 0.005$; *E. bovis*/1.2% vs. control: $p = 0.0274$; stigmasterol: *E. bovis*/10% vs. control: $p = 0.012$; *E. bovis*/1.2% vs. control: $p = 0.0218$) (Fig. 2). As such, no statistical differences in the phytosterol contents between infected cell cultures in 1.2% and 10% FCS-supplemented medium were stated. However, based on higher phytosterol contents in 10% FCS-supplemented control cells, the relative *n*-fold increase of campesterol (*E. bovis*/1.2% FCS vs. control: 9.3-fold; *E. bovis*/10% FCS vs. control: 2.5-

4

Modulation of cholesterol-related sterols during *Eimeria bovis* macromeront formation and impact of selected oxysterols on parasite development

A. Taubert et al.

Molecular & Biochemical Parasitology 223 (2018) 1–12

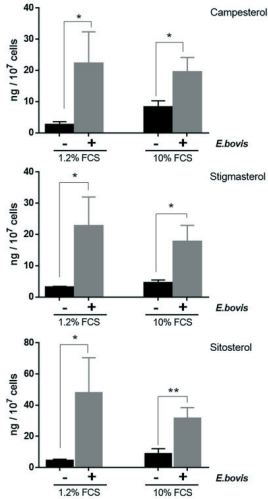


Fig. 2. Phytosterol contents in *E. bovis*-infected host cells. Bovine umbilical vein endothelial cells were cultured in cell culture medium containing 1.2% or 10% FCS and infected with vital *E. bovis* sporozoites. At 14 days p. i. *E. bovis*-infected BUVEC (grey bars) and non-infected control cells (black bars) were harvested and subjected to GC-MS-based measurements of cellular campesterol, stigmaterol and sitosterol contents. Arithmetic mean and standard deviation of three biological with four technical replicates, each. ** = $p \leq 0.01$, * = $p \leq 0.05$.

fold), sitosterol (*E. bovis*/1.2% FCS vs. control: 10.2-fold; *E. bovis*/10% FCS vs. control: 3.9-fold) and stigmaterol (*E. bovis*/1.2% FCS vs. control: 7-fold; *E. bovis*/10% FCS vs. control: 4.1-fold) cellular contents was higher in those conditions that supported improved parasite proliferation (1.2% FCS). Phytosterol:cholesterol ratios mirrored these data and revealed a significant enhancement for campesterol-, sitosterol- and stigmaterol-related ratios in *E. bovis*-infected cells irrespective of the FCS conditions but with higher n-fold increases found in those cells cultured in 1.2% FCS (Table 1).

Referring to the induction of endogenous cholesterol synthesis, a parasite proliferation-dependent effect was evident since under high FCS (10%) conditions no difference in absolute cholesterol precursor contents was detected between infected and non-infected host cells (Fig. 3) whilst under low FCS conditions (1.2%), promoting optimal merozoite I production (Fig. 1), several cholesterol precursors were found to be upregulated in their absolute contents when compared to respective controls or to infected cells cultured under high FCS conditions. Thus, enhanced levels of lanosterol (3.3-fold and 3.5-fold compared to non-infected controls and *E. bovis*/10% FCS cultures, respectively), lanosterol (7.1-fold and 4.7-fold compared to non-infected controls and *E. bovis*/10% FCS cultures, respectively), dihydrolanosterol (10.5-fold and 7.8-fold compared to non-infected controls and *E. bovis*/10% FCS cultures, respectively), desmosterol (3-fold and 7.8-fold compared to non-infected controls and *E. bovis*/10% FCS cultures, respectively) and 7 dehydrocholesterol (30.7-fold and 3.5-fold compared to non-infected controls and *E. bovis*/10% FCS cultures, respectively) were found indicating a parasite-driven induction of endogenous host cellular cholesterol synthesis in times of boosted *E. bovis* proliferation (Fig. 3). Unfortunately, the individual variation of primary bovine endothelial cell isolates which were already observed between non-infected BUVEC often hampered significant outcomes. Thus, statistically significant differences could only be stated for desmosterol (*E. bovis*/1.2% FCS vs. controls; $p = 0.0107$). These reactions were also reflected by sterol:cholesterol-ratios since n-fold change of cholesterol precursor:cholesterol-ratios was higher between infected and non-infected cells in case of low FCS conditions when compared to high FCS conditions (Table 1). However, due to strong individual variations, the enhancement of sterol:cholesterol-ratios in *E. bovis*-infected host cells proved statistically significant only in the case of 7 dehydrocholesterol ($p < 0.0001$), nevertheless underlying the assumption that endogenous cholesterol synthesis is increased under parasite-busting conditions.

The current data further indicated an enhanced conversion of cholesterol in *E. bovis*-infected endothelial host cells. Thus, *E. bovis*-infected cell layers experienced a significant, 2.5-fold increase of cholesterol

Table 1
Ratios of sterol/oxysterol to cholesterol in *E. bovis*-infected and non-infected BUVEC.

Molecule	sterol:chol ratio n.i./1.2% FCS	sterol:chol ratio E.b./1.2% FCS	n-fold 1.2% FCS	sterol:chol ratio n.i./10% FCS	sterol:chol ratio E.b./10% FCS	n-fold 10% FCS
lanosterol	0.687 ± 0.403	1.979 ± 0.714	2.88	0.395 ± 0.260	0.524 ± 0.195	1.33
dihydrolanosterol	0.087 ± 0.048	0.308 ± 0.240	3.54	0.045 ± 0.020	0.067 ± 0.022	1.49
lanosterol	9.533 ± 5.474	18.330 ± 9.862	1.92	3.001 ± 1.296	3.206 ± 0.631	1.07
7 dehydrocholesterol	0.049 ± 0.046	4.227 ± 7.008	85.60	0.977 ± 1.451	2.597 ± 3.837	2.66
desmosterol	2.854 ± 1.048	7.367 ± 4.222	2.58	0.729 ± 0.362	0.798 ± 0.280	1.08
7α hydroxycholesterol	0.094 ± 0.019	0.240 ± 0.110	2.56	0.134 ± 0.036	0.310 ± 0.104	2.32
24 hydroxycholesterol	0.233 ± 0.054	0.201 ± 0.063	0.86	0.073 ± 0.029	0.069 ± 0.034	0.95
25 hydroxycholesterol	0.041 ± 0.032	1.911 ± 1.382	46.93	0.028 ± 0.011	0.341 ± 0.121	12.35
27 hydroxycholesterol	0.055 ± 0.011	0.103 ± 0.045	1.85	0.033 ± 0.006	0.044 ± 0.018	1.32
4β cholesterol	0.064 ± 0.006	0.141 ± 0.054	2.20	0.059 ± 0.013	0.103 ± 0.042	1.76
7β cholesterol	0.210 ± 0.043	0.490 ± 0.261	2.34	0.289 ± 0.045	0.581 ± 0.243	2.01
7 keto cholesterol	2.094 ± 0.638	3.600 ± 1.704	1.72	1.736 ± 0.572	2.245 ± 0.987	1.29
campesterol	0.041 ± 0.016	0.313 ± 0.223	7.64	0.123 ± 0.052	0.243 ± 0.077	1.98
stigmaterol	0.050 ± 0.006	0.303 ± 0.122	6.01	0.069 ± 0.037	0.213 ± 0.036	3.07
sitosterol	0.077 ± 0.013	0.653 ± 0.384	8.48	0.141 ± 0.074	0.387 ± 0.036	2.74

Data in **bold**: data differ significantly from respective control data with $p \leq 0.05$.

Data in **bold + Italic**: data differ significantly from respective control data with $p \leq 0.01$.

Modulation of cholesterol-related sterols during *Eimeria bovis* macromeront formation and impact of selected oxysterols on parasite development

A. Tauber et al.

Molecular & Biochemical Parasitology 223 (2018) 1–12

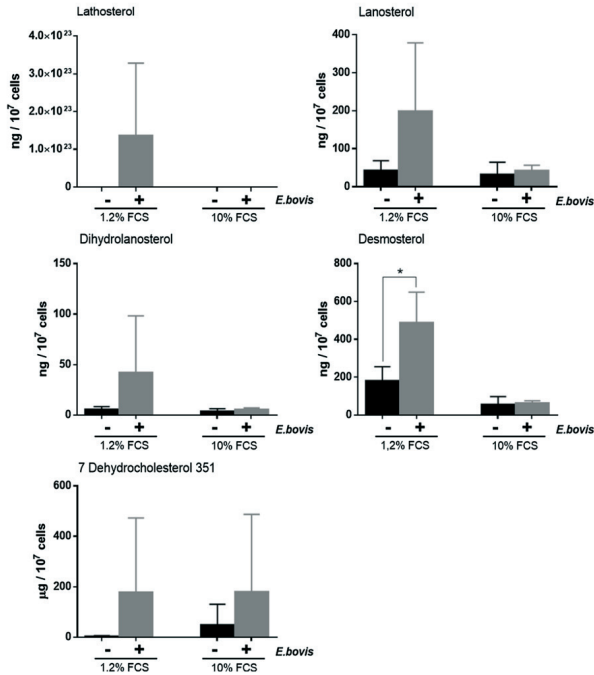


Fig. 3. Cholesterol precursor contents in *E. bovis*-infected host cells. Bovine umbilical vein endothelial cells were cultured in cell culture medium containing 1.2% or 10% FCS and infected with vital *E. bovis* sporozoites. At 14 days p.i. *E. bovis*-infected BUVEC (grey bars) and non-infected control cells (black bars) were harvested and subjected to GC-MS-based measurements of cellular lathosterol, lanosterol, dihydrolanosterol, desmosterol and 7 dehydrocholesterol 351 contents. Arithmetic mean and standard deviation of three biological with four technical replicates, each. * = $p \leq 0.05$.

esterification compared to non-infected controls ($p = 0.0101$; Fig. 4). Due to restricted oocyst/sporozyte availability these analyses were only performed at high (10%) FCS conditions. In addition, selective side-chain oxysterol formation was detected in *E. bovis*-infected BUVEC: whilst the cellular content of 24 hydroxycholesterol and 27 hydroxycholesterol was not significantly altered, 25 hydroxycholesterol was found up-regulated in *E. bovis*-infected host cells cultured under both, 1.2% FCS (63.2-fold upregulation) and 10% FCS (15.2-fold up-regulation) conditions (*E. bovis*/10% vs. control: $p = 0.0239$; *E. bovis*/1.2% vs. control: $p = 0.0569$) (Fig. 4). Comparing the two different FCS conditions in *E. bovis*-infected cells, 25 hydroxycholesterol was found 4.5-fold increased in those FCS conditions (1.2%) that boosted merozoite I

production. Overall, 25 hydroxycholesterol signified the most upregulated molecule of the entire study. Oxysterol:cholesterol ratios confirmed the above described results and were found significantly increased in *E. bovis*-infected host cells for both FCS conditions in the case of 25 hydroxycholesterol (*E. bovis*/10% vs. control: $p = 0.0164$; *E. bovis*/1.2% vs. control: $p = 0.0011$) whilst 24 hydroxycholesterol- and 27 hydroxycholesterol-related ratios were not significantly altered (Table 1).

Besides enzymatically synthesized side-chain oxysterols, non-enzymatically oxidized, ring-modified oxysterols indicating oxidative stress reactions were also found upregulated in *E. bovis*-infected host cell layers. It is worth noting that 7 ketocholesterol, 4 β cholesterol, 7 β

Modulation of cholesterol-related sterols during *Eimeria bovis* macromeront formation and impact of selected oxysterols on parasite development

A. Tauber et al.

Molecular & Biochemical Parasitology 223 (2018) 1–12

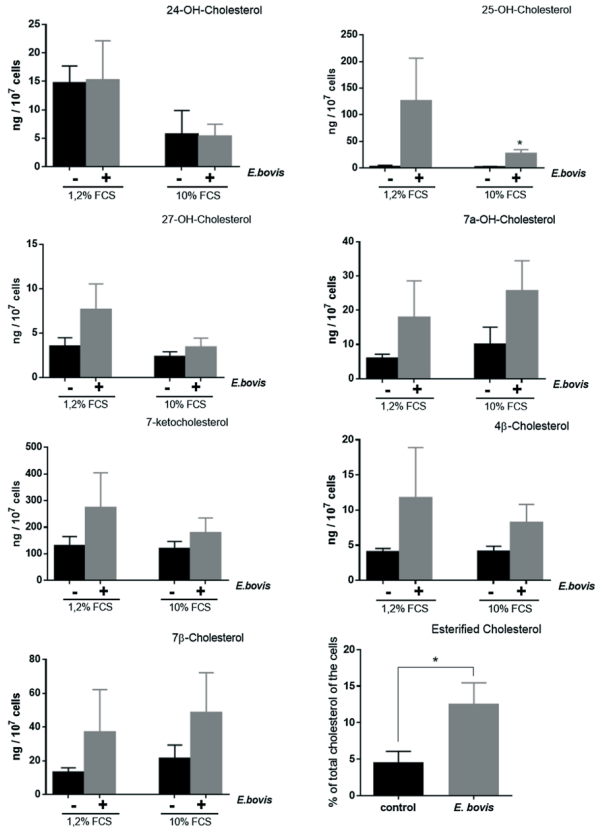


Fig. 4. Oxysterol and cholesterol ester contents in *E. bovis*-infected host cells. Bovine umbilical vein endothelial cells were cultured in cell culture medium containing 1.2% or 10% FCS and infected with vital *E. bovis* sporozoites. At 14 days p. i. *E. bovis*-infected BUVEC (grey bars) and non-infected control cells (black bars) were harvested and subjected to GC-MS-based measurements of cellular 24 hydroxycholesterol, 25 hydroxycholesterol, 27 hydroxycholesterol, 7α-OHC, 7 ketocholesterol, 7α-OHC, 7 ketocholesterol, 4β cholesterol and 7β cholesterol contents. Furthermore, the degree of cholesterol esterification was analyzed. Arithmetic mean and standard deviation of three biological with four technical replicates, each. * = $p \leq 0.05$.

Modulation of cholesterol-related sterols during *Eimeria bovis* macromeront formation and impact of selected oxysterols on parasite development

A. Tauber et al.

Molecular & Biochemical Parasitology 223 (2018) 1–12

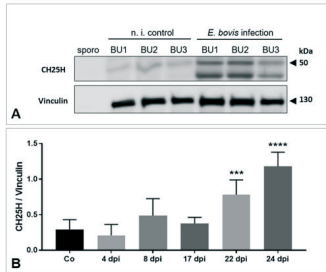


Fig. 5. Cholesterol 25 hydroxylase protein expression in *E. bovis*-infected host cells.

Different bovine umbilical vein endothelial cell isolates (= BUV) were infected with vital *E. bovis* sporozoites. Protein extraction from *E. bovis*-infected BUVEC was performed at days 4, 8, 17, 22 and 24 p. i. The samples were analyzed for cholesterol 25 hydroxylase protein abundance via immunoblotting and densitometric analyses of the respective protein bands. Vinculin was analyzed as reference protein for the normalization of the samples. For control reasons, protein extracts of *E. bovis* sporozoites (= sporo) were analyzed in parallel. (A) Exemplary blot of three BUVEC isolates (22 days p. i.). (B) Quantitative assessment of cholesterol 25 hydroxylase relative to vinculin expression in three BUVEC isolates. **** = $p \leq 0.0001$; *** = $p \leq 0.001$.

cholesterol and 7α hydroxycholesterol were found almost equally increased in both FCS conditions. However, these reactions revealed statistically insignificant. Nevertheless, enhanced oxysterol:cholesterol ratios reflected these results and proved statistically significant in the case of 4β cholesterol (1.2% FCS: $p = 0.0244$) and were barely not significant for 7α hydroxycholesterol (1.2% FCS: $p = 0.0579$) and β cholesterol (1.2% FCS: $p = 0.0529$; 10% FCS: $p = 0.0663$) (Table 1).

3.2. Cholesterol 25 hydroxylase protein expression is enhanced in *E. bovis* infected host cells

25 hydroxycholesterol is well-known as a potent regulator of cholesterol metabolism and additionally exhibits antiviral effects. It is mainly enzymatically synthesized via cholesterol 25 hydroxylase activities. Given that 25 hydroxycholesterol was the most upregulated molecule in this study, we here analyzed whether cholesterol 25 hydroxylase protein expression was increased in *E. bovis*-infected host cells. Immunoblotting-based analyses on cell homogenates of *E. bovis*-infected and control cells indeed showed a higher cholesterol 25 hydroxylase protein abundance in infected cells towards the end of macromeront formation (Fig. 5). As also described in the murine and human system [26], two protein bands with slightly differing masses were detected via immunoblotting. According to Lund et al. [26] these different forms result from a different glycosylation status of the protein. Interestingly, especially the lower protein band of cholesterol 25 hydroxylase was increasingly expressed at the late phase of infection and was almost undetectable in non-infected control cells (Fig. 5).

3.3. Oxysterol treatments of *E. bovis*-infected cells block parasite development and proliferation

Given that 25 hydroxycholesterol was found significantly enhanced in its contents in *E. bovis*-infected BUVEC and may also be secreted into the extracellular compartment [27], we here analyzed the effects of

different exogenous oxysterol (25 hydroxycholesterol, 27 hydroxycholesterol, 7 ketocholesterol) treatments on *E. bovis* intracellular development. Therefore, we here chose a fixed dose which is commonly used and generally promotes control of several viruses *in vitro*. Overall, 25 hydroxycholesterol, 27 hydroxycholesterol and 7 ketocholesterol treatments all exhibited significant adverse effects on *E. bovis* development and proliferation. Thus, the number and size of developing macromeronts as well as the merozoite I production was significantly decreased in treated cells when compared with solvent-treated controls (Fig. 6). When infected cells were treated from 10 days p. i. onwards (i. e. beginning with the onset of macromeront enlargement), the most prominent effects were driven by 25 hydroxycholesterol leading to a significant reduction of macromeront numbers [15 days p. i.: 80.5% reduction, barely not significant ($p < 0.0566$), 19 days p. i.: 92% reduction, $p < 0.0001$] and sizes [15 days p. i.: 76.5% reduction, $p = 0.0004$, 19 days p. i.: 87.2% reduction, $p < 0.0001$] and to an almost total blockage of merozoite I production (98.7% reduction, $p < 0.0001$) (Fig. 6). Slightly less pronounced effects were obtained by 27 hydroxycholesterol treatments [reduction of macromeront numbers: 75.5% at 15 days p. i. ($p = 0.0899$), 88% at 19 days p. i. ($p = 0.0001$), reduction of size: 64% at 15 days p. i. ($p = 0.003$) and 83.5% at 19 days p. i. ($p < 0.0001$) and reduction of merozoite I production: 96.3% ($p < 0.0001$)]. The least pronounced but still significant effects were driven by 7 ketocholesterol treatments leading to a reduction of macromeront numbers of 49.8% at 15 days p. i. (n. s.) and 62.5% at 19 days p. i. ($p = 0.0098$) and of meront sizes [15 days p. i.: 44.8% ($p = 0.0452$) and 19 days p. i.: 63.8% ($p < 0.0001$)] and to a reduced merozoite I replication of 93.1% ($p < 0.0001$). Overall, treatment-induced effects on macromeront sizes and numbers were found enhanced with prolonged treatment duration in the case of 27 hydroxycholesterol and 7 ketocholesterol treatments [7 days vs. 5 days of treatment: 27 hydroxycholesterol: $p < 0.01$ (meront size); 7 ketocholesterol: $p < 0.01$ (meront size) and $p < 0.0001$ (meront number)]. When oxysterol treatments were started early after infection from day 1 p. i. onwards, the detrimental effects on macromeront development were comparable to treatments from days 10 p. i. onwards, but led to a total blockage of merozoite I production (Table 2).

We further analyzed whether direct exogenous treatments of sporozoites as infective stages influenced their infectivity. Short-term (1 h) exogenous treatments with 25 hydroxycholesterol, 27 hydroxycholesterol or 7 ketocholesterol prior to BUVEC infection had no significant effects on sporozoite infectivity as illustrated in Fig. 7A. Prolonged treatments were only performed in the case of 25 hydroxycholesterol. As expected, prolonged presence in an extracellular condition led to reduced infectivity of sporozoites in both, treated and non-treated sporozoites (Fig. 7B). When sporozoites were treated for 3 h with the higher dose of 10 μ M 25 hydroxycholesterol ($p = 0.027$), a significant but moderate decrease of parasite infectivity was observed in comparison to solvent-treated parasite stages (Fig. 7B).

4. Discussion

Apicomplexan parasite species differ considerably in their intracellular replication modes depending on the genus, species or developmental stage and, in consequence, may favour different strategies of cholesterol acquisition, e. g. for offspring membrane biosynthesis. In the current study cholesterol-related sterol profiles revealed that the slow proliferating species *E. bovis* partially follows a similar strategy of cholesterol acquisition as fast proliferating coccidians since it induces sterol uptake from exogenous sources but also differs considerably in its strategy from fast proliferating species (i) by a simultaneous induction of host cellular endogenous cholesterol synthesis in times of optimized offspring production and (ii) by a selective upregulation of the side-chain oxysterol 25 hydroxycholesterol.

As a simple but important finding we here demonstrated that massive *E. bovis* merozoite I production in bovine endothelial host cells

Modulation of cholesterol-related sterols during *Eimeria bovis* macromeront formation and impact of selected oxysterols on parasite development

A. Tauber et al.

Molecular & Biochemical Parasitology 223 (2018) 1–12

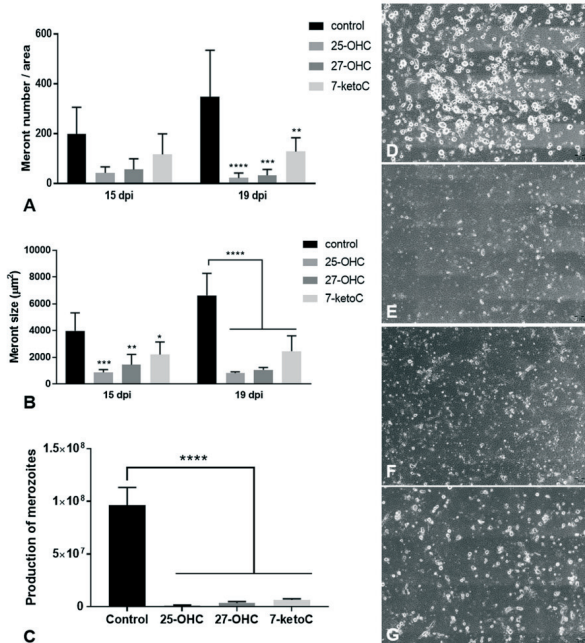


Fig. 6. Effects of 25 hydroxycholesterol, 27 hydroxycholesterol and 7 ketocholesterol treatments on *E. bovis* macromeront formation and merozoite I production. Bovine umbilical vein endothelial cells (BUVEC; n = 3) were infected with *E. bovis* sporozoites. From 10 days p. i. onwards, parasite cultures were treated with 25 hydroxycholesterol, 27 hydroxycholesterol or 7 ketocholesterol. Solvent-treated cultures served as controls. At days 15 and 19 p. i. the number (A) and size (B) of macromeronts were estimated. Additionally, the number of merozoites I (C) in treated cultures and controls was analyzed via qPCR at 24 days p. i. Exemplary illustrations of non-treated controls (D), 25 hydroxycholesterol- (E), 27 hydroxycholesterol- (F) and 7 ketocholesterol-treated (G) BUVEC at 19 days p. i. **** = p ≤ 0.0001; *** = p ≤ 0.001; ** = p ≤ 0.01; * = p ≤ 0.05.

depends on FCS supplementation of the medium in that sense, that, unexpectedly, lower FCS contents boost offspring formation. This finding gave us the unique opportunity to test for cholesterol-related sterols in conditions suboptimal and optimal for parasite replication.

The phytosterols campesterol, sitosterol and stigmasterol represent cholesterol analogs that are exclusive of plant dietary origin [28] and are derived from FCS-enriched media via the herbivore nutrition of cattle. Thus, phytosterols are commonly accepted as indicators of cellular sterol uptake from the extracellular environment [28–30]. Irrespective of FCS supplementation, all three plant sterols were significantly enhanced in *E. bovis*-infected endothelial host cells indicating that the basic infection-driven needs for cholesterol are primarily satisfied via extracellular sources. Phytosterols are transported via

lipoproteins (mainly LDL) and may then be taken-up by the cells via the LDL receptor (LDLR) or certain scavenger receptors [29–31]. Accordingly, we recently reported on the upregulation of both, LDLR and the scavenger receptor OLR1 (syn. LOX1) in *E. bovis*-infected host endothelial cells during macromeront formation [1]. The pivotal role of exogenous cholesterol sources, mainly LDL, for optimal parasite proliferation was also demonstrated for other apicomplexan parasites, such as *T. gondii*, *N. caninum* or *C. parvum* [2,3,6] and appears an important strategy of sterol supply that is exploited in a species-specific and host cell-specific manner. Thus, hepatic *Plasmodium* spp. stages or *T. gondii* tachyzoites developing in macrophages do not rely on LDL for replication [5,7], whilst *T. gondii* tachyzoites replicating in CHO cells [2] or *C. parvum* merozoite formation in epithelial cells [3] indeed need

Modulation of cholesterol-related sterols during *Eimeria bovis* macromeront formation and impact of selected oxysterols on parasite development

A. Tauber et al.

Molecular & Biochemical Parasitology 223 (2018) 1–12

Table 2
Relative reduction of *E. bovis* macromeront numbers, size and merozoite I production by 25 hydroxycholesterol, 27 hydroxycholesterol and 7 ketocholesterol treatments from day 1 p. i. onwards.

treatment	reduction (%) of macromeront numbers ^a	reduction (%) of macromeront size ^a	reduction (%) of merozoite I production ^b
25-OHC	95.6 ± 3.6	84.4 ± 6.8	100
27-OHC	87.0 ± 6.8	79.9 ± 8.8	100
7 keto cholesterol	85.9 ± 5.3	58.9 ± 16.7	100

^a Estimated at 19 days p. i.

^b Estimated at 24 days p. i.

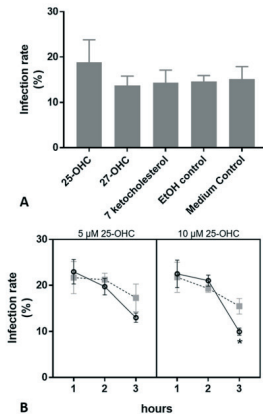


Fig. 7. Effects of 25 hydroxycholesterol, 27 hydroxycholesterol and 7 ketocholesterol treatments on *E. bovis* sporozoite infectivity.

(A) *E. bovis* sporozoites were treated for 60 min with 25 hydroxycholesterol, 27 hydroxycholesterol or 7 ketocholesterol (all 5 μM) prior to BUVEC infection. (B) In case of 25 hydroxycholesterol treatments (open black circles), time (1–3 h of incubation) and dose- (5 μM, 10 μM) dependent experiments were performed and analyzed in comparison to solvent-treated controls (grey squares). In all experimental settings the infection rate was estimated microscopically at 2 days p. i. * = $p \leq 0.05$.

these molecules for optimal parasite development.

Cholesterol precursors are generally accepted as reflecting the activity of the endogenous sterol biosynthetic pathway [29,30]. Obviously, in 10% FCS-supplemented control cells, higher contents of phytosterols reflecting an enhanced sterol uptake and no signs of enhanced endogenous cholesterol synthesis were noted when compared to low FCS conditions. The 10% FCS condition supported *E. bovis* development on a basic level, but to a minor degree than 1.2% FCS-supplementation. However, when low FCS was applied in infected cells, a higher content of several cholesterol precursors was found compared to non-infected controls and to high FCS-supplemented *E. bovis*-infected host cells indicating that available exogenous sterol sources were not

sufficient in these conditions to satisfy the parasite needs for massive merozoite I synthesis. Interestingly, the parallel induction of both modes of cholesterol acquisition, i. e. of endogenous cholesterol synthesis and exogenous sterol uptake, improved parasite development and boosted merozoite I production to a significantly higher degree than high dose FCS supplementation. Consequently, it may be concluded that optimal *E. bovis* development depends on the simultaneous orchestration of different modes of cholesterol acquisition. The assumption that endogenous cholesterol synthesis also plays a role in *E. bovis* macromeront development is supported by recent reports showing that chemical blockage of HMG-CoA reductase and squalene synthase via lovastatin and zaragozic acid, respectively, resulted in a highly significant inhibition of *E. bovis* merozoite I production [9]. Since these data contrast with findings on *T. gondii*, *Plasmodium* spp. or *C. parvum* infections [2,3,5] parasite-, stage- and/or even host cell type-specific reactions must be assumed.

For detoxifying reasons and cholesterol efflux, excess intracellular cholesterol is biochemically converted, e. g. to cholesteryl esters or oxysterols. In accordance, in the current study the degree of esterified cholesterol was found significantly increased in *E. bovis*-infected endothelial cells when compared to non-infected controls. These data are strengthened by the fact that blockage of cholesterol esterification resulted in highly diminished *E. bovis* proliferation and merozoite I production [9]. Accordingly, the absence of host SOAT or SOAT inhibition also induced a considerable decrease of *T. gondii* replication [11]. Since excess cholesteryl esters are mainly stored in lipid droplets, these organelles were consistently found increased on a high level in host cells being infected with *E. bovis* [1] or on a more moderate level in other intracellular protozoans, such as *Trypanosoma cruzi*, *T. gondii*, *P. berghei* or *P. falciparum* [2,11–15,17,18,32].

Besides cholesterol esterification, *E. bovis* infection also triggered differential oxysterol formation in endothelial host cells. Given that ring-modified oxysterols are mainly formed by interactions with reactive oxidative species (ROS), upregulation of several of these molecules (e. g. 7 ketocholesterol, 4β cholesterol, 7α hydroxycholesterol) indicated that endothelial host cells experienced a considerable oxidative cell stress in response to *E. bovis* infection. Interestingly, these reactions occurred independent of FCS supplementation indicating that they are independent of the degree of parasite development.

Whilst the levels of 24 hydroxycholesterol and 27 hydroxycholesterol were not significantly influenced, a significant increase of 25 hydroxycholesterol levels indicated a selective synthesis of side-chain oxysterols in *E. bovis*-infected host cells. An infection-triggered increase of 25 hydroxycholesterol contents was in principle found at both FCS conditions but obviously was parasite proliferation-dependent since a higher *n*-fold increase of 25 hydroxycholesterol occurred in conditions of boosted merozoite I production (1.2% FCS). However, in both FCS-conditions, 25 hydroxycholesterol revealed as the most up-regulated molecule of all sterols investigated. It is worth noting, that enhancement of 25 hydroxycholesterol synthesis in *E. bovis*-infected host cells appears to be parasite-specific since infections of BUVEC with the fast proliferating apicomplexan parasite *B. besnoiti* failed to influence 25 hydroxycholesterol contents (A. Tauber, personal observation). Given that 25 hydroxycholesterol is mainly enzymatically synthesized by cholesterol 25 hydroxylase, we here additionally studied the protein expression of this enzyme in *E. bovis*-infected cells. In agreement to recent data on upregulated cholesterol 25 hydroxylase gene transcription in *E. bovis*-infected BUVEC [1,8], we here indeed showed an increase in cholesterol 25 hydroxylase protein abundance in *E. bovis*-infected host cells. Interestingly, especially the lower protein band of cholesterol 25 hydroxylase, most probably signifying the non-glycosylated form of the protein, was almost selectively enhanced in its expression towards the end of merogony I. This effect may have been driven by a continuous exhaustion of cholesterol 25 hydroxylase enzymatic activity, but this is speculative and has to be studied in further detail. So far, it also remains unclear whether enhanced cellular

Modulation of cholesterol-related sterols during *Eimeria bovis* macromeront formation and impact of selected oxysterols on parasite development

A. Taubert et al.

Molecular & Biochemical Parasitology 223 (2018) 1–12

contents of 25 hydroxycholesterol are beneficial for parasite development in the sense of optimized building block supply or whether these must be considered as a host cellular regulative or innate immune mechanism. Overall, multiple functions have been reported for 25 hydroxycholesterol. Firstly, 25 hydroxycholesterol represents a pivotal regulator of cholesterol homeostasis via indicating the presence of excess cholesterol and down-regulating *de novo* synthesis. Secondly, the hydrophilic 25 hydroxycholesterol is redistributed among cellular membranes and contributes to altered membrane properties [20,33,34] by promoting lipid disordering and expansion of membranes. Whether such effects may be beneficial for the parasite with respect to the massive enlargement of *E. bovis*-infected host cell membranes has to be elucidated. Interestingly, enhanced levels of 25 hydroxycholesterol also seem to increase the availability of active cholesterol [20,33], which may then be accessible to the parasites. Finally, 25 hydroxycholesterol is well-known for its immunomodulatory functions and antiviral properties (summarized in [19]). However, so far, no reports exist on anti-parasitic properties of 25 hydroxycholesterol. Given that oxysterols are also known to be secreted by cells [27], we here additionally analyzed whether exogenous treatments with distinct oxysterols (25 hydroxycholesterol, 27 hydroxycholesterol and 7 ketocholesterol) would influence intracellular *E. bovis* development. For these experiments, we chose a fixed 5 μ M 25 hydroxycholesterol concentration which is commonly used and proved effective in antiviral treatments (see e. g. [35]). Overall, the physiological concentration of oxysterols varies greatly depending on the host cell type and host species. In humans and animal plasma, different oxysterol measurements vary greatly from 20 to 1200 nM (8–400 ng/ml [36]) and normally account for 1–5% of total cholesterol in the haematic pool [19]. However, depending on the detection method, 1–56 ng/ml 25-OHC was detected in serum/plasma samples of healthy humans [37]. Important to note, oxysterol concentrations are also highly influenced by nutrition and disease (as also shown in the current study). However, the concentration of the here chosen exogenous treatments can hardly be related to the current intracellular oxysterol values in *E. bovis*-infected cell layers, especially since only a small proportion of the cells produced this molecule within the infected cell layer (12.1% infection rate) and only a small proportion of exogenously supplied 25-OHC in fact reaches the intracellular compartment and can therefore be recovered [35]. Interestingly, 25 hydroxycholesterol, 27 hydroxycholesterol and 7 ketocholesterol treatments all blocked parasite development and led to a highly significant reduction of macromeront size and numbers as well as merozoite I production. Notably, when treated from day one p. i. onwards, no merozoites I were formed at all indicating a massive direct or indirect oxysterol-triggered interference with *E. bovis* development. Given that these molecules had no direct adverse effect on sporozoite infectivity after short-term treatments (given that the sporozoites are obligate intracellular stages and invade host cells rather fast, long-term exposure to extracellular oxysterols appear rather implausible), other functions of oxysterols may have contributed to their anti-parasitic effects. Since 25 hydroxycholesterol and 27 hydroxycholesterol both downregulate cholesterol *de novo* synthesis and receptor-mediated LDL uptake, it is tempting to speculate that these molecules may interfere with successful intracellular *E. bovis* development.

5. Conclusions

Overall, the current study confirms that *E. bovis* macromeront formation has a considerable impact on the host cellular cholesterol metabolism by simultaneously inducing both, extracellular sterol up-take and *de novo* synthesis in times of massive offspring production. For detoxifying and efflux reasons cholesterol is additionally increasingly converted into cholesterol esters and oxysterols. Interestingly, distinct oxysterols exhibit antiparasitic effects when applied exogenously. To sum up, the current report strengthens the hypothesis that *E. bovis* has an extraordinary need of cholesterol for successful parasite

development and replication and indeed differs in its metabolic actions and requirements from other fast proliferating apicomplexan parasites of humans, domestic animals, and wildlife animals.

Funding sources

This study was supported by the German Research Foundation (DFG, project no. TA291/10-1).

Competing interest statement

The authors have no competing interests to declare.

Acknowledgements

Authors thank Axel Wehrend (Clinic for Obstetrics, Gynecology, and Andrology of Large and Small Animals, Justus Liebig University, Giessen, Germany) for the continuous supply of bovine umbilical cords. We also acknowledge the outstanding work of Brigitte Hofmann and Christin Ritter in all cell culture experiments.

References

- [1] P.H. Hamid, J. Hirzmann, K. Kermer, G. Gimpl, G. Lochini, C.R. Hermosilla, A. Taubert, *Eimeria bovis* infection modulates endothelial host cell cholesterol metabolism for successful replication. *Vet. Res.* 46 (2015).
- [2] I. Coppens, A.P. Sinai, K.A. Joiner, *Toxoplasma gondii* exploits host low-density lipoprotein receptor-mediated endocytosis for cholesterol acquisition. *J. Cell Biol.* 149 (1) (2000) 167–180.
- [3] K. Ehrenman, J.W. Wanyiri, N. Bhat, H.D. Ward, I. Coppens, *Cryptosporidium parvum* scavenges LDL-derived cholesterol and micellar cholesterol internalized into enterocytes. *Cell. Microbiol.* 15 (7) (2013) 1182–1197.
- [4] P. Grellier, A. Valentin, V. Milleroux, J. Schreve, D. Rigomont, 3-Hydroxy-3-methylglutaryl coenzyme A reductase inhibitors lovastatin and simvastatin inhibit in vitro development of *Plasmodium falciparum* and *Babesia divergens* in human erythrocytes. *Antimicrob. Agents Chemother.* 38 (5) (1994) 1144–1148.
- [5] M. Labadie, B. Jayabalasingham, N. Bano, S.J. Cha, J. Sandvol, G. Guan, I. Coppens, *Plasmodium* salvages cholesterol internalized by LDL and synthesized *de novo* in the liver. *Cell. Microbiol.* 13 (4) (2011) 569–586.
- [6] S.J. Nolan, J.D. Romano, T. Luechtefeld, I. Coppens, *Neospora caninum* recruits host cell structures to its parasitophorous vacuole and salvages lipids from organelles. *Eukaryot. Cell* 14 (5) (2015) 454–473.
- [7] Y. Nishikawa, H.M. Ibrahim, K. Kameyama, I. Shiga, J. Hissa, X. Xuan, Host cholesterol synthesis contributes to growth of intracellular *Toxoplasma gondii* in macrophages. *J. Vet. Med. Sci.* 73 (5) (2011) 632–639.
- [8] A. Taubert, K. Wimmers, S. Ponsuksilli, C.A. Jimenez, H. Zahner, C. Hermosilla, Microarray-based transcriptional profiling of *Eimeria bovis*-infected bovine endothelial host cells. *Vet. Res.* 41 (5) (2010).
- [9] P.H. Hamid, J. Hirzmann, C. Hermosilla, A. Taubert, Differential inhibition of host cell cholesterol *de novo* biosynthesis and processing abrogates *Eimeria bovis* intracellular development. *Parasitol. Res.* 113 (11) (2014) 4165–4176.
- [10] B. Feng, P.M. Yao, Y. Li, C.M. Devlin, D. Zhang, H.P. Harding, M. Sweeney, J.X. Rong, C. Kurikose, E.A. Fisher, A.R. Marks, D. Ron, I. Tabas, The endoplasmic reticulum is the site of cholesterol-induced cytotoxicity in macrophages. *Nat. Cell Biol.* 5 (9) (2003) 781–792.
- [11] S. Sonda, L.M. Ting, S. Novak, K. Kim, J.J. Maher, R.V. Farese Jr., J.D. Ernst, Cholesterol esterification by host and parasite is essential for optimal proliferation of *Toxoplasma gondii*. *J. Biol. Chem.* 276 (37) (2001) 34434–34440.
- [12] I. Coppens, O. Vloeberghs, Insights into unique physiological features of neutral lipids in Apicomplexa: from storage to potential mediation in parasite metabolic activities. *Int. J. Parasitol.* 35 (6) (2005) 597–615.
- [13] A.P. Gomes, K.G. Magalhães, R.M. Rodrigues, L. de Carvalho, R. Molinaro, P.T. Bozza, S.J. Barbosa, *Toxoplasma gondii*-skeletal muscle cells interaction increases lipid droplet biogenesis and positively modulates the production of IL-12, IFN- γ and PGE $_2$. *Parasites Vectors* 7 (2014) 47.
- [14] R.C. Melo, H. D'Avila, D.L. Palumbo, P.E. Almeida, P.T. Bozza, Macrophage lipid body induction by Chagas disease in vivo: putative intracellular domains for riceo-spondium formation during infection. *Tissue Cell* 35 (1) (2003) 59–67.
- [15] Y. Nishikawa, F. Quirina, T.T. Stedman, D.R. Voelker, J.Y. Choi, M. Zahn, M. Yang, M. Pypart, K.A. Joiner, I. Coppens, Host cell lipids control cholesterol ester synthesis and storage in intracellular *Toxoplasma gondii*. *Microbiol. J.* 6 (2005) 849–867.
- [16] S.J. Nolan, J.D. Romano, I. Coppens, Host lipid droplets: an important source of lipids salvaged by the intracellular parasite *Toxoplasma gondii*. *PLoS Pathog.* 13 (6) (2017) e1006362.
- [17] A. Rodriguez-Acosta, H.J. Finol, M. Palleiro-Mendez, A. Marquez, G. Andrade, N. Gonzalez, I. Aguilar, M.E. Giron, A. Pinto, Liver ultrastructural pathology in mice infected with *Plasmodium berghei*. *J. Submicrosc. Cytol. Pathol.* 30 (2) (1998) 299–307.

Modulation of cholesterol-related sterols during *Eimeria bovis* macromeront formation and impact of selected oxysterols on parasite development

A. Taubert et al.

Molecular & Biochemical Parasitology 223 (2018) 1–12

- [18] O. Vielemeyer, M.T. McIntosh, K.A. Joiner, L. Coppens, Neutral lipid synthesis and storage in the intrareplicative stages of *Plasmodium falciparum*, Mol. Biochem. Parasitol. 135 (2) (2004) 197–209.
- [19] D. Lembo, V. Cagno, A. Cibra, G. Poli, Oxysterols: an emerging class of broad spectrum antiviral effectors, Mol. Aspects Med. 49 (2016) 23–30.
- [20] A.A. Bielska, P. Schlesinger, D.F. Covey, D.S. Ory, Oxysterols as non-genomic regulators of cholesterol homeostasis, Trends Endocrinol. Metab. 23 (3) (2012) 99–106.
- [21] U. Diczfalussy, On the formation and possible biological role of 25-hydroxycholesterol, Biochimie 95 (3) (2013) 455–460.
- [22] A.R. Jackson, The isolation of viable coccidial sporozoites, Parasitology 54 (1964) 87–93.
- [23] E.A. Jaffe, R.L. Nachman, C.G. Becker, C.R. Minick, Culture of human endothelial cells derived from umbilical veins. Identification by morphologic and immunologic criteria, J. Clin. Invest. 52 (11) (1973) 2745–2756.
- [24] D. Lütjohann, A. Brazzaitka, E. Barth, D. Abramowski, M. Staufenbiel, K. von Bergmann, K. Beyreuther, G. Multhaup, T.A. Bayer, Profile of cholesterol-related sterols in aged amyloid precursor protein transgenic mouse brain, J. Lipid Res. 43 (7) (2002) 1078–1085.
- [25] D.S. Mackay, P.J. Jones, S.B. Myrie, J. Plat, D. Lütjohann, Methodological considerations for the harmonization of non-cholesterol sterol bio-analysis, J. Chromatogr. B Anal. Technol. Biomed. Life Sci. 957 (2014) 116–122.
- [26] E.G. Land, T.A. Kerr, J. Sakai, W.P. Li, D.W. Russell, cDNA cloning of mouse and human cholesterol 25-hydroxylases, polytopic membrane proteins that synthesize a potent oxysterol regulator of lipid metabolism, J. Biol. Chem. 273 (51) (1998) 34316–34327.
- [27] A. Frolov, S.E. Zielinski, J.R. Crowley, N. Dudley-Rucker, J.E. Schaffer, D.S. Ory, NPC1 and NPC2 regulate cellular cholesterol homeostasis through generation of low density lipoprotein cholesterol-derived oxysterols, J. Biol. Chem. 278 (28) (2003) 25517–25525.
- [28] D. Lütjohann, Methodological aspects of plant sterol and stanol measurement, J. AOAC Int. 98 (3) (2015) 674–676.
- [29] V.M. Oikarinen, H. Gylling, E. Ikonen, Plant sterols, cholesterol precursors and oxysterols: small amounts, big effects, Duodecim 131 (3) (2015) 235–241.
- [30] V.M. Oikarinen, H. Gylling, E. Ikonen, Plant sterols, cholesterol precursors and oxysterols: minute concentrations-major physiological effects, J. Steroid Biochem. Mol. Biol. 169 (2017) 4–9.
- [31] H. Gylling, P. Simonen, Phytosterols, phytosterols, and lipoprotein metabolism, Nutrients 7 (9) (2015) 7965–7977.
- [32] I. Coppens, Contribution of host lipids to *Toxoplasma* pathogenesis, Cell. Microbiol. 8 (1) (2006) 1–9.
- [33] B.N. Olsen, P.H. Schlesinger, D.S. Ory, N.A. Baker, 25-Hydroxycholesterol increases the availability of cholesterol in phospholipid membranes, Biophys. J. 100 (4) (2011) 948–956.
- [34] B.N. Olsen, P.H. Schlesinger, D.S. Ory, N.A. Baker, Side-chain oxysterols: from cells to membranes to molecules, Biochim. Biophys. Acta 1818 (2) (2012) 330–336.
- [35] V. Cagno, A. Cibra, D. Rossin, S. Gallipieri, C. Ceccia, V. Lenzi, N. Dorma, F. Biasi, G. Poli, D. Lembo, Inhibition of herpes simplex 1 virus replication by 25-hydroxycholesterol and 27-hydroxycholesterol, Redox Biol. 12 (2017) 522–527.
- [36] C.Y.M. Lin, D.W. Morel, Distribution of oxysterols in human serum: characterization of 25-hydroxycholesterol association with serum albumin, Nutr. Biochem. 6 (1995) 618–625.
- [37] W.J. Griffiths, J. Abdel-khalik, P.J. Crick, E. Yunus, Y. Wang, New methods for analysis of oxysterols and related compounds by LC-MS, J. Steroid Biochem. Mol. Biol. 162 (2016) 4–26.

2.3. EZETIMIBE BLOCKS *TOXOPLASMA GONDII*-, *NEOSPORA CANINUM*- AND *BESNOITIA BESNOITI*-TACHYZOITE INFECTIVITY AND REPLICATION IN PRIMARY BOVINE ENDOTHELIAL HOST CELLS

Larrazabal, C., Silva, L.M.R., Hermosilla, C., and Taubert, A. (2021).

Parasitology 148, 1107–1115.

Own part in the publication:

- Project planning: 50 %, Together with co-authors and supervisors
- Development of experiments: 80 %, Mainly independent
- Evaluation of experiments: 80 %, Mainly independent
- Writing of the manuscript: 80 %, Mainly independent

Ezetimibe blocks *Toxoplasma gondii*-, *Neospora caninum*- and *Besnoitia besnoiti*-tachyzoite infectivity and replication in primary bovine endothelial host cells



Parasitology

cambridge.org/par

Research Article

Cite this article: Larrazabal C, Silva LMR, Hermosilla C, Taubert A (2021). Ezetimibe blocks *Toxoplasma gondii*-, *Neospora caninum*- and *Besnoitia besnoiti*-tachyzoite infectivity and replication in primary bovine endothelial host cells. *Parasitology* **148**, 1107–1115. <https://doi.org/10.1017/S0031182021000822>

Received: 12 March 2021

Revised: 23 April 2021

Accepted: 19 May 2021

First published online: 24 May 2021

Key words:

Besnoitia besnoiti; Ezetimibe; *Neospora caninum*; NPC1L1; *Toxoplasma gondii*

Author for correspondence:

Camilo Larrazabal, E-mail: Camilo.Larrazabal@vetmed.uni-giessen.de

Ezetimibe blocks *Toxoplasma gondii*-, *Neospora caninum*- and *Besnoitia besnoiti*-tachyzoite infectivity and replication in primary bovine endothelial host cells

Camilo Larrazabal , Liliana M. R. Silva, Carlos Hermosilla and Anja Taubert

Institute of Parasitology, Biomedical Research Center Settersberg, Justus Liebig University Giessen, 35392 Giessen, Germany

Abstract

Coccidia are obligate apicomplexan parasites that affect humans and animals. In fast replicating species, *in vitro* merogony takes only 24–48 h. In this context, successful parasite proliferation requires nutrients and other building blocks. Coccidian parasites are auxotrophic for cholesterol, so they need to obtain this molecule from host cells. In humans, ezetimibe has been applied successfully as hypolipidaemic compound, since it reduces intestinal cholesterol absorption *via* blockage of Niemann–Pick C-1 like-1 protein (NPC1L1), a transmembrane protein expressed in enterocytes. To date, few data are available on its potential anti-parasitic effects in primary host cells infected with apicomplexan parasites of human and veterinary importance, such as *Toxoplasma gondii*, *Neospora caninum* and *Besnoitia besnoiti*. Current inhibition experiments show that ezetimibe effectively blocks *T. gondii*, *B. besnoiti* and *N. caninum* tachyzoite infectivity and replication in primary bovine endothelial host cells. Thus, 20 μ M ezetimibe blocked parasite proliferation by 73.1–99.2%, *via* marked reduction of the number of tachyzoites per meront, confirmed by 3D-holotomographic analyses. The effects were parasitostatic since withdrawal of the compound led to parasite recovery with resumed proliferation. Ezetimibe-glucuronide, the *in vivo* most effective metabolite, failed to affect parasite proliferation *in vitro*, thereby suggesting that ezetimibe effects might be NPC1L1-independent.

Introduction

Toxoplasma gondii, *Neospora caninum* and *Besnoitia besnoiti* are cyst-forming species belonging to the Apicomplexa phylum, which consists of a large group of obligatory intracellular protozoan parasites that affect both humans and animals. Despite morphological similarities between coccidian species, host specificity and clinical consequences greatly differ among them. In this context, *T. gondii* is considered a major public health problem and an abortive agent especially in ovines (Benavides *et al.*, 2017) and humans (Nayeri *et al.*, 2020). The closely related coccidian parasite *N. caninum* is currently considered as a major cause of abortions in cattle (Reichel *et al.*, 2013). In contrast, *B. besnoiti* causes bovine besnoitiosis, an emerging disease within Europe, which is characterized by massive alterations of skin and mucosae and also bull infertility (Álvarez-García *et al.*, 2013).

During the acute stage of infection, coccidian parasites undergo asexual replication within host cells. In this context, host endothelial cells have shown high permissiveness for tachyzoite infection and proliferation *in vivo* (Álvarez-García *et al.*, 2013; Konradt *et al.*, 2016). Likewise, primary bovine endothelial cells have consistently been reported as suitable for *in vitro* replication of *T. gondii*, *N. caninum* and *B. besnoiti* (Taubert *et al.*, 2006, 2016; Silva *et al.*, 2019; Velásquez *et al.*, 2019), allowing high tachyzoite proliferation rates in an experimental set up close to the *in vivo* scenario. During the fast proliferation phase, tachyzoites need significant amounts of nutrients for offspring development, which may be obtained from the host cell or newly synthesized. Specifically during coccidian replication high amounts of cholesterol are needed for new membrane biosynthesis (Coppens, 2013). Given that apicomplexan parasites are considered auxotrophic for cholesterol (Coppens, 2013), their replication within the parasitophorous vacuole (PV) highly depends on cholesterol supply by the host cell. In general, cellular cholesterol supply may be achieved either by enhancement of cellular endogenous *de novo* biosynthesis or by an increased cholesterol uptake from extracellular sources (Luo *et al.*, 2020). In line, apicomplexan parasites can differentially exploit cholesterol sources depending on host cell type and parasite species. LDL internalization appears the main pathway for cholesterol uptake, and cholesterol esterification allows for storage in lipid-rich organelles (Luo *et al.*, 2020). Recently, LDL-mediated cholesterol incorporation was described as pivotal, but not exclusive mechanism to fulfil cholesterol requirement during fast replicating coccidia proliferation (Nolan *et al.*, 2015; Silva *et al.*, 2019).

Based on pathophysiological consequences of human hyperlipidaemia, several pharmacological lipid-lowering compounds have been developed (Barter and Rye, 2016). Amongst these, ezetimibe is one of the most common hypolipidaemic drugs, which is capable of

© The Author(s), 2021. Published by Cambridge University Press. This is an Open Access article, distributed under the terms of the Creative Commons Attribution licence (<http://creativecommons.org/licenses/by/4.0/>), which permits unrestricted re-use, distribution, and reproduction in any medium, provided the original work is properly cited.

CAMBRIDGE
UNIVERSITY PRESS

<https://doi.org/10.1017/S0031182021000822> Published online by Cambridge University Press

Ezetimibe blocks *Toxoplasma gondii*-, *Neospora caninum*- and *Besnoitia besnoiti*-tachyzoite infectivity and replication in primary bovine endothelial host cells

1108

Camilo Larrazabal et al.

reducing intestinal cholesterol absorption by its interaction with Niemann–Pick C-1 like-1 protein (NPC1L1) in enterocytes (Davis et al., 2004; Garcia-Calvo et al., 2005). In detail, ezetimibe binds to NPC1L1, resulting in the blockage of NPC1L1 endocytosis into clathrin-coated vesicles and thereby diminishing cholesterol internalization into enterocytes (Ge et al., 2008; Wang et al., 2009). Despite that, the participation of other potential ezetimibe targets as the class B type 1 scavenger receptor (SR-BI) and the aminopeptidase N (CD13) have been linked to its hypolipidaemic effect (Kramer et al., 2005; Labonté et al., 2007). In general, the efficacy and safety of ezetimibe has been reported in mice and human studies (Bays et al., 2001; van Heek et al., 2001). As such, ezetimibe might represent a promising anti-parasitic drug candidate (Andrade-Neto et al., 2016). In line, ezetimibe treatments significantly reduced *Cryptosporidium parvum* growth in Caco-2 cells (Ehrenman et al., 2013). However, other evidences are incongruent: whilst ezetimibe reduced the parasite burden of *Leishmania amazonensis* in vivo, and diminished the *L. infantum* replication in vitro and in vivo (alone or in binary and ternary combination with miltefosine and itraconazole) (Andrade-Neto et al., 2016, 2021), this treatment did not affect *Plasmodium yoelii* parasitaemia in mice, while reduced the intraerythrocytic proliferation of *P. falciparum* in vitro (Kume et al., 2016; Hayakawa et al., 2021), thereby suggesting parasite-specific effects for this compound.

So far, no data are available on the impact of this drug on typical fast replicating coccidian parasites. Therefore, the aim of this study was to evaluate anti-parasitic efficacy of ezetimibe in *T. gondii*, *N. caninum* and *B. besnoiti*-infected primary bovine host endothelial cells.

Materials and methods

Host cell culture

Primary bovine umbilical vein endothelial cells (BUVEC) were isolated as described elsewhere (Taubert et al., 2006). BUVEC were cultured at 37°C and 5% CO₂ atmosphere in modified endothelial cell growth medium (modECGM), by diluting ECGM medium (Promocell™) with M199 (Sigma-Aldrich) at a ratio of 1:3, supplemented with 500 U/mL penicillin (Sigma-Aldrich) and 50 µg/mL streptomycin (Sigma-Aldrich) and 5% FCS (foetal calf serum; Biocrom). BUVEC of less than three passages were used in this study.

Parasites

Toxoplasma gondii (strain RH) and *Neospora caninum* (strain NC-1) tachyzoites were cultivated in vitro as described elsewhere (Taubert et al., 2006; Velásquez et al., 2019), by maintaining them at several passages in permanent African green monkey kidney epithelial cells (MARC 145) in Dubelcco's modified eagle medium (DMEM) (Sigma-Aldrich). *Besnoitia besnoiti* (strain Bb Evor04) tachyzoite stages were propagated in Madin–Darby bovine kidney cells (MDBK) (Velásquez et al., 2020) in Roswell Park Memorial Institute (RPMI) medium (Sigma-Aldrich). All culture media were supplemented with 500 U/mL penicillin and 50 µg/mL streptomycin and 5% foetal calf serum (FCS; Sigma-Aldrich). Infected and non-infected cells were cultured at 37°C and 5% CO₂ atmosphere. Vital tachyzoites were collected from supernatants of infected host cells (800 × g, 5 min) and re-suspended in modECGM for further experiments.

For infection rate-related experiments, tachyzoites of each species were pre-incubated in 20 µM ezetimibe for 1 h. After washing in modECGM (800 × g, 5 min), tachyzoites were used for infection experiments.

Treatments of host cells and infections

BUVEC ($n = 5$) were seeded in 12-well plates (Sarstedt) pre-coated with fibronectin (1:400, Sigma-Aldrich). Ezetimibe (Cayman Chemical) and ezetimibe-glucuronide (Santa Cruz Biotechnology) stock solutions were prepared in dimethyl sulphoxide (DMSO; Sigma-Aldrich, 33 mM), diluted in modECGM at 2.5, 5, 10 and 20 µM and administered to fully confluent cell monolayers 48 h before infection. ModECGM with DMSO (0.06%) served as vehicle control. Following pre-treatments, the medium was entirely removed and cells were infected with tachyzoites of *T. gondii*, *B. besnoiti* or *N. caninum* at a multiplicity of infection of 1:5 for 4 h under inhibitor-free conditions. Then, extracellular tachyzoites were removed and fresh medium with inhibitors was re-administered. At 4 h post infection (p. i.), phase-contrast images for infection rate estimation ((infected cells/total cells) × 100) were acquired by an inverted microscope (IX81, Olympus™) equipped with a digital camera (XM10, Olympus™). Tachyzoites present in cell culture supernatants were collected (800 × g, 5 min) at 48 h p. i. and counted in a Neubauer chamber.

Additionally, withdrawal experiments were carried out. Therefore, ezetimibe-containing medium was replaced by control medium at 24 h p. i. and parasite replication was estimated 24 h later ($n = 5$). Finally, further assays were performed to estimate the effect of ezetimibe over time as cells were treated as described above with a daily replacement of medium containing ezetimibe (20 µM) at 24, 48 and 72 h p. i., and tachyzoite proliferation was observed at 48, 72 and 96 h p. i., respectively ($n = 5$).

Live cell 3D holotomographic microscopy to illustrate parasite development

BUVEC were seeded into 35 mm tissue culture µ-dishes (Ibidi™) and cultured (37°C, 5% CO₂) until confluence. Ezetimibe treatment (20 µM) was performed as described above. Thereafter, *T. gondii*, *N. caninum* and *B. besnoiti* tachyzoites were used to infect cell layers (MOI = 3:1). At 24 h p. i., holotomographic images were obtained by using 3D Cell-Explorer-fluo microscope (Nanolive) equipped with a 60 × magnification ($\lambda = 520$ nm, sample exposure 0.2 mW/mm²) and a depth of field of 30 µM. Images were analysed using STEVE software (Nanolive) to obtain refractive index (RI)-based z-stacks (Silva et al., 2019). Additionally, digital staining was applied according to the RI of intracellular tachyzoites. Finally, intracellular meront development was evaluated by counting intra-meront tachyzoites in at least six 3D holotomographic z-stacks of infected host cells (= 500 cells per condition) in presence or absence of ezetimibe (20 µM).

RT-qPCR for relative quantification of NPC1L1 mRNA

BUVEC ($n = 5$) grown in 25 cm² culture tissue flasks (Greiner Bio-One) were infected with *T. gondii*, *N. caninum* or *B. besnoiti* tachyzoites (MOI = 5:1). Infected- and non-infected host cells were processed for total RNA isolation at four different time points after infection (3, 6, 12, 24 h p. i.). Tissue samples from bovine small intestine obtained at a local slaughterhouse were used as positive controls for NPC1L1. For total RNA isolation, the RNeasy kit (Qiagen) was used according to the manufacturer's instructions. Total RNAs were stored at -80°C until further use. In order to remove any genomic DNA leftover, DNA digestion step was performed. Therefore, 1 µg of total RNA was treated with 10 U DNase I (Thermo Scientific) in 1 × DNase reaction buffer (37°C, 30 min). DNase was inactivated by heating the samples (65°C, 10 min). The efficiency of genomic DNA digestion was confirmed by no-RT-controls in each RT-qPCR experiment. cDNA synthesis was performed using the SuperScript IV

Ezetimibe blocks *Toxoplasma gondii*-, *Neospora caninum*- and *Besnoitia besnoiti*-tachyzoite infectivity and replication in primary bovine endothelial host cells

(Invitrogen™) according to the manufacturer's instructions. Briefly, for first-strand cDNA synthesis, 1 µg of DNase treated total RNA was added to 0.5 µL of 50 µM oligo(dt), 1 µL of 50 ng/µL random hexamer primer, 1 µL of 10 mM dNTP mix in a total volume of 10 µL. Thereafter, the samples were incubated at 65°C for 5 min and then immediately cooled on ice. Additionally, 4 µL of 5× SSIV buffer, 1 µL 0.1 M DTT, 1 µL RNase free H₂O and 0.5 µL SuperScript IV enzyme were added obtaining a total volume of 20 µL. The samples were incubated at 23°C for 10 min followed by 50°C for 10 min and an 80°C inactivation step for 10 min.

Probes were labelled at the 5'-end with a reporter dye FAM (6-carboxyfluorescein) and at the 3'-end with the quencher dye TAMRA (6-carboxytetramethyl-rhodamine). bNPC11 primer sequences were designed as follows: *Bos taurus* NPC11 forward 5'-CTTCCCTGATATGCTTAC-3'; reverse 5'-GACCAGAGA TATAAAGGC-3' probe AGCCAGTCAATGAAGTCGCCA. qPCR amplification was performed on a Rotor-Gene Q Thermocycler (Qiagen) in duplicates in a 10 µL total volume containing 400 nM forward and reverse primers, 200 nM probe, 10 ng cDNA and 5 µL 2× PerfeCTa qPCR FastMix (Quanta Biosciences). The reaction conditions were as follows: 95°C for 10 min, 40 cycles at 95°C for 10 s, 60°C for 15 s and 72°C for 30 s. No-template controls and no-RT reactions were included in each experiment. As reference gene GAPDH was used as previously reported (Taubert et al., 2006; Hamid et al., 2014; Hamid et al., 2015).

Viability assessment

For experiments on parasite viability, 5×10^5 tachyzoites of each parasite species were treated for 1 h with vehicle (DMSO 0.06%) or ezetimibe (20 µM) (37°C, 5% CO₂). Thereafter, viability of tachyzoites was determined by the trypan blue (Sigma-Aldrich) exclusion staining assay as described elsewhere (Cervantes-Valencia et al., 2019). Non-stained parasites were considered as viable. Additionally, cell viability after compound treatments was assessed by the colorimetric XTT test (Promega®) according to the manufacturer instructions. Briefly, BUVEC seeded in 96-well plate (Greiner) were incubated with DMSO, ezetimibe or ezetimibe-glucuronide (both 20 µM) in a total volume of 50 µL for 72 h. Thereafter, 50 µL of XTT working solution was added, and samples were incubated for 4 h (37°C, 5% CO₂, atmosphere). The resulting formazan product was estimated via optical density (OD) measurements at 590 nm and reference filter 620-nm wavelength using Varioskan™ Flash Multimode Reader (Thermo Scientific).

Statistical analysis

For statistical analyses, the statistical software GraphPad® Prism 8 (version 8.4.3.) was used. Data description was performed by presenting arithmetic mean ± standard deviation. In addition, the non-parametric statistical test Mann–Whitney for comparison of two experimental conditions was applied. In cases of three or more conditions, Kruskal–Wallis test was used. Whenever global comparison by Kruskal–Wallis test indicated significance, *post hoc* multiple comparison tests were carried out by Dunn tests to compare test with control conditions. Outcomes of statistical tests were considered to indicate significant differences when $P < 0.05$ (significance level).

Results

Ezetimibe treatments effectively block *T. gondii*, *N. caninum* and *B. besnoiti* tachyzoite proliferation

To analyse the effects of ezetimibe on intracellular tachyzoite replication, functional inhibition experiments were performed,

thereby evaluating the number of freshly released tachyzoites at 48 h p. i. from cells pre-treated and exposed to ezetimibe during the intracellular parasite proliferation stage. Overall, ezetimibe treatments significantly inhibited tachyzoite replication of *T. gondii* (10 µM, $P = 0.0397$; 20 µM, $P = 0.0010$; Figure 1A), *N. caninum* (20 µM, $P = 0.0078$; Figure 1B) and *B. besnoiti* (10 µM, $P = 0.0059$; 20 µM, $P < 0.0001$; Figure 1C) in BUVEC in a dose-dependent manner. Overall, the strongest effect of ezetimibe treatments at 20 µM was observed in case of *B. besnoiti* (99.2 ± 0.5% replication reduction), followed by *T. gondii* (95.7 ± 2.3% reduction) and *N. caninum* (73.1 ± 2.8% reduction). In line, phase-contrast microscopy showed an impairment in meront development for *T. gondii* (Fig. 1A1 and 1A2), *N. caninum* (Fig. 1B1 and 1B2) and *B. besnoiti* (Fig. 1C1 and 1C2) infected BUVEC at 24 h p. i. To better visualize ezetimibe-based effects on parasite development, additionally live cell 3D holotomographic microscopy were performed. As illustrated in Fig. 2, treatments with ezetimibe led to reduced meront sizes in *T. gondii*, *N. caninum* and *B. besnoiti* infections (Fig. 2), without apparently affecting the morphology of non-infected host cells (data not shown). Additionally, the number of tachyzoites per PV was determined to better understand ezetimibe-derived impact on parasite development (Fig. 2). Ezetimibe treatments markedly reduced the number of tachyzoites per meront in all three parasite species (all: $P < 0.0001$), however, the strongest effect was observed for *B. besnoiti*, with a reduction of 68.2% on the mean number of tachyzoites per meront, followed by *T. gondii* and *N. caninum* showing more than 50% reduction (56.5% and 50.2%, respectively).

Fast replicating coccidian fulfil their replication cycle within 36–48 h p. i. in BUVEC layers *in vitro* (Taubert et al., 2006; Silva et al., 2019; Velásquez et al., 2019). In this context, the sustained inhibitory effect of ezetimibe over time was evaluated by counting tachyzoite production daily at 48, 72 and 92 h p. i. As depicted in Fig. 3, ezetimibe (20 µM) effectively blocked *T. gondii* (99.1 ± 0.0% reduction; A1–A4), *N. caninum* (75.9 ± 7.6% reduction; B1–B4) and *B. besnoiti* (99.6 ± 0.1% reduction; C1–C4) replication over time (48, 72 and 96 h p. i.).

To estimate whether ezetimibe induces either parasitostatic or parasitocidal effects, compound withdrawal experiments were performed at 24 h p. i. As illustrated in Fig. 4, remnant *T. gondii* and *N. caninum* tachyzoites quickly recovered and regained proliferative capacities 24 h after ezetimibe withdrawal. In contrast, *B. besnoiti* proved more sensitive for ezetimibe treatments showing an ongoing reduction (31.6 ± 5.3%) of tachyzoite production when compared to non-treated cells ($P = 0.15$).

Ezetimibe treatments reduce tachyzoite infectivity but fail to affect host cell permissiveness

To fulfil intracellular replication tachyzoites must first actively invade the host cells. To determine if anti-parasitic effects of ezetimibe also relied on reduced infection rates, both compartments, i. e. host cells and parasites, were separately treated with ezetimibe and then tested for infection rates 4 h after infection. Therefore, BUVEC were pre-treated with ezetimibe for 48 h before infection. At 4 h p. i. non-treated control cells presented an infection rate of 50.2% (Fig. 5A), 51.8% (Fig. 5B) and 47.0% (Fig. 5C), for *T. gondii*, *N. caninum* and *B. besnoiti*, respectively. In pre-treated cells, similar infection rates were observed for each parasite species (Fig. 5A–C), thereby denying any effect of ezetimibe pre-treatments. In contrast, ezetimibe pre-treatments of fresh tachyzoites significantly reduced invasive capacities of *T. gondii* ($P = 0.0079$; Figure 5A), *N. caninum* ($P = 0.0159$; Figure 5B) and *B. besnoiti* ($P = 0.0079$; Figure 5C) tachyzoites, when compared to non-treated control stages. Here, species-dependent effects

Ezetimibe blocks *Toxoplasma gondii*-, *Neospora caninum*- and *Besnoitia besnoiti*-tachyzoite infectivity and replication in primary bovine endothelial host cells

1110

Camilo Larrazabal et al.

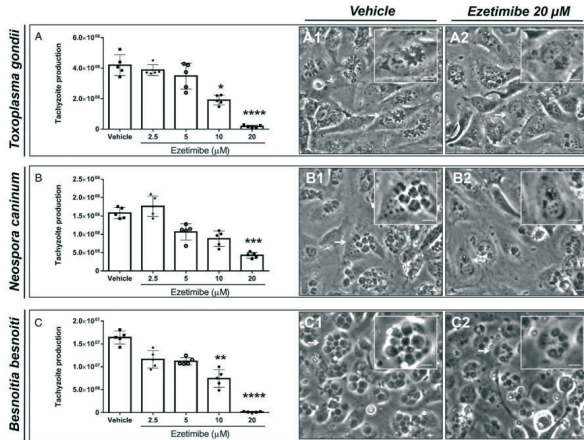


Fig. 1. Ezetimibe treatments inhibit *T. gondii*, *N. caninum* and *B. besnoiti* tachyzoite proliferation in primary endothelial cells. BVUEC were treated with ezetimibe (2.5, 5, 10 and 20 μM) 48 h before (A) *T. gondii*, (B) *N. caninum* or (C) *B. besnoiti* infection (MOI 1:5). 48 h after infection, the number of tachyzoites present in cell culture supernatants were counted (A–C). Exemplary illustration of *T. gondii* (A1–A2), *N. caninum* (B1–B2) or *B. besnoiti* (C1–C2) meront development at 24 h post infection. Scale bar represents 5 μm. Bars represent means of five biological replicates ± standard deviation. * $P \leq 0.05$; ** $P \leq 0.01$; *** $P \leq 0.001$; **** $P \leq 0.0001$.

were observed since the impact of ezetimibe pre-treatments were more prominent in case of *B. besnoiti* (28.1% reduction) than in *T. gondii* (22.2% reduction) or *N. caninum* (17.3% reduction).

Ezetimibe glucuronidation causes loss of anti-parasitic efficacy

Ezetimibe glucuronide is the major and pharmacologically active metabolite of ezetimibe following *in vivo* liver biotransformation. Thus, a functional assay to evaluate the effect of this chemically modified molecule on tachyzoite proliferation *in vitro* was performed (Fig. 6). Here, only ezetimibe but not its glucuronated derivative led to a reduction of *T. gondii*, *N. caninum* nor *B. besnoiti* tachyzoite proliferation.

NPCL1L gene is inconsistently transcribed in *T. gondii*-, *N. caninum*- and *B. besnoiti*-infected BVUEC

Given that NPCL1L is described as the main target of ezetimibe in humans, the profile of gene transcription of NPCL1L was estimated over infection kinetics (3–24 h p. i.) on *T. gondii*-, *N. caninum*- and *B. besnoiti*-infected BVUEC by qRT-PCR. Using bovine small intestine tissue samples, the functionality of the qPCR system was proved. However, infection-related data showed that neither *T. gondii*-, *N. caninum*- and *B. besnoiti*-infected BVUEC nor non-infected controls have a reliable amplification of NPCL1L mRNAs. Specifically, as illustrated in supplementary Table 1, NPCL1L was not detected in a consistent manner, thereby showing amplification only in some of the replicates at a rather high threshold cycle (CT > 30). Consequently, no

infection-driven effect on NPCL1L gene transcription was assumed.

Treatments does not cause cytotoxic damage to host cells or tachyzoites

To evaluate if ezetimibe (20 μM) treatment induced tachyzoite dead trypan blue exclusion test was performed. Our data showed an average viability of 95.2% ± 1.3, 90.7% ± 1.9 and 93.7% ± 2.1 for *T. gondii*-, *N. caninum* and *B. besnoiti* tachyzoites treated for 1 h with vehicle control (DMSO 0.06%) without significant effects provoked by ezetimibe (Fig. S1 A–C). Moreover, the cytotoxicity of ezetimibe or ezetimibe-glucuronide on endothelial host cells XTT test was performed. As illustrated in Fig. S1 D, treatments with ezetimibe or ezetimibe-glucuronide did not induce significant colorimetric changes in the formazan product compared to the vehicle control (DMSO 0.06%).

Discussion

Cholesterol is a major component of eukaryotic cell membranes (Luo et al., 2020). Given that apicomplexan parasites are generally considered as defective in cholesterol synthesis, they need to obtain this molecule from the host cell. Thus, LDL-driven cholesterol uptake is considered as a key pathway to fulfil cholesterol requirements during parasite merogony in different parasite species (Lababied et al., 2011; Coppens, 2013; Ehrenman et al., 2013; Hamid et al., 2014; Hamid et al., 2015; Nolan et al., 2015; Taubert et al., 2018; Silva et al., 2019). Additionally, in case

Ezetimibe blocks *Toxoplasma gondii*-, *Neospora caninum*- and *Besnoitia besnoiti*-tachyzoite infectivity and replication in primary bovine endothelial host cells

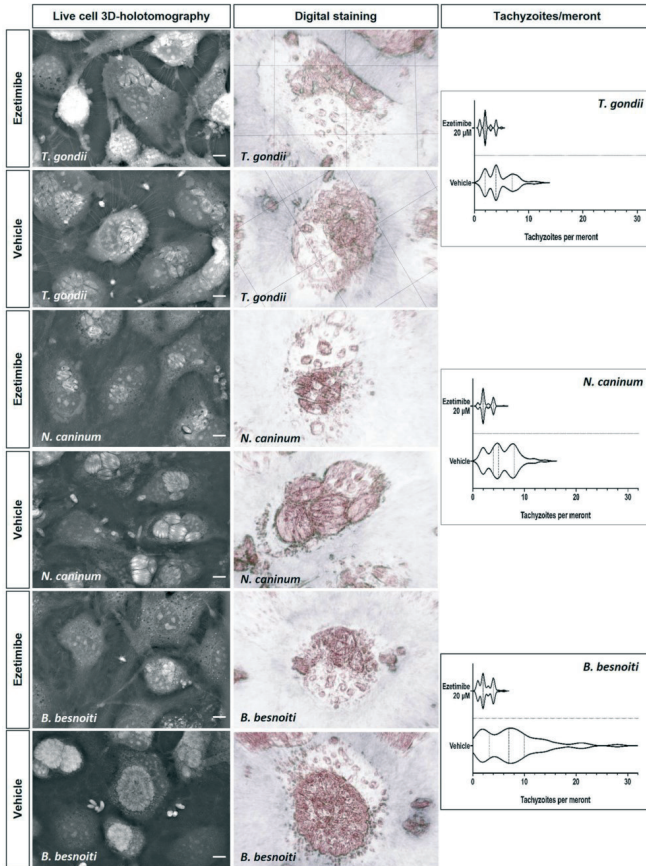


Fig. 2. Ezetimibe treatment affects intracellular meront formation and reduces the number of *T. gondii*, *N. caninum* and *B. besnoiti* intra-meront tachyzoites. Ezetimibe-pretreated BUVEC were infected with *T. gondii*, *N. caninum* and *B. besnoiti* tachyzoites and live cell 3D holographic microscopy was performed at 24 h p.i. Digital staining was achieved via STEVE software analysis. Violin plots depict the distribution of absolute *T. gondii*, *N. caninum* and *B. besnoiti* tachyzoite number per meront.

Ezetimibe blocks *Toxoplasma gondii*-, *Neospora caninum*- and *Besnoitia besnoiti*-tachyzoite infectivity and replication in primary bovine endothelial host cells

1112

Camilo Larrazabal *et al.*

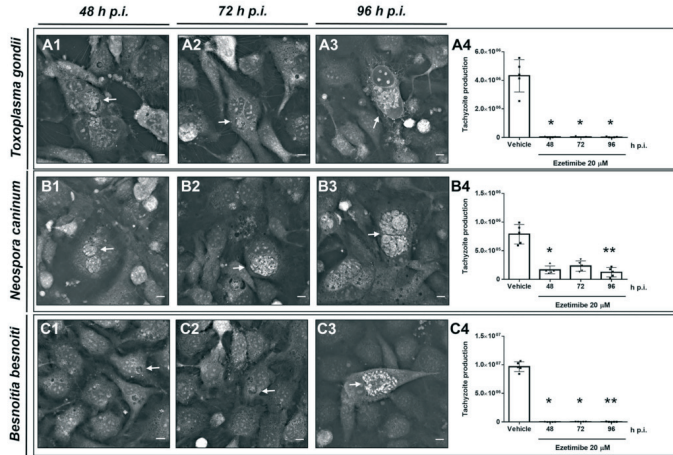


Fig. 3. Ezetimibe blocks *T. gondii*, *N. caninum* and *B. besnoiti* tachyzoite proliferation over time. BUVEC were treated with ezetimibe (20 μ M) 48 h before infection and then infected with *T. gondii* (A), *N. caninum* (B) and *B. besnoiti* (C) tachyzoites. Exemplary live cell 3D holotomographic illustration of *T. gondii* (A1–A3) *N. caninum* (B1–B3) or *B. besnoiti* (C1–C3) meront development (arrows) at 48, 72 and 96 h p. i., respectively. At 48, 72 and 96 h p. i., the number of tachyzoites present in cell culture supernatants were counted (A4, B4, C4). Bars represent means of five biological replicates \pm standard deviation. * $P < 0.05$; ** $P < 0.01$; *** $P < 0.001$; **** $P < 0.0001$.

of *C. parvum*-infected Caco-2 cells, cholesterol is incorporated via NPC1L1-mediated micellar uptake (Ehrenman *et al.*, 2013). NPC1L1 is a trans-membrane protein highly expressed in enterocytes that mediates sterol internalization via clathrin-coated vesicles and it has widely been accepted as main target of the lipid-lowering drug ezetimibe (Altmann *et al.*, 2004; Garcia-Calvo *et al.*, 2005; Beters and Yu, 2010).

Current data demonstrate for the first time that ezetimibe has inhibitory effects on *T. gondii*, *N. caninum*, and *B. besnoiti* tachyzoite replication in primary host endothelial cells, i.e. a host cell type that is parasitized *in vivo* during the acute phase of toxoplasmosis, neosporosis and besnoitiosis (Maley *et al.*, 2003; Alvarez-Garcia *et al.*, 2013; Konradt *et al.*, 2016). Here, 10 μ M ezetimibe treatment effectively blocked *T. gondii* and *B. besnoiti* proliferation, while *N. caninum* revealed less sensitive and inhibition needed a higher concentration of 20 μ M. However, both concentrations are in range or even lie below the concentration known to block effectively NPC1L1 endocytosis (25–100 μ M, Ehrenman *et al.*, 2013). Applying 20 μ M ezetimibe as effective concentration to all species studied, the anti-parasitic effects of this compound over time were explored. Its inhibitory effect on tachyzoite proliferation was consistent over time, since the number of newly released tachyzoites at 48, 72 and 96 h p. i. was consistently low. Thus, an overall reduction of tachyzoite production of 95.7, 73.1 and 93.2% was obtained for *T. gondii*, *N. caninum* and *B. besnoiti*, respectively. These findings in principle match data from *C. parvum*-infected Caco-2 cells (permanent cell line), where a growth reduction of 65% was achieved at 25–100 μ M

concentrations (Ehrenman *et al.*, 2013). *In vitro* anti-parasitic efficacy of ezetimibe was also reported for *L. amazonensis* where 10 μ M ezetimibe reduced promastigote replication, however, amastigote production was only affected at double doses (20 μ M; Andrade-Neto *et al.*, 2016). This stage-specific discrepancy might be explained by a lower sensitivity of intracellular stages to ezetimibe treatments. Still, the concentrations here used do not necessarily support this assumption, since high effects were found at 10 μ M ezetimibe in case of *T. gondii* and *B. besnoiti*-infected BUVEC. Thus, stage- and species-related or even host cell type-related sensitivities may play a role. In line, *P. falciparum*-merozoite replication was effectively blocked only at much higher concentrations of 80 μ M ezetimibe *in vitro* (Hayakawa *et al.*, 2020).

Successful parasite offspring formation relies on several defined processes starting with active cell invasion, formation of the PV, replication and egress (Black and Boothroyd, 2000). In this context, ezetimibe pre-treated extracellular tachyzoites showed impaired infection capacities, thereby hampering the replication process at the starting point. Of note, *B. besnoiti* tachyzoites appeared more sensitive to this treatment than *T. gondii* and *N. caninum* tachyzoites, the latter of which were hardly affected in their host cell invasion capacity.

A more detailed analysis of parasite intracellular development revealed an altered morphology of meronts in the case of all three parasites in treated host cells, suggesting that prolonged ezetimibe exposition indeed affected tachyzoite physiology, thereby reducing or hampering their ability to proliferate. Residual effects of ezetimibe on *in vitro* tachyzoite replication were evaluated by drug-

Ezetimibe blocks *Toxoplasma gondii*-, *Neospora caninum*- and *Besnoitia besnoiti*-tachyzoite infectivity and replication in primary bovine endothelial host cells

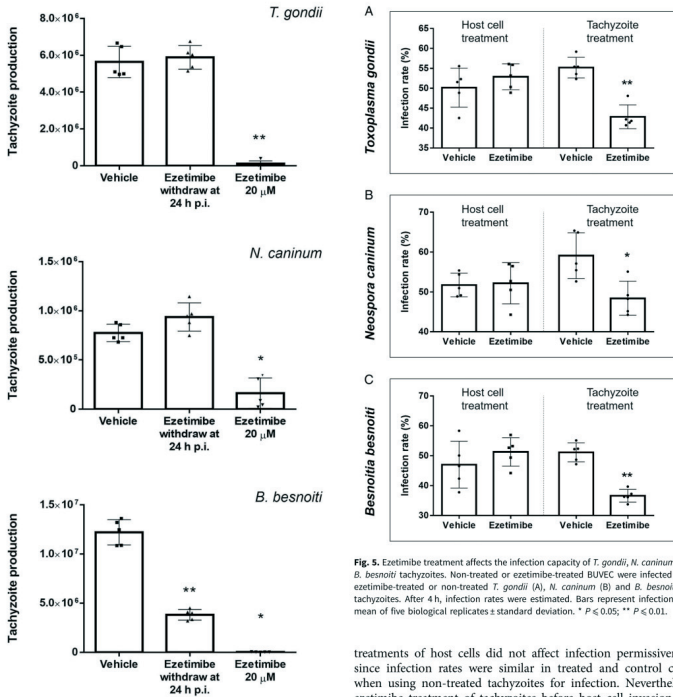


Fig. 4. Ezetimibe withdrawal restores *T. gondii* and *N. caninum* tachyzoite replication but hardly affects *B. besnoiti* recovery. Ezetimibe-treated BUEVC were infected with *T. gondii*, *N. caninum* and *B. besnoiti* tachyzoites. At 24 h p.i., ezetimibe was removed from cultures and tachyzoites present in supernatants 24 h after withdrawal were counted. Bars represent means of five biological replicates, standard deviation. * $P \leq 0.05$; ** $P \leq 0.01$; *** $P \leq 0.001$; **** $P \leq 0.0001$.

withdrawal experiments. Notably, *T. gondii* and *N. caninum* tachyzoites recovered within 24 h post withdrawal and proliferated at normal replication rates thereby showing that ezetimibe mainly induced developmental arrest but did not kill the parasites. In contrast, *B. besnoiti* tachyzoites suffered more profoundly from ezetimibe treatments since drug removal did not result in full recovery of parasite replication. These reactions indeed indicated species-specific sensitivity towards ezetimibe.

Overall, it is challenging to dissect if ezetimibe exclusively affects the parasites and/or the host cells, or if cumulative effects are to be considered. However, the current data showed that pre-

Fig. 5. Ezetimibe treatment affects the infection capacity of *T. gondii*, *N. caninum* and *B. besnoiti* tachyzoites. Non-treated or ezetimibe-treated BUEVC were infected with ezetimibe-treated or non-treated *T. gondii* (A), *N. caninum* (B) and *B. besnoiti* (C) tachyzoites. After 4 h, infection rates were estimated. Bars represent infection rate mean of five biological replicates \pm standard deviation. * $P \leq 0.05$; ** $P \leq 0.01$.

treatments of host cells did not affect infection permissiveness since infection rates were similar in treated and control cells, when using non-treated tachyzoites for infection. Nevertheless, ezetimibe treatment of tachyzoites before host cell invasion led to a significant reduction of infection rates, suggesting that ezetimibe also directly acts on tachyzoite invasive capacity in a rather species-dependent manner. Besides this mode of action, anti-parasitic activity of ezetimibe was also associated with inhibition of parasite replication within PV. By using live cell 3D holotomographic microscopy as a reliable tool for 3D cell visualization *in vivo* (Silva *et al.*, 2019; Velásquez *et al.*, 2019), we showed that ezetimibe-treated host cells infected with *T. gondii*, *N. caninum* and *B. besnoiti* presented a reduced number of tachyzoites per meront. Summarizing these data, ezetimibe might act on both, extra- and intracellular tachyzoites.

Hypolipidaemic/cholesterol-lowering properties of ezetimibe have previously been reported for humans as well as animals (Bays *et al.*, 2001; van Heek *et al.*, 2001; Knopp *et al.*, 2003). *In vivo*, this compound undergoes phase II metabolism to form a glucuronide conjugate thereby improving NPC1L1-specific affinity and binding capacities (García-Calvo *et al.*, 2005). Besides being the major metabolite detected in plasma (García-Calvo *et al.*, 2005), ezetimibe-glucuronide is therefore

Ezetimibe blocks *Toxoplasma gondii*-, *Neospora caninum*- and *Besnoitia besnoiti*-tachyzoite infectivity and replication in primary bovine endothelial host cells

1114

Camilo Larrazabal et al.

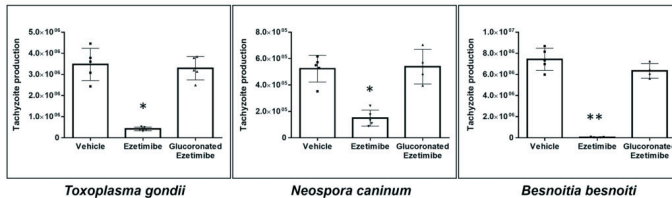


Fig. 6. Ezetimibe-mediated anti-parasitic effects are abolished by glucuronation. Ezetimibe- or ezetimibe-glucuronide-pre-treated BUEVC were infected with *T. gondii* (A), *N. caninum* (B) and *B. besnoiti* (C) tachyzoites. 48 h after infection, the number of tachyzoites present in cell culture supernatants were counted. Bars represent means of five biological replicates \pm standard deviation. * $P < 0.05$; ** $P < 0.01$; *** $P < 0.001$; **** $P < 0.0001$.

considered as main active metabolite in ezetimibe treatments *in vivo*. To parallel *in vivo* situation, additional studies on the effect of ezetimibe-glucuronide on *T. gondii*, *B. besnoiti* and *N. caninum* tachyzoite proliferation *in vitro* were performed. Unexpectedly, treatments with ezetimibe-glucuronide failed to hamper intracellular tachyzoite replication thereby implicating that ezetimibe-mediated anti-parasitic effects might be NPC1L1-independent. In line, we were not able to demonstrate a consistent infection-driven induction of NPC1L1 mRNAs since these gene transcripts could hardly be detected in infected BUEVC or control cells even though intestinal control tissues gave good PCR signals. Consequently, we here assume a very low expression of this transporter in BUEVC. Likewise, the presence of NPC1L1 protein expression by Western blotting was not achieved, so far (unpublished data). Noteworthy, ezetimibe was originally identified as an ACAT II inhibitor (Clader, 2004) and therefore as acting on other potential targets besides NPC1L1. Irrespective of this, it is well documented that NPC1L1 incorporates cholesterol through an ezetimibe-sensitive pathway, however, the binding mechanism between ezetimibe and NPC1L1 remains unknown (Betters and Yu, 2010). Recently, it has been reported that ezetimibe, but not ezetimibe-glucuronide, reduces the cellular content of cholesterol esters in a NPC1L1-independent manner in human monocytes, implying an inhibition of ACAT II (Orso et al., 2019). Likewise, we here propose that the current ezetimibe-mediated anti-coccidial effects may rather be linked to an inhibition of cholesterol esterification. In agreement, the importance of functional cholesterol esterification for coccidial replication was already confirmed for *T. gondii* (Sonda et al., 2001), *B. besnoiti* (Silva et al., 2019) and *E. bovis* (Hamid et al., 2014). However, the actual role of ezetimibe in cholesterol esterification and its cytosolic targets in primary bovine endothelial host cells should be further addressed in future studies. Even though *in vitro* studies have been published reporting anti-parasitic activities of ezetimibe treatments, *in vivo* evidence still needs to be addressed. Nevertheless, administration of ezetimibe to *L. amazonensis*-infected mice led to reduced parasite burden and boosted anti-leishmanial activity of ketoconazole (Andrade-Neto et al., 2016). However, given that ezetimibe treatments of *P. yoelii*-infected mice failed to affect parasitaemia (Kume et al., 2016) phylum-derived differences have to be assumed. In conclusion, the current study shows that ezetimibe effectively inhibits *T. gondii*, *N. caninum* and *B. besnoiti* tachyzoite replication in BUEVC in a time-sustained but reversible manner. Apparently, the anti-coccidial effect of ezetimibe is associated with both impairment of tachyzoite infectivity and intracellular replication blockage. Of note, we additionally observed that

ezetimibe-glucuronide does not interfere with parasite replication thereby suggesting an NPC1L1-independent anti-parasitic mechanism.

Supplementary material. The supplementary material for this article can be found at <https://doi.org/10.1017/S0031182021000822>.

Data. All data are available in the manuscript and Supplementary data files.

Acknowledgements. The authors would like to thank Christine Henrich, Dr Christin Ritter and Hannah Salecker for their outstanding technical support. We also are very thankful to Prof. Dr A. Wehrend (Clinic for Obstetrics, Gynaecology and Andrology of Large and Small Animals, Justus Liebig University, Giessen, Germany) for the continuous supply of bovine umbilical cords. Further, we thank Oliver Bender (Übl butcher shop, Langsdorf, Germany) for the supply of bovine small intestine samples.

Author contributions.

AT, CH, CL and LS conceived and designed the experiments. CL and LS performed the experiments. All authors performed analyses and interpretation of the data, preparation of the manuscript and approved final version of manuscript.

Financial support. CL was funded by the National Agency for Research and Development [(ANID), DOCTORADO BECAS CHILE/2017-72180349].

Conflict of interest. The authors declare there are no conflicts of interest.

Ethical standards. Not applicable

References

- Altmann SW, Davis HR Jr., Zhu JJ, Yao X, Hoos LM, Tetzloff G, Iyer SP, Maguire M, Golovko A, Zeng M, Wang L, Murgolo N and Graziano MP (2004) Niemann-Pick C1 like 1 protein is critical for intestinal cholesterol absorption. *Science (New York, N.Y.)* **303**, 1201–1204.
- Alvarez-García G, Frey CF, Mora LM and Schares G (2013) A century of bovine besnoitosis: an unknown disease re-emerging in Europe. *Trends in Parasitology* **29**, 407–415.
- Andrade-Neto VV, Cunha-Junior EF, Canto-Cavalheiro MM, Atella GC, Fernandes TA, Costa PR and Torres-Santos EC (2016) Antileishmanial activity of ezetimibe: inhibition of sterol biosynthesis, *in vitro* synergy with azoles, and efficacy in experimental cutaneous leishmaniasis. *Antimicrobial Agents and Chemotherapy* **60**, 6844–6852.
- Andrade-Neto VV, Rebelo KM, Pereira TM and Torres-Santos EC (2021) Effect of itraconazole-ezetimibe-miltefosine ternary therapy in murine visceral leishmaniasis. *Antimicrobial Agents and Chemotherapy* **65**, e02676–20, [/aac/65/5/AAC.02676-20.atom](https://doi.org/10.1128/AAC.02676-20.atom).
- Barter PJ and Rye KA (2016) New era of lipid-lowering drugs. *Pharmacological Reviews* **68**, 458–475.
- Bays HE, Moore PB, Drechsel MA, Rosenblatt S, Toth PD, Djouane CA, Knapp RH, Lipka LJ, Lebeaut AP, Yang B, Mellars LE, Caffie-Jackson C, Veltri EP and Ezetimibe Study G (2001) Effectiveness and tolerability

Ezetimibe blocks *Toxoplasma gondii*-, *Neospora caninum*- and *Besnoitia besnoiti*-tachyzoite infectivity and replication in primary bovine endothelial host cells

Parasitology

1115

- of ezetimibe in patients with primary hypercholesterolemia: pooled analysis of two phase II studies. *Clinical Therapeutics* 23, 1209–1230.
- Benavides J, Fernandez M, Castano P, Ferreras MC, Ortega-Mora I and Perez V (2017)** Ovine toxoplasmosis: a new look at its pathogenesis. *Journal of Comparative Pathology* 157, 34–38.
- Beters JL and Yu L (2010)** NPC1L1 And cholesterol transport. *FEBS Letters* 584, 2740–2747.
- Black MW and Boothroyd JC (2000)** Lytic cycle of *Toxoplasma gondii*. *Microbiology and Molecular Biology Reviews* 64, 607–623.
- Cervantes-Valencia ME, Hermosilla C, Alcalá-Canto Y, Tapia G, Taubert A and Silva LMR (2019)** Antiparasitic efficacy of curcumin against *Besnoitia besnoiti* tachyzoites in vitro. *Frontiers in Veterinary Science* 5, 333. doi: 10.3389/fvets.2019.00333
- Chader JW (2004)** The discovery of ezetimibe: a view from outside the receptor. *Journal of Medicinal Chemistry* 47, 1–9.
- Coppens I (2013)** Targeting lipid biosynthesis and salvage in apicomplexan parasites for improved chemotherapies. *Nature Reviews Microbiology* 11, 823–835.
- Davis HR Jr, Zhu LJ, Hoos LM, Tetloff G, Maguire M, Liu J, Yao X, Iyer SP, Lam MH, Lund EG, Detmers PA, Graziano MP and Altmann SW (2004)** Niemann-Pick C1 like 1 (NPC1L1) is the intestinal phytosterol and cholesterol transporter and a key modulator of whole-body cholesterol homeostasis. *Journal of Biological Chemistry* 279, 33586–33592.
- Ehrenman K, Wanjiyri JW, Bhat N, Ward HD and Coppens I (2013)** *Cryptosporidium parvum* scavenges LDL-derived cholesterol and micellar cholesterol internalized into enterocytes. *Cellular Microbiology* 15, 1182–1197.
- García-Calvo M, Lissnock J, Bull HG, Haves BE, Burnett DA, Braun MP, Crona JH, Davis HR Jr, Dean DC, Detmers PA, Graziano MP, Hughes M, Macintyre DE, Ogawa A, O'Neill K A, Iyer SP, Shevell DE, Smith MM, Tang YS, Makarewicz AM, Ujjainwalla F, Altmann SW, Chapman KT and Thornberry NA (2005)** The target of ezetimibe is Niemann-Pick C1 like 1 (NPC1L1). *Proceedings of the National Academy of Sciences of the United States of America* 102, 8132–8137.
- Ge L, Wang J, Qi W, Miao HH, Cao J, Qu YX, Li BL and Song BL (2008)** The cholesterol absorption inhibitor ezetimibe acts by blocking the sterol-induced internalization of NPC1L1. *Cell Metabolism* 7, 508–519.
- Hamid PH, Hirschman J, Hermosilla C and Taubert A (2014)** Differential inhibition of host cell cholesterol de novo biosynthesis and processing abrogates *Eimeria bovis* intracellular development. *Parasitology Research* 113, 4165–4176.
- Hamid PH, Hirschman J, Kerner K, Gimpl G, Lochnit G, Hermosilla CR and Taubert A (2015)** *Eimeria bovis* infection modulates endothelial host cell cholesterol metabolism for successful replication. *Veterinary Parasitology* 46, 100.
- Hayakawa EH, Yamaguchi K, Mori M and Nardone G (2020)** Real-time cholesterol sorting in *Plasmodium falciparum*-erythrocytes as revealed by 3D label-free imaging. *Scientific Reports* 10, 2794.
- Hayakawa EH, Kato H, Nardone GA and Usukura J (2021)** A prospective mechanism and source of cholesterol uptake by *Plasmodium falciparum*-infected erythrocytes co-cultured with HepG2 cells. *Parasitology International* 80, 102179.
- Knopp RH, Gitter H, Traut T, Bays H, Manion CV, Lipka LJ, LeBeant AP, Suresh R, Yang B, Vaturi EP and Ezetimibe Study G (2003)** Effects of ezetimibe, a new cholesterol absorption inhibitor, on plasma lipids in patients with primary hypercholesterolemia. *European Heart Journal* 24, 729–741.
- Konradt C, Ueno N, Christian DA, Delong JH, Pritchard GH, Herz J, Bzik DJ, Koshy AA, McGavern DB, Lodoen MB and Hunter CA (2016)** Endothelial cells are a replicative niche for entry of *Toxoplasma gondii* to the central nervous system. *Nature Microbiology* 1, 16001.
- Kramer W, Girbig F, Gosiero D, Pfenninger A, Frick W, Jähne G, Rhein M, Wendler W, Lottspeich F, Hochleitner EO, Erosé E and Schmitz G (2005)** Aminopeptidase N (CD13) is a molecular target of the cholesterol absorption inhibitor ezetimibe in the enterocyte brush border membrane. *Journal of Biological Chemistry* 280, 1306–1320.
- Kume A, Herbas MS, Shichiri M, Ishida N and Suzuki H (2016)** Effect of anti-hyperlipidemia drugs on the alpha-tocopherol concentration and their potential for murine malaria infection. *Parasitology Research* 115, 69–75.
- Labelled M, Jayabalasingham B, Bano N, Cha SJ, Sandoval J, Guan G and Coppens I (2011)** *Plasmodium* salvages cholesterol internalized by LDL and synthesized de novo in the liver. *Cellular Microbiology* 13, 569–586.
- Labonté ED, Howles PN, Granholm NA, Rojas JC, Davies JP, Ioannou YA and Hui DY (2007)** Class B type I scavenger receptor is responsible for the high affinity cholesterol binding activity of intestinal brush border membrane vesicles. *Biochimica et Biophysica Acta* 1771, 1132–1139.
- Lao J, Yang H and Song B-L (2020)** Mechanisms and regulation of cholesterol homeostasis. *Nature Reviews Molecular Cell Biology* 21, 225–245.
- Maley SW, Buxton D, Rae AG, Wright SE, Schock A, Bartley PM, Esteban-Redondo I, Swales C, Hamilton CM, Sales J and Innes EA (2003)** The pathogenesis of neosporosis in pregnant cattle: inoculation at mid-gestation. *Journal of Comparative Pathology* 119, 186–195.
- Nayeri T, Sarvi S, Moosazadeh M, Amouei A, Hosseinijad Z and Daryani A (2020)** The global seroprevalence of anti-*Toxoplasma gondii* antibodies in women who had spontaneous abortion: a systematic review and meta-analysis. *PLoS Neglected Tropical Diseases* 14, e0008103. doi: 10.1371/journal.pntd.0008103.
- Nolan SJ, Romano JD, Luechtfeld T and Coppens I (2015)** *Neospora caninum* recruits host cell structures to its parasitophorous vacuole and salvages lipids from organelles. *Eukaryotic Cell* 14, 454–473.
- Osw E, Robenek H, Boettcher A, Wolf Z, Lieblich G, Kramer W and Schmitz G (2019)** Nongluconidated ezetimibe disrupts CD13- and CD64-cosmelly in membrane microdomains and decreases cellular cholesterol content in human monocytes/macrophages. *Cytometry, Part A: The Journal of the International Society for Analytical Cytology* 95, 869–884.
- Reichel MP, Alejandra Ayanequi-Alcérrea M, Gondim LF and Ellis JT (2013)** What is the global economic impact of *Neospora caninum* in cattle – the billion dollar question. *International Journal for Parasitology* 43, 133–142.
- Silva LMR, Lütjohann D, Hamid P, Velásquez ZD, Kerner K, Larrazabal C, Fälling K, Hermosilla C and Taubert A (2019)** *Besnoitia besnoiti* infection alters both endogenous cholesterol de novo synthesis and exogenous LDL uptake in host endothelial cells. *Scientific Reports* 9, 6650.
- Sonda S, Ting LM, Novak S, Kim K, Maher JP, Farese RV Jr and Ernst JD (2001)** Cholesterol esterification by host and parasite is essential for optimal proliferation of *Toxoplasma gondii*. *Journal of Biological Chemistry* 276, 34434–34440.
- Taubert A, Zahner H and Hermosilla C (2006)** Dynamics of transcription of immunomodulatory genes in endothelial cells infected with different ocidial parasites. *Veterinary Parasitology* 142, 214–222.
- Taubert A, Hermosilla C, Silva LM, Wiek A, Fälling K and Mazurek S (2016)** Metabolic signatures of *Besnoitia besnoiti*-infected endothelial host cells and blockage of key metabolic pathways indicate high glycolytic and glutaminolytic needs of the parasite. *Parasitology Research* 115, 2023–2034.
- Taubert A, Silva LMR, Velásquez ZD, Larrazabal C, Lütjohann D and Hermosilla C (2018)** Modulation of cholesterol-related sterols during *Eimeria bovis* macronemont formation and impact of selected oxysterols on parasite development. *Molecular and Biochemical Parasitology* 223, 1–12.
- van Heck M, Farley C, Compton DS, Hoos L and Davis HR (2001)** Ezetimibe selectively inhibits intestinal cholesterol absorption in rodents in the presence and absence of exocrine pancreatic function. *British Journal of Pharmacology* 134, 409–417.
- Velásquez ZD, Conjejeros I, Larrazabal C, Kerner K, Hermosilla C and Taubert A (2019)** *Toxoplasma gondii*-induced host cellular cell cycle dysregulation is linked to chromosome missegregation and cytokinesis failure in primary endothelial host cells. *Scientific Reports* 9, 12496.
- Velásquez ZD, Lopez-Ovorio S, Perizán-Orozqui I, Herold S, Hermosilla C and Taubert A (2020)** *Besnoitia besnoiti*-driven endothelial host cell cycle alteration. *Parasitology Research* 119, 2563–2577.
- Wang J, Chu BB, Ge L, Li BL, Yan Y and Song BL (2009)** Membrane topology of human NPC1L1, a key protein in enterohepatic cholesterol absorption. *Journal of Lipid Research* 50, 1653–1662.

2.4. P-GLYCOPROTEIN INHIBITORS DIFFERENTLY AFFECT TOXOPLASMA GONDII, NEOSPORA CANINUM AND BESNOITIA BESNOITI PROLIFERATION IN BOVINE PRIMARY ENDOTHELIAL CELLS

Larrazabal, C., Silva, L.M.R., Pervizaj-Oruqaj, L., Herold, S., Hermosilla, C., and Taubert, A. (2021).

Pathogens 10 (4):395; doi: 10.3390/pathogens10040395

Own part in the publication:

- Project planning: 50 %, Together with co-authors and supervisors
- Development of experiments: 80 %, Mainly independent
- Evaluation of experiments: 60 %, Together with co-authors
- Writing of the manuscript: 80 %, Mainly independent

P-glycoprotein inhibitors differently affect *Toxoplasma gondii*, *Neospora caninum* and *Besnoitia besnoiti* proliferation in bovine primary endothelial cells



Article

P-Glycoprotein Inhibitors Differently Affect *Toxoplasma gondii*, *Neospora caninum* and *Besnoitia besnoiti* Proliferation in Bovine Primary Endothelial Cells

Camilo Larrazabal ^{1,*}, Liliana M. R. Silva ¹, Learta Pervizaj-Oruqaj ^{2,3}, Susanne Herold ^{2,3}, Carlos Hermosilla ¹ and Anja Taubert ¹

¹ Biomedical Research Center Seltersberg, Institute of Parasitology, Justus Liebig University Giessen, 35392 Giessen, Germany; Liliana.Silva@vetmed.uni-giessen.de (L.M.R.S.); Carlos.R.Hermosilla@vetmed.uni-giessen.de (C.H.); Anja.Taubert@vetmed.uni-giessen.de (A.T.)

² The Cardio-Pulmonary Institute (CPI), 35392 Giessen, Germany; Learta.Pervizaj-Oruqaj@innere.med.uni-giessen.de (L.P.-O.); Susanne.Herold@innere.med.uni-giessen.de (S.H.)

³ Member of the German Center for Lung Research (DZL), Department of Pulmonary and Critical Care Medicine and Infectious Diseases, Universities of Giessen and Marburg Lung Center (UGMLC), Justus-Liebig University Giessen, 35392 Giessen, Germany

* Correspondence: Camilo.Larrazabal@vetmed.uni-giessen.de



Citation: Larrazabal, C.; Silva, L.M.R.; Pervizaj-Oruqaj, L.; Herold, S.; Hermosilla, C.; Taubert, A. P-glycoprotein Inhibitors Differently Affect *Toxoplasma gondii*, *Neospora caninum* and *Besnoitia besnoiti* Proliferation in Bovine Primary Endothelial Cells. *Pathogens* **2021**, *10*, 395. <https://doi.org/10.3390/pathogens10040395>

Academic Editor: Geoff Hide

Received: 18 February 2021

Accepted: 24 March 2021

Published: 25 March 2021

Publisher's Note: MDPI stays neutral with regard to jurisdictional claims in published maps and institutional affiliations.



Copyright: © 2021 by the authors. Licensee MDPI, Basel, Switzerland. This article is an open access article distributed under the terms and conditions of the Creative Commons Attribution (CC BY) license (<https://creativecommons.org/licenses/by/4.0/>).

Abstract: Apicomplexan parasites are obligatory intracellular protozoa. In the case of *Toxoplasma gondii*, *Neospora caninum* or *Besnoitia besnoiti*, to ensure proper tachyzoite production, they need nutrients and cell building blocks. However, apicomplexans are auxotrophic for cholesterol, which is required for membrane biosynthesis. P-glycoprotein (P-gp) is a transmembrane transporter involved in xenobiotic efflux. However, the physiological role of P-gp in cholesterol metabolism is unclear. Here, we analyzed its impact on parasite proliferation in *T. gondii*-, *N. caninum*- and *B. besnoiti*-infected primary endothelial cells by applying different generations of P-gp inhibitors. Host cell treatment with verapamil and valsopodar significantly diminished tachyzoite production in all three parasite species, whereas tariquidar treatment affected proliferation only in *B. besnoiti*. 3D-holotomographic analyses illustrated impaired meront development driven by valsopodar treatment being accompanied by swollen parasitophorous vacuoles in the case of *T. gondii*. Tachyzoite and host cell pre-treatment with valsopodar affected infection rates in all parasites. Flow cytometric analyses revealed verapamil treatment to induce neutral lipid accumulation. The absence of a pronounced anti-parasitic impact of tariquidar, which represents here the most selective P-gp inhibitor, suggests that the observed effects of verapamil and valsopodar are associated with mechanisms independent of P-gp. Out of the three species tested here, this compound affected only *B. besnoiti* proliferation and its effect was much milder as compared to verapamil and valsopodar.

Keywords: P-glycoprotein; ABCB1-transporter; *Toxoplasma gondii*; *Neospora caninum*; *Besnoitia besnoiti*; verapamil; valsopodar; tariquidar

1. Introduction

Toxoplasma gondii, *Neospora caninum* and *Besnoitia besnoiti* are obligatory intracellular parasitic protists known as cyst-forming coccidia and belonging to the family Sarcocystidae of the phylum Apicomplexa. Many apicomplexans are causal agents of important human and animal diseases with variable host specificity and clinical outcomes [1]. In specific, *T. gondii* has the widest known host range among eukaryotic parasites as virtually all mammals and even some birds can be infected. This species represents a serious health threat [2] as prenatal infections may lead to abortions in humans and sheep [3,4]. In contrast, the closely related coccidian *N. caninum* does not infect humans, but it is one of the most important abortive agents in cattle worldwide [5,6]. The third species, *B. besnoiti*,

P-glycoprotein inhibitors differently affect *Toxoplasma gondii*, *Neospora caninum* and *Besnoitia besnoiti* proliferation in bovine primary endothelial cells

causes bovine besnoitiosis, which is emergent in Europe and leads to massive alterations of the skin and mucosa of cattle as well as infertility in bulls [7]. During the acute stage of infection, cyst-forming coccidian parasites undergo asexual intracellular proliferation, quickly releasing a considerable number of offspring (tachyzoites). This stage is linked with clinical manifestations of the parasite infection, and is followed by a slow replicative process with bradyzoites enclosed in cysts, which are infective for the definitive hosts (felids and canids) [1].

Considering the relevance of the tachyzoite replication in the acute phase of infection, several reports demonstrated that primary bovine umbilical vein endothelial cells (BUVEC) represent suitable host cells for in vitro replication of all three species [8–12], allowing fast tachyzoite replication in a setting close to the in vivo situation. During this replication process, one of the most demanded molecules is cholesterol. Being auxotrophic for cholesterol synthesis, coccidian parasites either trigger its uptake from exogenous sources or induce the de novo synthesis of this compound by infected host cells [8,13–16]. Low density lipoprotein (LDL)-mediated endocytosis represents the main uptake mechanism in many types of host cells [17]. *T. gondii*, *N. caninum* and *B. besnoiti* were reported to rely on host cell LDL endocytosis for cholesterol uptake during tachyzoite replication [8,13,14]. To prevent toxic accumulation of free cholesterol in the cell, most excess of it is esterified and stored in lipid-rich organelles, such as lipid droplets [18,19], being available for parasite consumption [8,13]. Thus, to satisfy an increased need of cholesterol and other lipids in infected host cells, lipid droplet size and number are reported to be significantly increased [8,20].

Other strategy to face the challenge of lipid imbalance is the use of ATP binding cassette (ABC) transporter-mediated efflux mechanisms [21,22]. ABC transporters are highly evolutionarily conserved and ubiquitous molecules that mediate a broad range of physiological functions [21]. In eukaryotic cells, one of the most extensively studied members of the ABC transporter family is P-glycoprotein (P-gp; syn. ABCB1) [21], the expression of which is frequently correlated with the removal of hydrophobic compounds from the cell [22,23]. This transmembrane protein, also called multidrug resistance protein 1 (MDR1), is vastly associated with drug resistance phenomena in cancer cells [24]. Noteworthy, the participation of this transporter in drug resistance has been proposed also for protozoan parasites, such as *T. gondii* [25], *Leishmania* spp. [26] and *Plasmodium falciparum* [27], as well as for helminths like *Schistosoma mansoni* [28], *Teladorsagia circumcincta*, *Haemonchus contortus* [29] and *Echinococcus granulosus* [30]. Despite the well-known role of P-gp in drug resistance development, little is known about its impact on cell metabolism. As such, this protein seems to be involved in host cellular cholesterol transport to the parasitophorous vacuole (PV) during *T. gondii* and *N. caninum* replication [31], and might be necessary to maintain cholesterol homeostasis during coccidian infections. P-gp inhibition was demonstrated to suppress replication in some coccidia and microsporidia [31,32]. However, P-gp blockers represent a heterogeneous group of compounds. By now, three generations of pharmacological P-gp blockers have been developed, differing greatly in chemical and pharmacological terms [33].

In this work, we explored the effects of P-gp inhibitors on in vitro proliferation of different fast-replicating coccidian species (*T. gondii*, *N. caninum* and *B. besnoiti*) by testing the L-type Ca⁺⁺ channel blocker verapamil [34], the non-immunosuppressive cyclosporine D derivative valsopodar [35,36] and the highly selective allosteric inhibitor tariquidar [37,38], as representative compounds of each P-gp blocker generation. The aim of this work was to identify and compare anti-coccidial properties of well-known compounds for future drug repurposing reasons.

2. Results

2.1. Different Generations of P-Gp Inhibitors Vary in Their Impact on Tachyzoite Replication

The efficacy of verapamil, valsopodar and tariquidar treatment on tachyzoite replication was evaluated via functional inhibition assays, determining the number of freshly released

P-glycoprotein inhibitors differently affect *Toxoplasma gondii*, *Neospora caninum* and *Besnoitia besnoiti* proliferation in bovine primary endothelial cells

tachyzoites present in the medium at 48 h post infection (p. i.). The current data showed that verapamil effectively inhibited parasite replication in a dose-dependent manner (Figure 1). Thus, *T. gondii* replication (Figure 1A) was diminished by $45.7 \pm 11.7\%$ ($p = 0.0508$) and $84.04 \pm 7.6\%$ ($p = 0.001$) at 20 and 40 μM , respectively. At the same concentrations, this compound led to a reduction of *N. caninum* replication (Figure 1B) by $64.9 \pm 10.4\%$ ($p = 0.009$) and $84.5 \pm 2.7\%$ ($p = 0.0001$), respectively, and to a decrease of *B. besnoiti* parasite production (Figure 1C) by $36.6 \pm 5.9\%$ ($p = 0.07$) and $84.5 \pm 2.7\%$ ($p = 0.0005$). Lower concentrations of verapamil (5 and 10 μM) failed to significantly affect tachyzoite proliferation in any species studied here.

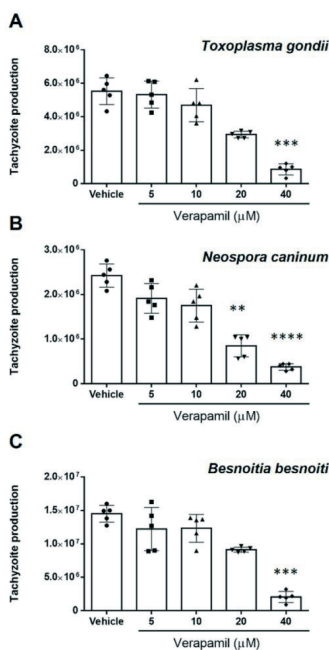


Figure 1. Verapamil treatment reduces *T. gondii*, *N. caninum* and *B. besnoiti* tachyzoite proliferation in a dose-dependent manner. The hosts cells pre-treated with verapamil (5, 10, 20 and 40 μM) were infected with *T. gondii* (A), *N. caninum* (B) or *B. besnoiti* (C) tachyzoites in inhibitor-free medium for 4 h, followed by the compound re-administration. At 48 h after infection, the number of tachyzoites present in cell culture supernatants were counted. Bars represent means of five biological replicates \pm standard deviation.

P-glycoprotein inhibitors differently affect *Toxoplasma gondii*, *Neospora caninum* and *Besnoitia besnoiti* proliferation in bovine primary endothelial cells

Alike verapamil, treatment with valsopodar also caused a dose-dependent reduction of tachyzoite proliferation (Figure 2). Thus, *T. gondii* replication (Figure 2A) was reduced by $67.8 \pm 10.4\%$ ($p = 0.78$), $91.6 \pm 3.4\%$ ($p = 0.07$) and $98.9 \pm 0.3\%$ ($p = 0.002$) at 1.25, 2.5 and 5 μM concentration, respectively. Likewise, *N. caninum* replication (Figure 2B) was reduced at 2.5 and 5 μM concentrations, leading to a proliferation diminishment of $64.0 \pm 5.0\%$ ($p = 0.0068$) and $92.8 \pm 2.5\%$ ($p = 0.0001$), respectively. Furthermore, *B. besnoiti* replication (Figure 2C) was blocked at 1.25, 2.5 and 5 μM valsopodar by $37.94 \pm 18.3\%$ ($p = 0.9$), $94.6 \pm 2.5\%$ ($p = 0.09$) and $99.6 \pm 0.3\%$ ($p = 0.003$), respectively.

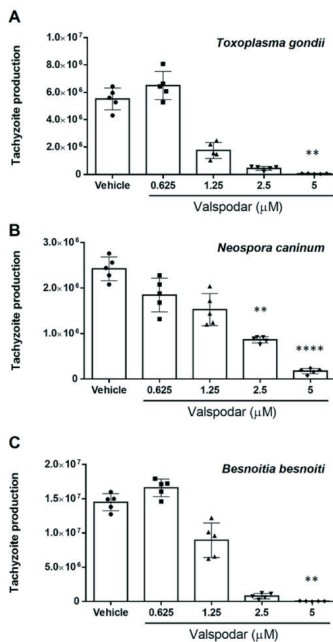


Figure 2. Valsopodar treatment induces a dose-dependent effect on *T. gondii*, *N. caninum* and *B. besnoiti* proliferation. The host cells pre-treated with valsopodar (0.625, 1.25, 2.5 and 5 μM) were infected with *T. gondii* (A), *N. caninum* (B) or *B. besnoiti* (C) tachyzoites in inhibitor-free medium for 4 h, followed by the compound re-administration. At 48 h after infection, the number of tachyzoites present in cell culture supernatants were counted. Bars represent means of five biological replicates \pm standard deviation.

P-glycoprotein inhibitors differently affect *Toxoplasma gondii*, *Neospora caninum* and *Besnoitia besnoiti* proliferation in bovine primary endothelial cells

In contrast to valsopodar and verapamil, tariquidar treatment had differential impact on tachyzoite replication (Figure 3) by exhibiting inhibitory efficacy against *B. besnoiti* proliferation at 1 and 2 μM , showing a reduction of $35.9 \pm 15.2\%$, ($p = 0.023$) and 51.7 ± 14.8 ($p = 0.002$) of tachyzoite replication, respectively, but failing to block either *T. gondii* or *N. caninum* proliferation.

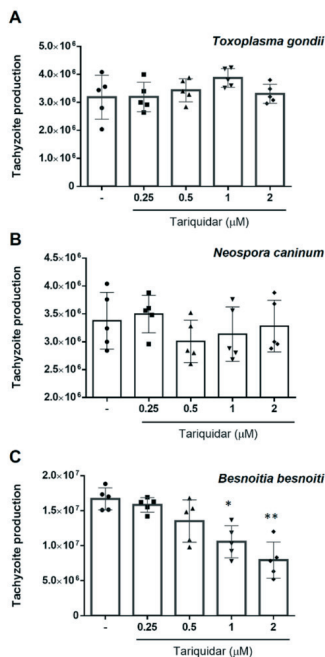


Figure 3. Tariquidar treatment differentially affects *T. gondii*, *N. caninum* and *B. besnoiti* tachyzoite production. The hosts cells pre-treated with tariquidar (0.25, 0.5 and 2 μM) were infected with *T. gondii* (A), *N. caninum* (B) or *B. besnoiti* (C) tachyzoites in inhibitor-free medium for 4 h, followed by the compound re-administration. At 48 h after infection, the number of tachyzoites present in cell culture supernatants were counted. Bars represent means of five biological replicates \pm standard deviation.

2.2. Infection Rates Are Differentially Influenced by Different P-Cp Inhibitors

Host cell infection is the earliest step necessary for successful parasite proliferation and progression. To assess direct effects of inhibitors on tachyzoite stages, we first treated live tachyzoites and then evaluated their invasive capacities for BUVEC (Figure 4, tachyzoite

P-glycoprotein inhibitors differently affect *Toxoplasma gondii*, *Neospora caninum* and *Besnoitia besnoiti* proliferation in bovine primary endothelial cells

treatment). Non-treated tachyzoites infected $47.6\% \pm 1.2$, 62.0 ± 2.3 and 55.1 ± 6.6 of the host cells in the case of *T. gondii*, *N. caninum* and *B. besnoiti*, respectively. Tachyzoite infectivity was not affected by verapamil (40 μM) treatment. In contrast, valsopodar (5 μM) treatment resulted in a decrease of infection rates with *T. gondii*, *N. caninum*, and *B. besnoiti* by 7.8% ($p = 0.009$), 14.13% ($p = 0.013$) and 19.3% ($p = 0.022$), respectively. Tariquidar tachyzoite treatment (2 μM) affected exclusively *B. besnoiti* infectivity, thereby reducing the infection rate by 16.41% ($p = 0.03$).

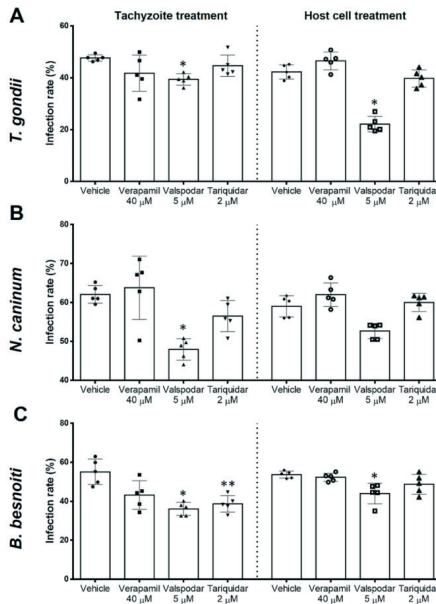


Figure 4. P-gp blockers differentially decrease *T. gondii*, *N. caninum* and *B. besnoiti* infection rates. Host cells or tachyzoites were pre-treated with verapamil (40 μM), valsopodar (5 μM) or tariquidar (2 μM). Infection rates were determined 4 h p. i. with *T. gondii* (A), *N. caninum* (B) or *B. besnoiti* (C) tachyzoites. Bars represent means of five biological replicates \pm standard deviation.

Host cell pre-treatments were performed to assess inhibitor-related effects on its permissiveness for parasite invasion (Figure 4, host cell treatment). In non-treated host cells, $42.2 \pm 2.7\%$, $59.0 \pm 2.7\%$ and $53.7 \pm 1.8\%$ of the host cells were found infected with *T. gondii*, *N. caninum* and *B. besnoiti* tachyzoites, respectively. Host cell treatment with verapamil (40 μM) and tariquidar (2 μM) had no effect on permissiveness as judged by

P-glycoprotein inhibitors differently affect *Toxoplasma gondii*, *Neospora caninum* and *Besnoitia besnoiti* proliferation in bovine primary endothelial cells

comparable infection rates at 4 h p. i. In contrast, host cell pre-treatment with valsopodar (5 μ M) led to reduced infection rates with all three parasites (reduction of 20.12% ($p = 0.036$), 6.35% ($p = 0.085$) and 9.7% ($p = 0.008$) in the case of *T. gondii*, *N. caninum* and *B. besnoiti*, respectively).

2.3. P-Gp Inhibitor-Driven Morphological Alterations in Primary Bovine Endothelial Cells

To assess the impact of inhibitor treatments on host cell physiology, BUVEC morphology was analyzed via live cell 3D-holotomographic microscopy. In uninfected BUVEC cells, 48 h verapamil treatment induced a considerable accumulation of the dense globular structures (refractive index of 1.3488 ± 0.0048) in the cytoplasm and their displacement from the center to the periphery of the cells (Supplementary Figure S2). As for infected cells, this effect could clearly be observed only in the case of *N. caninum*, whilst for the two other coccidian species the results were inconclusive (Figure 5). A change of meront morphology was not observed in verapamil-treated host cells. Given that the globular structures resembled cytoplasmic lipid droplets, we here additionally performed experiments applying BODIPY 493/503, which is a well-accepted probe for neutral lipids and often used for lipid droplet detection. When using BODIPY 493/503 staining in live cell 3D-holotomography, identical globular structures were marked by bright green fluorescence (Figure 6A) as observed before, and these structures were much less evident in vehicle-treated control cells (Figure 6A). Moreover, the same observation was made in infected host cells (Supplementary Figure S3). Given that neutral lipids are typically stored in lipid droplets, these data indicated a verapamil-driven increase of lipid droplet formation in BUVEC. Quantitative flow cytometric analyses confirmed a verapamil-induced increase in BODIPY 493/503-driven signals, whilst valsopodar and tariquidar treatment had no effect on lipid droplet formation (Figure 6B). Thus, treatment with verapamil led to a 74.1% increase of BODIPY-derived mean fluorescence intensity when compared to control conditions ($p = 0.026$)

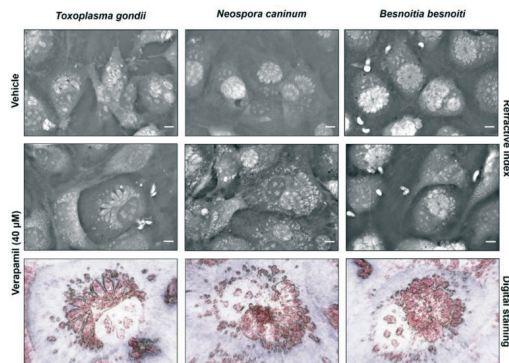


Figure 5. Live cell 3D-holotomography of *T. gondii*-, *N. caninum*- and *B. besnoiti*-infected and verapamil-treated BUVEC. Host cells were treated with verapamil (40 μ M) and infected with *T. gondii*, *N. caninum* or *B. besnoiti* tachyzoites. Cell morphology was illustrated at 24 h p. i. via live 3D-holotomography. Images mirror refractive indices and used digital staining.

P-glycoprotein inhibitors differently affect *Toxoplasma gondii*, *Neospora caninum* and *Besnoitia besnoiti* proliferation in bovine primary endothelial cells

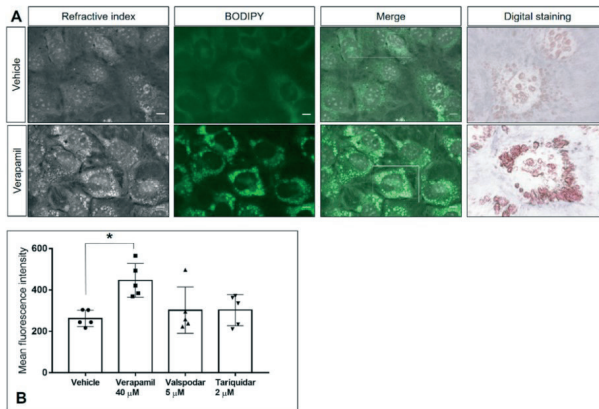


Figure 6. Lipid droplet accumulation induced by verapamil treatment. Lipid droplet formation was measured by FACS analysis in host cells 48 h after treatment with verapamil (40 μM), valspodar (5 μM) or tariquidar (2 μM) via Bodipy 493/503 staining. (A) Representative live cell 3D-holographic images of vehicle- or verapamil-treated BUVEC stained with Bodipy 493/503. The white frame indicates the area of digital staining, which was based on dense granule refractive indices. (B) Quantitative analysis of neutral lipid accumulation; graph bars represent the means of five biological replicates ± standard deviation.

In contrast to verapamil-treated cells, valspodar- and tariquidar-treated BUVEC showed normal cytoplasmic morphology lacking any vesicular accumulation. In the case of tariquidar, no effects on host cell or meront morphology could be detected in any parasite species tested here (data not shown). In contrast, valspodar treatment led to impaired meront development in all parasite species studied here (Figure 7). Thus, a considerable decrease in meront sizes was observed (Figure 7A). Specifically, valspodar treatment reduced the meront diameter by 45.2%, 40.2% and 29.2% for *T. gondii*, *N. caninum* and *B. besnoiti* ($p < 0.0001$ for all three species) (Supplementary Figure S4). Interestingly, exclusively in the case of *T. gondii* infections, valspodar treatment caused alterations in some of the PV as these parasitic structures appeared swollen. Moreover, parasite replication was consistently arrested at one-tachyzoite-stage/PV as detected throughout the entire experiment and still observed at 36 and 46 h p. i. (Figure 7B, arrows).

2.4. P-Gp Inhibitor Treatment Does Not Cause Cytotoxic Damage to Host Cells or Tachyzoites

To determine if the treatment with P-gp inhibitors evoke a cytotoxic effect on endothelial host cells or tachyzoites cytotoxicity assays were performed. As illustrated in Figure S1A, treatments with verapamil (40 μM), valspodar (5 μM) and tariquidar (2 μM) did not induce significant colorimetric changes in the formazan product compared to the vehicle control (DMSO 0.01%). Similarly, the trypan blue exclusion test showed an average viability of $88.9 \pm 3.8\%$ for *T. gondii*, *N. caninum* and *B. besnoiti* treated for 1 h with vehicle control (DMSO 0.01%) without significant effects provoked by verapamil (40 μM), valspodar (5 μM) or tariquidar (2 μM) treatments (Figure S1B–D).

P-glycoprotein inhibitors differently affect *Toxoplasma gondii*, *Neospora caninum* and *Besnoitia besnoiti* proliferation in bovine primary endothelial cells

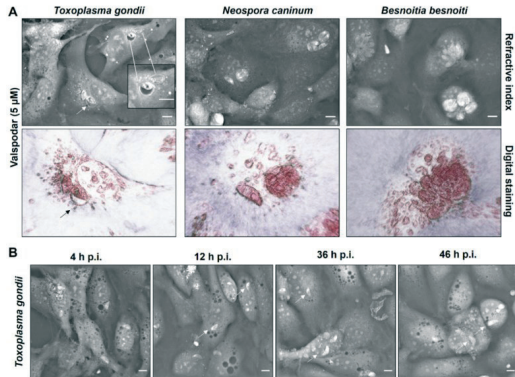


Figure 7. Live cell 3D-holography of *T. gondii*-, *N. caninum*- and *B. besnoiti*-infected and valsopodar-treated BUVEC. (A) Host cells were treated with valsopodar (5 μM) and infected with *T. gondii*, *N. caninum* or *B. besnoiti* tachyzoites. Cell morphology was illustrated at 24 h p. i. via live cell 3D-holography. Images mirror refractive indices (RI) and digital staining. Arrows point to the swollen PV in *T. gondii*-infected host cells treated with valsopodar, in the zoomed image. (B) Time lapse of *T. gondii* development in valsopodar (5 μM)-treated host cells illustrating the RI at 4, 12, 36 and 46 h p. i. Arrows point to non-dividing tachyzoites.

3. Discussion

The cyst-forming coccidia studied here, i.e., *T. gondii*, *N. caninum* and *B. besnoiti*, represent fast-replicating parasites that share the capacity of massive offspring production within 1–3 days after infection in vivo. Consequently, they all require significant amounts of building blocks to ensure successful parasite proliferation. Being auxotrophic for cholesterol, they strongly depend on the availability and efficient uptake of this nutrient for the successful proliferation [39]. Hence, P-gp implicated in the cholesterol uptake represents a promising anti-coccidial target. Here we investigated the effects of different P-gp inhibitors on the three above-mentioned parasite species. We found that verapamil treatment diminished intracellular parasite proliferation in a dose-dependent manner without cytotoxic effects on the host cells nor tachyzoites. At 40 μM, verapamil significantly reduced the replication of *T. gondii*, *N. caninum* and *B. besnoiti* tachyzoites in BUVEC by an average of 84 ± 0.8%. Comparable effects of verapamil (at concentrations of 10–100 μM) were already reported in *T. gondii* infections of mouse embryonic fibroblasts and enterocytes [40,41]. In addition, anti-parasitic effects were also documented for *P. falciparum* erythrocytic stages [42,43]. Here, we demonstrated that verapamil treatment of tachyzoites and host cells failed to affect infection rates, indicating that its anti-parasitic effect seems exclusively associated with parasite division processes, but not with active tachyzoite invasion or PV formation. In line with this, live cell 3D holography revealed no morphological changes of newly formed PVs and tachyzoites but indicated an accumulation of dense vesicles surrounding the PV. Thus, the anti-coccidial effect of verapamil might also be linked to intracellular lipid transport mechanisms. Interestingly, for other primary cell cultures, the impact of verapamil on cellular proliferation has been previously demonstrated

P-glycoprotein inhibitors differently affect *Toxoplasma gondii*, *Neospora caninum* and *Besnoitia besnoiti* proliferation in bovine primary endothelial cells

to depend on calcium-dependent mechanisms [44–46]. Considering the importance of calcium homeostasis for tachyzoite proliferation [47], it is likely that verapamil-triggered effects were driven by a calcium-mediated pathway in the current endothelium system. However, additional mechanisms may play a role as verapamil also interacts with other key channels and transporters, such as the glucose transporter GLUT1, which mediates constitutive glucose uptake in various cell types, including endothelial cells [48]. In fibroblasts, verapamil blocks GLUT1-mediated glucose transport at both basal and stress-induced conditions [49]. Thus, glucose-related effects may have contributed to the anti-proliferative impact of verapamil reported in this study, however further experiments are necessary to address this possibility.

Besides verapamil, we analyzed anti-coccidial effects of one of the most promising second-generation P-gp inhibitors, namely valsopodar [35,36]. Current data showed that valsopodar treatment significantly blocked *T. gondii*, *N. caninum* and *B. besnoiti* tachyzoite replication in infected BUEVC, without affecting the host cell and tachyzoites viability. Thus, 5 μM valsopodar—depending on the studied species—reduced tachyzoite production by 92.8 ± 2.5 – $99.6 \pm 0.3\%$, with an effective inhibitory concentration being eight times smaller than that of verapamil. In accordance with this, live cell 3D holotomography illustrated a marked reduction in meront sizes. In *T. gondii*, 3D-holotomographic microscopy also revealed an arrest at the single tachyzoite-stage. The mechanism underlying species-specific sensitivity is still unclear. However, anti-proliferative effects of valsopodar were already demonstrated for *T. gondii* tachyzoites in permanent cell lines (Vero cells; [50]), for *P. falciparum* erythrocytic stages [51] and for *Cryptosporidium parvum*-infected Caco-2 cells [52], suggesting that valsopodar-mediated effects are conserved among these apicomplexans. Given that valsopodar is a derivative of cyclosporine, for which anti-parasitic activity against the same three species has been demonstrated [50–52], these two compounds may have common effects. Here, we furthermore documented that valsopodar treatment led to altered tachyzoite infectivity in the three coccidian species studied here without any significant effect on tachyzoite viability, which is in agreement with previous data on *T. gondii* (10 μM ; [25]). More interestingly, current data showed that host cell pre-treatment with this compound led to a moderate reduction of *T. gondii* and *B. besnoiti* infection rates, suggesting that valsopodar additionally reduces host cell permissiveness, thereby hampering parasite invasion, even though it is an active process mainly driven by tachyzoites [53]. However, treatment with the endocytosis inhibitor dynasore also impairs *T. gondii* infectivity, proving that both tachyzoite- and host cell-derived actions are crucial for invasion [54]. Overall, the current data evidence that valsopodar affected several aspects of parasite infection, i.e., tachyzoite infectivity, host cell permissiveness and tachyzoite division.

Considering that the promiscuity associated with derivative drug design strategies was greatly overcome for P-gp third-generation inhibitors, we also evaluated effects of the selective P-gp blocker tariquidar. Tariquidar is a potent P-gp-specific allosteric inhibitor with an average IC_{50} of 50 nM [28,37,38]. Overall, tariquidar treatments were not toxic for the host cell or tachyzoites and concentrations of 1–2 μM showed a moderate effect on *B. besnoiti* proliferation but failed to influence *T. gondii* and *N. caninum* intracellular replication. Interestingly, tariquidar tachyzoite pre-treatment also affected *B. besnoiti* host-cell infectivity, thereby emphasizing species-specific effects. So far, little is known on the impact of third-generation P-gp inhibitors on apicomplexan parasite proliferation. In line with the current data, it has been previously reported that elacridar (10 μM) treatment reduced *T. gondii* proliferation and, by affecting Ca^{++} homeostasis of tachyzoites, led to hypermotility and untimely microneme secretion [40]. Thus, the current tariquidar-mediated effects on *B. besnoiti* tachyzoites may rely on a species-specific reduction of infectivity blockage and replication.

Until now, the role of P-gp in cholesterol homeostasis is still under debate [23]. Whilst one report argues that P-gp expression does not play a major role in cholesterol homeostasis in P-gp-inducible cells, another evidenced a physiological role of P-gp in intracellular

P-glycoprotein inhibitors differently affect *Toxoplasma gondii*, *Neospora caninum* and *Besnoitia besnoiti* proliferation in bovine primary endothelial cells

cholesterol trafficking in *T. gondii*-infected fibroblasts [31,55]. However, the fact that different studies were performed on different types of host cells can explain such oppositional findings. Interestingly, P-gp inhibitors have shown pharmacological activities beyond P-gp. Some of these compounds can also interact with other transporters affecting cellular cholesterol homeostasis [56,57]. In this context, we aimed to find out if anti-coccidial effects could be related to cholesterol homeostasis-related mechanisms. Therefore, we evaluated if inhibitor treatments affected neutral lipid accumulation. Indeed, verapamil treatment resulted in neutral lipid accumulation in BUVEC as measured by BODIPY-derived signals, whilst valsopodar and tariquidar treatment did not have such an effect. So far, analyses of neutral lipid accumulation driven by P-gp are limited as some dyes may act as P-gp substrates and be actively exported from the cell [33]. To avoid data misinterpretation, we also confirmed neutral lipid accumulation via live cell 3D-holography. Co-localization of the RI and BODIPY fluorescence in vesicles confirmed verapamil as an inducer of neutral lipid accumulation in BUVEC. In line with this, verapamil-induced cholesterol accumulation was also reported in rabbit aortic smooth cells [46] and mouse myocardium [58].

In summary, as shown in Table 1 here we demonstrated that verapamil and valsopodar treatments inhibited intracellular *T. gondii*, *N. caninum* and *B. besnoiti* tachyzoite replication in BUVEC and possess significant differences in anti-coccidial and cholesterol-related side effects. We assume that the high efficacy of valsopodar is based on its effects on both infectivity and replication, and is independent of cholesterol-related pathways. In contrast, treatment with tariquidar revealed species-specific effects and led to reduced tachyzoite infectivity and proliferation only in *B. besnoiti*.

Table 1. Summary of the effects of verapamil, valsopodar and tariquidar on *T. gondii*, *N. caninum* and *B. besnoiti* as well as the host cells.

Effect	Verapamil	Valsopodar	Tariquidar
Reduced tachyzoite proliferation	yes	yes	only <i>B. besnoiti</i>
Diminished meront size at 24 h p. i.	no	yes	no
Reduced infection rate	no	yes	only <i>B. besnoiti</i>
Decreased host cell permissiveness	no	only <i>T. gondii</i> and <i>B. besnoiti</i>	no
Neutral lipid accumulation	yes	no	no

4. Materials and Methods

4.1. Host Cell Culture

Primary bovine umbilical vein endothelial cells (BUVEC) were isolated as described elsewhere [9,10]. BUVEC were cultured at 37 °C and 5% CO₂ atmosphere in modified ECGM (modECGM) medium, by diluting ECGM medium (Promocell, Heidelberg, Germany) with M199 (Sigma-Aldrich, Munich, Germany) at a ratio of 1:3, supplemented with 500 U/mL penicillin (Sigma-Aldrich), 50 µg/mL streptomycin (Sigma-Aldrich) and 5% FCS (fetal calf serum; Biochrom, Cambridge, UK). Only BUVEC of less than three passages were used in this study.

4.2. Parasite Cultures

T. gondii (strain RH) and *N. caninum* (strain NC-1) were maintained in vitro in permanent African green monkey kidney epithelial cells (MARC145) in DMEM (Sigma-Aldrich) as described elsewhere [12]. *B. besnoiti* (strain Bb Evora04) was propagated in Madin-Darby bovine kidney cells (MDBK) [11,59] in RPMI medium (Sigma-Aldrich). All cell culture media were supplemented with 500 U/mL penicillin, 50 µg/mL streptomycin (Sigma-Aldrich) and 5% FCS (Gibco™). Infected and non-infected cells were cultured at 37 °C and 5% CO₂ atmosphere. Live tachyzoites were collected from supernatants of infected host cells (400 × g; 10 min) and re-suspended in modECGM for further experiments.

P-glycoprotein inhibitors differently affect *Toxoplasma gondii*, *Neospora caninum* and *Besnoitia besnoiti* proliferation in bovine primary endothelial cells

4.3. Inhibitor Treatment

BUVEC ($n = 5$) were cultured in 12-well plates (Sarstedt, Nümbrecht Germany) previously coated with fibronectin (1:400; Sigma-Aldrich). Verapamil (Cayman Chemical, Ann Arbor, MI, USA), valsopodar and tariquidar (both Sigma-Aldrich) were solved in DMSO (dimethyl sulfoxide; Sigma-Aldrich) and diluted in modECGM. Inhibitor treatments were performed by supplementation with verapamil (5–40 μM), valsopodar (0.6–5 μM) or tariquidar (0.2–2 μM) to fully confluent cell layers 48 h prior to infection. ModECGM with DMSO (0.01%) served as control medium. After 48 h of treatment, the inhibitors were removed by washing with plain medium. The cells were incubated with tachyzoites of *T. gondii*, *B. besnoiti* or *N. caninum* at a multiplicity of infection of 5 for 4 h. This was followed by the removal of remaining extracellular tachyzoites by washing with plain medium and inhibitor re-administration. At 48 h post infection (p. i.), tachyzoites present in cell culture supernatants were collected (800 \times g; 5 min) and counted in a Neubauer chamber.

To estimate inhibitor effects on tachyzoite infectivity, fresh tachyzoites were treated for 1 h (37 $^{\circ}\text{C}$, 5% CO_2) with verapamil, valsopodar or tariquidar. After washing in plain medium (800 \times g; 5 min), inhibitor-treated tachyzoites and non-treated control parasites were used for infection as described above. In addition, for host cell permissiveness assays the host cells were incubated with the inhibitors as described above (48 h pre infection) and then the inhibitors were removed and cells infected with live tachyzoites in medium without inhibitors. In both cases, at 4 h p. i., phase-contrast images (3 per experimental condition, $n = 5$) were acquired with an inverted microscope (IX81, Olympus, Tokyo, Japan) for infection rate estimation.

4.4. Flow Cytometry Analysis

BUVEC ($n = 5$) were seeded into T-25 cm^2 flasks (Sarstedt) and cultured until confluence. Thereafter, the cells were treated with verapamil (40 μM), valsopodar (5 μM) or tariquidar (2 μM) for 48 h. To determine if inhibitor treatment exerted an effect on neutral lipids, pre-treated cells were stained with BODIPY 493/503 (2.5 μM , Cayman Chemical, 1 h, 37 $^{\circ}\text{C}$, 5% CO_2). Afterwards, cells were washed twice in PBS 1 \times (600 \times g; 5 min), fixed in 4% PFA (paraformaldehyde; Sigma-Aldrich) and stored at -80°C until further analysis. The samples were analyzed by a BD LSRFortessa[®] cell analyzer (Becton-Dickinson, Heidelberg, Germany). Cells were gated according to their size and granularity. Moreover, BODIPY 493/503-derived signals were assessed in the FL-1 channel. Data analysis was performed via FlowJo[®] (version 10.5.0) flow cytometry analysis software (FlowJo LLC, Ashland, OR, USA).

4.5. Live Cell 3D-Holotomographic Microscopy

BUVEC were seeded into 35 mm tissue culture μ -dishes (Ibidi, Planegg, Germany) and cultured (37 $^{\circ}\text{C}$, 5% CO_2) to confluence. P-gp inhibitor treatment and parasite infections were performed as described above. Treated cell layers were placed in a top-stage incubator (Ibidi[®]) at 5% CO_2 and 37 $^{\circ}\text{C}$ during the entire experiment. Holotomographic images were obtained via 3D cell-explorer microscope (Nanolive, Eublens, Switzerland) equipped with a 60 \times magnification ($\lambda = 520$ nm, sample exposure 0.2 mW/mm²) and a depth of field of 30 μm . Images were analyzed using STEVE software (Nanolive) to obtain refractive index (RI)-based z-stacks. In addition, digital staining was applied according to the RI of cell organelles and intracellular tachyzoites. For neutral lipid visualization, cells were loaded with BODIPY 493/503 (2.5 μM , 1 h, 37 $^{\circ}\text{C}$). Live cell 3D-holotomographic microscopy and analysis of BODIPY 493/503-based fluorescence were performed in parallel to prove the nature of lipid-rich organelles. Image processing was carried out by Fiji ImageJ[®] using Z-projection and merged-channel-plugins.

4.6. Cell Toxicity Assays

Cell toxicity of P-gp inhibitors was assessed by colorimetric XTT tests (Promega, Madison, WI, USA) according to the manufacturer instructions. Briefly, BUVEC ($n = 3$)

P-glycoprotein inhibitors differently affect *Toxoplasma gondii*, *Neospora caninum* and *Besnoitia besnoiti* proliferation in bovine primary endothelial cells

were cultured in 96-well plates (Greiner) and treated with verapamil (40 μ M), valsopodar (5 μ M) or tariquidar (2 μ M) in a total volume of 50 μ l for 96 h. Thereafter, 50 μ L of XTT working solution were added and the samples were incubated for 4 h (37 $^{\circ}$ C, 5% CO₂ atmosphere). The resulting formazan products were estimated via optical density (OD) measurements at 590 nm and reference filter 620-nm wavelength using VarioskanTM Flash Multimode Reader (Thermo Scientific, Waltham, MA, USA). BUVEC treated with the solvent (DMSO; 0.01%) were used as negative controls.

Additionally, for experiments on parasite viability, 5×10^5 tachyzoites of each parasite species were treated for 1 h with each of the studied compounds (verapamil 40 μ M, valsopodar 5 μ M and tariquidar 2 μ M; 37 $^{\circ}$ C, 5% CO₂). Viability of tachyzoites was determined by the trypan blue (Sigma-Aldrich) exclusion staining assay [60]. Non-stained parasites were considered as viable.

4.7. Statistical Analysis

Statistical analyses were performed by the software GraphPad Prism[®] 8 (version 8.4.3., www.graphpad.com) Data description was performed by presenting the arithmetic mean \pm standard deviation. In addition, the non-parametric Mann–Whitney test was applied for the comparison of two experimental conditions, while Kruskal–Wallis test was used for the comparison of three or more conditions. Whenever a global comparison by the Kruskal–Wallis test indicated significance, post hoc multiple comparison was carried out using the Dunn test to compare with control conditions. The outcomes of the statistical tests were considered to indicate significant differences at $p \leq 0.05$ (significance level).

Supplementary Materials: The following are available online at <https://www.mdpi.com/2076-0817/10/4/395/s1>, Supplementary Figure S1: Viability assessment for host cells and tachyzoites, Supplementary Figure S2: Live cell 3D-holographic analysis of P-gp inhibitor-treated control cells, Supplementary Figure S3: Analysis of verapamil-induced lipid accumulation in infected BUVEC at 24 h p. i., Supplementary Figure S4: Effect of valsopodar treatment on meront diameter of *T. gondii*, *N. caninum* and *B. besnoiti*.

Author Contributions: A.T., C.L., L.P.-O. and L.M.R.S. conceived and designed the experiments; C.L., L.P.-O. and L.M.R.S. performed the experiments; all authors performed analyses and interpretation of the data; A.T., C.H., C.L. and L.M.R.S. prepared the manuscript. C.L., L.M.R.S., L.P.-O., S.H., C.H. and A.T. approved the final version of the manuscript. All authors have read and agreed to the published version of the manuscript.

Funding: This research received no external funding.

Institutional Review Board Statement: Not applicable.

Informed Consent Statement: Not applicable.

Data Availability Statement: All data are included in the manuscript.

Acknowledgments: Authors would like to thank Christin Ritter and Hannah Salecker (both at the Institute of Parasitology, Justus Liebig University Giessen) for the outstanding technical support. We also are very thankful to Axel Wehrend (Clinic for Obstetrics, Gynecology and Andrology of Large and Small Animals, Justus Liebig University, Giessen, Germany) for continuous supply of bovine umbilical cords. C.L. was funded by the National Agency for Research and Development [(ANID), DOCTORADO BECAS CHILE/2017–72180349].

Conflicts of Interest: The authors declare no conflict of interest.

References

1. Votyčka, J.; Modrý, D.; Obornik, M.; Šlapeta, J.; Lukeš, J. Apicomplexa. In *Handbook of the Protists*; Archibald, J.M., Simpson, A.G.B., Slamovits, C.H., Eds.; Springer International Publishing: Cham, Switzerland, 2017; pp. 567–624. [CrossRef]
2. Innes, E.A. A brief history and overview of *Toxoplasma gondii*. *Zoonoses Public Health* **2010**, *57*, 1–7. [CrossRef]
3. Benavides, J.; Fernandez, M.; Castano, P.; Ferreras, M.C.; Ortega-Mora, L.; Perez, V. Ovine Toxoplasmosis: A New Look at its Pathogenesis. *J. Comp. Pathol.* **2017**, *157*, 34–38. [CrossRef]

P-glycoprotein inhibitors differently affect *Toxoplasma gondii*, *Neospora caninum* and *Besnoitia besnoiti* proliferation in bovine primary endothelial cells

4. Nayeri, T.; Sarvi, S.; Moosazadeh, M.; Amouei, A.; Hosseininejad, Z.; Daryani, A. The global seroprevalence of anti-*Toxoplasma gondii* antibodies in women who had spontaneous abortion: A systematic review and meta-analysis. *PLoS Negl. Trop. Dis.* **2020**, *14*, e0008103. [CrossRef]
5. Lagomarsino, H.; Scialò, A.; Rodríguez, A.; Armendano, J.; Fiorani, F.; Bence, Á.; García, J.; Hecker, Y.; Gual, I.; Cantón, G.; et al. Controlling Endemic *Neospora caninum*-Related Abortions in a Dairy Herd From Argentina. *Front. Vet. Sci.* **2019**, *6*, 446. [CrossRef]
6. Reichel, M.P.; Alejandra Ayaguey-Alcárcera, M.; Gondim, L.F.; Ellis, J.T. What is the global economic impact of *Neospora caninum* in cattle—the billion dollar question. *Int. J. Parasitol.* **2013**, *43*, 133–142. [CrossRef] [PubMed]
7. Alvarez-García, G.; Frey, C.F.; Mora, L.M.; Schares, G. A century of bovine besnoitiosis: An unknown disease re-emerging in Europe. *Trends Parasitol.* **2013**, *29*, 407–415. [CrossRef] [PubMed]
8. Silva, L.M.R.; Lufjohann, D.; Hamid, P.; Velásquez, Z.D.; Kerner, K.; Larrazabal, C.; Failing, K.; Hermosilla, C.; Taubert, A. *Besnoitia besnoiti* infection alters both endogenous cholesterol de novo synthesis and exogenous LDL uptake in host endothelial cells. *Sci. Rep.* **2019**, *9*, 6650. [CrossRef] [PubMed]
9. Taubert, A.; Zahner, H.; Hermosilla, C. Dynamics of transcription of immunomodulatory genes in endothelial cells infected with different coccidian parasites. *Vet. Parasitol.* **2006**, *142*, 214–222. [CrossRef] [PubMed]
10. Taubert, A.; Krüll, M.; Zahner, H.; Hermosilla, C. *Toxoplasma gondii* and *Neospora caninum* infections of bovine endothelial cells induce endothelial adhesion molecule gene transcription and subsequent PMN adhesion. *Vet. Immunol. Immunopathol.* **2006**, *112*, 272–283. [CrossRef]
11. Velásquez, Z.D.; Lopez-Osorio, S.; Perviza]-Oruqaj, L.; Herold, S.; Hermosilla, C.; Taubert, A. *Besnoitia besnoiti*-driven endothelial host cell cycle alteration. *Parasitol. Res.* **2020**, *119*, 2563–2577. [CrossRef]
12. Velásquez, Z.D.; Conejeros, I.; Larrazabal, C.; Kerner, K.; Hermosilla, C.; Taubert, A. *Toxoplasma gondii*-induced host cellular cycle dysregulation is linked to chromosome missegregation and cytokinesis failure in primary endothelial host cells. *Sci. Rep.* **2019**, *9*, 12496. [CrossRef] [PubMed]
13. Nolan, S.J.; Romano, J.D.; Luechtefeld, T.; Coppens, I. *Neospora caninum* Recruits Host Cell Structures to Its Parasitophorous Vacuole and Salvages Lipids from Organelles. *Eukaryot. Cell* **2015**, *14*, 454–473. [CrossRef] [PubMed]
14. Coppens, I.; Sinai, A.F.; Joiner, K.A. *Toxoplasma gondii* exploits host low-density lipoprotein receptor-mediated endocytosis for cholesterol acquisition. *J. Cell Biol.* **2000**, *149*, 167–180. [CrossRef] [PubMed]
15. Ehrenman, K.; Wanyiri, J.W.; Bhat, N.; Ward, H.D.; Coppens, I. *Cryptosporidium parvum* scavenges LDL-derived cholesterol and micellar cholesterol internalized into enterocytes. *Cell. Microbiol.* **2013**, *15*, 1182–1197. [CrossRef]
16. Nishikawa, Y.; Ibrahim, H.M.; Kameyama, K.; Shiga, I.; Hiasa, J.; Xuan, X. Host cholesterol synthesis contributes to growth of intracellular *Toxoplasma gondii* in macrophages. *J. Vet. Med. Sci.* **2011**, *73*, 633–639. [CrossRef]
17. Simons, K.; Ikonen, E. How cells handle cholesterol. *Science* **2000**, *290*, 1721–1726. [CrossRef]
18. Yamauchi, Y.; Rogers, M.A. Sterol Metabolism and Transport in Atherosclerosis and Cancer. *Front. Endocrinol.* **2018**, *9*, 509. [CrossRef]
19. Chang, T.Y.; Li, B.L.; Chang, C.C.; Urano, Y. Acyl-coenzyme A:cholesterol acyltransferases. *Am. J. Physiol. Endocrinol. Metab.* **2009**, *297*, E1–E9. [CrossRef]
20. Hu, X.; Binns, D.; Reese, M.L. The Coccidian Parasites *Toxoplasma* and *Neospora* Dysregulate Mammalian Lipid Droplet Biogenesis. *J. Biol. Chem.* **2017**, *292*, 11009–11020. [CrossRef] [PubMed]
21. Dean, M.; Hamon, Y.; Chimini, G. The human ATP-binding cassette (ABC) transporter superfamily. *J. Lipid Res.* **2001**, *42*, 1007–1017. [CrossRef]
22. Ehrenman, K.; Sehgal, A.; Lige, B.; Stedman, T.T.; Joiner, K.A.; Coppens, I. Novel roles for ATP-binding cassette G transporters in lipid redistribution in *Toxoplasma*. *Mol. Microbiol.* **2010**, *76*, 1232–1249. [CrossRef]
23. Satyamoorthy, K.; Sharom, F.J. Complex Interplay between the P-Glycoprotein Multidrug Efflux Pump and the Membrane: Its Role in Modulating Protein Function. *PLoS ONE* **2014**, *4*, 41. [CrossRef]
24. Robinson, K.; Tiriveedhi, V. Perplexing Role of P-Glycoprotein in Tumor Microenvironment. *Front. Oncol.* **2020**, *10*, 265. [CrossRef] [PubMed]
25. Schmid, A.; Sauvage, V.; Escotte-Binet, S.; Aubert, D.; Terryn, C.; Garnotel, R.; Villena, I. Molecular characterization and expression analysis of a P-glycoprotein homologue in *Toxoplasma gondii*. *Mol. Biochem. Parasitol.* **2009**, *163*, 54–60. [CrossRef] [PubMed]
26. Castans-Muñoz, E.; Pérez-Victoria, J.M.; Gamarro, F.; Castans, S. Characterization of an ABCG-like transporter from the protozoan parasite *Leishmania* with a role in drug resistance and transbilayer lipid movement. *Antimicrob. Agents Chemother.* **2008**, *52*, 3573–3579. [CrossRef] [PubMed]
27. Riordan, J.R.; Deuchars, K.; Kartner, N.; Alon, N.; Trent, J.; Ling, V. Amplification of P-glycoprotein genes in multidrug-resistant mammalian cell lines. *Nature* **1985**, *316*, 817–819. [CrossRef]
28. Kasinathan, R.S.; Morgan, W.M.; Greenberg, R.M. Genetic knockdown and pharmacological inhibition of parasite multidrug resistance transporters disrupts egg production in *Schistosoma mansoni*. *PLoS Negl. Trop. Dis.* **2011**, *5*, e1425. [CrossRef]
29. Bartley, D.J.; McAllister, H.; Bartley, Y.; Dupuy, J.; Ménez, C.; Alvierie, M.; Jackson, F.; Lespine, A. P-glycoprotein interfering agents potentiate ivermectin susceptibility in ivermectin sensitive and resistant isolates of *Teladorsagia circumcincta* and *Haemonchus contortus*. *Parasitology* **2009**, *136*, 1081–1088. [CrossRef]
30. Nicolao, M.C.; Denegri, G.M.; Cárcamo, J.G.; Cumino, A.C. P-glycoprotein expression and pharmacological modulation in larval stages of *Echinoococcus granulosis*. *Parasitol. Int.* **2014**, *63*, 1–8. [CrossRef]

P-glycoprotein inhibitors differently affect *Toxoplasma gondii*, *Neospora caninum* and *Besnoitia besnoiti* proliferation in bovine primary endothelial cells

31. Bottova, L.; Hehl, A.B.; Stefanic, S.; Fabrias, G.; Casas, J.; Schraner, E.; Pieters, J.; Sonda, S. Host cell P-glycoprotein is essential for cholesterol uptake and replication of *Toxoplasma gondii*. *J. Biol. Chem.* **2009**, *284*, 17438–17448. [[CrossRef](#)] [[PubMed](#)]
32. Leitch, G.J.; Scanton, M.; Shaw, A.; Visvesvara, G.S. Role of P-glycoprotein in the course and treatment of *Encephalitozoon microsporidiosis*. *Antimicrob. Agents Chemother.* **2001**, *45*, 75–78. [[CrossRef](#)]
33. Palmeira, A.; Sousa, E.; Vasconcelos, M.H.; Pinto, M.M. Three decades of P-gp inhibitors: Skimming through several generations and scaffolds. *Curr. Med. Chem.* **2012**, *19*, 1946–2025. [[CrossRef](#)]
34. Tsuruo, T.; Iida, H.; Tsukagoshi, S.; Sakurai, Y. Overcoming of vincristine resistance in P388 leukemia in vivo and in vitro through enhanced cytotoxicity of vincristine and vinblastine by verapamil. *Cancer Res.* **1981**, *41*, 1967–1972.
35. Archinal-Matheis, A.; Rezeka, R.W.; Watanabe, T.; Kokubu, N.; Itoh, Y.; Combates, N.J.; Bair, K.W.; Cohen, D. Analysis of the interactions of SDZ PSC 833 ([3'-keto-Bmt1]-Val2]-Cyclosporine), a multidrug resistance modulator, with P-glycoprotein. *Oncol. Rep.* **1995**, *7*, 603–610.
36. Atadja, P.; Watanabe, T.; Xu, H.; Cohen, D. PSC-833, a frontier in modulation of P-glycoprotein mediated multidrug resistance. *Cancer Metastasis Rev.* **1998**, *17*, 163–168. [[CrossRef](#)]
37. Martin, C.; Berridge, G.; Mistry, P.; Higgins, C.; Charlton, P.; Callaghan, R. The molecular interaction of the high affinity reversal agent XR9576 with P-glycoprotein. *Br. J. Pharmacol.* **1999**, *128*, 403–411. [[CrossRef](#)]
38. Roe, M.; Folkes, A.; Ashworth, P.; Brumwell, J.; Chima, L.; Hunjan, S.; Pretswell, I.; Dangerfield, W.; Ryder, H.; Charlton, P. Reversal of P-glycoprotein mediated multidrug resistance by novel anthranilamide derivatives. *Bioorg. Med. Chem. Lett.* **1999**, *9*, 595–600. [[CrossRef](#)]
39. Coppens, I. Targeting lipid biosynthesis and salvage in apicomplexan parasites for improved chemotherapy. *Nat. Rev. Microbiol.* **2013**, *11*, 823–835. [[CrossRef](#)] [[PubMed](#)]
40. Bottova, L.; Sauder, U.; Olivieri, V.; Hehl, A.B.; Sonda, S. The P-glycoprotein inhibitor GF120918 modulates Ca²⁺-dependent processes and lipid metabolism in *Toxoplasma gondii*. *PLoS ONE* **2010**, *5*, e10062. [[CrossRef](#)]
41. Hofels, E.; McAuley, J.; Mack, D.; Milhous, W.K.; McLeod, R. In vitro effects of artemisinin ether, cycloguanil hydrochloride (alone and in combination with sulfadiazine), quinine sulfate, mefloquine, primaquine phosphate, trifluoperazine hydrochloride, and verapamil on *Toxoplasma gondii*. *Antimicrob. Agents Chemother.* **1994**, *38*, 1392–1396. [[CrossRef](#)] [[PubMed](#)]
42. Adovelande, J.; Deleze, J.; Schreve, J. Synergy between two calcium channel blockers, verapamil and fantofarone (SR33557), in reversing chloroquine resistance in *Plasmodium falciparum*. *Biochem. Pharmacol.* **1998**, *55*, 433–440. [[CrossRef](#)]
43. Martiney, J.A.; Cerami, A.; Slater, A.F. Verapamil reversal of chloroquine resistance in the malaria parasite *Plasmodium falciparum* is specific for resistant parasites and independent of the weak base effect. *J. Biol. Chem.* **1995**, *270*, 22393–22398. [[CrossRef](#)]
44. Orekhov, A.N.; Tertov, V.V.; Kudryashov, S.A.; Khashimov, Kh, A.; Smirnov, V.N. Primary culture of human aortic intima cells as a model for testing antiatherosclerotic drugs. Effects of cyclic AMP, prostaglandins, calcium antagonists, antioxidants, and lipid-lowering agents. *Atherosclerosis* **1986**, *60*, 101–110. [[CrossRef](#)]
45. Rokosova, B.; Bentley, J.P. Effect of calcium on cell proliferation and extracellular matrix synthesis in arterial smooth muscle cells and dermal fibroblasts. *Exp. Mol. Pathol.* **1986**, *44*, 307–317. [[CrossRef](#)]
46. Stein, O.; Halperin, G.; Stein, Y. Long-term effects of verapamil on aortic smooth muscle cells cultured in the presence of hypercholesterolemic serum. *Arteriosclerosis* **1987**, *7*, 585–592. [[CrossRef](#)]
47. Hupe, D.J.; Pfefferkorn, E.R.; Behrens, N.D.; Peters, K. L-651,582 inhibition of intracellular parasitic protozoal growth correlates with host-cell directed effects. *J. Pharmacol. Exp. Ther.* **1991**, *256*, 462–467.
48. Polin, R.A.; Fox, W.W.; Abman, S.H. *Fetal and Neonatal Physiology*, 3rd ed.; W.B. Saunders Co.: Philadelphia, PA, USA, 2004.
49. Louters, L.L.; Stehouwer, N.; Rekan, J.; Tidball, A.; Cok, A.; Holstege, C.P. Verapamil inhibits the glucose transport activity of GLUT1. *J. Med. Toxicol. Off. J. Am. Coll. Med Toxicol.* **2010**, *6*, 100–105. [[CrossRef](#)]
50. Silverman, J.A.; Hayes, M.L.; Luft, B.J.; Joiner, K.A. Characterization of anti-*Toxoplasma* activity of SDZ 215-918, a cyclosporin derivative lacking immunosuppressive and peptidyl-prolyl-isomerase-inhibiting activity: Possible role of a P-glycoprotein in *Toxoplasma* physiology. *Antimicrob. Agents Chemother.* **1997**, *41*, 1859–1866. [[CrossRef](#)]
51. Bell, A.; Wernli, B.; Franklin, R.M. Roles of peptidyl-prolyl cis-trans isomerase and calcineurin in the mechanisms of antimalarial action of cyclosporin A, FK506, and rapamycin. *Biochem. Pharmacol.* **1994**, *48*, 495–503. [[CrossRef](#)]
52. Perkins, M.E.; Wu, T.W.; Le Blancq, S.M. Cyclosporin analogs inhibit in vitro growth of *Cryptosporidium parvum*. *Antimicrob. Agents Chemother.* **1998**, *42*, 843–848. [[CrossRef](#)]
53. Black, M.W.; Boothroyd, J.C. Lytic cycle of *Toxoplasma gondii*. *Microbiol. Mol. Biol. Rev. MMBR* **2000**, *64*, 607–623. [[CrossRef](#)]
54. Caldas, L.A.; Attias, M.; de Souza, W. Dynamin inhibitor impairs *Toxoplasma gondii* invasion. *FEMS Microbiol. Lett.* **2009**, *301*, 103–108. [[CrossRef](#)]
55. Le Goff, W.; Settle, M.; Greene, D.J.; Morton, R.E.; Smith, J.D. Reevaluation of the role of the multidrug-resistant P-glycoprotein in cellular cholesterol homeostasis. *J. Lipid Res.* **2006**, *47*, 51–58. [[CrossRef](#)] [[PubMed](#)]
56. Nagao, K.; Maeda, M.; Manucat, N.B.; Ueda, K. Cyclosporine A and PSC833 inhibit ABCA1 function via direct binding. *Biochim. Biophys. Acta* **2013**, *1831*, 398–406. [[CrossRef](#)] [[PubMed](#)]
57. Suzuki, S.; Nishimaki-Mogami, T.; Tamehiro, N.; Inoue, K.; Arakawa, R.; Abe-Dohmae, S.; Tanaka, A.R.; Ueda, K.; Yokoyama, S. Verapamil increases the apolipoprotein-mediated release of cellular cholesterol by induction of ABCA1 expression via Liver X receptor-independent mechanism. *Arterioscler. Thromb. Vasc. Biol.* **2004**, *24*, 519–525. [[CrossRef](#)] [[PubMed](#)]

P-glycoprotein inhibitors differently affect *Toxoplasma gondii*, *Neospora caninum* and *Besnoitia besnoiti* proliferation in bovine primary endothelial cells

58. Saetersdal, T.; Røh, J.; Engedal, H.; Jodalen, H.; Rotevatn, S. Protective effects of verapamil against isoprenaline- induced mobilization of mitochondrial calcium and cellular lipid droplets in the myocardium. *Res. Exp. Med. Z. Für Die Gesamte Exp. Med. Einschl. Exp. Chir.* **1982**, *181*, 39–47. [[CrossRef](#)]
59. Munoz-Caro, T.; Silva, L.M.; Ritter, C.; Taubert, A.; Hermosilla, C. *Besnoitia besnoiti* tachyzoites induce monocyte extracellular trap formation. *Parasitol. Res.* **2014**, *113*, 4189–4197. [[CrossRef](#)]
60. Cervantes-Valencia, M.E.; Hermosilla, C.; Alcalá-Canto, Y.; Tapia, G.; Taubert, A.; Silva, L.M.R. Antiparasitic Efficacy of Curcumin Against *Besnoitia besnoiti* Tachyzoites in vitro. *Front. Vet. Sci.* **2018**, *5*, 333. [[CrossRef](#)] [[PubMed](#)]

2.5. THIOSEMICARBAZONE COPPER CHELATOR BLT-1 BLOCKS APICOMPLEXAN PARASITE REPLICATION BY SELECTIVE INHIBITION OF THE SCAVENGER RECEPTOR B TYPE I (SR-BI)

Larrazabal C, López-Osorio S, Velásquez ZD, Hermosilla C, Taubert A, Silva LMR. (2021)

Microorganisms 9 (11); doi.org/10.3390/microorganisms9112372

Own part in the publication:

- Project planning: 50 %, Together with co-authors and supervisors
- Development of experiments: 60 %, Together with co-authors
- Evaluation of experiments: 60 %, Together with co-authors
- Writing of the manuscript: 60 %, Together with co-authors

Thiosemicarbazone copper chelator BLT-1 blocks apicomplexan parasite replication by selective inhibition of the scavenger receptor B type I (SR-BI)



Article

Thiosemicarbazone Copper Chelator BLT-1 Blocks Apicomplexan Parasite Replication by Selective Inhibition of Scavenger Receptor B Type 1 (SR-BI)

Camilo Larrazabal ^{1,*}, Sara López-Osorio ^{1,2}, Zahady D. Velásquez ¹, Carlos Hermosilla ¹, Anja Taubert ¹ and Liliana M. R. Silva ^{1,*}

¹ Institute of Parasitology, Biomedical Research Center Seltersberg, Justus Liebig University Giessen, 35392 Giessen, Germany; sara.lopez@udea.edu.co (S.L.-O.); zahady.velasquez@vetmed.uni-giessen.de (Z.D.V.); carlos.r.hermosilla@vetmed.uni-giessen.de (C.H.); anja.taubert@vetmed.uni-giessen.de (A.T.)

² CIBAV Research Group, Veterinary Medicine School, Faculty of Agrarian Sciences, University of Antioquia, Medellín 050010, Colombia

* Correspondence: Camilo.Larrazabal@vetmed.uni-giessen.de (C.L.); Liliana.Silva@vetmed.uni-giessen.de (L.M.R.S.)



Citation: Larrazabal, C.; López-Osorio, S.; Velásquez, Z.D.; Hermosilla, C.; Taubert, A.; Silva, L.M.R. Thiosemicarbazone Copper Chelator BLT-1 Blocks Apicomplexan Parasite Replication by Selective Inhibition of Scavenger Receptor B Type 1 (SR-BI). *Microorganisms* **2021**, *9*, 2372. <https://doi.org/10.3390/microorganisms9112372>

Academic Editor: Anna Olivieri

Received: 21 October 2021

Accepted: 11 November 2021

Published: 17 November 2021

Publisher's Note: MDPI stays neutral with regard to jurisdictional claims in published maps and institutional affiliations.



Copyright: © 2021 by the authors. Licensee MDPI, Basel, Switzerland. This article is an open access article distributed under the terms and conditions of the Creative Commons Attribution (CC BY) license (<https://creativecommons.org/licenses/by/4.0/>).

Abstract: Coccidian parasites are obligate intracellular pathogens that affect humans and animals. Apicomplexans are defective in de novo synthesis of cholesterol, which is required for membrane biosynthesis and offspring formation. In consequence, cholesterol has to be scavenged from host cells. It is mainly taken up from extracellular sources via LDL particles; however, little is known on the role of HDL and its receptor SR-BI in this process. Here, we studied effects of the SR-BI-specific blocker BLT-1 on the development of different fast (*Toxoplasma gondii*, *Neospora caninum*, *Besnoitia besnoiti*) and slow (*Eimeria bovis* and *Eimeria arloingi*) replicating coccidian species. Overall, development of all these parasites was significantly inhibited by BLT-1 treatment indicating a common SR-BI-related key mechanism in the replication process. However, SR-BI gene transcription was not affected by *T. gondii*, *N. caninum* and *B. besnoiti* infections. Interestingly, BLT-1 treatment of infective stages reduced invasive capacities of all fast replicating parasites paralleled by a sustained increase in cytoplasmic Ca⁺⁺ levels. Moreover, BLT1-mediated blockage of SR-BI led to enhanced host cell lipid droplet abundance and neutral lipid content, thereby confirming the importance of this receptor in general lipid metabolism. Finally, the current data suggest a conserved role of SR-BI for successful coccidian infections.

Keywords: *Toxoplasma gondii*; *Neospora caninum*; *Besnoitia besnoiti*; *Eimeria bovis*; *Eimeria arloingi*; SR-BI; HDL; BLT-1

1. Introduction

Coccidia comprise a large group of protozoan parasites belonging to the apicomplexan phylum. In general, coccidian parasites are distributed in two families, Sarcocystidae and Eimeriidae. Sarcocystidae parasites have a heteroxenic life cycle, while the majority of Eimeriidae species present with a monoxenic life cycle [1]. Despite several conserved features among these families, coccidian parasites also show a tremendous divergence in host range, host cell specificity and clinical outcomes. In Sarcocystidae, the clinical scenario is largely a consequence of an extraintestinal merogonic (asexual) replication. In particular, *Toxoplasma gondii*, which is a widely distributed zoonotic parasite with a broad range of suitable intermediate hosts, commonly induces abortions in humans and sheep [2,3]. In contrast, the closely related coccidian *Neospora caninum* is not zoonotic, but it is considered to be a major abortive agent in the bovine industry [4,5]. Additionally, *Besnoitia besnoiti* is the causal agent of bovine besnoitiosis, a re-emerging disease in Europe, which leads to massive alterations of skin and mucosa in cattle and to infertility in bulls [6,7]. Interestingly,

Thiosemicarbazone copper chelator BLT-1 blocks apicomplexan parasite replication by selective inhibition of the scavenger receptor B type I (SR-BI)

Eimeriidae parasites are species-specific pathogens, most of them with a marked tropism towards intestinal tissues. Two of the most pathogenic species in ruminants, *Eimeria bovis* (cattle) and *Eimeria arloingi* (goats), develop macromeronts in highly immunoreactive endothelial host cells during their first merogony and can provoke life-threatening diarrhoea in young calves and goat kids, respectively, thereby generating an enormous economic impact on bovine and caprine industries worldwide [8].

During early host infection, coccidian parasites proliferate asexually within suitable nucleated host cells. Nevertheless, major differences exist within coccidian families regarding cell tropism and kinetics of development, largely driven by parasite stage and species [1]. Sarcocystidae parasites rapidly proliferate within a rather wide range of host cell types releasing their progeny (tachyzoites) a few days or even hours after infection [9,10]. In contrast, some pathogenic ruminant *Eimeria* species perform the long-lasting first merogony within distinct host cells, such as endothelial cells in the lacteal of the intestinal villi [11], releasing a high number of merozoites I (>120.0000) after 15–18 days in vitro [12,13]. In this context, primary endothelial cells were proven to be appropriate for the development of several coccidian species. This in vitro system, which is closely related to the in vivo scenario, allows intracellular replication [12–16] and consequently delivers a methodological bridge for analysing these divergent families in the same host cell type, thereby avoiding host cell type-driven variations.

During merogonic replication, considerable amounts of nutrients are required to support high proliferation rates. However, apicomplexans miss some pivotal metabolic pathways, which may be suitable targets for novel therapeutic strategies. In particular, apicomplexan species rely on host cells to fulfil their cholesterol requirements [17]. From a physiological perspective, cells mainly acquire cholesterol from circulating low-density lipoproteins (LDL) with the LDLR (LDL receptor)-related endocytic pathway representing the best-characterized cholesterol uptake route [18,19]. Exogenous LDL supply proved essential for several fast replicating coccidia, such as *T. gondii*, *N. caninum* and *B. besnoiti* [20–22]. Referring to this mechanism, cholesterol is internalized by clathrin-mediated endocytosis of the LDL–LDLR complex and delivered to lysosomes where cholesteryl esters are cleaved by acid lipase, thereby releasing free cholesterol for cellular needs [23,24]. The mechanism of cholesterol exit from late endosomes is still under debate; nevertheless, the involvement of Niemann–Pick type C protein 1/2 (NPC1-2) is largely accepted [23]. This protein promotes transfer of cholesterol into other membranes (i.e., cytoplasmic, endosomal, mitochondrial) or its incorporation into the endoplasmic reticulum for formation of lipid droplets (LDs), which indeed are the key cholesterol sources for intracellular pathogens [25].

As excess accumulation of free cholesterol is toxic, it should be effluxed from the cell. This process requires high-density lipoprotein (HDL) particles functioning as extracellular acceptors and is driven by transporters from the ATP-binding cassette (ABC) family, such as ABCA1 [18,19,26]. Additionally, cholesterol efflux in other cell types, such as endotheliocytes and macrophages, is modulated by the HDL receptor, scavenger receptor B I (SR-BI) [27–29]. This transmembrane protein mediates a gradient-dependent bidirectional flux of cholesteryl esters from HDL and other lipoproteins via a unique non-endocytic route [30,31]. Thus, SR-BI plays a dual role in reverse cholesterol transport, promoting not only cholesterol efflux from peripheral cells, but also its uptake by hepatocytes for biliary disposal [28,29]. In this context, SR-BI has a marked tissue-specific expression, which is enhanced especially in steroidogenic tissue and hepatocytes. Nevertheless, its considerable expression in neoplastic cells, such as prostate and breast cancer cells additionally indicates its tight association with high proliferative activities and malignant cell phenotypes [32]. Of note, SR-BI is also capable of incorporating cholesteryl esters from LDL particles via a non-endocytic route [31], representing an alternative route for LDL-related cholesterol acquisition. Interestingly, the apicomplexan parasite *Plasmodium* spp. significantly relies on SR-BI interactions for hepatocyte invasion and intracellular proliferation during hepatic

Thiosemicarbazone copper chelator BLT-1 blocks apicomplexan parasite replication by selective inhibition of the scavenger receptor B type I (SR-BI)

stage of its life cycle [33,34]. However, for other apicomplexan parasites, no SR-BI-related data are available so far.

The aim of this work was to evaluate the role of SR-BI in coccidian host cell invasion and obligate intracellular replication. To additionally address potentially conserved SR-BI-related mechanisms, comparative inhibitor studies were performed on several protozoan parasites covering both fast (*T. gondii*, *N. caninum*, *B. besnoiti*) and slow (*E. bovis* and *E. arloingi*) replicating coccidian species. Overall, here, we confirmed that SR-BI indeed seems to be involved in successful replication of all these parasites when replicating in bovine primary endothelial cells.

2. Materials and Methods

2.1. Host Cell Culture

Primary bovine umbilical vein endothelial cells (BUVEC) were isolated as described elsewhere [35]. BUVEC were cultured at 37 °C in 5% CO₂ atmosphere in a modified ECGM (modECGM) medium by diluting the ECGM medium (Promocell, Heidelberg, Germany) with M199 (Sigma-Aldrich, St. Louis, MO, USA) at a 1:3 ratio, supplemented with 500 U/mL penicillin (Sigma-Aldrich, St. Louis, MO, USA), 50 µg/mL streptomycin (Sigma-Aldrich) and 5% FCS (foetal calf serum; Biochrom, Cambridge, UK). BUVEC of fewer than three passages were used in this study.

2.2. Parasites

T. gondii (strain RH) and *N. caninum* (strain NC-1) tachyzoites were cultured in vitro as previously described [16,35] by continuous passages in permanent African green monkey kidney epithelial cells (MARC 145) in DMEM (Sigma-Aldrich) supplemented with 5% FCS (Biochrom). *B. besnoiti* (strain Bb Evara04) tachyzoites were propagated in Madin Darby bovine kidney cells (MDBK) in RPMI medium (Sigma-Aldrich) supplemented with 5% FCS [16,36]. For *E. bovis* (strain H) and *E. arloingi* (strain A) cultures, parasites were maintained by passages in parasite-free Holstein Friesian male calves and male White German goat kids, respectively [12,13]. For oocyst production, the animals were infected orally with either 3×10^4 *E. bovis* or 1×10^4 *E. arloingi* sporulated oocysts. Experimental infections were conducted in accordance with the Institutional Ethics Commission of the Justus Liebig University (JLU) Giessen, Germany (allowance No. GI 18/10 Nr. A 51/2012 and GI 18/10 Nr. A 2/2016). Excreted oocysts were isolated from faeces beginning at day 18 post-infection (p.i.) and sporulated by incubation in a 2% (*w/v*) potassium dichromate (Merck, Darmstadt, Germany) solution at room temperature (RT) and frequent aeration. Sporulated oocysts were stored in this solution at 4 °C until further use. Sporozoites were excysted from sporulated oocysts as previously described [37]. All culture media were supplemented with 500 U/mL penicillin, 50 µg/mL streptomycin and 5% FCS (Sigma-Aldrich). Infected and non-infected host cells were cultured at 37 °C in 5% CO₂ atmosphere. Vital tachyzoites were collected from supernatants of infected host cells (800 × g; 5 min) and re-suspended in modECGM for further experiments.

2.3. BLT-1 Treatments of Host Cells and Parasite Infections

For infection experiments on fast replicating coccidia (*T. gondii*, *N. caninum* and *B. besnoiti*), BUVEC (*n* = 5) were seeded in 12-well plates (Sarstedt, Nümbrecht, Germany) pre-coated with fibronectin (1:400; Sigma-Aldrich). A BLT-1 (Sigma-Aldrich) stock solution was prepared in dimethyl sulfoxide (DMSO; Sigma-Aldrich, 10 mM, stored at −20 °C), diluted in modECGM and administered at different concentrations (0.25–2 µM) to fully confluent cell monolayers 48 h before infection. Plain modECGM with DMSO (0.02%) served as vehicle control. Following pre-treatments, the inhibitor-supplemented medium was removed, and host cells were infected with tachyzoites at a multiplicity of infection (MOI) of 5:1 for 4 h under inhibitor-free conditions. Then, extracellular tachyzoites were removed and a fresh BLT-1-supplemented medium was re-administered. For infection rate estimation, phase-contrast images were acquired at 24 h p.i. with an inverted microscope

Thiosemicarbazone copper chelator BLT-1 blocks apicomplexan parasite replication by selective inhibition of the scavenger receptor B type I (SR-BI)

(IX81, Olympus, Shinjuku City, Tokyo, Japan) equipped with a digital camera (XM10, Olympus). For the evaluation of inhibitory efficacy, tachyzoites present in cell culture supernatants at 48 h p.i. of BLT-1-treated cells and non-treated controls were collected ($800\times$; 5 min) and counted in a Neubauer chamber.

For analysis of *E. bovis* or *E. arloingi* first merogony and merozoite I production, BUVEC were cultured in 12-well plates (Sarstedt). Thereafter, confluent cell layers were infected with either 7.8×10^4 *E. bovis* or *E. arloingi* sporozoites for 24 h. Every third day, the culture medium was replaced with fresh modCEGM. From 10 (*E. bovis*) or 15 (*E. arloingi*) days p.i. onwards, infected cell cultures were treated with BLT-1 (2 μ M) or vehicle (DMSO 0.02%), with inhibitor-supplemented fresh medium being replaced every 2–3 d. For analyses of *E. bovis*- or *E. arloingi* first merogony development over time, 50 (*E. bovis*) or 40 (*E. arloingi*) macromeronts were analysed per BUVEC isolate ($n = 3$ and 4, respectively). In case of *E. bovis* cultures, BLT-1-driven effects on macromeront development were assessed via estimating the number and size of meronts per area at days 15 and 19 p.i. using the CellSens Dimension[®] v1.7 software (Olympus, Shinjuku City, Tokyo, Japan). Moreover, *E. bovis* proliferation was determined via qPCR-based (EBM1C4-qPCR) analyses of merozoite I production at 24 d p.i., as previously described [14,38]. In case of the *E. arloingi* cultures, macromeront numbers and sizes were studied at days 17, 19, 21, 24 and 26 p.i. From day 21 p.i. onwards, supernatants of infected monolayers were harvested and stored at -80°C for qPCR-based merozoite I quantification, as previously reported [13].

2.4. Live Cell 3D Holotomographic Microscopy and Lipid Droplet (LD) Visualization

BUVEC were seeded into 35 mm tissue culture μ -dishes (Ibidi[®], Gräfelfing, Germany) and cultured (37°C , 5% CO_2) until confluence. BLT-1 pre-treatments (2 μ M) of BUVEC were performed as described above. Thereafter, pre-treated BUVEC were infected with *T. gondii*, *N. caninum* and *B. besnoiti* tachyzoites (MOI = 3:1). At 24 h p.i., live cell holotomographic images were obtained by using a 3D Cell-Explorer microscope (Nanolive[®], Tolothenaz, Switzerland) with $60\times$ magnification ($\lambda = 520$ nm; sample exposure, 0.2 mW/mm²) and a depth of field of 30 μ m. The images were analysed using the STEVE[®] software v 1.1 (Nanolive[®]) to obtain refractive index (RI)-based z -stacks, being projected by the mean average projection plugin tool in the Image J v1.52 software. Further image changes were limited to brightness and contrast adjustments. For *E. arloingi*, infected host cells treated with BLT-1 (2 μ M) from day 15 p.i. were analysed via live cell 3D holotomographic microscopy at day 26 p.i.

For LD visualization, BUVEC were seeded into 35 mm tissue culture μ -dishes (Ibidi[®]) and treated with the vehicle and BLT-1 for 48 h as described above. Then, the treated cells were loaded with BODIPY 493/503 (2 $\mu\text{g}/\text{mL}$, 1 h, 37°C , 5% CO_2 ; Cayman Chemical, Ann Arbor, MI, USA) as described elsewhere [15]. Cellular LDs in the BLT-1-treated cells and non-treated controls ($n = 50$ per condition) were manually counted based on morphology and BODIPY 493/503-driven signal accumulation in endothelial cells [39] and expressed as the number of LDs per cell.

2.5. Ca^{++} Flux Measurements

Calcium signals were registered by staining with Ca^{++} -sensitive dye Fluo-4 (Invitrogen, Waltham, MA, USA) according to the manufacturer's instructions. Briefly, *T. gondii*, *N. caninum* or *B. besnoiti* tachyzoites were loaded with Fluo-4 (2.5 μM in HBSS, 30 min, 37°C); the excess dye was removed by washing with PBS ($600\times$; 5 min), and fresh HBSS was added. For Ca^{++} flux measurement, Fluo-4-loaded tachyzoites were placed into 96-well plates (Greiner, Frickenhausen, Germany) at the concentration of 25×10^6 tachyzoites/mL and exposed to BLT-1 (2 μ M). Spectrofluorometric recording of Ca^{++} signals was performed at an excitation wavelength of 488 nm and emission wavelength of 530 nm in an automated multi-plate reader (Varioskan[®] Flash Multimode Reader, Thermo Scientific, Waltham, MA, USA).

Thiosemicarbazone copper chelator BLT-1 blocks apicomplexan parasite replication by selective inhibition of the scavenger receptor B type I (SR-BI)

2.6. Flow Cytometric Analysis (FACS) of Neutral Lipids in BUVEC

BUVEC ($n = 5$) were seeded into 25 cm² flasks (Sarstedt) and cultured until confluence. Then, the cells were treated with BLT-1 (2 μ M) for 48 h. To determine if inhibitor treatments exerted an effect on neutral lipids, pre-treated cells were stained with BODIPY 493/503 (2 μ g/mL, 1 h, 37 °C, 5% CO₂, Cayman Chemical). Afterwards, cells were washed twice in 1 × PBS (600 × g; 5 min) and samples were analyzed with a BD Accuri C6[®] FACS cell analyzer (Becton-Dickinson, Heidelberg, Germany). The cells were gated according to their size and granularity, while BODIPY 493/503-derived signals were assessed in the FL-1 channel as described elsewhere [15].

2.7. RT-qPCR for Relative Quantification of SR-BI Gene Transcripts

BUVEC ($n = 5$) grown in 25 cm² culture tissue flasks (Greiner, Frickenhausen, Germany) were infected with *T. gondii*, *N. caninum* or *B. besnoiti* tachyzoites (MOI = 5:1). Infected and non-infected host cells were equally processed for total RNA isolation at four different time points after infection (3, 6, 12, 24 h p.i.). For total RNA isolation, the RNeasy kit (Qiagen, Germantown, MD, USA) was used according to the manufacturer's instructions. Total RNAs were stored at −80 °C until further use. In order to remove any traces of genomic DNA, a DNA digestion step was performed. Therefore, 1 μ g of total RNA was treated with 10 U DNase I (Thermo Scientific, Waltham, MA, USA) in 1 × DNase reaction buffer (37 °C, 30 min). Thereafter, DNase was inactivated by heating the samples (65 °C, 10 min). The efficiency of genomic DNA digestion was confirmed by no-RT-controls in each RT-qPCR experiment, while cDNA synthesis was performed using SuperScript IV (Invitrogen[™], Waltham, MA, USA) according to the manufacturer's instructions. Briefly, for first-strand cDNA synthesis, 1 μ g of DNase-treated total RNA was added to 0.5 μ L of 50 μ M oligo(dt), 1 μ L of 50 ng/ μ L random hexamer primer, 1 μ L of 10 mM dNTP mix in a total volume of 10 μ L. Thereafter, the samples were incubated at 65 °C for 5 min and then immediately cooled on ice. Then, 4 μ L of 5 × SSIV buffer, 1 μ L 0.1 M DTT, 1 μ L RNase-free H₂O and 0.5 μ L SuperScript IV enzyme were added, obtaining a total volume of 16.5 μ L. The samples were incubated at 23 °C for 10 min followed by 50 °C for 10 min and an 80 °C inactivation step for 10 min.

The probes were labelled at the 5'-end with reporter dye FAM (6-carboxyfluorescein) and at the 3'-end with quencher dye TAMRA (6-carboxytetramethyl-rhodamine). The SR-BI primer and the probe sequence were designed as follows: *Bos taurus* SR-BI forward 5'-CCACCTCATCAATCAGTAC-3'; reverse 5'-TCGGAATGCCAATAGTTG-3' and probe ACTCCATCCACTTGTCCACGA; qPCR amplification was performed on a Rotor-Gene Q Thermocycler (Qiagen) in duplicates in 10 μ L total volume containing 400 nM forward and reverse primers, 200 nM probe, 10 ng cDNA and 5 μ L 2 × PerfeCTa qPCR FastMix (Quanta Biosciences, Gaithersburg, MD, USA). The reaction conditions were as follows: 95 °C for 10 min, 40 cycles at 95 °C for 10 s, 60 °C for 15 s and 72 °C for 30 s. No-template controls and no-RT reactions were included in each experiment. As the reference housekeeping gene, GAPDH was used as previously reported [14,35].

2.8. Cell Viability Assessment

Cell toxicity of BLT-1 was evaluated by colorimetric XTT tests (Promega, Madison, WI, USA) according to the manufacturer's instructions. Briefly, BUVEC ($n = 3$) were cultured in 96-well plates (Greiner) and treated with BLT-1 (2 μ M) in a total volume of 50 μ L for 72 h. Thereafter, 50 μ L of the XTT working solution were added and the samples were incubated for 4 h (37 °C, 5% CO₂ atmosphere). The resulting formazan products were estimated via optical density (OD) measurements at 590 nm and reference filter 620 nm wavelength using a Varioskan[®] Flash Multimode Reader (Thermo Scientific). BUVEC treated with a solvent (DMSO; 0.02%) were used as the negative control.

For experiments on parasite viability, 5 × 10⁹ tachyzoites/sporozoites of each parasite species were treated for 2 h with BLT-1 (2 μ M; 37 °C, 5% CO₂). The viability was deter-

Thiosemicarbazone copper chelator BLT-1 blocks apicomplexan parasite replication by selective inhibition of the scavenger receptor B type I (SR-BI)

mined using the trypan blue (Sigma-Aldrich) exclusion test. Non-stained parasites were considered to be viable, as reported elsewhere [40].

2.9. Statistical Analysis

For statistical analyses, the GraphPad® Prism 8 (version 8.4.3) software was used. Calculation of Ca^{++} fluxes over time was performed by the analysis of the area under the curve (AUC), using the first 90 s before stimulation as the base line and estimating a total duration of 1100 s. Data description was carried out by presenting the arithmetic mean \pm standard deviation. In addition, the nonparametric statistical Mann–Whitney test for the comparison of two experimental conditions was applied. In cases of three or more conditions, the Kruskal–Wallis test was used. Whenever global comparison using the Kruskal–Wallis test indicated significance, post hoc multiple comparison tests were carried out by means of Dunn’s tests to compare the test conditions with the control ones. Outcomes of the statistical tests were considered to indicate significant differences when $p \leq 0.05$ (significance level).

3. Results

3.1. BLT-1 Treatments Induce Dose-Dependent Blockage of Tachyzoite Replication

Before conducting any further experimentation, potential cytotoxic effects of BLT-1 on BUVEC or tachyzoites were monitored via cytotoxicity assays. As depicted in Supplementary Figure S1A, treatments with BLT-1 (2 μ M) did not induce significant changes in formazan product formation compared to the vehicle controls (DMSO, 0.02%). Similarly, trypan blue exclusion tests showed a similar average viability for *T. gondii*, *N. caninum* and *B. besnoiti* tachyzoites either treated with 0.02% DMSO (vehicle control) or BLT-1 (2 μ M) (Supplementary Figure S1B).

The impact of BLT-1 treatments on the replication of fast proliferating coccidian species (*T. gondii*, *N. caninum* and *B. besnoiti*) was determined by functional assays via counting tachyzoites being released into the medium after 48 h p.i. In principle, BLT-1 treatments induced dose-dependent inhibition of tachyzoite proliferation in all three coccidian species (Figure 1); however, a difference in single parasite sensitivities was apparent since the effects of different inhibitor doses varied in their magnitude in a species-specific manner. In particular, BLT-1 treatments reduced *T. gondii* replication by $90.80 \pm 2.00\%$ ($p < 0.01$) and $97.99 \pm 1.25\%$ ($p < 0.001$) at 1 and 2 μ M, respectively, without any significant effect at lower concentrations (Figure 1A). In the case of *N. caninum* (Figure 1B) and *B. besnoiti* (Figure 1C), 2 μ M BLT-1 reduced tachyzoite replication by $64.59 \pm 7.76\%$ ($p < 0.001$) and $47.24 \pm 4.39\%$ ($p < 0.01$), respectively, with no significant inhibitory effects at lower concentrations. Thus, *B. besnoiti* appeared as the less BLT-1-sensitive and *T. gondii* as the most sensitive of these three coccidian species. In addition, live cell 3D holotomography confirmed respective effects of BLT-1 treatments (2 μ M) in all three parasites species, illustrating a reduction in meront size in *T. gondii*- (Figure 1(A1,A2)), *N. caninum*- (Figure 1(B1,B2)) and *B. besnoiti*-infected (Figure 1(C1,C2)) BUVEC, which was mainly driven by a reduction in tachyzoite numbers within meronts.

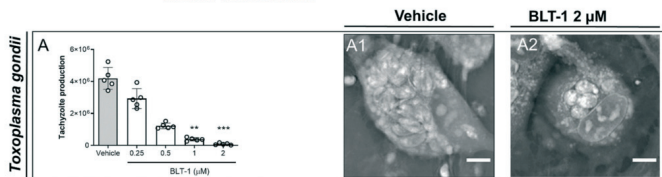


Figure 1. Cont.

Thiosemicarbazone copper chelator BLT-1 blocks apicomplexan parasite replication by selective inhibition of the scavenger receptor B type I (SR-BI)

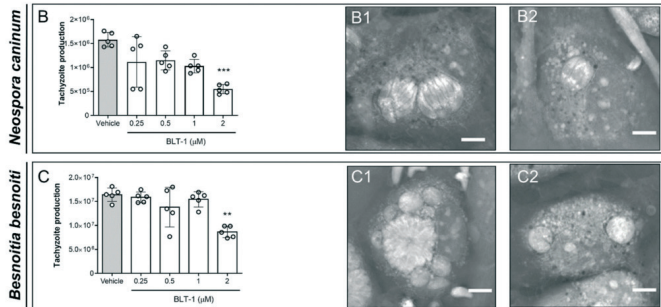


Figure 1. BLT-1 treatments inhibit *T. gondii*, *N. caninum* and *B. besnoiti* intracellular tachyzoite proliferation in primary bovine umbilical vein endothelial cells (BUVEC). BUVEC were treated with BLT-1 (0.25, 0.5, 1 and 2 μM) 48 h before (A) *T. gondii*, (B) *N. caninum* or (C) *B. besnoiti* infection. The number of tachyzoites present in cell culture supernatants were counted 48 h after infection (A–C). Exemplary live cell 3D holotomographic illustration of BLT-1-treated and non-treated *T. gondii*- (A1,A2), *N. caninum*- (B1,B2) or *B. besnoiti*-infected (C1,C2) BUVEC at 24 h p.i. Scale bar: 5 μm. Bars represent the means of five biological replicates ± standard deviation; ** $p \leq 0.01$; *** $p \leq 0.001$.

3.2. BLT-1 Treatments Interfere with *E. bovis* and *E. arloingi* Macromeront Formation and Block Merozoite I Production

The highly pathogenic ruminant *Eimeria* species *E. bovis* (cattle) and *E. arloingi* (goats) develop in host endothelial cells during the first merogony with macromeront formation. The impact of BLT-1 treatment was studied throughout the first merogony of both species by estimating macromeront sizes and numbers in addition to merozoite I production. Overall, a detrimental effect of BLT-1 treatments on macromeront development and merozoite I production was stated in both *Eimeria* species.

In case of *E. bovis*, infected host cells were treated from 10 days p.i. onwards, i.e., the treatments started at immature meront stages. Microscopic monitoring revealed dramatic effects of BLT-1 treatments since immature meronts hardly developed any further under treatment (Figure 2A). Overall, blockage of SR-BI via 2 μM BLT-1 treatments induced a reduction in macromeront numbers per area, as observed on days 15 ($p = 0.0721$; 80% reduction) and 19 ($p = 0.0141$; 87% reduction) p.i. (Figure 2B). Moreover, those meronts that were still able to form proved to be smaller (Figure 2C; 15 d p.i.: $p = 0.1149$; 19 d p.i.: $p = 0.0075$) than the ones in non-treated control cells. Consequently, merozoite I proliferation was significantly blocked by 95% when compared to the controls (Figure 2D; $p = 0.0286$).

E. arloingi-infected BUVEC were treated with BLT-1 from day 15 p.i. onwards, i.e., when macromeronts were still immature, and were thoroughly monitored microscopically (Figure 3A). Overall, the microscopic effects differed substantially from those observed in *E. bovis* cultures and appeared to be less prominent. Thus, in terms of macromeront size, parasite development seemed to be similar in the treated and non-treated *E. arloingi*-infected BUVEC. However, from day 17 p.i. onwards, merozoite I formation started in the control cells but was absent in the treated cells. From day 21 p.i. onwards, mature merozoites I were visible in macromeronts of the non-treated cells, while macromeronts of BLT-1-treated cultures showed degradation, vacuolization, and a lack of merozoites I until the end of the experiment. In contrast to the treated cells, fully developed merozoites I were released into the cell culture supernatant beginning at 24 days p.i. (Figure 3A, 24 d p.i.). In order

Thiosemicarbazone copper chelator BLT-1 blocks apicomplexan parasite replication by selective inhibition of the scavenger receptor B type I (SR-BI)

to control delayed merozoite I formation under BLT-1 treatment, BUVEC cultures were microscopically monitored until day 35 p.i. During this timeframe, no merozoites I were formed, and continuous macromeront degradation was observed. To investigate further the inner structure of macromeronts in the BLT-1-treated cells, 3D holotomographic imaging was performed at day 22 p.i. (Figure 3A, right panel). Here, macromeronts presented equal inhibitor-driven effects of vacuolization in both compartments, the host cell and the macromeront. Furthermore, merozoites I could not be identified since macromeront content appeared as an undistinguishable mass, which is a characteristic feature for degrading *Eimeria* macromeronts. Interestingly, even if new offspring failed to form, macromeronts continued to grow until day 26 p.i., thereby hampering any significant effects of BLT-1-treatments on meront size (Figure 3B).

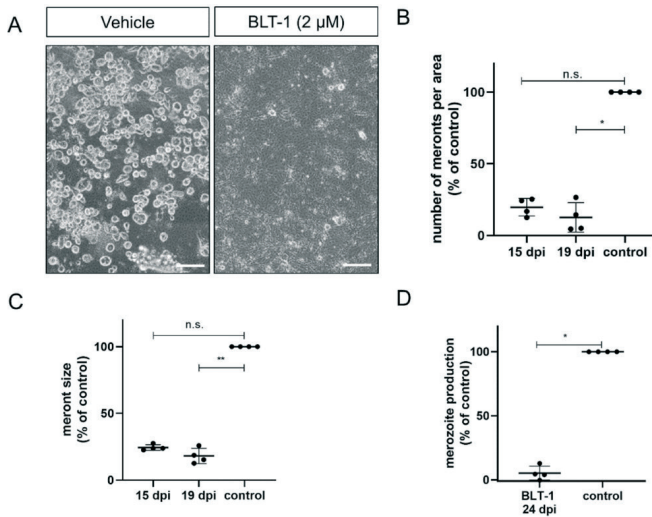


Figure 2. Inhibition of *E. bovis* macromeront development by BLT-1 treatments. (A) Representative illustration of *E. bovis*-infected primary bovine umbilical vein endothelial cells (BUVEC) treated with the vehicle or BLT-1 at day 19 p.i. Normalized number of macromeronts (B) and macromeront sizes (C) at days 15 and 19 p.i. in the vehicle- or BLT-1-treated *E. bovis*-infected BUVEC layers. (D) Normalized merozoite I production at day 24 p.i. in the vehicle- or BLT-1-treated *E. bovis*-infected BUVEC. Scatter plots illustrate the mean of four biological replicates \pm standard deviation. Scale bar: 200 μ m. * $p \leq 0.05$; ** $p \leq 0.01$.

Thiosemicarbazone copper chelator BLT-1 blocks apicomplexan parasite replication by selective inhibition of the scavenger receptor B type I (SR-BI)

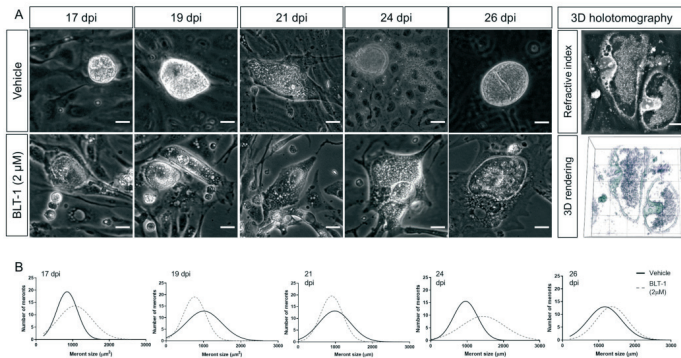


Figure 3. Effects of BLT-1 treatments on *E. arloingi* macromeront development in primary bovine umbilical vein endothelial cells (BUVEC). (A) Representative phase-contrast imaging of *E. arloingi* macromeronts at days 17, 19, 21, 24, 26 p.i. in the vehicle- or BLT-1-treated BUVEC and exemplary live cell 3D holotomography analysis of the BLT-1-treated *E. arloingi*-infected BUVEC at 22 d p.i. Note: vacuolization of host cells and macromeronts. (B) Macromeront numbers over time in the vehicle- and BLT-1-treated *E. arloingi*-infected BUVEC as a frequency distribution histogram. Scale bar: 5 μm.

3.3. BLT-1 Treatment Impairs Infectivity of Fast Replicating Tachyzoites but Has No Effect on Slow Replicating Sporozoites

Fulfilment of intracellular replication relies on active parasite-driven host cell invasion. To estimate if BLT-1 also had direct effects on the capacities of infective stages, here, we treated free infective stages (tachyzoites of *T. gondii*, *N. caninum* and *B. besnoiti* or sporozoites of *E. bovis* and *E. arloingi*) with BLT-1. As illustrated in Figure 4A–C, BLT-1 treatments moderately reduced tachyzoite invasive capacities since lower infection rates were detected in all cases of BLT-1 pre-treatments. Thus, an average infection rate of $33.41 \pm 3.90\%$, $43.59 \pm 5.91\%$ and $26.74 \pm 3.74\%$ was found in case of non-treated *T. gondii*-, *N. caninum*- and *B. besnoiti* tachyzoites, respectively, which was reduced to $28.4 \pm 14.9\%$ ($p = 0.043$), $40.0 \pm 7.7\%$ ($p = 0.002$) and $22.7 \pm 19.2\%$ ($p = 0.056$) for BLT-1-treated tachyzoites, respectively. Of note, BLT-1 pre-treatments of BUVEC did not affect their permissiveness for subsequent *T. gondii*-, *N. caninum*- or *B. besnoiti* tachyzoite infections (Supplementary Figure S2). Referring to the slow replicating species *E. bovis* and *E. arloingi*, treatments with 2 μM BLT-1 did not affect sporozoites viability (2 h; data not shown). However, in contrast to fast replicating coccidia, preincubation of freshly excysted sporozoites with 2 μM BLT-1 did not significantly affect subsequent host cell infection. Thus, an infection rate of $15.72 \pm 1.39\%$ and $14.55 \pm 2.18\%$ was registered for the *E. bovis*-infected non-treated and BLT-1-treated cells, respectively ($p = 0.700$). *E. arloingi*-treated sporozoites infected $7.75 \pm 0.90\%$ of host cells, while an infection rate of $8.21 \pm 0.67\%$ was recorded for non-treated parasite stages ($p = 0.486$). Additionally, BLT-1 pre-treatments of host cells did not affect their permissiveness for subsequent *E. arloingi* sporozoite infection (reduction to 6.5%).

Thiosemicarbazone copper chelator BLT-1 blocks apicomplexan parasite replication by selective inhibition of the scavenger receptor B type I (SR-BI)

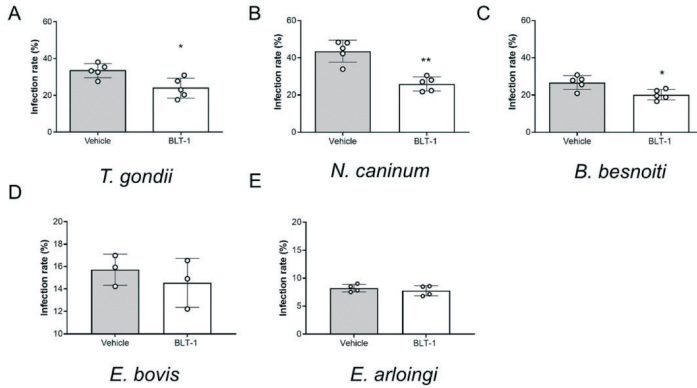


Figure 4. Impairment of *T. gondii*, *N. caninum* and *B. besnoiti* tachyzoite infectivity by BLT-1 treatments. Infection rates of the vehicle-treated or BLT1-treated *T. gondii* (A), *N. caninum* (B) and *B. besnoiti* (C) tachyzoites and the *E. bovis* (D) and *E. arloingi* (E) sporozoites. Bars represent the means of five biological replicates \pm standard deviation; * $p \leq 0.05$; ** $p \leq 0.01$.

3.4. BLT-1 Treatments Trigger Ca^{++} Fluxes in Free Tachyzoites

Given that infectivity-related inhibitor effects were stated for fast proliferating coccidia, here, we additionally measured potential effects of BLT-1 on the tachyzoite own Ca^{++} responses. Given that Ca^{++} acts as an early second messenger and is pivotal for tachyzoite invasion, we evaluated the impact of BLT-1 treatments on Ca^{++} fluxes in Fluo-4-loaded tachyzoites. In principle, 2 μ M BLT-1 treatments induced an increase in Ca^{++} signals over time when compared with the controls (vehicle treatment) in all *T. gondii*, *N. caninum* and *B. besnoiti* tachyzoites, showing only minor differences between parasite species in terms of signal kinetics. This effect was similar for *T. gondii* (Figure 5(A1)), *N. caninum* (Figure 5(B1)) and *B. besnoiti* (Figure 5(C1)) tachyzoites. Likewise, AUC analysis revealed a total increase in Ca^{++} mobilized by BLT-1 treatments (Figure 5(A2,B2,C2)), demonstrating inhibitor-driven enhancement in Ca^{++} signals of 402.52 \pm 354.14% ($p = 0.0079$), 53.98 \pm 22.73% ($p = 0.0079$) and 43.30 \pm 7.60% ($p = 0.0079$) for *T. gondii*, *N. caninum* and *B. besnoiti*, respectively.

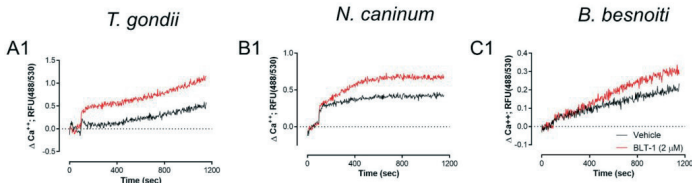


Figure 5. Cont.

Thiosemicarbazone copper chelator BLT-1 blocks apicomplexan parasite replication by selective inhibition of the scavenger receptor B type I (SR-BI)

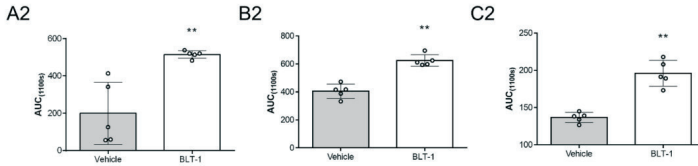


Figure 5. BLT-1 affects Ca^{2+} homeostasis in *T. gondii*, *N. caninum* and *B. besnoiti* tachyzoites. Vehicle- or BLT1-induced Ca^{2+} flux in and the related AUC data from Fluo-4-loaded *T. gondii* (A1,A2), *N. caninum* (B1,B2) and *B. besnoiti* (C1,C2) tachyzoites. Bars represent the means of five biological replicates \pm standard deviation; ** $p \leq 0.01$.

3.5. BLT-1 Treatments Alter Neutral Lipid Contents and Cholesterol Distribution in BUVEC

Given that anti-parasitic effects of BLT-1 primarily seemed to be attributed to host cell alterations and considering that all *T. gondii*, *N. caninum* and *B. besnoiti* species have already been reported to depend on host cell lipid disposal [22,25], we next evaluated BLT-1-mediated effects on endothelial cell phenotype by performing RI-based 3D holographic live cell imaging. As illustrated in Figure 6, 2 μ M BLT-1 treatments did not induce major phenotypic changes of living BUVEC; nevertheless, we found a discrete increase in small dense globular structures within the cytoplasm of treated cells (Figure 6 arrows). These vesicle-like structures showed the average RI of 1.366 ± 0.011 ($n = 50$) which is consistent with prior reports on LDs [22]. To confirm this finding, we additionally stained BUVEC for cellular distribution of neutral lipids via BODIPY 493/503. BLT-1 treatments induced a change in neutral lipid signal distribution by increasing the cytoplasmic presence of BODIPY 493/503-positive vesicles throughout the cell by 45.1% when compared with vehicle-treated controls ($p = 0.004$) (Figure 6A,B). We also confirmed these microscope-based observations in a quantitative manner via FACS analysis on BODIPY 493/503-stained live endothelial cells. As expected, BLT-1 treatments induced a significant increase in the neutral lipid-related mean fluorescence intensity (26.1%, $p = 0.0159$, Figure 6C).

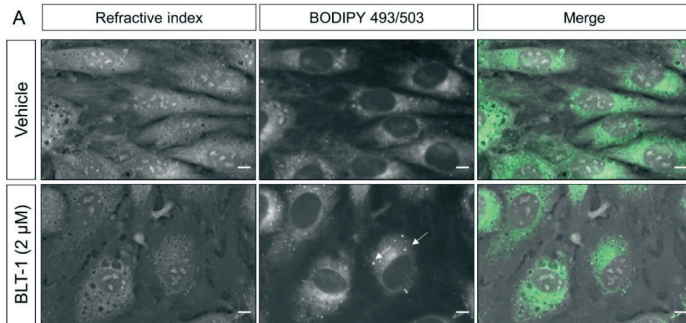


Figure 6. Cont.

Thiosemicarbazone copper chelator BLT-1 blocks apicomplexan parasite replication by selective inhibition of the scavenger receptor B type I (SR-BI)



Figure 6. BLT-1-induced changes in cytoplasmic neutral lipid accumulation in primary bovine umbilical vein endothelial cells (BUVEC). (A) Live cell 3D holotomography analysis in combination with BODIPY 493/503-driven epifluorescence of the vehicle- or BLT-1-treated BUVEC. (B) Violin plot depicting the number of LDs in the vehicle- or BLT-1-treated BUVEC. (C) BODIPY 493/503-based mean fluorescence intensity in the vehicle- or BLT-1-treated BUVEC detected by FACS analyses. Bars represent the means of five biological replicates \pm standard deviation. White arrows indicate LD-like structures. Scale bar: 5 μ m. * $p \leq 0.05$; *** $p \leq 0.001$.

3.6. SR-BI Gene Transcription Is Not Affected by *T. gondii*, *N. caninum* and *B. besnoiti* Tachyzoite Infections

Since coccidian parasites are well-known to modulate host cell gene expression throughout infection to ensure their obligate intracellular replication requirements [41–43], we also evaluated the impact of *T. gondii*, *N. caninum* and *B. besnoiti* infections on SR-BI gene transcription in BUVEC by RT-qPCR. Even though SR-BI gene transcription seemed slightly enhanced at 3 and 6 h p.i. (*T. gondii*, Figure 7A), 12 and 24 h p.i. (*N. caninum*, Figure 7B) or 6 and 12 h p.i. (*B. besnoiti*, Figure 7C) in single endothelial cell isolates, no significant *T. gondii*-, *N. caninum*- or *B. besnoiti*-driven changes in SR-BI mRNA abundance was detected over time in tachyzoite-infected BUVEC.

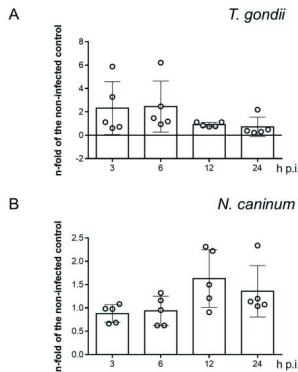


Figure 7. Cont.

Thiosemicarbazone copper chelator BLT-1 blocks apicomplexan parasite replication by selective inhibition of the scavenger receptor B type I (SR-BI)

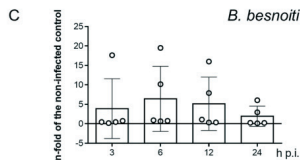


Figure 7. SR-BI gene transcription in *T. gondii*- (A), *N. caninum*- (B) and *B. besnoiti*-infected (C) primary bovine umbilical vein endothelial cells (BUVEC). Bars represent the means of five biological replicates \pm standard deviation. Significant level $p < 0.05$.

4. Discussion

Since apicomplexan parasites are auxotrophic for cholesterol biosynthesis, they need to obtain this molecule from their host cells to ensure successful proliferation [17]. During merogonic replication of coccidian parasites, host cell uptake of exogenous LDL represents the major mechanism of cholesterol acquisition to fulfil parasite metabolic requirements [20–22,44]. This route relies on endocytosis of LDL–LDLR, being thereafter LDL-derived cholesterol released for cell requirements in a NPC1-dependent process [18]. Interestingly, alternative non-endocytic mechanisms of cholesterol uptake have also been suggested for endothelial cells [27]. In this context, endothelocytes might obtain cholesterol from acetylated or oxidized LDL via the acLDL receptor and the lectin-type oxidized LDL receptor 1 (LOX-1, syn. OLR1) [27]. Moreover, participation of scavenger receptor B type I (SR-BI) representing the canonical HDL receptor in an alternative non-endocytic route for cholesteryl ester uptake from plasmatic LDL molecules was proposed [28,31], thereby offering an alternative and LDLR-independent scavenging pathway for endothelial coccidian infections.

To analyse involvement of SR-BI in coccidian parasite proliferation, the SR-BI-specific inhibitor BLT-1 was used [45,46]. This compound has a high inhibitory capacity without affecting LDL-endocytic cholesterol acquisition delivering a suitable tool for SR-BI-related analyses [45,46]. The current data show that BLT-1 treatments significantly reduced *T. gondii*-, *N. caninum*- and *B. besnoiti* tachyzoite replication in primary host endothelial cells, *T. gondii* being the most affected by this treatment. So far, this is the first report on antiproliferative capacity of BLT-1 treatments in fast proliferating coccidian species. Of note, prior reports showed importance of SR-BI in Huh7 cell infections with the apicomplexan parasite *P. berghei* via BLT-1 treatments and siRNA assays [33]. Interestingly, these findings were corroborated by reduction of parasite burden in SR-BI-deficient mice, demonstrating participation of SR-BI-mediated pathways in hepatic *P. berghei* replication in vivo [33], suggesting a common mechanism for apicomplexans. However, apparent differences in host cell type and parasite biology limit valid comparisons with present data. In this context, it should be highlighted that the capacity of SR-BI to incorporate cholesteryl esters and other lipids from HDL particles is largely accepted for the hepatic tissue [27–29]. In contrast, its function in endothelial cell cholesterol metabolism currently seems limited to its typical role as HDL receptor [28,29]. It is worth noting that *T. gondii*, *N. caninum* and *B. besnoiti* generate their offspring via endodyogeny, whilst species of the genus *Plasmodium*, such as *P. berghei* and *P. falciparum*, undergo schizogony during their hepatic phase in vivo [47]. In this scenario, to address if current anti-coccidian effects of BLT-1 in endothelial cells represented a conserved phenomenon or rather a consequence of particular characteristics of host cell type or of specific parasite asexual division mechanisms, we additionally evaluated the impact of this inhibitor on *E. bovis* and *E. arloingi* merogony I in BUVEC. These eimerian parasites undergo schizogony during their long-lasting first merogony (more than 18 days in vitro), which is restricted to endothelial host cells and which requires considerable amounts of cholesterol to fulfil macromeront formation and massive offspring

Thiosemicarbazone copper chelator BLT-1 blocks apicomplexan parasite replication by selective inhibition of the scavenger receptor B type I (SR-BI)

production, resulting in $\geq 120,000$ merozoites I per macromeront [12,14,22,48]. In line with the fast proliferating species, BLT-1 treatment effectively reduced macromeront development in both pathogenic ruminant *Eimeria* species, suggesting conserved involvement of SR-BI in apicomplexan replication. However, as reported here for fast proliferating coccidian species, we also detected slight species-specific differences in BLT-1 effects on *E. bovis* and *E. arloingi* macromeront development. Thus, whilst *E. bovis* macromeronts hardly developed at all under BLT-1 treatments, *E. arloingi* macromeronts seemed to be formed but failed to produce merozoites I and were prone to degradation. So far, this is the first report on the participation of cholesterol-related routes in caprine *E. arloingi* first merogony. In contrast, for *E. bovis*, its dependence on host cell de novo cholesterol biosynthesis and LDL uptake was already reported [14,49].

Due to their characteristic obligate intracellular life style, coccidian parasites must actively invade host cells [9]. Therefore, here, we evaluated the impact of BLT-1 treatments on free infective stages (tachyzoites in case of *T. gondii*, *N. caninum* and *B. besnoiti* and sporozoites for *E. bovis* and *E. arloingi*) and additionally controlled whether host cell pre-treatments may impair active parasite invasion. Referring to infective stages, interestingly, we found stage-specific effects of BLT-1 treatments. Thus, tachyzoite treatments resulted in an impairment of *T. gondii*, *N. caninum* and *B. besnoiti* host cell invasion process, thereby either indicating the presence of parasite molecules interacting with BLT-1 in tachyzoites or non-specific side effects of this treatment. In contrast, *Eimeria* spp. sporozoites were not at all affected by BLT-1 treatments and subsequent infection rates did not differ from those of untreated stages, thereby eventually questioning the hypothesis of non-specific side effects. Referring to host cells, BLT-1 pre-treatments had neither an effect on subsequent parasite invasion nor host cell permissiveness in none of parasites studied here. The latter finding contrasts with observations on *Plasmodium* spp. infections since SR-BI is considered to be the key surface molecule for host cell recognition during sporozoite invasion [33,34]. Given that no data are available on detailed mechanism of direct anti-invasive BLT-1-triggered effects in tachyzoites, we additionally evaluated effects of treatments on tachyzoite Ca^{++} homeostasis. In parallel with impaired invasion, BLT-1 triggered enhanced Ca^{++} fluxes in free tachyzoites of *T. gondii*, *N. caninum* and *B. besnoiti* over time. This is of special interest since Ca^{++} is well-recognised as a pivotal second messenger for coccidian host cell invasion [9,50], suggesting that BLT-1 treatments could result in untimely Ca^{++} mobilization during the invasion process. Possible implications of BLT-1 on Ca^{++} homeostasis have not been addressed previously, but BLT-1 treatment has been linked to phenotypical changes in zebrafish development [51], implying possible side effects driven by this compound. Nonetheless, further detailed studies are necessary to establish the impact of BLT-1 on coccidian Ca^{++} homeostasis.

From a mechanistic perspective, exogenous cholesterol is mainly incorporated by LDL via the canonical LDL-LDLR endocytic route [18,24]. Considering possible involvement of SR-BI in BUVEC-mediated cholesterol acquisition, we functionally evaluated the impact of BLT-1 treatments on cellular neutral lipid contents. Overall, microscopic analyses showed that BLT-1 treatment incremented the number of neutral lipid (marker = BODIPY 493/503)-positive vesicles, and FACS analyses confirmed this effect in a quantitative manner. In agreement, live cell 3D holotomographic analysis suggested these globular structures as LDs based on their characteristic RI-values. These findings are in line with the function of SR-BI in endothelial cell cholesterol efflux [27], being a consequence of SR-BI blockage, thereby impairing its capacity for HDL-dependent cholesterol efflux and finally resulting in cellular neutral lipid accumulation [52]. Interestingly, we recently reported that verapamil treatments also reduced *T. gondii*-, *N. caninum*- and *B. besnoiti* tachyzoite replication, which was accompanied by enhanced neutral lipid accumulation [15]. It seems, therefore, plausible to speculate that cholesterol efflux impairment may generally affect obligate intracellular coccidian development. However, BLT-1-mediated anti-coccidian effects may also be a consequence of inhibitor-driven impairment of SR-BI HDL-dependent signaling pathways, e.g., via PI3K or ERK1/2 [32].

Thiosemicarbazone copper chelator BLT-1 blocks apicomplexan parasite replication by selective inhibition of the scavenger receptor B type I (SR-BI)

At the transcriptomic level, steroidogenic and hepatic tissues present higher levels of SR-BI mRNAs [32]. In mammalian endothelial cells, SR-BI gene transcription has been linked to liver X receptor (LXR) activation and 17 β -estradiol exposure [53,54]. In this context, the capacity of coccidian parasites to modulate host cell gene transcription and their phenotype to sustain metabolic requirements of parasite replication has already been reported [22,41–43]. Considering this, we evaluated whether *T. gondii*, *N. caninum* and *B. besnoiti* infections modulate SR-BI gene transcription in BUVEC over time. Unexpectedly, no infection-mediated changes in SR-BI gene transcription were detected over time, suggesting that constitutive receptor expression is sufficient to mediate current BLT-1-driven effects.

In summary, here, we reported for the first time anti-proliferative effects of BLT-1 on several coccidian species of medical and veterinary importance. These data suggest SR-BI participation in asexual replication of *T. gondii*, *N. caninum*, *B. besnoiti*, *E. bovis* and *E. arloingi*, thereby implying conserved mechanisms in these species. Given that BLT-1 treatments additionally drive Ca²⁺ fluxes and impair infectivity in free tachyzoites, a non-specific side effect of this treatment may eventually occur in this parasitic stage. Finally, BLT-1-induced neutral lipid accumulation demonstrates that SR-BI is involved in neutral lipid metabolism and efflux in primary bovine endothelial cells.

Supplementary Materials: The following are available online at <https://www.mdpi.com/article/10.3390/microorganisms9112372/s1>, Figure S1: Viability of BLT-1-treated host cells, Figure S2: Infection rates of fast replicating coccidian parasites after BLT-1 pre-treatment of host cells.

Author Contributions: C.L., L.M.R.S., C.H. and A.T. conceived and designed the studies. Collection of data: C.L. and L.M.R.S. carried out experiments on fast replicating coccidian experiments; A.T. and L.M.R.S. performed *E. bovis*-related experiments; S.L.-O., L.M.R.S. and Z.D.V., carried out *E. arloingi*-based experiments. C.L. and L.M.R.S. performed statistical analyses. All authors contributed to data analyses. C.L. and L.M.R.S. wrote the manuscript. All authors have read and agreed to the published version of the manuscript.

Funding: Selected experiments were supported and financed by the German Research Foundation (Deutsche Forschungsgemeinschaft (DFG); grant No. TA 291/10-1). The publication fees were partially funded by the Open Access Funds of Justus Liebig University Giessen.

Institutional Review Board Statement: Not applicable.

Informed Consent Statement: Not applicable.

Data Availability Statement: All data are included in the manuscript.

Acknowledgments: The authors would like to thank Christine Henrich, Christin Ritter and Hannah Salecker for their outstanding technical support. We are very thankful to A. Wehrend (Clinic for Obstetrics, Gynaecology and Andrology of Large and Small Animals, Justus Liebig University Giessen, Germany) for the continuous supply of bovine umbilical cords. C.L. was funded by the National Agency for Research and Development ((ANID), DOCTORADO BECAS CHILE/2017—1780349). S.L.O. was a recipient of a PhD fellowship financed by the German Academic Exchange Service (DAAD Research Grants—One-Year Grants 2018–19).

Conflicts of Interest: The authors declare no conflict of interest.

References

1. Votýpka, J.; Modrý, D.; Oborník, M.; Šlapeta, J.; Lukeš, J. Apicomplexa. In *Handbook of the Protists*; Archibald, J.M., Simpson, A.G.B., Slamovits, C.H., Eds.; Springer International Publishing: Cham, Switzerland, 2017; pp. 567–624, ISBN 978-3-319-28149-0.
2. Benavides, J.; Fernández, M.; Castaño, P.; Ferreras, M.C.; Ortega-Mora, L.; Pérez, V. Ovine Toxoplasmosis: A New Look at Its Pathogenesis. *J. Comp. Pathol.* **2017**, *157*, 34–38. [CrossRef] [PubMed]
3. Innes, E.A. A Brief History and Overview of *Toxoplasma gondii*. *Zoonoses Public Health* **2010**, *57*, 1–7. [CrossRef] [PubMed]
4. Dubey, J.P. Review of *Neospora caninum* and Neosporosis in Animals. *Korean J. Parasitol.* **2003**, *41*, 1–16. [CrossRef] [PubMed]
5. Reichel, M.P.; Alejandra Ayanegui-Alcérreca, M.; Gondim, L.F.P.; Ellis, J.T. What Is the Global Economic Impact of *Neospora caninum* in Cattle—The Billion Dollar Question. *Int. J. Parasitol.* **2013**, *43*, 133–142. [CrossRef] [PubMed]

Thiosemicarbazone copper chelator BLT-1 blocks apicomplexan parasite replication by selective inhibition of the scavenger receptor B type I (SR-BI)

6. Alvarez-García, G.; García-Lunar, P.; Gutiérrez-Expósito, D.; Shkap, V.; Ortega-Mora, L.M. Dynamics of *Besnoitia besnoiti* Infection in Cattle. *Parasitology* **2014**, *141*, 1419–1435. [CrossRef]
7. Cortes, H.; Leitão, A.; Gottstein, B.; Hemphill, A. A Review on Bovine Besnoitiosis: A Disease with Economic Impact in Herd Health Management, Caused by *Besnoitia besnoiti* (Franco and Borges, 1916). *Parasitology* **2014**, *141*, 1406–1417. [CrossRef]
8. Dausgries, A.; Najdrowski, M. Eimeriosis in Cattle: Current Understanding. *J. Vet. Med. B Infect. Dis. Vet. Public Health* **2005**, *52*, 417–427. [CrossRef]
9. Black, M.W.; Boothroyd, J.C. Lytic Cycle of *Toxoplasma gondii*. *Microbiol. Mol. Biol. Rev.* **2000**, *64*, 607–623. [CrossRef]
10. Lindsay, D.S.; Dubey, J.P. Neosporosis, Toxoplasmosis, and Sarcocystosis in Ruminants: An Update. *Vet. Clin. N. Am. Food Anim. Pract.* **2020**, *36*, 205–222. [CrossRef]
11. Pellerdy, L.P. *Coccidia and Coccidiosis*, 2nd ed.; Parey: Berlin/Hamburg, Germany, 1974; ISBN 978-3-489-73317-1.
12. López-Osorio, S.; Silva, L.M.R.; Taubert, A.; Chaparro-Gutiérrez, J.J.; Hermosilla, C.R. Concomitant In Vitro Development of *Eimeria zuernii*- and *Eimeria bovis*-Macromeronts in Primary Host Endothelial Cells. *Parasitol. Int.* **2018**, *67*, 742–750. [CrossRef]
13. Silva, L.M.R.; Vila-Vieira, M.J.M.; Cortes, H.C.E.; Taubert, A.; Hermosilla, C. Suitable In Vitro *Eimeria arloingi* Macromeront Formation in Host Endothelial Cells and Modulation of Adhesion Molecule, Cytokine and Chemokine Gene Transcription. *Parasitol. Res.* **2015**, *114*, 113–124. [CrossRef]
14. Hamid, P.H.; Hinzmann, J.; Kermer, K.; Gimpl, G.; Lochnit, G.; Hermosilla, C.R.; Taubert, A. *Eimeria bovis* Infection Modulates Endothelial Host Cell Cholesterol Metabolism for Successful Replication. *Vet. Res.* **2015**, *46*, 100. [CrossRef]
15. Larrazabal, C.; Silva, L.M.R.; Pervizaj-Oruqaj, L.; Herold, S.; Hermosilla, C.; Taubert, A. P-Glycoprotein Inhibitors Differently Affect *Toxoplasma gondii*, *Neospora caninum* and *Besnoitia besnoiti* Proliferation in Bovine Primary Endothelial Cells. *Pathogens* **2021**, *10*, 395. [CrossRef]
16. Larrazabal, C.; Silva, L.M.R.; Hermosilla, C.; Taubert, A. Ezetimibe Blocks *Toxoplasma gondii*-, *Neospora caninum*- and *Besnoitia besnoiti*-Tachyzoite Infectivity and Replication in Primary Bovine Endothelial Host Cells. *Parasitology* **2021**, *148*, 1107–1115. [CrossRef] [PubMed]
17. Coppens, I. Targeting Lipid Biosynthesis and Salvage in Apicomplexan Parasites for Improved Chemotherapies. *Nat. Rev. Microbiol.* **2013**, *11*, 823–835. [CrossRef] [PubMed]
18. Ikonen, E. Cellular Cholesterol Trafficking and Compartmentalization. *Nat. Rev. Mol. Cell. Biol.* **2008**, *9*, 125–138. [CrossRef] [PubMed]
19. Luo, J.; Yang, H.; Song, B.-L. Mechanisms and Regulation of Cholesterol Homeostasis. *Nat. Rev. Mol. Cell. Biol.* **2020**, *21*, 225–245. [CrossRef]
20. Coppens, I.; Sinai, A.P.; Joiner, K.A. *Toxoplasma gondii* Exploits Host Low-Density Lipoprotein Receptor-Mediated Endocytosis for Cholesterol Acquisition. *J. Cell Biol.* **2000**, *149*, 167–180. [CrossRef]
21. Nolan, S.J.; Romano, J.D.; Luetchefeld, T.; Coppens, I. *Neospora caninum* Recruits Host Cell Structures to Its Parasitophorous Vacuole and Salvages Lipids from Organelles. *Eukaryot. Cell* **2015**, *14*, 454–473. [CrossRef]
22. Silva, L.M.R.; Lütjohann, D.; Hamid, P.; Velasquez, Z.D.; Kermer, K.; Larrazabal, C.; Failing, K.; Hermosilla, C.; Taubert, A. *Besnoitia besnoiti* Infection Alters Both Endogenous Cholesterol de Novo Synthesis and Exogenous LDL Uptake in Host Endothelial Cells. *Sci. Rep.* **2019**, *9*, 6660. [CrossRef]
23. Meng, Y.; Heybrock, S.; Neucil, D.; Saftig, P. Cholesterol Handling in Lysosomes and Beyond. *Trends Cell Biol.* **2020**, *30*, 452–466. [CrossRef] [PubMed]
24. Simons, K.; Ikonen, E. How Cells Handle Cholesterol. *Science* **2000**, *290*, 1721–1726. [CrossRef] [PubMed]
25. Nolan, S.J.; Romano, J.D.; Coppens, I. Host Lipid Droplets: An Important Source of Lipids Salvaged by the Intracellular Parasite *Toxoplasma gondii*. *PLoS Pathog.* **2017**, *13*, e1006362. [CrossRef]
26. Dean, M.; Rzhetsky, A.; Allikmets, R. The Human ATP-Binding Cassette (ABC) Transporter Superfamily. *Genome Res.* **2001**, *11*, 1156–1166. [CrossRef] [PubMed]
27. Adachi, H.; Tsujimoto, M. Endothelial Scavenger Receptors. *Prog. Lipid Res.* **2006**, *45*, 379–404. [CrossRef] [PubMed]
28. Hoekstra, M.; Van Berkel, T.-J.; Van Eck, M. Scavenger Receptor BI: A Multi-Purpose Player in Cholesterol and Steroid Metabolism. *World J. Gastroenterol.* **2010**, *16*, 5916–5924. [CrossRef]
29. Van Eck, M.; Twisk, J.; Hoekstra, M.; Van Rij, B.T.; Van der Lans, C.A.C.; Bos, I.S.T.; Kruijt, J.K.; Kuipers, F.; Van Berkel, T.J.C. Differential Effects of Scavenger Receptor BI Deficiency on Lipid Metabolism in Cells of the Arterial Wall and in the Liver. *J. Biol. Chem.* **2003**, *278*, 23699–23705. [CrossRef]
30. Linton, M.F.; Tao, H.; Linton, E.F.; Yancey, P.G. SR-BI: A Multifunctional Receptor in Cholesterol Homeostasis and Atherosclerosis. *Trends Endocrinol. Metab.* **2017**, *28*, 461–472. [CrossRef]
31. Vishnyakova, T.G.; Bocharov, A.V.; Baranova, I.N.; Kurlander, R.; Drake, S.K.; Chen, Z.; Amar, M.; Sviridov, D.; Vaisman, B.; Poliakov, E.; et al. SR-BI Mediates Neutral Lipid Sorting from LDL to Lipid Droplets and Facilitates Their Formation. *PLoS ONE* **2020**, *15*, e0240659. [CrossRef]
32. Gutierrez-Pajares, J.L.; Ben Hassen, C.; Chevalier, S.; Frank, P.G. SR-BI: Linking Cholesterol and Lipoprotein Metabolism with Breast and Prostate Cancer. *Front. Pharmacol.* **2016**, *7*, 338. [CrossRef]
33. Rodrigues, C.D.; Hannus, M.; Prudêncio, M.; Martin, C.; Gonçalves, L.A.; Portugal, S.; Epiphanyo, S.; Akinc, A.; Hadwiger, P.; Jahn-Hofmann, K.; et al. Host Scavenger Receptor SR-BI Plays a Dual Role in the Establishment of Malaria Parasite Liver Infection. *Cell Host Microbe* **2008**, *4*, 271–282. [CrossRef]

Thiosemicarbazone copper chelator BLT-1 blocks apicomplexan parasite replication by selective inhibition of the scavenger receptor B type I (SR-B1)

34. Yalaoui, S.; Huby, T.; Franetich, J.-F.; Gego, A.; Rametti, A.; Moreau, M.; Collet, X.; Siau, A.; van Gemert, G.-J.; Sauerwein, R.W.; et al. Scavenger Receptor BI Boosts Hepatocyte Permissiveness to *Plasmodium* Infection. *Cell Host Microbe* **2008**, *4*, 283–292. [[CrossRef](#)]
35. Taubert, A.; Zahner, H.; Hermosilla, C. Dynamics of Transcription of Immunomodulatory Genes in Endothelial Cells Infected with Different Coccidian Parasites. *Vet. Parasitol.* **2006**, *142*, 214–222. [[CrossRef](#)] [[PubMed](#)]
36. Maksimov, P.; Hermosilla, C.; Kleinertz, S.; Hirtzmann, J.; Taubert, A. *Besnoitia besnoiti* Infections Activate Primary Bovine Endothelial Cells and Promote PMN Adhesion and NET Formation under Physiological Flow Condition. *Parasitol. Res.* **2016**, *115*, 1991–2001. [[CrossRef](#)] [[PubMed](#)]
37. López-Osorio, S.; Silva, L.M.R.; Chaparro-Gutiérrez, J.J.; Velásquez, Z.D.; Taubert, A.; Hermosilla, C. Optimized Excystation Protocol for Ruminant *Eimeria bovis*- and *Eimeria arloingi*-Sporulated Oocysts and First 3D Holotomographic Microscopy Analysis of Differing Sporozoite Egress. *Parasitol. Int.* **2020**, *76*, 102068. [[CrossRef](#)] [[PubMed](#)]
38. Taubert, A.; Silva, L.M.R.; Velásquez, Z.D.; Larrazabal, C.; Lütjohann, D.; Hermosilla, C. Modulation of Cholesterol-Related Sterols during *Eimeria bovis* Macromeront Formation and Impact of Selected Oxysterols on Parasite Development. *Mol. Biochem. Parasitol.* **2018**, *223*, 1–12. [[CrossRef](#)]
39. Astanina, K.; Koch, M.; Jüngst, C.; Zumbusch, A.; Kiemer, A.K. Lipid Droplets as a Novel Cargo of Tunnelling Nanotubes in Endothelial Cells. *Sci. Rep.* **2015**, *5*, 11453. [[CrossRef](#)]
40. Cervantes-Valencia, M.E.; Hermosilla, C.; Alcalá-Canto, Y.; Tapia, G.; Taubert, A.; Silva, L.M.R. Antiparasitic Efficacy of Curcumin Against *Besnoitia besnoiti* Tachyzoites In Vitro. *Front. Vet. Sci.* **2018**, *5*, 333. [[CrossRef](#)]
41. Horcajo, P.; Xia, D.; Randle, L.; Collantes-Fernández, E.; Wastling, J.; Ortega-Mora, L.M.; Regidor-Cerrillo, J. Integrative Transcriptome and Proteome Analyses Define Marked Differences between *Neospora caninum* Isolates throughout the Tachyzoite Lytic Cycle. *J. Proteom.* **2018**, *180*, 108–119. [[CrossRef](#)]
42. Jiménez-Meléndez, A.; Ramakrishnan, C.; Hehl, A.B.; Russo, G.; Álvarez-García, G. RNA-Seq Analyses Reveal That Endothelial Activation and Fibrosis Are Induced Early and Progressively by *Besnoitia besnoiti* Host Cell Invasion and Proliferation. *Front. Cell. Infect. Microbiol.* **2020**, *10*, 218. [[CrossRef](#)]
43. Taubert, A.; Wimmers, K.; Ponsuksili, S.; Jimenez, C.A.; Zahner, H.; Hermosilla, C. Microarray-Based Transcriptional Profiling of *Eimeria bovis*-Infected Bovine Endothelial Host Cells. *Vet. Res.* **2010**, *41*, 70. [[CrossRef](#)]
44. Ehrenman, K.; Wányiri, J.W.; Bhat, N.; Ward, H.D.; Coppens, I. *Cryptosporidium parvum* Scavenges LDL-Derived Cholesterol and Micellar Cholesterol Internalized into Enterocytes. *Cell. Microbiol.* **2013**, *15*, 1182–1197. [[CrossRef](#)] [[PubMed](#)]
45. Dockendorff, C.; Faloon, P.W.; Germain, A.; Yu, M.; Youngsaye, W.; Nag, P.P.; Bennion, M.; Penman, M.; Nieland, T.J.F.; Dadapani, S.; et al. Discovery of Bisamide-Heterocycles as Inhibitors of Scavenger Receptor BI (SR-BI)-Mediated Lipid Uptake. *Bioorg. Med. Chem. Lett.* **2015**, *25*, 2594–2598. [[CrossRef](#)] [[PubMed](#)]
46. Yu, M.; Romer, K.A.; Nieland, T.J.F.; Xu, S.; Saenz-Vash, V.; Penman, M.; Yesilaltay, A.; Carr, S.A.; Krieger, M. Exoplasmic Cysteine Cys384 of the HDL Receptor SR-B1 Is Critical for Its Sensitivity to a Small-Molecule Inhibitor and Normal Lipid Transport Activity. *Proc. Natl. Acad. Sci. USA* **2011**, *108*, 12243–12248. [[CrossRef](#)] [[PubMed](#)]
47. Francia, M.E.; Stripien, B. Cell Division in Apicomplexan Parasites. *Nat. Rev. Microbiol.* **2014**, *12*, 125–136. [[CrossRef](#)]
48. Hermosilla, C.; Barbisch, B.; Heise, A.; Kowalik, S.; Zahner, H. Development of *Eimeria bovis* In Vitro: Suitability of Several Bovine, Human and Porcine Endothelial Cell Lines, Bovine Fetal Gastrointestinal, Madin-Darby Bovine Kidney (MDBK) and African Green Monkey Kidney (VERO) Cells. *Parasitol. Res.* **2002**, *88*, 301–307. [[CrossRef](#)] [[PubMed](#)]
49. Hamid, P.H.; Hirtzmann, J.; Hermosilla, C.; Taubert, A. Differential Inhibition of Host Cell Cholesterol *de Novo* Biosynthesis and Processing Abrogates *Eimeria bovis* Intracellular Development. *Parasitol. Res.* **2014**, *113*, 4165–4176. [[CrossRef](#)] [[PubMed](#)]
50. Lourido, S.; Moreno, S.N.J. The Calcium Signaling Toolkit of the Apicomplexan Parasites *Toxoplasma gondii* and *Plasmodium* spp. *Cell Calcium* **2015**, *57*, 186–193. [[CrossRef](#)]
51. Raldúa, D.; Babin, P.J. BLT-1, a Specific Inhibitor of the HDL Receptor SR-B1, Induces a Copper-Dependent Phenotype during Zebrafish Development. *Toxicol. Lett.* **2007**, *175*, 1–7. [[CrossRef](#)]
52. Pagler, T.A.; Rhode, S.; Neuhofer, A.; Laggner, H.; Strobl, W.; Hintnerdorfer, C.; Volf, I.; Pavelka, M.; Eckhardt, E.R.M.; van der Westhuyzen, D.R.; et al. SR-BI-Mediated High Density Lipoprotein (HDL) Endocytosis Leads to HDL Resecretion Facilitating Cholesterol Efflux. *J. Biol. Chem.* **2006**, *281*, 11193–11204. [[CrossRef](#)]
53. Fukata, Y.; Yu, X.; Imachi, H.; Nishiuchi, T.; Lyu, J.; Seo, K.; Takeuchi, A.; Iwama, H.; Masugata, H.; Hoshikawa, H.; et al. 17 β -Estradiol Regulates Scavenger Receptor Class BI Gene Expression via Protein Kinase C in Vascular Endothelial Cells. *Endocrine* **2014**, *46*, 644–650. [[CrossRef](#)] [[PubMed](#)]
54. Norata, G.D.; Ongari, M.; Uboldi, P.; Pellegatta, F.; Catapano, A.L. Liver X Receptor and Retinoic X Receptor Agonists Modulate the Expression of Genes Involved in Lipid Metabolism in Human Endothelial Cells. *Int. J. Mol. Med.* **2005**, *16*, 717–722. [[PubMed](#)]

2.6. 3D HOLOTOMOGRAPHIC MONITORING OF CA⁺⁺ DYNAMICS DURING IONOPHOR-INDUCED NEOSPORA CANINUM TACHYZOITE EGRESS FROM PRIMARY BOVINE HOST ENDOTHELIAL CELLS

Larrazabal, C., Hermosilla, C., Taubert, A. and Conejeros, I. (2021).

Parasitol Res 121 1169-1177; doi: 10.1007/s00436-021-07260-2

Own part in the publication:

- Project planning: 80 %, Together with co-authors and supervisors
- Development of experiments: 80 %, Mainly independent
- Evaluation of experiments: 80 %, Mainly independent
- Writing of the manuscript: 80 %, Mainly independent

3D holotomographic monitoring of Ca^{++} dynamics during ionophore-induced *Neospora caninum* tachyzoite egress from primary bovine host endothelial cells

Parasitology Research (2022) 121:1169–1177
https://doi.org/10.1007/s00436-021-07260-2

PROTOZOLOGY - ORIGINAL PAPER



3D holotomographic monitoring of Ca^{++} dynamics during ionophore-induced *Neospora caninum* tachyzoite egress from primary bovine host endothelial cells

C. Larrazabal¹ · C. Hermosilla¹ · A. Taubert¹ · I. Conejeros¹

Received: 25 March 2021 / Accepted: 18 July 2021 / Published online: 13 August 2021
© The Author(s) 2021

Abstract

Neospora caninum represents an obligate intracellular parasite that belongs to the phylum Apicomplexa and is a major abortive agent in bovines. During merogony, *N. caninum* tachyzoites invade and proliferate in host cells in vivo, including endothelial cells of lymphatic and blood vessels. The egress at the end of the lytic cycle is tightly regulated in apicomplexans. Evidence in *Toxoplasma gondii* shows that Ca^{++} signalling governs tachyzoite egress. Much less is known on egress mechanisms of *N. caninum*. Here, we show, using 3D live cell holotomographic microscopy in fluo-4 AM-loaded *N. caninum*-infected BUV-EC, that treatments with the calcium ionophore A23187 at 24- and 42-h post-infection (h p. i.) induced a fast and sustained increase in Ca^{++} signals in parallel to tachyzoite egress. A23187 treatments exclusively triggered tachyzoite release at 42-h p. i. but failed to do so at 24-h p. i. indicating a role for meront maturation in calcium-induced tachyzoite egress. Overall, we show that live cell 3D holotomographic analysis in combination with epifluorescence is a suitable tool to study calcium dynamics related to coccidian egress or other important cell functions.

Keywords *Neospora caninum* · Egress · A23187 · 3D microscopy · Holotomography · Cattle

Introduction

Neospora caninum is a heteroxenic apicomplexan parasite which belongs to the coccidian cyst-forming Sarcocystidae family (Lindsay and Dubey 2020). This family includes other important representatives of the phylum Apicomplexa for domestic, wild animal and human health, such as *Toxoplasma gondii*, *Sarcocystis suihominis* or *Besnoitia besnoiti*. *N. caninum* is a primary cause of abortion in bovines as well as other small ruminant species and has a substantial economic impact on livestock industry (Reichel et al. 2013). Since *N. caninum* is an obligate intracellular parasite, asexual formation of offspring stages (tachyzoites) strictly occurs in and depends on nucleated host cells. In vivo, *N. caninum*

preferentially infects endothelium but may also invade other nucleated cell types, thereby provoking major changes in host cell functions (Horcajo et al. 2017; Velásquez et al. 2019; Regidor-Cerrillo et al. 2020) and finally leading to cell lysis. In this context, primary bovine endothelial cells have been proven as suitable for *N. caninum* in vitro replication, allowing high proliferation rate of tachyzoites (Taubert et al. 2006a, 2006b).

The successful replication cycle of tachyzoites starts with an active cell invasion, continues with intracellular parasite replication after parasitophorous vacuole (PV) formation and ends with active tachyzoite release which occurs after achieving full maturation (Behrendt et al. 2008). All these intracellular steps are critical for rapid parasite development (Black and Boothroyd 2000). From a physiological perspective, intracellular Ca^{++} acts as coupling factor or essential second messenger for a variety of cellular functions (Carafoli and Krebs 2016). Overall, Ca^{++} -related studies on the closely related coccidian parasite *T. gondii* have shown that increase in intracellular Ca^{++} concentration is pivotal for adequate tachyzoite motility, invasion (Mondragon and Frixione 1996) and egress (Endo et al. 1982). The egress process allows tachyzoites to disseminate within the infected organism,

Section Editor: Xing-Qun ZHU

✉ C. Larrazabal
Camilo.Larrazabal@vetmed.uni-giessen.de

¹ Institute of Parasitology, Biomedical Research Center Seltersberg, Justus Liebig University Giessen, Schubertstr., 81, 35392 Giessen, Germany

3D holotomographic monitoring of Ca^{++} dynamics during ionophor-induced *Neospora caninum* tachyzoite egress from primary bovine host endothelial cells

1170

Parasitol Res (2022) 121:1169–1177

thereby influencing the outcome of disease. However, and despite the well-described role of Ca^{++} in coccidian biology at functional level, the precise mechanisms underlying parasite egress are not fully understood (Caldas and de Souza 2018). In this context, egress-related studies on *T. gondii* have consistently demonstrated that treatments with calcium ionophores, such as A23187 or ionomycin, induce an early egress of tachyzoites in a Ca^{++} -dependent manner (Endo et al. 1982; Black et al. 2000; Caldas et al. 2007; Behrendt et al. 2008). Moreover, Ca^{++} -driven egress is a general mechanism, since not only other chemicals including ethanol (Arrizabalaga and Boothroyd 2004), DTT (Stommel et al. 1997) and nigericine (Fruth and Arrizabalaga 2007), but also physiological signals, such as nitric oxide (Yan et al. 2015) or interferon gamma ($\text{IFN-}\gamma$) (Niedelman et al. 2013), can evoke *T. gondii* egress by modulating calcium dynamics. Interestingly, in case of the coccidian parasite *Eimeria bovis*, treatments with A23187 failed to induce egress of merozoite I stages from macromeronts, but promoted a fast exit of sporozoites from recently invaded endothelial cells (Behrendt et al. 2008), suggesting not only parasite species but also stage-specific egress mechanisms in apicomplexan parasites.

Calcium flux imaging is a classical approach to study cellular Ca^{++} homeostasis (Russell 2011). However, conventional microscopy-based approaches have rather been problematic for characterizing the role of intracellular calcium dynamics in host-coccidian parasites interactions (Lovett and Sibley 2003) since microscopic techniques are often limited to the post-experimental merge of signals coming from the phase (PH) or differential interference contrast (DIC). Alternative approaches include the use of genetically modified parasites or suitable dyes for live cell imaging (Frigault et al. 2009). However, in case of these approaches, the difficulties of working with genetically modified organisms in addition to fluorescence-associated challenges like quenching or phototoxicity must be solved (Brown 2007). In this context, the recently developed holotomographic microscopy allows non-phototoxic and high-resolution imaging in live cells (Sandoz et al. 2019). The digital holotomographic reconstruction is based on the refractive index (RI) of the different cell structures, thereby enhancing the information possible to obtain in cell systems. In line, holotomographic acquisition permits a 3D reconstruction of the RI-based tomogram, allowing not only the generation of high-resolution images, but also bringing novel information regarding the spatial distribution of cellular structures (Sandoz et al. 2019). In addition, one of the key advantages is that RI-based registries can be directly merged with fluorescence with a suitable frame rate, allowing direct analysis of host-parasite interactions. The aim of this work was to study the role of calcium influx in *N. caninum* tachyzoite egress in bovine endothelial primary cells, using a combined approach of 3D holotomographic microscopy and calcium probe fluo-4 AM-mediated fluorescence analysis.

Material and methods

Host cell culture

Primary bovine umbilical vein endothelial cells (BUVEC) were isolated as described previously (Taubert et al. 2006a). BUVEC were cultured at 37 °C and 5% CO_2 atmosphere in modified ECGM (modECGM) medium, by diluting ECGM medium (Promocell) with M199 (Sigma-Aldrich) at a ratio of 1:3, supplemented with 500 U/mL penicillin (Sigma-Aldrich), 50 $\mu\text{g}/\text{mL}$ streptomycin (Sigma-Aldrich) and 5% FCS (foetal calf serum; Biochrom). Only BUVEC monolayers of less than three passages were used in this study.

Parasites and treatments

Neospora caninum (strain NC-1) was maintained in vitro as described elsewhere (Taubert et al. 2006a, 2006b) by culturing it for several passages in permanent African green monkey kidney epithelial cells (MARCI45) in DMEM (Sigma-Aldrich), supplemented with 500 U/mL penicillin, 50 $\mu\text{g}/\text{mL}$ streptomycin and 5% FCS. Cells were cultured at 37 °C and 5% CO_2 atmosphere. Vital tachyzoites were collected from supernatants of infected cells by a centrifugation step (800 \times g; 5 min) and suspended in modECGM for further experiments. For parasite infection experiments, BUVEC were seeded in 35-mm tissue culture μ -dishes (Ibidi®) and cultured (37 °C, 5% CO_2) until confluence. Vital *N. caninum* tachyzoites (MOI 3:1) were added to BUVEC cultures for 4 h for infection. Thereafter, non-invaded or dead tachyzoites were removed by a complete medium change.

Live cell 3D holotomographic microscopy and image analysis

3D holotomographic images and videos were obtained for *N. caninum*-infected host cells at 24- and 42-h p. i. using a 3D Cell Explorer-fluo microscope (Nanolive®) equipped with 60 \times magnification ($\lambda = 520$ nm, sample exposure 0.2 mW/mm^2 and a depth of field of 30 μm) and a fluorescence unit (CoolLED pE-300ultra). Each experiment was performed independently three times (i.e. newly seeded BUVEC and new infections each time). Images were acquired every 6 s in both refractive index (RI) and fluorescence channels. The raw data were analysed using STEVE software (Nanolive®) to obtain refractive index-based z-stacks. Digital staining of subcellular structures was performed based on generated RI data.

Tracking of intracellular Ca^{++} fluxes

Intracellular Ca^{++} fluxes were visualized by the Ca^{++} -sensitive dye fluo-4 AM (Invitrogen) following the manufacturer's

3D holotomographic monitoring of Ca⁺⁺ dynamics during ionophore-induced *Neospora caninum* tachyzoite egress from primary bovine host endothelial cells

Parasitol Res (2022) 121:1169–1177

1171

recommendations. Briefly, host cells were incubated for 30 min in fluo-4 AM (2.5- μ M final concentration) at 37 °C and supplemented with pluronic acid (Invitrogen) in a dye/pluronic acid ratio of 1:1. Non-incorporated dye was removed by washing in sterile PBS and adding fresh modECGM. Calcium influx induction was induced by calcium ionophore A23187 treatments (15 μ M, Sigma-Aldrich).

Post-processing analysis was performed by the use of Image J v1.52p software (Schneider et al. 2012). Z Project plugin was applied to holotomographic z-stacks with the average intensity of the images as projection output. For calcium flux measurements over time, defined areas surrounding resting host cells were defined as regions of interest (ROI) (Silvestre-Roig et al. 2019). Thereafter, the multi-measurement tool (roiManager “Multi Measure”) was used to quantify the mean grey value as indicator of fluorescence intensity over time. Finally, for better visualization of Ca⁺⁺ flux, fluorescence images were displayed in pseudo-colours, using fire lookup tables as described elsewhere (Ardiel et al. 2017; Liu and Baraban 2019; Wakida et al. 2020).

Assessment of ionophore-induced tachyzoite egress

To estimate the impact of A23187 treatments, quantification of egressed *N. caninum* tachyzoites was performed at 24- and 42-h p. i. Briefly, at 24- and 42-h p. i., the number of meronts in *N. caninum*-infected BUVEC was determined (time 0). Then, the *N. caninum*-infected BUVEC cell monolayer was incubated with A23187 (15 μ M) for 10 min and the number of meronts that released tachyzoites was determined by comparison with the image obtained at time 0. The result was expressed as percentage of meronts showing tachyzoite release, defining as the 100% the number of meronts with tachyzoites at the beginning of the experiment. At least 15 meronts per experimental condition were analysed.

Statistical analysis

The statistical analyses were performed by GraphPad® Prism software (version 8.4.3). Ca⁺⁺ fluxes were normalized as percentage of the maximal response in order to compare kinetic differences among experimental conditions. Global comparisons of Ca⁺⁺ flux magnitudes were assessed by area under the curve (AUC) analysis at 1200-s post-stimulation. Data description was carried out by presenting arithmetic mean \pm standard deviation (SD). In addition, the non-parametric statistical Kruskal-Wallis was applied to compare three or more experimental conditions. Whenever global comparison by Kruskal-Wallis test indicated significance, post hoc multiple comparison tests were carried out by Dunn tests to compare test with control (non-infected) conditions. Outcomes of

statistical tests were considered to indicate significant differences when $p \leq 0.05$ (significance level).

Results

Cellular Ca⁺⁺ signals mainly originated from intracellular *N. caninum* meronts

To characterize the localization of Ca⁺⁺ signals within host cells, we performed a fluorescence and 3D holotomographic microscopy-based approach in *N. caninum*-infected (24- and 42-h p. i.) and non-infected BUVEC. Therefore, BUVEC were loaded with the Ca⁺⁺-sensitive fluorescent dye fluo-4. As exemplarily illustrated in Fig. 1, we observed a vesicle-like pattern of Ca⁺⁺ accumulation in the perinuclear area of the cytoplasm in non-infected cells (Fig. 1 A3 arrow). Moreover, at 24- and 42-h p. i., *N. caninum*-infected BUVEC revealed a marked signal accumulation within meronts, specifically associated to the perinuclear area of tachyzoites (Fig. 1 B3; B4 arrow). No major differences in Ca⁺⁺ signal pattern of infected cells were observed between 24- and 42-h p. i.

A23187 treatments induced a fast and sustained Ca⁺⁺ entry in *N. caninum*-infected host cells

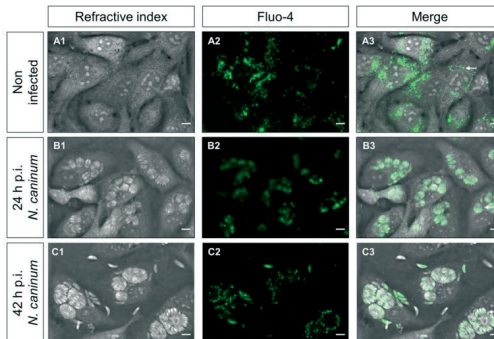
Given that ionophore A23187 is capable of permeating cytoplasmic membranes for Ca⁺⁺ ions, its use in cell systems allows to determine the role of Ca⁺⁺ entry. As depicted in Fig. 2A, A23187 treatments of BUVEC induced an increase in Ca⁺⁺-related fluorescent signals over time. Moreover, a time-dependent redistribution of Ca⁺⁺-driven signals was detected at 24- and 42-h p. i. in *N. caninum*-infected host cells (Supplementary Videos 1 and 2). In addition, no evident cytotoxic effect like cell lysis or membrane protrusions during the first 5 min was observed. When referring to subcellular areas, an enhancement in fluorescent signals over time was detected within *N. caninum* meronts (Fig. 2A, arrows). Furthermore, quantitative image-based fluorescence registries showed an A23187-induced fast and sustained increase of Ca⁺⁺-related fluorescence signals in both *N. caninum*-infected host cells and non-infected controls (Fig. 2B). Here, the current data showed that A23187 stimulation increased the fluo-4-driven signals reaching a peak after 500-s post-exposure in the non-infected and 24-h p. i.-infected cells, which was faster reached (60-s post-exposure) in 42-h p. i.-infected cells. This was followed by a plateau phase being in general sustained over time in all experimental conditions: non-infected cells, 24-h p. i. and 42-h p. i. Differences in the dynamics of the calcium flux were observed (Fig. 2B) whilst the magnitude of the Ca⁺⁺ influx (defined as the AUC of the registries) was not

3D holotomographic monitoring of Ca^{++} dynamics during ionophor-induced *Neospora caninum* tachyzoite egress from primary bovine host endothelial cells

1172

Parasitol Res (2022) 121:1169–1177

Figure 1. Calcium distribution in *N. caninum*-infected BUVEC determined by 3D tomographic microscopy. Refractive index (A1, B1 and C1) and fluorescent signal-based images (A2, B2, C2) of fluo-4-loaded BUVEC were obtained at 24- and 42-h p. i. Non-infected BUVEC were used as controls. Images exemplarily illustrate calcium-derived signals (green fluorescence) of non-infected (A) and *N. caninum*-infected BUVEC at 24- (B) and 42-h p. i. (C). The white arrow in (A3) highlights perinuclear vesicle distribution and subapical calcium accumulation in intracellular tachyzoites (B3-C3). The full registry in video format can be found in the supplementary material. Size scale bars correspond to 5 μm



significantly affected by the different experimental conditions ($p = 0.47$) (Fig. Sup. 1).

Ionophore-induced *N. caninum* egress is tachyzoite maturation-dependent

During *N. caninum* meront development, tachyzoites divide several times within the infected cell and finally egress in a Ca^{++} -dependent process. To evaluate the dependence of egress on meront maturation, the number of meronts showing tachyzoite release was determined at 24- and 42-h p. i. The data revealed that at 24-h p. i., no *N. caninum* meronts (0%) showed tachyzoite egress upon ionophore treatment. On the contrary, at 42-h p. i., $88.9 \pm 19.0\%$ of meronts released tachyzoites after 10 min of treatment (Fig. 3C). Interestingly, holotomographic videos revealed that at 24-h p. i., intracellular tachyzoites showed little or no motility within meronts after A23187 exposure (Supplementary Video 1). In contrast, at 42-h p. i., tachyzoite movements highly increased and calcium localization changed upon A23187 treatment finally leading to tachyzoites egress shortly after exposure (Fig. 3, Supplementary Video 2). These results were consistently illustrated by RI-based digital staining, showing rapid parasite rosette breakdown and hypermotility of intracellular tachyzoites within the PV (Fig. 3 Supplementary Videos 3–4).

Discussion

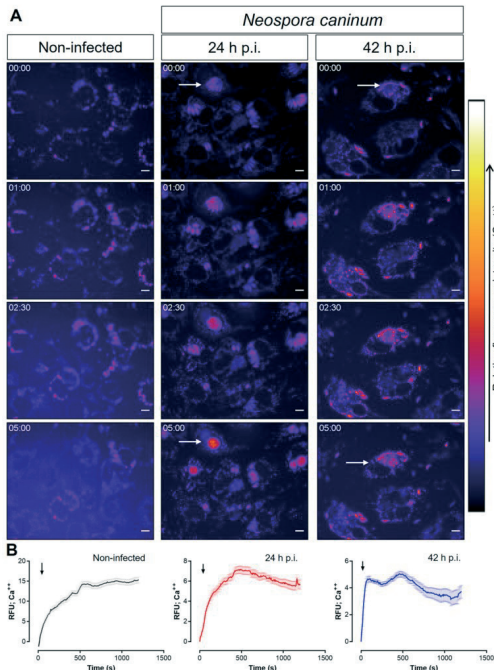
Calcium flux imaging represents a suitable and reliable tool for the study of cellular Ca^{++} physiology (Russell 2011).

Moreover, the use of microscopy-based approaches of host cell-parasite interaction studies allows to characterize the role of Ca^{++} fluxes in coccidian biology (Lovett and Sibley 2003). Despite that, using live cell fluorescence microscopy, the characterization of host cell-parasite interactions is usually limited to overlay approaches using light microscopic images (phase or differential interference contrast). These limitations can be overcome by the use of genetically modified fluorescent parasites or dyes suitable for live cell imaging (Frigault et al. 2009). However, the complexity of genetic manipulations and multi-channel fluorescence-associated problematics, such as quenching or phototoxicity (Brown 2007), generates a complex experimental set-up for studying intracellular parasites. Within this scenario, the current report shows for the first time that changes in Ca^{++} fluorescence signal intensities can be documented by RI-based illustration using a holotomographic microscope. Here, this technique allowed us to simultaneously monitor 3D holotomographic and epifluorescent signals to characterize the dynamics of intracellular Ca^{++} fluxes induced by A23187 treatments in vitro. In addition, the use of fluo-4 AM as Ca^{++} -sensitive dye delivered sensitive and specific signals with reduced interference from other bivalent cations (Gee et al. 2000). In detail, we here found that Ca^{++} -mediated fluorescent signals in non-infected endothelial control cells mainly originated from a perinuclear position, showing a vesicle-like pattern in the cytoplasmic region. This finding is in line with previous reports on bovine aortic endothelial cells and human umbilical endothelial cells (Chang et al. 2001; Son et al. 2010).

Cytoplasmic Ca^{++} distribution processes are highly conserved among eukaryotic cells, where endoplasmic reticulum

3D holotomographic monitoring of Ca^{++} dynamics during ionophor-induced *Neospora caninum* tachyzoite egress from primary bovine host endothelial cells

Figure 2. A23187 treatments induce a rapid and sustained calcium flux in non-infected and *N. caninum*-infected BUVEC. Fluorescence-derived images and measurements on calcium fluxes induced by A23187. **A** The images illustrate the changes in cellular calcium (pseudo-colour) dynamics in non-infected and *N. caninum*-infected BUVEC. Arrows highlight Ca^{++} -driven signal accumulation in meronts over time. **B** Image-derived fluorescence intensity measurements over time in A23187-treated cells. Error bars express standard error of at least 5 cells. **C** The full registry in video format and the AUC analyses of image-derived fluorescence can be found in the supplementary material. Size scale bars correspond to 5 μm



(ER), mitochondria and Golgi are considered Ca^{++} -rich organelles in resting cells (Russell 2011; Carafoli and Krebs 2016). The current study of apicomplexan-infected host cells proved fluorescence signals mainly to be located within *N. caninum* meronts, most possibly due to a redistribution of host cellular cytosolic Ca^{++} . This observation is in agreement with previous reports on *T. gondii*-infected cells, where the Ca^{++} concentration was significantly higher in the PV than in the cytosolic area of human epidermoid carcinoma epithelial cells (24-h p. i., Pingret et al. 1996), indicating that the PV represents a specialized calcium-rich subcellular compartment. In detail, we here found that fluo-4-based signals predominantly

translocated into the subapical region of intracellular *N. caninum* tachyzoites. In line with other eukaryotic organisms, tachyzoites in principle possess above described Ca^{++} -rich organelles (Lourido and Moreno 2015) but they additionally own other Ca^{++} stores, the so-called acidocalcisomes, as described for *T. gondii* and *Plasmodium berghei* (Moreno and Zhong 1996; Marchesini et al. 2000).

The calcium ionophore A23187 is a mobile ion carrier that forms stable complexes with cations, such as Ca^{++} (Pressman 1976). As already reported in the past, treatments with this compound effectively triggered Ca^{++} fluxes and other apicomplexan tachyzoite egresses (Endo et al. 1982; Black

3D holotomographic monitoring of Ca^{++} dynamics during ionophore-induced *Neospora caninum* tachyzoite egress from primary bovine host endothelial cells

1174

Parasitol Res (2022) 121:1169–1177

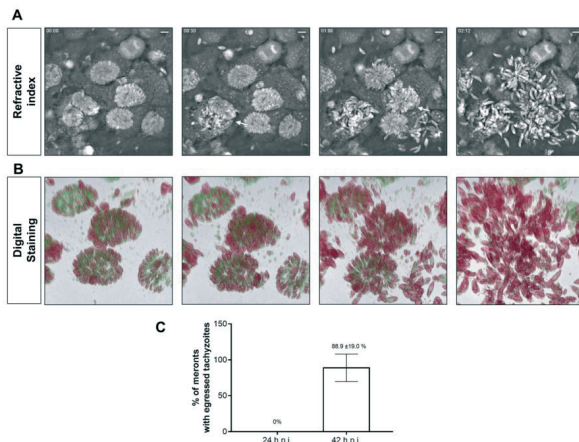


Figure 3. Calcium influx induced by A23187 treatment triggers a fast tachyzoite egress from *N. caninum*-infected BUEVC at 42-h p. i. Holotomographic images show a fast tachyzoite egress induced by A23187 treatments from *N. caninum*-infected BUEVC. Refractive index (A) or digital staining (B). Arrows highlight an early rosette disassembly

and massive egress of motile tachyzoites from mature meronts. (C) Bar graph illustrating the mean of the percentage of meronts releasing tachyzoites after 10-min post-A23187 treatments \pm standard deviation. The full registry in video format can be found in the supplementary material. Size scale bars correspond to 5 μm

and Boothroyd 2000; Behrendt et al. 2008). As here illustrated, A23187 treatments effectively induced increases in Ca^{++} -derived fluorescent signals over time in *N. caninum*-infected and control BUEVC. Considering cellular compartments, Ca^{++} signals mainly accumulated in vesicle-like structures within the cytoplasmic compartment of non-infected host endothelial cells. More interesting, in *N. caninum*-infected BUEVC, cytoplasmic signals were quickly redistributed to tachyzoite stages within meronts, thereby demonstrating a rise in tachyzoite intracellular Ca^{++} levels; nevertheless, the possibility that this Ca^{++} signal enhancement is a consequence of a Ca^{++} flux from *N. caninum* tachyzoite intracellular stores originated by the egress induction should not be excluded. This represents the first report on Ca^{++} flux evaluation during *N. caninum* tachyzoite egress. Furthermore, quantitative analyses on fluorescence intensities using defined ROIs demonstrated that A23187 treatments provoked a fast calcium flux in 42-h p. i. *N. caninum*-infected cells and with a similar kinetic in non-infected and 24-h p. i.-infected cells. The latter was followed by a sustained plateau phase, most probably reflecting the stabilization of extra- and intracellular Ca^{++}

concentrations. Interestingly, during Ca^{++} induction at 42-h p. i., slight changes in Ca^{++} flux over time were observed; however, this can be consequence of the movement of tachyzoites during the ionophore-induced egress, rather than reflecting an alternative kinetic profile, which, in general, matches with a receptor-independent mechanism and seems consequence of channel formation in cytoplasmic membranes (Tang et al. 2007).

Mechanisms of coccidian egress have extensively been studied in *T. gondii* (Caldas and de Souza 2018). In contrast, much less data are available on other closely related apicomplexan parasites, such as *N. caninum*. So far, a pivotal role of Ca^{++} -sensitive mechanisms has been proposed previously. As such, treatments with DTT and thiazolides derivatives induced a BAPTA-sensitive tachyzoite egress from *N. caninum*-infected human foreskin fibroblasts (evaluated 30-min post-induction at 48-h p. i.; Esposito et al. 2007). Likewise, 10- μM A23187 treatments evoked egress in infected BUEVC 10-min post-treatment at 60-h p. i. (Behrendt et al. 2008). Unfortunately, and despite the relevance of these works, the mere use of phase contrast microscopy hindered

3D holotomographic monitoring of Ca^{++} dynamics during ionophore-induced *Neospora caninum* tachyzoite egress from primary bovine host endothelial cells

Parasitol Res (2022) 121:1169–1177

1175

precise characterization of calcium influx signals in tachyzoite egress in living cells and only allowed for limited data interpretation. Using the current technique, *N. caninum* tachyzoites showed highly motile activities and egressed after 30 s of ionophore exposition at 42-h p. i. but failed to do so at 24-h p. i. In line, low intracellular tachyzoite motility was observed in reaction to A23187 exposition at 24-h p. i. Since *N. caninum*-infected BUVEC showed a similar calcium dynamic profile at 24- and 42-h p. i., we speculate that egress rather depends on meront maturity than on the mode of calcium influx. This is in agreement with previous observations showing that the maturity of meront-contained *T. gondii* and *N. caninum* tachyzoites significantly influenced A23187-triggered egress in BUVEC (Behrendt et al. 2008). Interestingly, *T. gondii* egress seems to involve an additional pathway, namely an active process from the tachyzoite side (Caldas and de Souza 2018). Specifically, studies on *T. gondii* demonstrated the participation of a perforin-like protein (tgPLP-1) and a lectin:cholesterol acyltransferase (tgLCAT), which are secreted from the parasite micronemes and dense granules, respectively, and which both proved pivotal for PV disintegration and tachyzoite release (Kafsack et al. 2009; Pzenny et al. 2016). In line, electron microscopy-based analyses confirmed that tubular network disintegration within the PV is an early event during *T. gondii* egress (Caldas et al. 2010). Considering this, motility seems crucial for ionophore-induced *T. gondii* egress (Lavine and Arrizabalaga 2008). Consequently, forming tachyzoites within immature *N. caninum* meronts may indeed be fixed in a tubular network within the PV, thereby failing to egress upon ionophore treatments. Comparative studies on *T. gondii* and *N. caninum* have shown that A23187-induced egress is highly influenced by infection kinetic and maturity of intracellular meront stages (Behrendt et al. 2008), thereby indicating that ionophore-induced early egress is highly affected by parasite-specific characteristics. However, and despite the well-documented role of Ca^{++} in *T. gondii*-induced cellular egress, the correlation of calcium flux and coccidian egress has not sufficiently been characterized via microscopy-based approaches, yet.

In summary, current data showed that *N. caninum* tachyzoites egress is a Ca^{++} -sensitive mechanism. Also, differences in tachyzoite egress behaviour depending on the time post-infection and resulting maturation status were here documented. These differences were not necessarily dependent on the Ca^{++} influx and further investigations are needed to better understand this cellular process. From a methodological perspective, the current study shows the usefulness of novel live cell 3D holotomography in combination with the use of fluo-4-AM as a suitable tool for calcium-related studies dealing with coccidian egress and development in host cells.

Supplementary information The online version contains supplementary material available at <https://doi.org/10.1007/s00436-021-07260-2>.

Acknowledgements Authors would like to thank Axel Wehrend (Clinic for Obstetrics, Gynecology and Andrology of Large and Small Animals, Justus Liebig University, Giessen, Germany) for the continuous supply of bovine umbilical cords. The PhD project of C. Larrazabal was funded by the National Agency for Research and Development (ANID), fellowship number DOCTORADO BECAS CHILE/2017–72180349. The publication fees were partially funded by the open access (OA) fund of the Justus Liebig University Giessen (JLU).

Funding Open Access funding enabled and organized by Projekt DEAL.

Data Availability All data are included in the manuscript.

Code availability Not applicable.

Declarations

Conflict of interest The authors declare no competing interests.

Open Access This article is licensed under a Creative Commons Attribution 4.0 International License, which permits use, sharing, adaptation, distribution and reproduction in any medium or format, as long as you give appropriate credit to the original author(s) and the source, provide a link to the Creative Commons licence, and indicate if changes were made. The images or other third party material in this article are included in the article's Creative Commons licence, unless indicated otherwise in a credit line to the material. If material is not included in the article's Creative Commons licence and your intended use is not permitted by statutory regulation or exceeds the permitted use, you will need to obtain permission directly from the copyright holder. To view a copy of this licence, visit <http://creativecommons.org/licenses/by/4.0/>.

References

- Ardiel EL, Kumar A, Marbach J, Christensen R, Gupta R, Duncan W, Daniels JS, Stuurman N, Colón-Ramos D, Shroff H (2017) Visualizing calcium flux in freely moving nematode embryos. *Biophys J* 112:1975–1983. <https://doi.org/10.1016/j.bpj.2017.02.035>
- Arrizabalaga G, Boothroyd JC (2004) Role of calcium during *Toxoplasma gondii* invasion and egress. *Int J Parasitol* 34:361–368. <https://doi.org/10.1016/j.ijpara.2003.11.017>
- Behrendt JH, Taubert A, Zahner H, Hermosilla C (2008) Studies on synchronous egress of coccidian parasites (*Neospora caninum*, *Toxoplasma gondii*, *Eimeria bovis*) from bovine endothelial host cells mediated by calcium ionophore A23187. *Vet Res Commun* 32:325–332. <https://doi.org/10.1007/s11259-007-9033-7>
- Black MW, Boothroyd JC (2000) Lytic cycle of *Toxoplasma gondii*. *Microbiol Mol Biol Res* MMBR 64:607–623. <https://doi.org/10.1128/mmb.64.3.607-623.2000>
- Black MW, Arrizabalaga G, Boothroyd JC (2000) Ionophore-resistant mutants of *Toxoplasma gondii* reveal host cell permeabilization as an early event in egress. *Mol Cell Biol* 20:9399–9408. <https://doi.org/10.1128/mcb.20.24.9399-9408.2000>
- Brown CM (2007) Fluorescence microscopy—avoiding the pitfalls. *J Cell Sci* 120:1703–1705. <https://doi.org/10.1242/jcs.03433>
- Caldas LA, de Souza W (2018) A window to *Toxoplasma gondii* egress. *Pathogens* 7:E69. <https://doi.org/10.3390/pathogens7030069>

3D holotomographic monitoring of Ca⁺⁺ dynamics during ionophore-induced *Neospora caninum* tachyzoite egress from primary bovine host endothelial cells

1176

Parasitol Res (2022) 121:1169–1177

- Caldas LA, de Souza W, Attias M (2007) Calcium ionophore-induced egress of *Toxoplasma gondii* shortly after host cell invasion. *Vet Parasitol* 147:210–220. <https://doi.org/10.1016/j.vetpar.2007.05.012>
- Caldas LA, de Souza W, Attias M (2010) Microscopic analysis of calcium ionophore activated egress of *Toxoplasma gondii* from the host cell. *Vet Parasitol* 167:8–18. <https://doi.org/10.1016/j.vetpar.2009.09.051>
- Carafoli E, Krebs J (2016) Why calcium? How calcium became the best communicator. *J Biol Chem* 291:20849–20857. <https://doi.org/10.1074/jbc.R116.735894>
- Chang HC, Tsai SY, Wu GJ, Lin YH, Chen RM, Chen TL (2001) Effects of propofol on mitochondrial function and intracellular calcium shift in bovine aortic endothelial model. *Acta Anaesthesiol Sin* 39:115–122
- Endo T, Sethi KK, Piekarski G (1982) *Toxoplasma gondii*: calcium ionophore A23187-mediated exit of trophozoites from infected murine macrophages. *Exp Parasitol* 53:179–188. [https://doi.org/10.1016/0014-4894\(82\)90059-5](https://doi.org/10.1016/0014-4894(82)90059-5)
- Esposito M, Moores S, Naguleswaran A, Müller J, Hemphill A (2007) Induction of tachyzoite egress from cells infected with the protozoan *Neospora caninum* by nitro- and bromo-thiazolides, a class of broad-spectrum anti-parasitic drugs. *Int J Parasitol* 37:1143–1152. <https://doi.org/10.1016/j.ijpara.2007.03.007>
- Frigault MM, Lacoste J, Swift JL, Brown CM (2009) Live-cell microscopy - tips and tools. *J Cell Sci* 122:753–767. <https://doi.org/10.1242/jcs.033833>
- Fruh LA, Arrizabalaga G (2007) *Toxoplasma gondii*: induction of egress by the potassium ionophore nigericin. *Int J Parasitol* 37:1559–1567. <https://doi.org/10.1016/j.ijpara.2007.05.010>
- Gee KR, Brown KA, Chen WN et al (2000) Chemical and physiological characterization of fluo-4 Ca²⁺-indicator dyes. *Cell Calcium* 27: 97–106. <https://doi.org/10.1054/ceca.1999.0095>
- Horcajo P, Jiménez-Pelayo L, García-Sánchez M, Regidor-Cerrillo J, Collantes-Fernández E, Rozas D, Hambroich N, Pfarrer C, Ortega-Mora LM (2017) Transcriptional modulation of bovine trophoblast cells in vitro by *Neospora caninum*. *Int J Parasitol* 47:791–799. <https://doi.org/10.1016/j.ijpara.2017.08.007>
- Kafsack BFC, Pena JDO, Coppens I, Ravindran S, Boothroyd JC, Carruthers VB (2009) Rapid membrane disruption by a perforin-like protein facilitates parasite exit from host cells. *Science* 323: 530–533. <https://doi.org/10.1126/science.1165740>
- Lavine MD, Arrizabalaga G (2008) Exit from host cells by the pathogenic parasite *Toxoplasma gondii* does not require motility. *Eukaryot Cell* 7:131–140. <https://doi.org/10.1128/EC.00301.07>
- Lindsay DS, Dubey JP (2020) Neosporosis, toxoplasmosis, and sarcocystosis in ruminants: an update. *Vet Clin North Am Food Anim Pract* 36:205–222. <https://doi.org/10.1016/j.cvfa.2019.11.004>
- Liu J, Baraban SC (2019) Network properties revealed during multi-scale calcium imaging of seizure activity in zebrafish. *eNeuro* 6:6–ENEUR19.2019. <https://doi.org/10.1523/ENEURO.0041-19.2019>
- Lourido S, Moreno SNJ (2015) The calcium signaling toolkit of the Apicomplexan parasites *Toxoplasma gondii* and *Plasmodium spp.* *Cell Calcium* 57:186–193. <https://doi.org/10.1016/j.ceca.2014.12.010>
- Lovett JL, Sibley LD (2003) Intracellular calcium stores in *Toxoplasma gondii* govern invasion of host cells. *J Cell Sci* 116:3009–3016. <https://doi.org/10.1242/jcs.00596>
- Marchesini N, Luo S, Rodrigues CO et al (2000) Acidocalcisomes and a vacuolar H⁺-pyrophosphatase in malaria parasites. *Biochem J* 347(Pt 1):243–253
- Mondragon R, Frictione E (1996) Ca²⁺-dependence of conoid extrusion in *Toxoplasma gondii* tachyzoites. *J Eukaryot Microbiol* 43:120–127. <https://doi.org/10.1111/j.1550-7408.1996.tb04491.x>
- Moreno SN, Zhong L (1996) Acidocalcisomes in *Toxoplasma gondii* tachyzoites. *Biochem J* 313(Pt 2):655–659. <https://doi.org/10.1042/bj3130655>
- Niedelmann W, Sprohloht JK, Clough B, Frickel EM, Saaji JPI (2013) Cell death of gamma interferon-stimulated human fibroblasts upon *Toxoplasma gondii* infection induces early parasite egress and limits parasite replication. *Infect Immun* 81:4341–4349. <https://doi.org/10.1128/IAI.00416-13>
- Pingret L, Millot JM, Sharonov S, Bonhomme A, Manfait M, Pinon JM (1996) Relationship between intracellular free calcium concentrations and the intracellular development of *Toxoplasma gondii*. *J Histochem Cytochem Off J Histochem Soc* 44:1123–1129. <https://doi.org/10.1177/44.10.8813077>
- Pressman BC (1976) Biological applications of ionophores. *Annu Rev Biochem* 45:501–530. <https://doi.org/10.1146/annurev.bi.45.070176.002441>
- Pszeny V, Ehrenman K, Romano JD, Kennard A, Schultz A, Roos DS, Grigg ME, Carruthers VB, Coppens I (2016) A lipolytic lecithin:cholesterol acyltransferase secreted by *Toxoplasma* facilitates parasite replication and egress. *J Biol Chem* 291:3725–3746. <https://doi.org/10.1074/jbc.M115.671974>
- Regidor-Cerrillo J, Xia D, Jiménez-Pelayo L, García-Sánchez M, Collantes-Fernández E, Randle N, Wasting J, Ortega-Mora LM, Horcajo P (2020) Proteomic characterization of host-pathogen interactions during bovine trophoblast cell line infection by *Neospora caninum*. *Pathogens* 9:749. <https://doi.org/10.3390/pathogens9090749>
- Reichel MP, Alejandra Ayaneque-Alecdrea M, Gondim LFP, Ellis JT (2013) What is the global economic impact of *Neospora caninum* in cattle - the billion dollar question. *Int J Parasitol* 43:133–142. <https://doi.org/10.1016/j.ijpara.2012.10.022>
- Russell JT (2011) Imaging calcium signals in vivo: a powerful tool in physiology and pharmacology. *Br J Pharmacol* 163:1605–1625. <https://doi.org/10.1111/j.1476-5381.2010.09988.x>
- Sandoz PA, Tremblay C, van der Goot FG, Frechin M (2019) Image-based analysis of living mammalian cells using label-free 3D refractive index maps reveals new organelle dynamics and dry mass flux. *PLoS Biol* 17:e3000553. <https://doi.org/10.1371/journal.pbio.3000553>
- Schneider CA, Rasband WS, Eliceiri KW (2012) NIH Image to ImageJ: 25 years of image analysis. *Nat Methods* 9:671–675. <https://doi.org/10.1038/nmeth.2089>
- Silvestre-Roig C, Braster O, Wichapong K, Lee EY, Teulon JM, Berrebeh N, Winter J, Adrover JM, Santos GS, Froese A, Lemnitz P, Ortega-Gómez A, Chevre R, Marschner J, Schumski A, Winter C, Perez-Olivares L, Pan C, Paulin N, Schoufouret J, Hartwig H, González-Ramos S, Kamp F, Megens RTA, Mowen KA, Gunzer M, Maedgessell L, Hackeng T, Luigens E, Daemen M, von Blumke J, Anders HJ, Nikolaev VO, Pelleguer JL, Weber C, Hidalgo A, Nicosches GAF, Wong GCL, Soehnlein O (2019) Externalized histone H4 orchestrates chronic inflammation by inducing lytic cell death. *Nature* 569:236–240. <https://doi.org/10.1038/s41586-019-1167-6>
- Son H-J, Lim Y-C, Ha K-S, Kang SS, Cheong IY, Lee SJ, Park SW, Hwang BM (2010) Propofol and aminophylline antagonize each other during the mobilization of intracellular calcium in human umbilical vein endothelial cells. *J Korean Med Sci* 25:1222–1227. <https://doi.org/10.1038/jkms.2010.25.8.1222>
- Stommel EW, Ely KH, Schwartzman JD, Kasper LH (1997) *Toxoplasma gondii*: diethyl-intra-endoxal Ca²⁺ flux causes egress of parasites from the parasitophorous vacuole. *Exp Parasitol* 87:88–97. <https://doi.org/10.1006/expr.1997.4187>
- Tang EHC, Leung FP, Huang Y, Feletou M, So KF, Man RYK, Vanhoutte PM (2007) Calcium and reactive oxygen species increase in endothelial cells in response to relaxers of endothelium-derived

3D holotomographic monitoring of Ca^{++} dynamics during ionophor-induced *Neospora caninum* tachyzoite egress from primary bovine host endothelial cells

Parasitol Res (2022) 121:1169–1177

1177

- contracting factor. *Br J Pharmacol* 151:15–23. <https://doi.org/10.1038/sj.bjp.0707190>
- Taubert A, Krüll M, Zahner H, Hermosilla C (2006a) *Toxoplasma gondii* and *Neospora caninum* infections of bovine endothelial cells induce endothelial adhesion molecule gene transcription and subsequent PMN adhesion. *Vet Immunol Immunopathol* 112:272–283. <https://doi.org/10.1016/j.vetimm.2006.03.017>
- Taubert A, Zahner H, Hermosilla C (2006b) Dynamics of transcription of immunomodulatory genes in endothelial cells infected with different coccidian parasites. *Vet Parasitol* 142:214–222. <https://doi.org/10.1016/j.vetpar.2006.07.021>
- Velásquez ZD, Concejeros I, Larrazabal C, Kerner K, Hermosilla C, Taubert A (2019) *Toxoplasma gondii*-induced host cellular cell cycle dysregulation is linked to chromosome missegregation and cytokinesis failure in primary endothelial host cells. *Sci Rep* 9:12496. <https://doi.org/10.1038/s41598-019-48961-0>
- Wakida NM, Gomez-Godinez V, Li H, Nguyen J, Kim EK, Dynes JL, Othby S, Lau AL, Ding P, Shi L, Carmona C, Thompson LM, Cahalan MD, Berns MW (2020) Calcium dynamics in astrocytes during cell injury. *Front Bioeng Biotechnol* 8:912. <https://doi.org/10.3389/fbioe.2020.00912>
- Yan X, Ji Y, Liu X, Suo X (2015) Nitric oxide stimulates early egress of *Toxoplasma gondii* tachyzoites from human foreskin fibroblast cells. *Parasit Vectors* 8:420. <https://doi.org/10.1186/s13071-015-1037-5>

Publisher's note Springer Nature remains neutral with regard to jurisdictional claims in published maps and institutional affiliations.

3. RESULTS AND DISCUSSION

This work mainly focused on the coccidian-driven modulation of the host cellular cholesterol metabolism and on anti-parasitic properties of selected cholesterol-associated compounds. In detail, the differential impact of *de novo* synthesis and LDL-dependent cholesterol acquisition on *B. besnoiti* intracellular replication and changes of sterol abundance during *E. bovis* macromeront formation were analyzed. Moreover, the relevance of the three important cholesterol-related proteins NPC1L1, P-gp and SR-BI was analyzed during intracellular replication of different coccidian species – *T. gondii*, *N. caninum*, *B. besnoiti*, *E. bovis* and *E. arloingi*. Finally, changes in Ca⁺⁺ dynamics during ionophore-induced tachyzoite egress were studied for *N. caninum*.

Coccidian parasites are generally considered as defective in cholesterol *de novo* biosynthesis and, consequently, have to scavenge this molecule from their host cells to sustain biomembrane synthesis during offspring formation. However, the mechanisms of cholesterol acquisition used by coccidia appear to be both species- and host cell type-dependent. *T. gondii*-driven reactions were previously studied by Coppens et al. (2000) stating that cholesterol acquisition largely depends on LDL and LDL-LDLR-related endocytic routes, attributing only a minor role to endogenous *de novo* cholesterol biosynthesis. Later reports confirmed that LDL-dependent cholesterol uptake is also pivotal for other apicomplexan parasites, such as *N. caninum* (Nolan et al., 2015), *Plasmodium* spp. (Labaied et al., 2011) or *C. parvum* (Ehrenman et al., 2013). Likewise, dependency on LDL as cholesterol source was also described for euglenozoan parasites like *Trypanosoma brucei* and *Trypanosoma cruzi* (Black and Vandeweerdt, 1989; Pereira et al., 2015). The conserved key role of LDL in protozoan cholesterol requirements is consequence of the predominant role of this lipoprotein in cholesterol delivery and transport in mammals (Coppens, 2013; Ikonen, 2008).

3.1. *B. besnoiti* relies on different strategies of cholesterol scavenging

Independent of well-documented *T. gondii*-driven changes in host cellular cholesterol metabolism, major gaps of knowledge are still present for other coccidian parasites, such as *B. besnoiti*. Therefore, acquisition routes used by *B. besnoiti* to fulfill its cholesterol requirements were analyzed in the current work (see 2.1). Hence, the influence of *B. besnoiti* infection on host cellular endogenous cholesterol synthesis and sterol uptake from exogenous

Results and discussion

sources was analyzed. GC-MS-based profiling of cholesterol-related sterols revealed enhanced cholesterol synthesis rates in *B. besnoiti*-infected cells. Accordingly, lovastatin and zaragozic acid treatments diminished tachyzoite production (see 2.1). Moreover, increased lipid droplet contents and enhanced cholesterol esterification was detected and inhibition of the latter significantly blocked parasite proliferation. Furthermore, the artificial increase of host cellular lipid droplet disposability boosted parasite proliferation (see 2.1).

We additionally found that *B. besnoiti* tachyzoite replication is influenced by LDL availability, since an increased tachyzoite proliferation was observed in BUVEC in presence of acetylated LDL (acLDL) (see 2.1). So far, no other report demonstrated the importance of modified lipoproteins for intracellular parasite proliferation. In this context, the incorporation of acLDL by endothelial cells represents a specific feature of this cell type (Adachi and Tsujimoto, 2006). Interestingly, lectin-like oxidized low density lipoprotein receptor 1 expression was upregulated in infected endothelial host cells, whilst LDLR was not affected by parasite infection (see 2.1). Mechanistically, acLDL uptake is mainly driven by the acLDL receptor, located on the surface of endothelial cells and macrophages (Adachi and Tsujimoto, 2006). This may be of special relevance considering the well-defined tropism that this coccidian exhibits towards endothelial cells *in vivo* (Alvarez-García et al., 2014; Langenmayer et al., 2015), eventually indicating a specific metabolic host cellular preference for *B. besnoiti* merogony. Nevertheless, since *B. besnoiti* infection also drives an enhancement of oxLDL (syn LOX-1) receptor expression over time, the participation of other endothelial scavenger receptors in cholesterol transport should also be considered.

Interestingly, a key aspect of LDL-LDLR-mediated cholesterol acquisition is the incorporation of this molecule into late endosomes shortly after its endocytosis, being afterwards trafficked into the E.R. for re-esterification and thereafter stored as cholesteryl esters in lipid droplets for further disposal (Ikonen, 2008). In consequence, lipid droplets represent an important neutral lipid source, which are exploited for replicative requirements in different parasite species (Hamid et al., 2015; Hu et al., 2017; Nolan et al., 2017). Moreover, in agreement with work on other coccidian species, such as *T. gondii*, *N. caninum* and *E. bovis* (Hamid et al., 2015; Hu et al., 2017), *B. besnoiti* infection induces an enhancement of host cellular lipid droplet numbers over time thereby serving as lipid sources

even in absence of other cholesterol sources (see 2.1). Overall, this finding corroborates the general importance of this specific organelle as source of neutral lipids in coccidian parasite replication (Hu et al., 2017; Nolan et al., 2017). Besides the role of LDL, treatments with lovastatin, zaragozic acid, CI976, and C75, demonstrated an involvement of HMG-CoA reductase, squalene synthase, ACAT and fatty acid synthase, respectively, in *B. besnoiti* replication suggesting an additional participation of *de novo* cholesterol biosynthesis (see 2.1). The precise role of this *de novo* synthesis route in apicomplexan replication is unclear so far, nevertheless it was already reported for other coccidian parasites, such as *E. bovis* and *T. gondii* (in macrophages) as well as for hemosporidian species like *Plasmodium* and *Babesia* (Grellier et al., 1994; Hamid et al., 2015; Nishikawa et al., 2011). In contrast, *T. gondii* replication in CHO cells revealed as statin-unresponsive (Coppens et al., 2000), while *Plasmodium* spp. mainly relies on *de novo* biosynthesis during its hepatic stage as alternative for LDL supply (Labaied et al., 2011), suggesting that both host cell type and parasite species significantly influence alternative route utilization.

Considering these evidences, we conclude that *B. besnoiti* in principle exploits different alternative cholesterol sources to sustain its intracellular replication.

3.2. *E. bovis* drives changes in host cellular sterol composition during first merogony

Differing significantly from fast replicating coccidian species, *E. bovis* owns a characteristic long-lasting first merogony. Thus, *E. bovis* possesses unique features in terms of division biology, replication rate and offspring prolificacy (Francia and Striepen, 2014; Hermosilla et al., 2002; Taubert et al., 2006, 2016). During first merogony, *E. bovis* modulates the host cellular transcriptome thereby triggering changes in sterol uptake, synthesis and metabolism (Taubert et al., 2010). To analyze the impact of extensive *E. bovis* proliferation on host cellular sterol metabolism we here compared the sterol profiles of *E. bovis*-infected primary endothelial host cells grown under optimized (1.2%) and non-optimized (10%) foetal calf serum (FCS) cell culture conditions (see 2.2). Therefore, several sterols indicating endogenous *de novo* cholesterol synthesis, cholesterol conversion and sterol uptake (phytosterols) were analyzed via GC-MS-based approaches. Overall, significantly enhanced levels of phytosterols were detected in both FCS conditions indicating infection-triggered sterol uptake from extracellular sources as a major pathway of sterol acquisition (see 2.2).

Results and discussion

Interestingly, a simultaneous induction of endogenous cholesterol synthesis based on increased levels of distinct cholesterol precursors was only observed in case of optimized parasite proliferation indicating a parasite proliferation-dependent effect (see 2.2). Overall, GC-MS analysis demonstrated a substantial accumulation of phytosterols (campesterol, stigmasterol and sitosterol) at 14 d p. i. (see 2.2). Phytosterols are not synthesized by mammalian cells but are exclusively taken up from (nutritional) exogenous sources and therefore represent reliable indicators of cellular sterol uptake. Consequently, plasma sterol composition in bovines, as in other herbivorous animals, is largely determined by nutritional intake. Moreover, since most cell culture systems rely on foetal bovine serum for exogenous cholesterol delivery, the chemical differentiation of phytosterols and cholesterol permits to discriminate the source of cellular cholesterol (*de novo* vs uptake) (Gachumi and El-Aneel, 2017). Therefore, enhanced phytosterol levels in *E. bovis*-infected host cells indicated a massive uptake of exogenous sterols driven by the parasite's replicative needs. However, it is necessary to highlight that too high cellular concentrations of phytosterols proved toxic for animal cells (Brown and Yu, 2010; Feng et al., 2020). In general, cellular phytosterol imbalances are prevented by counter-regulating cholesterol uptake via NPC1L1 during intestinal absorption (Betters and Yu, 2010). Likewise, ABC transporter activities remove these sterols from cells by incorporating them into HDL particles (Brown and Yu, 2010; Feng et al., 2020). Noteworthy, mutations in ABCG5 or ABCG8 transporters generates sitosterolemia and subsequent accumulation of phytosterols in different muscular structures, affecting the cytoplasmic membrane composition and fluidity, potentially leading premature coronary heart disease (Brown and Yu, 2010). Interestingly and contrasting with findings on *E. bovis*, GC-MS-based analyses on *B. besnoiti*-infected cells revealed a reduction in phytosterols (see 2.1), confirming marked species-dependent differences in sterol modulation. Of note, the higher sensitivity that *B. besnoiti* shows towards P-gp-specific inhibition (see 2.4), suggests a stronger dependency on ABC-mediated cholesterol efflux.

Downstream cholesterol requirements of *E. bovis* have previously been addressed and showed a time-dependent enhancement of both total cholesterol and neutral lipid content during first merogony in infected BUVEC (Hamid et al., 2015). In the current work, GC-MS based analysis of *E. bovis*-infected cells confirmed an enhancement of cholesteryl ester

Results and discussion

abundance at 14 d p. i. (see 2.2). This finding delivers a functional outcome to prior reports that showed an increase of ACAT 2 transcription driven by *E. bovis* infection in addition to merozoite I production inhibition by ACAT 2 inhibitors (Hamid et al., 2014). Considering side-chain oxysterols, 25 hydroxycholesterol levels were selectively found increased in *E. bovis*-infected host cells in the current work, while 24 hydroxycholesterol and 27 hydroxycholesterol contents were not significantly altered by infection (see 2.2). Interestingly, exogenous treatments with 25 hydroxycholesterol, 27 hydroxycholesterol, and 7 ketocholesterol induced significant adverse effects on *E. bovis* intracellular development. Thus, the number and size of developing macromeronts and merozoite I production was significantly reduced indicating that these oxysterols bear direct or indirect antiparasitic properties (see 2.2). Overall, downstream cholesterol metabolism permits the synthesis of more complex cholesterol derivatives and prevents potential cytotoxicity driven by this molecule (Simons and Ikonen, 2000). Moreover, beyond esterification, cholesterol is largely oxidized into oxysterols within cells (Lefort and Cani, 2021). Oxysterols represent a class of cholesterol derivatives generated by its oxidation (Griffiths and Wang, 2019). Furthermore, the biological interest towards these molecules is driven by a broad range of their biological implications, in e. g. cancer, atherosclerosis, and immunity (Griffiths and Wang, 2019). Interestingly, overexpression of cholesterol 25 hydroxylase at RNA level at 14 days p. i. in *E. bovis*-infected endothelial cells suggested downstream sterol conversion into oxysterols within infected host endothelial cells (Hamid et al., 2015). In that context, the overexpression of cholesterol 25 hydroxylase was confirmed for the first time at protein level at 22 and 24 days p. i. (see 2.2). Likewise, 25-OH-cholesterol levels were found increased in infected cells, thereby confirming a functional participation of this enzyme (see 2.2). Interestingly, this metabolite possesses potential immune properties since it is upregulated during inflammatory processes and it is capable to interfere with intracellular pathogen replication (Cyster et al., 2014). In specific, 25-OH-cholesterol can reduce porcine reproductive and respiratory syndrome virus host cell invasion by affecting the stability and integrity of cholesterol-enriched membranes (Dong et al., 2018; Yang et al., 2015), suggesting a protective effect against enveloped viruses. Nonetheless, its antiviral effect seems to be broader since it is extended to other non-enveloped viral species like human papillomavirus-16, human rotavirus and human rhinovirus (Civra et al., 2014). In this context, this oxysterol

could potentially reduce intracellular viral proliferation by interacting with host cell oxysterol-binding proteins and/or direct interactions with viral components (Zhao et al., 2020). Moreover, 25-OH-cholesterol seems to play a broader role in viral immune response, since it is released by macrophages upon interferon treatment and mouse cytomegalovirus (Blanc et al., 2013). In the case of coccidian parasites, the current data represent the first report on its increased synthesis during *E. bovis* infection (see 2.2). Noteworthy, exogenous supplementation of 25-OHC, 27-OHC, and 7-ketoChol reduced *E. bovis* macromeront development, thereby indicating enhanced host cell defense mechanisms during *E. bovis* infection. Worth noting and given that 25-OHC levels were not altered by *B. besnoiti* infection (see 2.1), parasite-driven modulation of cholesterol 25 hydroxylase activity and subsequent 25-OHC synthesis appear to mirror species-specific effects.

Overall, the current data indicate parasite-driven changes in the host cellular sterol profile reflecting the huge demand of *E. bovis* for cholesterol during macromeront formation and its versatility in the utilization of cholesterol sources.

3.3. NPC1L1 blockage as potential anti-coccidian strategy

Despite the importance of LDL as cholesterol source, studies on *C. parvum*-infected HCT-8 cells revealed that micellar sources and enhanced sterol uptake via a NPC1L1-dependent reactions may also reflect important mechanisms to sustain lipid availability (Ehrenman et al., 2013). In this context, the use of the NPC1L1 blocker ezetimibe, a molecule that is clinically applied as cholesterol-lowering drug, permits to explore the role of this receptor in tachyzoite proliferation of the important fast replicating coccidian parasites *T. gondii*, *N. caninum* and *B. besnoiti* (see 2.3). Interestingly, ezetimibe treatments effectively blocked tachyzoite proliferation of all three coccidian species and induced a significant coccidiostatic effect over time (see 2.3). Overall, this work represents the first *in vitro* report on the efficacy of ezetimibe treatments in fast replicating coccidian species. Of note, ezetimibe treatments seem to exert parasite-specific effects since their impact on other parasites is inconsistent: while this compound reduces the parasite burden of *Leishmania amazonensis in vivo* (Andrade-Neto et al., 2021) and diminishes *Leishmania infantum* burden *in vivo* and *in vitro* (Andrade-Neto et al., 2016), it fails to affect *Plasmodium yoelii* parasitemia in mice (Hayakawa et al., 2021), but reduces intraerythrocytic proliferation of *P. falciparum in vitro*

(Hayakawa et al., 2020). These findings suggest a marked divergence in sensitivity between parasite phylum and species. However, the methodological differences of *in vivo* and *in vitro* ezetimibe treatments must also be considered.

From a pharmacological perspective, ezetimibe is conjugated to a glucuronide group *in vivo* in liver after administration, thereby generating ezetimibe-glucuronide as the main biologically active metabolite (Clader, 2004; Garcia-Calvo et al., 2005). This metabolite owns a higher hypolipidemic activity associated with a higher NPC1L1 affinity than the non-modified compound (Garcia-Calvo et al., 2005). However, the use of this phase 2 metabolite in our *in vitro* system completely abolished the anti-coccidian efficacy of ezetimibe (see 2.3). Thus, it seems plausible that ezetimibe-driven anti-parasitic effects are indeed NPC1L1-independent. This hypothesis may largely explain the vast differences on anti-parasitic properties of ezetimibe in other works but raises new questions on the putative mechanism underlying the current findings. Given that sterol esterification was reported as pivotal for intracellular proliferation of different apicomplexan species [e. g. *T. gondii* (Sonda et al., 2001), *Plasmodium* spp. (Vielemeyer et al., 2004) and *E. bovis* (Hamid et al., 2014)], the inhibitory capacity of ezetimibe but not of ezetimibe-glucuronide targeting ACAT-1 (Clader, 2004) suggests a plausible mechanism for its *in vitro* anti-coccidian properties. Nevertheless, further studies are necessary to clarify the effector mechanism of ezetimibe on coccidian replication.

3.4. Chemical blockage of P-gp activity affects proliferation of fast replicating coccidia in an inhibitor generation-dependent manner

Cholesterol sequestering and trafficking represents a suitable target of novel therapeutics against coccidian parasite infections. In this context, treatments with U18666a (inhibitor of NPC1) dampens *T. gondii* and *Plasmodium* spp. replication (Coppens et al., 2000; Labaied et al., 2011; Petersen et al., 2017). However, this compound also induces a NPC1-defective phenotype, characterized by cholesterol accumulation within late endosomes at cellular level and by neurological disorders *in vivo* (Cenedella, 2009). These findings obviously limit the suitability of this inhibitor as anti-coccidian drug. Interestingly, the absence of pharmacological effects of U18666a against *T. gondii* replication in addition to the aberrant cholesterol distribution in P-gp-*knock out* cells, suggest an involvement of P-gp in host

Results and discussion

cellular cholesterol trafficking or efflux during coccidian replication (Bottova et al., 2009). Moreover, based on the importance of this ABC transporter in tumor resistance, several generations of pharmacologically active compounds blocking P-gp activity have been developed (Palmeira et al., 2012). As reported in chapter 2.4, the anti-coccidian properties of three different generations of P-gp inhibitors (verapamil, valsopodar and tariquidar) were explored in the current work. In this context, the first and second generation of P-gp inhibitors, represented by verapamil and valsopodar, respectively, include molecules or their derivatives with inhibitory capacities towards P-gp activity, amongst other effects. Third generation P-gp inhibitors, such as tariquidar, exhibit an improved selectivity and potency, thereby reducing side effects (Palmeira et al., 2012). By using primary cell lines, we here established a rather physiological model, since P-gp activity potentially is enhanced in tumoral or immortalized cell lines *per se* (Riordan et al., 1985). Overall, here we reported an average replication inhibition of *T. gondii*, *N. caninum* and *B. besnoiti* tachyzoites of 84 % and 95 % by verapamil (40 μ M) and valsopodar (5 μ M) treatments, respectively (see 2.4). Likewise, previous reports on other host cell types also showed that treatments with verapamil (at concentrations ranging 10–100 μ M) and valsopodar (1-10 μ M) impair *T. gondii* and *P. falciparum* replication (Archinal-Mattheis et al., 1995; Bottova et al., 2010; Martiney et al., 1995; Silverman et al., 1997). Moreover, the current work extends these findings to other coccidian parasites, i. e. to *N. caninum* and *B. besnoiti* (see 2.4). As an interesting cholesterol-related finding, exclusively verapamil treatments affected neutral lipid composition and distribution in primary endothelial cells, thereby suggesting valsopodar-driven anti-coccidian effects as independent of changes in sterol distribution. In this context, given the pharmacological properties of valsopodar as cyclosporine derivative, is possible to speculate that the anti-coccidian effects here reported could represent cyclosporine-related side effects (Palmeira et al., 2012), nonetheless further studies are necessary to address the specific mechanisms underlying this. Of note, treatments with tariquidar, the most specific P-gp blocker used in current work, showed least effects on parasite replication. Thus, this blocker exclusively inhibited *B. besnoiti* replication but not the other coccidian parasites, thereby revealing species-specific differences in efficacy. Interestingly, the inhibitory impact of another, closely related third generation inhibitor, elacridar, was confirmed for *T. gondii*

infections in mouse embryonic fibroblasts, since respective treatments reduced tachyzoite formation (Bottova et al., 2010).

3.5. Blockage of neutral lipid efflux impairs coccidian intracellular replication

Since neutral lipid accumulation represented a consistent finding in P-gp inhibitor-related studies, the blockage of cholesteryl ester efflux may also represent a mechanistic strategy for anti-coccidian drugs. Hence, a study on the role of the classical HDL receptor SR-BI was here performed (see 2.5). Here we found that chemical blockage of SR-BI with BLT-1 (2 μ M) enhances lipid droplets abundance and BODIPY 493/503-driven signals in non-infected BUVEC suggesting an overall increase in the neutral lipid content of endothelial cells. Furthermore, we observed that this compound interferes with *T. gondii*, *N. caninum* and *B. besnoiti* replication by reducing parasite proliferation by 97.99 %, 64.59 % and 47.24 %, respectively (see 2.5). Likewise, we found that this treatment also affects intracellular development of the pathogenic ruminant *Eimeria* species, i. e. *E. bovis* and *E. arloingi* (see 2.5), indicating a general involvement of SR-BI in intracellular proliferation of coccidian parasites in endothelial cells.

The main function of SR-BI as membrane receptor is to maintain and control cholesteryl ester efflux, thereby preventing toxic accumulation of these molecules in endothelial cells (Linton et al., 2017). The participation of this efflux route in intracellular parasite proliferation was here studied for the first time, not only for fast replicating coccidian species (*T. gondii*, *N. caninum* and *B. besnoiti*) but also for *E. bovis* and *E. arloingi*, which are characterized by a long lasting first merogony in endothelial cells leading to macromeront formation. Of note, prior reports on the role of SR-BI were limited to apicomplexan species from *Plasmodium* genera (Rodrigues et al., 2008; Yalaoui et al., 2008). In contrast to endothelial cells, liver-derived cell lines (primary human/murine hepatocytes or HepG2 cells) differ from endothelial cells in terms of SR-BI function, since its key role in hepatic tissue is to acquire HDL-contained cholesteryl esters for later biliary disposal (Adachi and Tsujimoto, 2006; Linton et al., 2017). Overall, the dual functionality of SR-BI for cholesteryl ester trafficking is driven by a unique mechanism that allows a gradient-dependent cholesteryl ester displacement from or to HDL particles, mimicking an ion channel pore (Linton et al., 2017). Therefore, the finding of an enhancement of BODIPY 493/503-related

signals and lipid droplet numbers in BUVEC treated with the specific SR-BI blocker BLT-1 strongly supports a functional blockage of SR-BI. At this point, the impact of SR-BI on coccidian replication somehow also appears contradictory since apicomplexan parasites generally use lipid droplets to sustain their lipid requirements (Nolan et al., 2017) and these organelles indeed are enhanced by SR-BI blockage. Additionally, since SR-BI expression was not influenced by *T. gondii*, *N. caninum* or *B. besnoiti* infections over time, it is possible to conclude that coccidian parasites do not modulate this receptor to a measurable extent during infection. Interestingly, the role of SR-BI in *Plasmodium* replication in hepatic cells has not directly been linked to the transfer of cholesteryl esters into the P.V. (Rodrigues et al., 2008; Yalaoui et al., 2008). Nevertheless, *P. berghei*-, *P. yoelii*-, *P. berghei*- and *P. falciparum*-invasion and development were clearly affected by chemical blockage of SR-BI or its genetic deletion (Rodrigues et al., 2008; Yalaoui et al., 2008). In contrast, the SR-BI-dependent host cell permissiveness was not affected in the coccidian species here studied, indicating different mechanisms compared to *Plasmodium* genera (see 2.5). The precise mechanism underlying these findings remains unclear, however, it was speculated that SR-BI blockage affects hepatic host cell permissiveness by modifying the cholesterol composition of the host cell membrane (Yalaoui et al., 2008). Furthermore, a participation of SR-BI in other cell pathways beyond cholesterol homeostasis has been reported (Gutierrez-Pajares et al., 2016). Likewise, SR-BI also activates distinct intracellular signaling pathways which are mediated by PI3K and ERK in endothelial cells (Kimura et al., 2010), thereby suggesting that anti-coccidian effects of SR-BI blockage might be not necessarily or exclusively depend on cholesterol homeostasis.

3.6. Changes in Ca⁺⁺ dynamics as pivotal early signal in coccidian parasite stages

Host cell invasion is essential for coccidian parasites to fulfil their intracellular lytic cycle (Black and Boothroyd, 2000). Noteworthy, considering the current work, several compounds were shown to affect parasite invasion. In specific, ezetimibe treatments consistently reduced *T. gondii*, *N. caninum* and *B. besnoiti* invasion rates by an average of 22.5%, when directly applied to free tachyzoite stages (see 2.3). Likewise, valsopodar treatments affected the tachyzoites invasive performance by 13.8% in these three parasitic species (see 2.4). The mechanisms behind these findings remain unclear. Of interest, studies on free *T. gondii* tachyzoites demonstrated a Ca⁺⁺ flux induced by elacridar treatments (Bottova et al., 2010),

Results and discussion

suggesting an untimely tachyzoite activation. In this context, we here report that BLT-1 (2 μ M) treatments of free *T. gondii*, *N. caninum* and *B. besnoiti* tachyzoites reduced their infectivity by 30% (see 2.5). Interestingly, fluorimetric analyses of fluo-4 (Ca⁺⁺sensitive dye)-loaded free tachyzoites revealed that BLT-1 treatment evokes a sustained increase in Ca⁺⁺ fluxes over time, producing an overall increase in the area under the curve (AUC) at 1100 s by $402.52 \pm 354.14\%$, $53.98 \pm 22.73\%$ and $43.30 \pm 7.60\%$ for *T. gondii*, *N. caninum* and *B. besnoiti*, respectively (see 2.5).

Overall, the modulation of Ca⁺⁺ homeostasis in apicomplexan stages has been proposed as pharmacological strategy against protozoal infections (Gupta et al., 2021). In general, drugs that affect apicomplexan Ca⁺⁺ homeostasis can be grouped according to their modes of action, with inhibition of Ca⁺⁺ entry and dysregulation of Ca⁺⁺ cytoplasmic storage representing the main mechanisms (Gupta et al., 2021). In this context, the efficacy of channel blocker-derived drugs leading to the reduction of Ca⁺⁺ entry were previously explored. In specific, the presence of a Ca⁺⁺ L-channel homologue in apicomplexa has been proposed since Ca⁺⁺ channel blockage by nifedipide reduced *T. gondii* tachyzoite invasion (Pace et al., 2014). On the contrary, current invasion assays after verapamil treatments of free tachyzoites revealed a minor impact of this treatment on their invasive capacity in case of *T. gondii*, *N. caninum* and *B. besnoiti* (see 2.4). Considering the efficacy of verapamil as Ca⁺⁺ L-channel blocker, these findings indicate that Ca⁺⁺ channels may play a minor role in this invasive stage. In line, studies on *T. gondii* proved extracellular Ca⁺⁺ chelation to exert only a minor impact on parasite invasion, whilst intracellular Ca⁺⁺ chelation had strong anti-invasive effects on free tachyzoites, suggesting that intracellular Ca⁺⁺ stores largely determine the Ca⁺⁺ requirements for invasion (Lovett and Sibley, 2003). The latter finding is of special relevance since the induction of an untimely Ca⁺⁺ flux potentially impairs parasite invasion (Gupta et al., 2021). Mechanistically, untimely Ca⁺⁺ fluxes may cause intracellular Ca⁺⁺ store depletion and early microneme secretion, leading to a reduced infective performance (Carruthers et al., 1999; Gupta et al., 2021; Pace et al., 2014). Considering that we here reported that BLT-1 evokes an unspecific Ca⁺⁺ flux over time in *T. gondii*, *B. besnoiti* and *N. caninum* tachyzoites (see 2.5), we may speculate that the effect of this compound on the tachyzoite invasion step may rely on an untimely activation of the invasion machinery. This hypothesis was recently studied by the use of the sarco/endoplasmic reticulum Ca⁺⁺

ATPase (SERCA) inhibitor thapsigargin in *T. gondii* tachyzoites. The use of this substance led to a Ca^{++} -dependent hypermotility and microneme secretion in tachyzoite stages, which also showed an impaired infection performance (Pace et al., 2014). In addition, the well-known anti-malarial drug artemisine also exhibited a SERCA-related inhibitory effect in *T. gondii* tachyzoites (Gupta et al., 2021; Nagamune et al., 2007). Similarly, curcumin, which is reported to affect SERCA activity (Bilmen et al., 2001), showed effective anti-proliferative properties in case of *Plasmodium* spp., *T. gondii* and *B. besnoiti* (Cervantes-Valencia et al., 2018; Dohutia et al., 2017; Goo et al., 2015). In conclusion, all these data highlight early Ca^{++} signaling events as potential drug target against apicomplexan parasites.

3.7. Intracellular Ca^{++} signals are relocated during parasite egress

Besides apicomplexan invasion processes, Ca^{++} fluxes are also associated with parasite egress from infected host cells (Caldas and de Souza, 2018). However, detailed characterization of Ca^{++} homeostasis and parasite egress has mainly been restricted to *T. gondii* and *Plasmodium* spp., so far (Caldas and de Souza, 2018; Lourido and Moreno, 2015; Tan and Blackman, 2021). To address potential species-specific differences in this context, Ca^{++} homeostasis and fluxes were here analyzed in *N. caninum*-infected host cells (see 2.6). Of note, this work represents the first study on cellular Ca^{++} distribution in *N. caninum*-infected primary cells and showed that host cell Ca^{++} distribution is largely affected by *N. caninum* infection and development. Thus, a change in Ca^{++} -driven fluorescence signal phenotypes from a vesicle-like pattern in the perinuclear area of the cytoplasm in non-infected cells to a marked signal accumulation within meronts, associated to the perinuclear area of tachyzoites was here documented (see 2.6). The current findings are in principle in line with prior studies on *T. gondii* and, more recently, on the blood stage of *P. falciparum* (Fraser et al., 2021; Pingret et al., 1996). Specifically, the considerable Ca^{++} accumulation within *T. gondii* P.V.s proved these parasitic structures as Ca^{++} -rich intracellular stores when compared to the cytosolic compartment of infected cells with low Ca^{++} signals (Pingret et al., 1996). Respective mechanisms remain unclear, however, sequestering of cytosolic Ca^{++} could also serve as immune evasion mechanism since cytosolic Ca^{++} is required for scramblase-dependent phosphatidylserine exposure, reducing the capacity of immune cells to detect infected cells by phosphatidylserine sensing (Nagata et al., 2016). Likewise, Ca^{++} accumulation within the P.V. was also proposed as evasion

Results and discussion

response of *P. falciparum*-infected erythrocytes (Fraser et al., 2021). However, further studies are necessary to verify underlying mechanisms.

In terms of host cell egress, Ca^{++} ionophores have largely been used to explore egress-related mechanisms in apicomplexan parasites (Caldas and de Souza, 2018). In the current work, treatments with the Ca^{++} ionophore A23187 evoked a fast egress of intracellular *N. caninum* tachyzoites from their host cells (see 2.6). As expected, A23187-induced tachyzoite egress seemed to be largely influenced by the maturity of the meronts, since respective treatments failed to induce parasite egress at the early phase of merogony (24 h p. i.). Interestingly, this finding occurs irrespective of Ca^{++} signaling, since A23187 evoked a fast Ca^{++} -signal redistribution into intracellular tachyzoites stage independent of meront maturity. The inability of *N. caninum* tachyzoites to egress at 24 h p.i. was in line with an earlier report showing a time-dependent egress of *N. caninum* but not of *T. gondii* tachyzoites from BUVEC (Behrendt et al., 2008). Maturity-dependent effects were also stated for other coccidian stages since *Eimeria tenella* sporozoites showed a higher nitric oxide-triggered egress ratio at 12 h p. i. than at 24 or 48 h p. i. (Yan et al., 2021) and *E. bovis* sporozoites egressed from their host cells early after infection (2 h p. i.) but were unresponsive to ionophore treatments when macromeronts were established intracellularly at 20-25 d p. i. (Behrendt et al., 2008). Taking this together, parasite egress seems to depend on both, the parasite species and the stimulant.

4. ZUSAMMENFASSUNG

Kokzidien sind Krankheitserreger von Mensch und Tier und gehören zu obligat intrazellulären Parasiten, die im Stamm der Apikomplexa eingeordnet werden. Veterinärmedizinisch relevante Kokzidien befinden sich in verschiedene Familien, wie den Sarcocystidae (z. B. *Toxoplasma gondii*, *Neospora caninum* und *Besnoitia besnoiti*) und Eimeriidae (z. B. *Eimeria bovis* und *Eimeria arloingi*), die sich hinsichtlich Lebenszyklus und Wirtsspezifität unterscheiden. Diese intrazellulär lebenden Parasiten sind für ihre Entwicklung vom Metabolismus ihrer Wirtszelle abhängig. So werden komplexe Moleküle - wie etwa Cholesterol - aus den Wirtszellen entnommen, um die proliferativen Anforderungen des Parasiten zu erfüllen. Grundsätzlich können Zellen Cholesterol durch *de-novo*-Biosynthese oder extrazelluläre Aufnahme bereitstellen. Letztere wird vornehmlich über die Aufnahme von LDL vermittelt. Vor allem diesen Weg scheinen Kokzidien für sich zu nutzen. Insgesamt sind jedoch sind die Kenntnisse zur Cholesterolaufnahme durch Kokzidien noch lückenhaft und nicht für alle Arten repräsentativ. So wurden alternative Aufnahmewege zum Cholesterol, die von bestimmten Rezeptoren und Transportern wie NPC1L1, P-pg oder SR-BI abhängig sind, bisher kaum in Betracht gezogen. Die vorliegende Arbeit befasst sich deshalb mit dieser Thematik und führte zu folgenden Ergebnissen:

Eine GC-MS-basierte Analyse von Cholesterol-assoziierten Sterolen in *B. besnoiti*-infizierten primären Endothelzellen zeigte eine Zunahme von Cholesterol-Vorstufen. Zusammen mit einer Statin-vermittelten Hemmung der *B. besnoiti*-Replikation deuten diese Daten auf eine wichtige Rolle der *de-novo* Biosynthese in infizierten Wirtszellen hin. Dass die acLDL-Supplementierung die *B. besnoiti*-Vermehrung verstärkte, weist zudem auf acLDL als zusätzliche, extrazelluläre Cholesterolquelle hin und zeigte auf, dass dieser Parasit alternative Wege zur Deckung des Cholesterolbedarfs nutzt. Im Falle von *E. bovis*-Infektionen belegten Sterolanalysen eine signifikante Zunahme von Phytosterolen während der ersten Merogonie, was auf eine Abhängigkeit der intrazellulären Parasitenentwicklung von extrazellulären Cholesterolquellen hinweist. Zudem ergab die Analyse von Cholesterinmetaboliten eine gesteigerte Bildung von Cholesterylestern und Oxysterolen (insbesondere 25-Hydroxycholesterin). Da der exogene Zusatz von Oxysterolen die Entwicklung von *E. bovis* Makromeronten behinderte, könnte die gesteigerte Synthese dieser Moleküle auch Ausdruck einer Abwehrreaktionen infizierter Wirtszellen sein.

Zusammenfassung

Eine Beteiligung weiterer cholesterolassoziierter Wege zeigte die Anwendung von Ezetimib als NPC1L1-Blocker, die signifikante parasitostatische Effekte auf die Proliferation von *T. gondii*-, *N. caninum*- und *B. besnoiti*-Tachyzoiten ergab. Behandlungen mit dem *in vivo* aktiven Metaboliten (glucuronisiertes Ezetimib) bewirkten jedoch keine parasitostatische Wirkungen. Zusammen mit der inkonsistenten Genexpression von NPC1L1 in infizierten Zellen legte dies nahe, dass Ezetimib die Parasitenreplikation durch einen NPC1L1-unabhängigen Mechanismus beeinflusst. Außerdem zeigte die chemische Blockade des im Cholesterolstoffwechsel eingebundenen ABC-Transporters P-gp durch verschiedene Inhibitorgenerationen (Verapamil, Valspodar, Tariquidar) deutliche Unterschiede in ihrer antiparasitären Wirksamkeit. Während Behandlungen mit Verapamil signifikant die Replikation von *T. gondii*, *N. caninum* und *B. besnoiti* hemmten und eine Anreicherung neutraler Lipide in Wirtszellen erzeugten, zeigten Valspodar-Behandlungen zwar ebenfalls anti-invasive und anti-proliferative Wirkungen, ohne jedoch die Abundanz neutraler Lipide zu beeinflussen. Im Gegensatz dazu verringerte der spezifischste P-gp-Inhibitor Tariquidar ausschließlich die Invasion und Replikation von *B. besnoiti*, wirkte sich jedoch nicht auf *T. gondii* oder *N. caninum* aus, was parasitenspezifische Reaktionen nahelegt. Interessanterweise induzierte die Blockade des Scavenger-Rezeptors SR-BI durch BLT-1-Behandlungen signifikante hemmende Effekte sowohl auf die schnell replizierenden Kokzidien *T. gondii*, *N. caninum* und *B. besnoiti* als auch auf die pathogenen *Eimeria*-Spezies *E. bovis* und *E. arloingi*, was konservierte, SR-BI-assoziierte Mechanismen bei der intrazellulären Kokzidien-Replikation nahelegt. BLT-1-Behandlungen freier Sporozysten und Tachyzoiten beeinflussten jedoch ausschließlich die invasive Kapazität der letzteren Gruppe, begleitet von einem anhaltenden Ca^{++} -Flux in diesen Parasitenstadien.

Schließlich belegten Studien zum Zellaustritt von *N. caninum* über Live-Cell-Imaging, dass dieser mit einer infektionsbedingten Ca^{++} -Umverteilung mit erhöhten Ca^{++} -Signalen innerhalb der Meronten verbunden war. Analysen zum ionophorinduzierten Austritt von *N. caninum* zeigten zudem, dass die Austrittsleistung des Parasiten hauptsächlich von der Merontenreife beeinflusst wurde und dass Ionophorbehandlungen keine Ca^{++} -Umverteilung zwischen unterschiedlichen Infektionszeitpunkten (24 oder 42 h p. i.) verursachte.

5. SUMMARY

Coccidia are a large family of obligate intracellular parasites that belong to the apicomplexan phylum and are responsible for diseases in human and animal populations. In this context, veterinary-relevant coccidian species are grouped into certain families, such as Sarcocistidae (i. e. *Toxoplasma gondii*, *Neospora caninum* and *Besnoitia besnoiti*) and Eimeriidae (i. e. *Eimeria bovis* and *Eimeria arloingi*) which largely differ in terms of life cycle and host specificity. It is well-known that coccidian parasites highly rely on host cell metabolism and their capacity to hijack their host cell to fulfill their metabolic requirements during intracellular development. In that context, complex molecules like cholesterol are scavenged from host cells to sustain proliferative requirements. Physiologically, cells obtain cholesterol either by *de novo* biosynthesis or by extracellular uptake. The latter is largely driven by LDL internalization in mammalian cells, which is accepted as pivotal route to be exploited by apicomplexan parasites. Nevertheless, since coccidian biology largely differs between species, the overall knowledge on cholesterol acquisition by coccidia has been oversimplified. As such, alternative cholesterol-related acquisition routes driven by NPC1L1, P-pg and SR-BI have scarcely been considered, so far. Related to these topics, the following results were achieved in the current work:

GC-MS-based profiling of cholesterol-related sterols in *B. besnoiti*-infected primary endothelial cells showed an enhancement of several cholesterol precursors. Together with the finding of statin-mediated inhibition of *B. besnoiti* replication, these data strongly suggest a key role of cholesterol *de novo* biosynthesis in infected host cells. Furthermore, beneficial effects of LDL-supplementation on parasite proliferation proved acLDL as pivotal extracellular cholesterol source for *B. besnoiti* replication, thereby indicating that this coccidian parasite exploits alternative routes to sustain its cholesterol requirements. Moreover, in the case of *E. bovis* first merogony, lipidomic profiling revealed an enhancement of phytosterols over time indicating that this coccidian parasite significantly relies on extracellular sources for cholesterol acquisition. Interestingly, analysis of downstream cholesterol metabolites additionally documented an accumulation of cholesteryl esters and oxysterols (especially 25 hydroxycholesterol) throughout first merogony. Considering that exogenous oxysterols treatments impeded *E. bovis* macromeront

Summary

development, these molecules may also result from anti-parasitic responses of infected-host cells.

Regarding the participation of alternative cholesterol-related routes, the use of ezetimibe as NPC1L1 blocker revealed strong parasitostatic effects on *T. gondii*, *N. caninum* and *B. besnoiti* tachzoite proliferation. However, the absence of anti-coccidian effects driven by the *in vivo* active metabolite (glucuronated ezetimibe), in addition to the inconsistent gene expression of NPC1L1 in infected cells suggest that ezetimibe might affect parasite replication by an NPC1L1-independent mechanism. Additionally, chemical blockage of the ABC transporter P-gp by different generations of inhibitors (verapamil, valsopodar, tariquidar) revealed differences in terms of anti-coccidian efficacies. Specifically, treatments with verapamil consistently reduced *T. gondii*, *N. caninum* and *B. besnoiti* replication and generated neutral lipid accumulation in host cells. Likewise, valsopodar treatments induced significant anti-invasive and anti-proliferative effects in these three parasite species but failed to influence cellular neutral lipid abundance. In contrast, the most specific P-gp inhibitor tariquidar exclusively diminished *B. besnoiti* invasion and replication but failed to affect *T. gondii* or *N. caninum*, thereby suggesting parasite-specific reactions. Interestingly, blockage of the scavenger receptor SR-BI by BLT-1 treatments induced significant anti-replicative effects not only in the fast-replicating coccidia *T. gondii*, *N. caninum* and *B. besnoiti*, but also in the pathogenic *Eimeria* species *E. bovis* and *E. arloingi*, thereby evidencing potentially conserved SR-BI-related mechanisms as key events for coccidian replication. However, BLT-1 treatments of free sporozoites and tachyzoites exclusively affected host cell invasion capacity in the latter group, being paralleled with a sustained Ca^{++} flux over time.

Finally, studies on *N. caninum* host cell egress by live cell imaging revealed an infection-driven Ca^{++} redistribution leading to increased Ca^{++} signals within intracellular *N. caninum* meronts. Furthermore, analyses on ionophore-induced *N. caninum* egress proved egress performance to be mainly influenced by meront maturity and showed no differences in Ca^{++} redistribution between time points of infection (24 or 42 h p. i.).

6. REFERENCES

- Adachi, H., and Tsujimoto, M. (2006). Endothelial scavenger receptors. *Prog Lipid Res* 45, 379–404. <https://doi.org/10.1016/j.plipres.2006.03.002>.
- Alvarez-García, G., Frey, C.F., Mora, L.M.O., and Schares, G. (2013). A century of bovine besnoitiosis: an unknown disease re-emerging in Europe. *Trends Parasitol* 29, 407–415. <https://doi.org/10.1016/j.pt.2013.06.002>.
- Alvarez-García, G., García-Lunar, P., Gutiérrez-Expósito, D., Shkap, V., and Ortega-Mora, L.M. (2014). Dynamics of *Besnoitia besnoiti* infection in cattle. *Parasitology* 141, 1419–1435. <https://doi.org/10.1017/S0031182014000729>.
- Anderson, M.L., Andrianarivo, A.G., and Conrad, P.A. (2000). Neosporosis in cattle. *Anim Reprod Sci* 60–61, 417–431. [https://doi.org/10.1016/s0378-4320\(00\)00117-2](https://doi.org/10.1016/s0378-4320(00)00117-2).
- Andrade-Neto, V.V., Cunha-Júnior, E.F., Canto-Cavalheiro, M.M. do, Atella, G.C., Fernandes, T. de A., Costa, P.R.R., and Torres-Santos, E.C. (2016). Antileishmanial activity of ezetimibe: inhibition of sterol biosynthesis, in vitro synergy with azoles, and efficacy in experimental cutaneous leishmaniasis. *Antimicrob Agents Chemother* 60, 6844–6852. <https://doi.org/10.1128/AAC.01545-16>.
- Andrade-Neto, V.V., Rebello, K.M., Pereira, T.M., and Torres-Santos, E.C. (2021). Effect of itraconazole-ezetimibe-miltefosine ternary therapy in murine visceral leishmaniasis. *Antimicrob Agents Chemother* 65. <https://doi.org/10.1128/AAC.02676-20>.
- Anvari, D., Saberli, R., Sharif, M., Sarvi, S., Hosseini, S.A., Moosazadeh, M., Hosseini, Z., Chegeni, T.N., and Daryani, A. (2020). Seroprevalence of *Neospora caninum* infection in dog population worldwide: a systematic review and meta-analysis. *Acta Parasitol* 65, 273–290. <https://doi.org/10.2478/s11686-019-00163-4>.
- Archinal-Mattheis, A., Rzepka, R.W., Watanabe, T., Kokubu, N., Itoh, Y., Combates, N.J., Bair, K.W., and Cohen, D. (1995). Analysis of the interactions of SDZ PSC 833 ([3'-keto-Bmt1]-Val2]-Cyclosporine), a multidrug resistance modulator, with P-glycoprotein. *Oncol Res* 7, 603–610. .

References

- Arrizabalaga, G., and Boothroyd, J.C. (2004). Role of calcium during *Toxoplasma gondii* invasion and egress. *Int J Parasitol* 34, 361–368. <https://doi.org/10.1016/j.ijpara.2003.11.017>.
- Baldacchino, F., Gardès, L., De Stordeur, E., Jay-Robert, P., and Garros, C. (2014). Blood-feeding patterns of horse flies in the French Pyrenees. *Vet Parasitol* 199, 283–288. <https://doi.org/10.1016/j.vetpar.2013.10.009>.
- Behrendt, J.H., Taubert, A., Zahner, H., and Hermosilla, C. (2008). Studies on synchronous egress of coccidian parasites (*Neospora caninum*, *Toxoplasma gondii*, *Eimeria bovis*) from bovine endothelial host cells mediated by calcium ionophore A23187. *Vet Res Commun* 32, 325–332. <https://doi.org/10.1007/s11259-007-9033-7>.
- Benavides, J., Maley, S., Pang, Y., Palarea, J., Eaton, S., Katzer, F., Innes, E.A., Buxton, D., and Chianini, F. (2011). Development of lesions and tissue distribution of parasite in lambs orally infected with sporulated oocysts of *Toxoplasma gondii*. *Vet Parasitol* 179, 209–215. <https://doi.org/10.1016/j.vetpar.2011.03.001>.
- Ben-Harari, R.R., and Connolly, M.P. (2019). High burden and low awareness of toxoplasmosis in the United States. *Postgrad Med* 131, 103–108. <https://doi.org/10.1080/00325481.2019.1568792>.
- Bettters, J.L., and Yu, L. (2010). NPC1L1 and cholesterol transport. *FEBS Lett* 584, 2740–2747. <https://doi.org/10.1016/j.febslet.2010.03.030>.
- Bilmen, J.G., Khan, S.Z., Javed, M.H., and Michelangeli, F. (2001). Inhibition of the SERCA Ca²⁺ pumps by curcumin. Curcumin putatively stabilizes the interaction between the nucleotide-binding and phosphorylation domains in the absence of ATP. *Eur J Biochem* 268, 6318–6327. <https://doi.org/10.1046/j.0014-2956.2001.02589.x>.
- Black, M.W., and Boothroyd, J.C. (2000). Lytic cycle of *Toxoplasma gondii*. *Microbiol Mol Biol Rev* 64, 607–623. <https://doi.org/10.1128/mmlr.64.3.607-623.2000>.
- Black, S., and Vandeweerdt, V. (1989). Serum lipoproteins are required for multiplication of *Trypanosoma brucei brucei* under axenic culture conditions. *Mol Biochem Parasitol* 37, 65–72. [https://doi.org/10.1016/0166-6851\(89\)90103-5](https://doi.org/10.1016/0166-6851(89)90103-5).

References

- Blanc, M., Hsieh, W.Y., Robertson, K.A., Kropp, K.A., Forster, T., Shui, G., Lacaze, P., Watterson, S., Griffiths, S.J., Spann, N.J., et al. (2013). The transcription factor STAT-1 couples macrophage synthesis of 25-hydroxycholesterol to the interferon antiviral response. *Immunity* 38, 106–118. <https://doi.org/10.1016/j.immuni.2012.11.004>.
- Bottova, I., Hehl, A.B., Stefanić, S., Fabriàs, G., Casas, J., Schraner, E., Pieters, J., and Sonda, S. (2009). Host cell P-glycoprotein is essential for cholesterol uptake and replication of *Toxoplasma gondii*. *J Biol Chem* 284, 17438–17448. <https://doi.org/10.1074/jbc.M809420200>.
- Bottova, I., Sauder, U., Olivieri, V., Hehl, A.B., and Sonda, S. (2010). The P-glycoprotein inhibitor GF120918 modulates Ca²⁺-dependent processes and lipid metabolism in *Toxoplasma gondii*. *PLoS One* 5, e10062. <https://doi.org/10.1371/journal.pone.0010062>.
- Brown, J.M., and Yu, L. (2010). Protein mediators of sterol transport across intestinal brush border membrane. *Subcell Biochem* 51, 337–380. https://doi.org/10.1007/978-90-481-8622-8_12.
- Buhaescu, I., and Izzedine, H. (2007). Mevalonate pathway: a review of clinical and therapeutical implications. *Clin Biochem* 40, 575–584. <https://doi.org/10.1016/j.clinbiochem.2007.03.016>.
- Carruthers, V.B., Moreno, S.N., and Sibley, L.D. (1999). Ethanol and acetaldehyde elevate intracellular [Ca²⁺] and stimulate microneme discharge in *Toxoplasma gondii*. *Biochem J* 342 (Pt 2), 379–386. .
- Cenedella, R.J. (2009). Cholesterol synthesis inhibitor U18666A and the role of sterol metabolism and trafficking in numerous pathophysiological processes. *Lipids* 44, 477–487. <https://doi.org/10.1007/s11745-009-3305-7>.
- Civra, A., Cagno, V., Donalizio, M., Biasi, F., Leonarduzzi, G., Poli, G., and Lembo, D. (2014). Inhibition of pathogenic non-enveloped viruses by 25-hydroxycholesterol and 27-hydroxycholesterol. *Sci Rep* 4, 7487. <https://doi.org/10.1038/srep07487>.
- Clader, J.W. (2004). The discovery of ezetimibe: a view from outside the receptor. *J Med Chem* 47, 1–9. <https://doi.org/10.1021/jm030283g>.

References

- Coppens, I. (2013). Targeting lipid biosynthesis and salvage in apicomplexan parasites for improved chemotherapies. *Nat Rev Microbiol* *11*, 823–835. <https://doi.org/10.1038/nrmicro3139>.
- Coppens, I. (2014). Exploitation of auxotrophies and metabolic defects in *Toxoplasma* as therapeutic approaches. *Int J Parasitol* *44*, 109–120. <https://doi.org/10.1016/j.ijpara.2013.09.003>.
- Coppens, I., Sinai, A.P., and Joiner, K.A. (2000). *Toxoplasma gondii* exploits host low-density lipoprotein receptor-mediated endocytosis for cholesterol acquisition. *J Cell Biol* *149*, 167–180. <https://doi.org/10.1083/jcb.149.1.167>.
- Cortes, H., Leitão, A., Gottstein, B., and Hemphill, A. (2014). A review on bovine besnoitiosis: a disease with economic impact in herd health management, caused by *Besnoitia besnoiti* (Franco and Borges, 1916). *Parasitology* *141*, 1406–1417. <https://doi.org/10.1017/S0031182014000262>.
- Cyster, J.G., Dang, E.V., Reboldi, A., and Yi, T. (2014). 25-Hydroxycholesterols in innate and adaptive immunity. *Nat Rev Immunol* *14*, 731–743. <https://doi.org/10.1038/nri3755>.
- D'Angelo, J.G., Bordón, C., Posner, G.H., Yolken, R., and Jones-Brando, L. (2009). Artemisinin derivatives inhibit *Toxoplasma gondii* in vitro at multiple steps in the lytic cycle. *J Antimicrob Chemother* *63*, 146–150. <https://doi.org/10.1093/jac/dkn451>.
- Dauguschies, A., and Najdrowski, M. (2005). Eimeriosis in cattle: current understanding. *J Vet Med B Infect Dis Vet Public Health* *52*, 417–427. <https://doi.org/10.1111/j.1439-0450.2005.00894.x>.
- Davis, H.R.J., Zhu, L.-J., Hoos, L.M., Tetzloff, G., Maguire, M., Liu, J., Yao, X., Iyer, S.P.N., Lam, M.-H., Lund, E.G., et al. (2004). Niemann-Pick C1 Like 1 (NPC1L1) is the intestinal phytosterol and cholesterol transporter and a key modulator of whole-body cholesterol homeostasis. *J Biol Chem* *279*, 33586–33592. <https://doi.org/10.1074/jbc.M405817200>.
- Dean, M., Rzhetsky, A., and Allikmets, R. (2001). The human ATP-binding cassette (ABC) transporter superfamily. *Genome Res* *11*, 1156–1166. <https://doi.org/10.1101/gr.184901>.

References

- Deplazes, P., Joachim, A., Mathis, A., Strube, C., Taubert, A., Samson-Himmelstjerna, G. von, and Zahner, H. (2021). *Parasitologie für die Tiermedizin* (Stuttgart New York: Georg Thieme Verlag).
- Dohutia, C., Chetia, D., Gogoi, K., and Sarma, K. (2017). Design, in silico and in vitro evaluation of curcumin analogues against *Plasmodium falciparum*. *Exp Parasitol* 175, 51–58. <https://doi.org/10.1016/j.exppara.2017.02.006>.
- Dong, H., Zhou, L., Ge, X., Guo, X., Han, J., and Yang, H. (2018). Antiviral effect of 25-hydroxycholesterol against porcine reproductive and respiratory syndrome virus in vitro. *Antivir Ther* 23, 395–404. <https://doi.org/10.3851/IMP3232>.
- Dubey, J.P. (2003). Review of *Neospora caninum* and neosporosis in animals. *Korean J Parasitol* 41, 1–16. <https://doi.org/10.3347/kjp.2003.41.1.1>.
- Dubey, J.P. (2008). The history of *Toxoplasma gondii*--the first 100 years. *J Eukaryot Microbiol* 55, 467–475. <https://doi.org/10.1111/j.1550-7408.2008.00345.x>.
- Dubey, J.P., and Sharma, S.P. (1980). Parasitemia and tissue infection in sheep fed *Toxoplasma gondii* oocysts. *J Parasitol* 66, 111–114. .
- Dubey, J.P., Lindsay, D.S., and Speer, C.A. (1998). Structures of *Toxoplasma gondii* tachyzoites, bradyzoites, and sporozoites and biology and development of tissue cysts. *Clin Microbiol Rev* 11, 267–299. <https://doi.org/10.1128/CMR.11.2.267>.
- Ehrenman, K., Wanyiri, J.W., Bhat, N., Ward, H.D., and Coppens, I. (2013). *Cryptosporidium parvum* scavenges LDL-derived cholesterol and micellar cholesterol internalized into enterocytes. *Cell Microbiol* 15, 1182–1197. <https://doi.org/10.1111/cmi.12107>.
- Elmore, S.A., Jones, J.L., Conrad, P.A., Patton, S., Lindsay, D.S., and Dubey, J.P. (2010). *Toxoplasma gondii*: epidemiology, feline clinical aspects, and prevention. *Trends Parasitol* 26, 190–196. <https://doi.org/10.1016/j.pt.2010.01.009>.
- Feng, S., Belwal, T., Li, L., Limwachiranon, J., Liu, X., and Luo, Z. (2020). Phytosterols and their derivatives: Potential health-promoting uses against lipid metabolism and associated

References

- diseases, mechanism, and safety issues. *Compr Rev Food Sci Food Saf* *19*, 1243–1267. <https://doi.org/10.1111/1541-4337.12560>.
- Ferguson, D.J.P., and Dubremetz, J.-F. (2014). Chapter 2 - The ultrastructure of *Toxoplasma gondii*. In *Toxoplasma gondii* (Second Edition), L.M. Weiss, and K. Kim, eds. (Boston: Academic Press), pp. 19–59.
- Francia, M.E., and Striepen, B. (2014). Cell division in apicomplexan parasites. *Nat Rev Microbiol* *12*, 125–136. <https://doi.org/10.1038/nrmicro3184>.
- Franklin-Murray, A.L., Mallya, S., Jankeel, A., Sureshchandra, S., Messaoudi, I., and Lodoen, M.B. (2020). *Toxoplasma gondii* dysregulates barrier function and mechanotransduction signaling in human endothelial cells. *MSphere* *5*. <https://doi.org/10.1128/mSphere.00550-19>.
- Fraser, M., Jing, W., Bröer, S., Kurth, F., Sander, L.-E., Matuschewski, K., and Maier, A.G. (2021). Breakdown in membrane asymmetry regulation leads to monocyte recognition of *P. falciparum*-infected red blood cells. *PLoS Pathog* *17*, e1009259. <https://doi.org/10.1371/journal.ppat.1009259>.
- Friend, S.C., and Stockdale, P.H. (1980). Experimental *Eimeria bovis* infection in calves: a histopathological study. *Can J Comp Med* *44*, 129–140. .
- Gachumi, G., and El-Aneed, A. (2017). Mass spectrometric approaches for the analysis of phytosterols in biological samples. *J Agric Food Chem* *65*, 10141–10156. <https://doi.org/10.1021/acs.jafc.7b03785>.
- Garcia, C.R.S., Alves, E., Pereira, P.H.S., Bartlett, P.J., Thomas, A.P., Mikoshiba, K., Plattner, H., and Sibley, L.D. (2017). InsP₃ signaling in apicomplexan parasites. *Curr Top Med Chem* *17*, 2158–2165. <https://doi.org/10.2174/1568026617666170130121042>.
- Garcia-Calvo, M., Lisnock, J., Bull, H.G., Hawes, B.E., Burnett, D.A., Braun, M.P., Crona, J.H., Davis, H.R.J., Dean, D.C., Detmers, P.A., et al. (2005). The target of ezetimibe is Niemann-Pick C1-Like 1 (NPC1L1). *Proc Natl Acad Sci U S A* *102*, 8132–8137. <https://doi.org/10.1073/pnas.0500269102>.

References

- Gigley, J.P. (2016). The diverse role of NK cells in immunity to *Toxoplasma gondii* infection. *PLoS Pathog* 12, e1005396. <https://doi.org/10.1371/journal.ppat.1005396>.
- Goldstein, J.L., and Brown, M.S. (1990). Regulation of the mevalonate pathway. *Nature* 343, 425–430. <https://doi.org/10.1038/343425a0>.
- Goo, Y.-K., Yamagishi, J., Ueno, A., Terkawi, M.A., Aboge, G.O., Kwak, D., Hong, Y., Chung, D.-I., Igarashi, M., Nishikawa, Y., et al. (2015). Characterization of *Toxoplasma gondii* glyoxalase 1 and evaluation of inhibitory effects of curcumin on the enzyme and parasite cultures. *Parasit Vectors* 8, 654. <https://doi.org/10.1186/s13071-015-1268-5>.
- Grellier, P., Valentin, A., Millerioux, V., Schrevel, J., and Rigomier, D. (1994). 3-Hydroxy-3-methylglutaryl coenzyme A reductase inhibitors lovastatin and simvastatin inhibit in vitro development of *Plasmodium falciparum* and *Babesia divergens* in human erythrocytes. *Antimicrob Agents Chemother* 38, 1144–1148. <https://doi.org/10.1128/AAC.38.5.1144>.
- Griffiths, W.J., and Wang, Y. (2019). Oxysterol research: a brief review. *Biochem Soc Trans* 47, 517–526. <https://doi.org/10.1042/BST20180135>.
- Gupta, Y., Goicoechea, S., Pearce, C.M., Mathur, R., Romero, J.G., Kwofie, S.K., Weyenberg, M.C., Daravath, B., Sharma, N., Poonam, et al. (2021). The emerging paradigm of calcium homeostasis as a new therapeutic target for protozoan parasites. *Med Res Rev* <https://doi.org/10.1002/med.21804>.
- Gutiérrez-Expósito, D., Arnal, M.C., Martínez-Durán, D., Regidor-Cerrillo, J., Revilla, M., L Fernández de Luco, D., Jiménez-Meléndez, A., Calero-Bernal, R., Habela, M.A., García-Bocanegra, I., et al. (2016). The role of wild ruminants as reservoirs of *Besnoitia besnoiti* infection in cattle. *Vet Parasitol* 223, 7–13. <https://doi.org/10.1016/j.vetpar.2016.04.005>.
- Gutierrez-Pajares, J.L., Ben Hassen, C., Chevalier, S., and Frank, P.G. (2016). SR-BI: Linking cholesterol and lipoprotein metabolism with breast and prostate cancer. *Front Pharmacol* 7, 338. <https://doi.org/10.3389/fphar.2016.00338>.
- Hamid, P.H., Hirzmann, J., Hermosilla, C., and Taubert, A. (2014). Differential inhibition of host cell cholesterol de novo biosynthesis and processing abrogates *Eimeria bovis*

References

- intracellular development. *Parasitol Res* 113, 4165–4176. <https://doi.org/10.1007/s00436-014-4092-5>.
- Hamid, P.H., Hirzmann, J., Kerner, K., Gimpl, G., Lochnit, G., Hermosilla, C.R., and Taubert, A. (2015). *Eimeria bovis* infection modulates endothelial host cell cholesterol metabolism for successful replication. *Vet Res* 46, 100. <https://doi.org/10.1186/s13567-015-0230-z>.
- Hayakawa, E.H., Yamaguchi, K., Mori, M., and Nardone, G. (2020). Real-time cholesterol sorting in *Plasmodium falciparum*-erythrocytes as revealed by 3D label-free imaging. *Sci Rep* 10, 2794. <https://doi.org/10.1038/s41598-020-59552-9>.
- Hayakawa, E.H., Kato, H., Nardone, G.A., and Usukura, J. (2021). A prospective mechanism and source of cholesterol uptake by *Plasmodium falciparum*-infected erythrocytes co-cultured with HepG2 cells. *Parasitol Int* 80, 102179. <https://doi.org/10.1016/j.parint.2020.102179>.
- He, J.-J., Ma, J., Elsheikha, H.M., Song, H.-Q., Zhou, D.-H., and Zhu, X.-Q. (2016). Proteomic profiling of mouse liver following acute *Toxoplasma gondii* infection. *PLoS One* 11, e0152022. <https://doi.org/10.1371/journal.pone.0152022>.
- He, J.-J., Ma, J., Wang, J.-L., Zhang, F.-K., Li, J.-X., Zhai, B.-T., Wang, Z.-X., Elsheikha, H.M., and Zhu, X.-Q. (2019). Global transcriptome profiling of multiple porcine organs reveals *Toxoplasma gondii*-induced transcriptional landscapes. *Front Immunol* 10, 1531. <https://doi.org/10.3389/fimmu.2019.01531>.
- Hermosilla, C., Barbisch, B., Heise, A., Kowalik, S., and Zahner, H. (2002). Development of *Eimeria bovis* in vitro: suitability of several bovine, human and porcine endothelial cell lines, bovine fetal gastrointestinal, Madin-Darby bovine kidney (MDBK) and African green monkey kidney (VERO) cells. *Parasitol Res* 88, 301–307. <https://doi.org/10.1007/s00436-001-0531-1>.
- Hoff, E.F., and Carruthers, V.B. (2002). Is *Toxoplasma* egress the first step in invasion? *Trends Parasitol* 18, 251–255. [https://doi.org/10.1016/s1471-4922\(02\)02240-7](https://doi.org/10.1016/s1471-4922(02)02240-7).

References

- Horcajo, P., Xia, D., Randle, N., Collantes-Fernández, E., Wastling, J., Ortega-Mora, L.M., and Regidor-Cerrillo, J. (2018). Integrative transcriptome and proteome analyses define marked differences between *Neospora caninum* isolates throughout the tachyzoite lytic cycle. *J Proteomics* 180, 108–119. <https://doi.org/10.1016/j.jprot.2017.11.007>.
- Hortua Triana, M.A., Márquez-Nogueras, K.M., Vella, S.A., and Moreno, S.N.J. (2018). Calcium signaling and the lytic cycle of the Apicomplexan parasite *Toxoplasma gondii*. *Biochim Biophys Acta Mol Cell Res* 1865, 1846–1856. <https://doi.org/10.1016/j.bbamcr.2018.08.004>.
- Hu, X., Binns, D., and Reese, M.L. (2017). The coccidian parasites *Toxoplasma* and *Neospora* dysregulate mammalian lipid droplet biogenesis. *J Biol Chem* 292, 11009–11020. <https://doi.org/10.1074/jbc.M116.768176>.
- Ikonen, E. (2008). Cellular cholesterol trafficking and compartmentalization. *Nat Rev Mol Cell Biol* 9, 125–138. <https://doi.org/10.1038/nrm2336>.
- Innes, E.A., Bartley, P.M., Buxton, D., and Katzer, F. (2009). Ovine toxoplasmosis. *Parasitology* 136, 1887–1894. <https://doi.org/10.1017/S0031182009991636>.
- Jiao, F., Zhang, D., Jiang, M., Mi, J., Liu, X., Zhang, H., Hu, Z., Xu, X., and Hu, X. (2017). Label-free proteomic analysis of placental proteins during *Toxoplasma gondii* infection. *J Proteomics* 150, 31–39. <https://doi.org/10.1016/j.jprot.2016.08.013>.
- Jiménez-Meléndez, A., Ramakrishnan, C., Hehl, A.B., Russo, G., and Álvarez-García, G. (2020). RNA-Seq analyses reveal that endothelial activation and fibrosis are induced early and progressively by *Besnoitia besnoiti* host cell invasion and proliferation. *Front Cell Infect Microbiol* 10, 218. <https://doi.org/10.3389/fcimb.2020.00218>.
- Juarez, D., and Fruman, D.A. (2021). Targeting the mevalonate pathway in cancer. *Trends Cancer* 7, 525–540. <https://doi.org/10.1016/j.trecan.2020.11.008>.
- Keeton, S.T.N., and Navarre, C.B. (2018). Coccidiosis in large and small ruminants. *Vet Clin North Am Food Anim Pract* 34, 201–208. <https://doi.org/10.1016/j.cvfa.2017.10.009>.
- Kimura, T., Tomura, H., Sato, K., Ito, M., Matsuoka, I., Im, D.-S., Kuwabara, A., Mogi, C., Itoh, H., Kurose, H., et al. (2010). Mechanism and role of high density lipoprotein-induced

References

- activation of AMP-activated protein kinase in endothelial cells. *J Biol Chem* 285, 4387–4397. <https://doi.org/10.1074/jbc.M109.043869>.
- Kume, A., Herbas, M.S., Shichiri, M., Ishida, N., and Suzuki, H. (2016). Effect of anti-hyperlipidemia drugs on the alpha-tocopherol concentration and their potential for murine malaria infection. *Parasitol Res* 115, 69–75. <https://doi.org/10.1007/s00436-015-4722-6>.
- Labaied, M., Jayabalasingham, B., Bano, N., Cha, S.-J., Sandoval, J., Guan, G., and Coppens, I. (2011). *Plasmodium* salvages cholesterol internalized by LDL and synthesized de novo in the liver. *Cell Microbiol* 13, 569–586. <https://doi.org/10.1111/j.1462-5822.2010.01555.x>.
- Lang, M., Kann, M., Zahner, H., Taubert, A., and Hermosilla, C. (2009). Inhibition of host cell apoptosis by *Eimeria bovis* sporozoites. *Vet Parasitol* 160, 25–33. <https://doi.org/10.1016/j.vetpar.2008.10.100>.
- Langenmayer, M.C., Gollnick, N.S., Majzoub-Altweck, M., Scharr, J.C., Schares, G., and Hermanns, W. (2015). Naturally acquired bovine besnoitiosis: histological and immunohistochemical findings in acute, subacute, and chronic disease. *Vet Pathol* 52, 476–488. <https://doi.org/10.1177/0300985814541705>.
- Lefort, C., and Cani, P.D. (2021). The liver under the spotlight: bile acids and oxysterols as pivotal actors controlling metabolism. *Cells* 10. <https://doi.org/10.3390/cells10020400>.
- Leprohon, P., L egar , D., and Ouellette, M. (2011). ABC transporters involved in drug resistance in human parasites. *Essays Biochem* 50, 121–144. <https://doi.org/10.1042/bse0500121>.
- Li nard, E., Salem, A., Jacquiet, P., Grisez, C., Pr vot, F., Blanchard, B., Bouhsira, E., and Franc, M. (2013). Development of a protocol testing the ability of *Stomoxys calcitrans* (Linnaeus, 1758) (Diptera: Muscidae) to transmit *Besnoitia besnoiti* (Henry, 1913) (Apicomplexa: Sarcocystidae). *Parasitol Res* 112, 479–486. <https://doi.org/10.1007/s00436-012-3157-6>.
- Lindsay, D.S., and Dubey, J.P. (2020). Neosporosis, Toxoplasmosis, and Sarcocystosis in Ruminants: An update. *Vet Clin North Am Food Anim Pract* 36, 205–222. <https://doi.org/10.1016/j.cvfa.2019.11.004>.

References

- Linton, M.F., Tao, H., Linton, E.F., and Yancey, P.G. (2017). SR-BI: a multifunctional receptor in cholesterol homeostasis and atherosclerosis. *Trends Endocrinol Metab* 28, 461–472. <https://doi.org/10.1016/j.tem.2017.02.001>.
- López-Osorio, S., Silva, L.M.R., Taubert, A., Chaparro-Gutiérrez, J.J., and Hermosilla, C.R. (2018). Concomitant in vitro development of *Eimeria zuernii*- and *Eimeria bovis*-macromeronts in primary host endothelial cells. *Parasitol Int* 67, 742–750. <https://doi.org/10.1016/j.parint.2018.07.009>.
- Lourido, S., and Moreno, S.N.J. (2015). The calcium signaling toolkit of the apicomplexan parasites *Toxoplasma gondii* and *Plasmodium spp.* *Cell Calcium* 57, 186–193. <https://doi.org/10.1016/j.cecca.2014.12.010>.
- Lovett, J.L., and Sibley, L.D. (2003). Intracellular calcium stores in *Toxoplasma gondii* govern invasion of host cells. *J Cell Sci* 116, 3009–3016. <https://doi.org/10.1242/jcs.00596>.
- Luo, J., Yang, H., and Song, B.-L. (2020). Mechanisms and regulation of cholesterol homeostasis. *Nat Rev Mol Cell Biol* 21, 225–245. <https://doi.org/10.1038/s41580-019-0190-7>.
- Maksimov, P., Hermosilla, C., Kleinertz, S., Hirzmann, J., and Taubert, A. (2016). *Besnoitia besnoiti* infections activate primary bovine endothelial cells and promote PMN adhesion and NET formation under physiological flow condition. *Parasitol Res* 115, 1991–2001. <https://doi.org/10.1007/s00436-016-4941-5>.
- Mammari, N., Halabi, M.A., Yaacoub, S., Chlala, H., Dardé, M.-L., and Courtioux, B. (2019). *Toxoplasma gondii* modulates the host cell responses: an overview of apoptosis pathways. *Biomed Res Int* 2019, 6152489. <https://doi.org/10.1155/2019/6152489>.
- Martiney, J.A., Cerami, A., and Slater, A.F. (1995). Verapamil reversal of chloroquine resistance in the malaria parasite *Plasmodium falciparum* is specific for resistant parasites and independent of the weak base effect. *J Biol Chem* 270, 22393–22398. <https://doi.org/10.1074/jbc.270.38.22393>.

References

- Martorelli Di Genova, B., and Knoll, L.J. (2020). Comparisons of the sexual cycles for the coccidian parasites *Eimeria* and *Toxoplasma*. *Front Cell Infect Microbiol* 10, 604897. <https://doi.org/10.3389/fcimb.2020.604897>.
- McAuley, J.B. (2014). Congenital Toxoplasmosis. *J Pediatric Infect Dis Soc* 3 *Suppl* 1, S30-35. <https://doi.org/10.1093/jpids/piu077>.
- Meng, Y., Heybrock, S., Neculai, D., and Saftig, P. (2020). Cholesterol handling in lysosomes and beyond. *Trends Cell Biol* 30, 452–466. <https://doi.org/10.1016/j.tcb.2020.02.007>.
- Milne, G., Webster, J.P., and Walker, M. (2020). *Toxoplasma gondii*: An underestimated threat? *Trends Parasitol* 36, 959–969. <https://doi.org/10.1016/j.pt.2020.08.005>.
- Molestina, R.E., El-Guendy, N., and Sinai, A.P. (2008). Infection with *Toxoplasma gondii* results in dysregulation of the host cell cycle. *Cell Microbiol* 10, 1153–1165. <https://doi.org/10.1111/j.1462-5822.2008.01117.x>.
- Montoya, J.G., and Liesenfeld, O. (2004). *Toxoplasmosis*. *Lancet* 363, 1965–1976. [https://doi.org/10.1016/S0140-6736\(04\)16412-X](https://doi.org/10.1016/S0140-6736(04)16412-X).
- Nagamune, K., Moreno, S.N.J., and Sibley, L.D. (2007). Artemisinin-resistant mutants of *Toxoplasma gondii* have altered calcium homeostasis. *Antimicrob Agents Chemother* 51, 3816–3823. <https://doi.org/10.1128/AAC.00582-07>.
- Nagata, S., Suzuki, J., Segawa, K., and Fujii, T. (2016). Exposure of phosphatidylserine on the cell surface. *Cell Death Differ* 23, 952–961. <https://doi.org/10.1038/cdd.2016.7>.
- Nelson, M.M., Jones, A.R., Carmen, J.C., Sinai, A.P., Burchmore, R., and Wastling, J.M. (2008). Modulation of the host cell proteome by the intracellular apicomplexan parasite *Toxoplasma gondii*. *Infect Immun* 76, 828–844. <https://doi.org/10.1128/IAI.01115-07>.
- Nishikawa, Y., Ibrahim, H.M., Kameyama, K., Shiga, I., Hiasa, J., and Xuan, X. (2011). Host cholesterol synthesis contributes to growth of intracellular *Toxoplasma gondii* in macrophages. *J Vet Med Sci* 73, 633–639. <https://doi.org/10.1292/jvms.10-0496>.

References

- Nolan, S.J., Romano, J.D., Luechtefeld, T., and Coppens, I. (2015). *Neospora caninum* recruits host cell structures to its parasitophorous vacuole and salvages lipids from organelles. *Eukaryot Cell* 14, 454–473. <https://doi.org/10.1128/EC.00262-14>.
- Nolan, S.J., Romano, J.D., and Coppens, I. (2017). Host lipid droplets: An important source of lipids salvaged by the intracellular parasite *Toxoplasma gondii*. *PLoS Pathog* 13, e1006362. <https://doi.org/10.1371/journal.ppat.1006362>.
- Norata, G.D., Ongari, M., Uboldi, P., Pellegatta, F., and Catapano, A.L. (2005). Liver X receptor and retinoic X receptor agonists modulate the expression of genes involved in lipid metabolism in human endothelial cells. *Int J Mol Med* 16, 717–722. .
- Olzmann, J.A., and Carvalho, P. (2019). Dynamics and functions of lipid droplets. *Nat Rev Mol Cell Biol* 20, 137–155. <https://doi.org/10.1038/s41580-018-0085-z>.
- Pace, D.A., McKnight, C.A., Liu, J., Jimenez, V., and Moreno, S.N.J. (2014). Calcium entry in *Toxoplasma gondii* and its enhancing effect of invasion-linked traits. *J Biol Chem* 289, 19637–19647. <https://doi.org/10.1074/jbc.M114.565390>.
- Palmeira, A., Sousa, E., Vasconcelos, M.H., and Pinto, M.M. (2012). Three decades of P-gp inhibitors: skimming through several generations and scaffolds. *Curr Med Chem* 19, 1946–2025. <https://doi.org/10.2174/092986712800167392>.
- Pereira, M.G., Visbal, G., Salgado, L.T., Vidal, J.C., Godinho, J.L.P., De Cicco, N.N.T., Atella, G.C., de Souza, W., and Cunha-e-Silva, N. (2015). *Trypanosoma cruzi* epimastigotes are able to manage internal cholesterol levels under nutritional lipid stress conditions. *PLoS One* 10, e0128949. <https://doi.org/10.1371/journal.pone.0128949>.
- Perkins, M.E., Wu, T.W., and Le Blancq, S.M. (1998). Cyclosporin analogs inhibit in vitro growth of *Cryptosporidium parvum*. *Antimicrob Agents Chemother* 42, 843–848. <https://doi.org/10.1128/AAC.42.4.843>.
- Petersen, W., Stenzel, W., Silvie, O., Blanz, J., Saftig, P., Matuschewski, K., and Ingmundson, A. (2017). Sequestration of cholesterol within the host late endocytic pathway restricts liver-stage *Plasmodium* development. *Mol Biol Cell* 28, 726–735. <https://doi.org/10.1091/mbc.E16-07-0531>.

References

- Phillips, M.C. (2014). Molecular mechanisms of cellular cholesterol efflux. *J Biol Chem* 289, 24020–24029. <https://doi.org/10.1074/jbc.R114.583658>.
- Pingret, L., Millot, J.M., Sharonov, S., Bonhomme, A., Manfait, M., and Pinon, J.M. (1996). Relationship between intracellular free calcium concentrations and the intracellular development of *Toxoplasma gondii*. *J Histochem Cytochem* 44, 1123–1129. <https://doi.org/10.1177/44.10.8813077>.
- Regidor-Cerrillo, J., Xia, D., Jiménez-Pelayo, L., García-Sánchez, M., Collantes-Fernández, E., Randle, N., Wastling, J., Ortega-Mora, L.-M., and Horcajo, P. (2020). Proteomic Characterization of Host-Pathogen Interactions during Bovine Trophoblast Cell Line Infection by *Neospora caninum*. *Pathogens* 9. <https://doi.org/10.3390/pathogens9090749>.
- Reichel, M.P., Alejandra Ayanegui-Alcérrec, M., Gondim, L.F.P., and Ellis, J.T. (2013). What is the global economic impact of *Neospora caninum* in cattle - the billion dollar question. *Int J Parasitol* 43, 133–142. <https://doi.org/10.1016/j.ijpara.2012.10.022>.
- Ribeiro, C.M., Soares, I.R., Mendes, R.G., de Santis Bastos, P.A., Katagiri, S., Zavilenski, R.B., de Abreu, H.F.P., and Afreixo, V. (2019). Meta-analysis of the prevalence and risk factors associated with bovine neosporosis. *Trop Anim Health Prod* 51, 1783–1800. <https://doi.org/10.1007/s11250-019-01929-8>.
- Rodrigues, C.D., Hannus, M., Prudêncio, M., Martin, C., Gonçalves, L.A., Portugal, S., Epiphanyo, S., Akinc, A., Hadwiger, P., Jahn-Hofmann, K., et al. (2008). Host scavenger receptor SR-BI plays a dual role in the establishment of malaria parasite liver infection. *Cell Host Microbe* 4, 271–282. <https://doi.org/10.1016/j.chom.2008.07.012>.
- Romano, J.D., Sonda, S., Bergbower, E., Smith, M.E., and Coppens, I. (2013). *Toxoplasma gondii* salvages sphingolipids from the host Golgi through the rerouting of selected Rab vesicles to the parasitophorous vacuole. *Mol Biol Cell* 24, 1974–1995. <https://doi.org/10.1091/mbc.E12-11-0827>.
- Rosypal, A.C., and Lindsay, D.S. (2005). The sylvatic cycle of *Neospora caninum*: where do we go from here? *Trends Parasitol* 21, 439–440. <https://doi.org/10.1016/j.pt.2005.08.003>.

References

- Ryan, U., Fayer, R., and Xiao, L. (2014). *Cryptosporidium* species in humans and animals: current understanding and research needs. *Parasitology* *141*, 1667–1685. <https://doi.org/10.1017/S0031182014001085>.
- Shapiro, K., Bahia-Oliveira, L., Dixon, B., Dumètre, A., de Wit, L.A., VanWormer, E., and Villena, I. (2019). Environmental transmission of *Toxoplasma gondii*: Oocysts in water, soil and food. *Food Waterborne Parasitol* *15*, e00049. <https://doi.org/10.1016/j.fawpar.2019.e00049>.
- Shunmugam, S., Arnold, C.-S., Dass, S., Katris, N.J., and Botté, C.Y. (2022). The flexibility of apicomplexa parasites in lipid metabolism. *PLoS Pathog* *18*, e1010313. <https://doi.org/10.1371/journal.ppat.1010313>.
- Silverman, J.A., Hayes, M.L., Luft, B.J., and Joiner, K.A. (1997). Characterization of anti-*Toxoplasma* activity of SDZ 215-918, a cyclosporin derivative lacking immunosuppressive and peptidyl-prolyl-isomerase-inhibiting activity: possible role of a P glycoprotein in *Toxoplasma* physiology. *Antimicrob Agents Chemother* *41*, 1859–1866. <https://doi.org/10.1128/AAC.41.9.1859>.
- Simons, K., and Ikonen, E. (2000). How cells handle cholesterol. *Science* *290*, 1721–1726. <https://doi.org/10.1126/science.290.5497.1721>.
- Sinai, A.P., Webster, P., and Joiner, K.A. (1997). Association of host cell endoplasmic reticulum and mitochondria with the *Toxoplasma gondii* parasitophorous vacuole membrane: a high affinity interaction. *J Cell Sci* *110 (Pt 17)*, 2117–2128. .
- Sonda, S., Ting, L.M., Novak, S., Kim, K., Maher, J.J., Farese, R.V.J., and Ernst, J.D. (2001). Cholesterol esterification by host and parasite is essential for optimal proliferation of *Toxoplasma gondii*. *J Biol Chem* *276*, 34434–34440. <https://doi.org/10.1074/jbc.M105025200>.
- Sow, S.O., Muhsen, K., Nasrin, D., Blackwelder, W.C., Wu, Y., Farag, T.H., Panchalingam, S., Sur, D., Zaidi, A.K.M., Faruque, A.S.G., et al. (2016). The burden of *Cryptosporidium* diarrheal disease among children < 24 months of age in moderate/high mortality regions of sub-Saharan Africa and south Asia, utilizing data from the global enteric multicenter study (GEMS). *PLoS Negl Trop Dis* *10*, e0004729. <https://doi.org/10.1371/journal.pntd.0004729>.

References

- Speer, C.A., Dubey, J.P., McAllister, M.M., and Blixt, J.A. (1999). Comparative ultrastructure of tachyzoites, bradyzoites, and tissue cysts of *Neospora caninum* and *Toxoplasma gondii*. *Int J Parasitol* 29, 1509–1519. [https://doi.org/10.1016/s0020-7519\(99\)00132-0](https://doi.org/10.1016/s0020-7519(99)00132-0).
- Sun, H., Li, J., Wang, L., Yin, K., Xu, C., Liu, G., Xiao, T., Huang, B., Wei, Q., Gong, M., et al. (2021). Comparative proteomics analysis for elucidating the interaction between host cells and *Toxoplasma gondii*. *Front Cell Infect Microbiol* 11, 643001. <https://doi.org/10.3389/fcimb.2021.643001>.
- Tan, M.S.Y., and Blackman, M.J. (2021). Malaria parasite egress at a glance. *J Cell Sci* 134. <https://doi.org/10.1242/jcs.257345>.
- Tanaka, S., Nishimura, M., Ihara, F., Yamagishi, J., Suzuki, Y., and Nishikawa, Y. (2013). Transcriptome analysis of mouse brain infected with *Toxoplasma gondii*. *Infect Immun* 81, 3609–3619. <https://doi.org/10.1128/IAI.00439-13>.
- Taubert, A., Krüll, M., Zahner, H., and Hermosilla, C. (2006a). *Toxoplasma gondii* and *Neospora caninum* infections of bovine endothelial cells induce endothelial adhesion molecule gene transcription and subsequent PMN adhesion. *Vet Immunol Immunopathol* 112, 272–283. <https://doi.org/10.1016/j.vetimm.2006.03.017>.
- Taubert, A., Zahner, H., and Hermosilla, C. (2006b). Dynamics of transcription of immunomodulatory genes in endothelial cells infected with different coccidian parasites. *Vet Parasitol* 142, 214–222. <https://doi.org/10.1016/j.vetpar.2006.07.021>.
- Taubert, A., Wimmers, K., Ponsuksili, S., Jimenez, C.A., Zahner, H., and Hermosilla, C. (2010). Microarray-based transcriptional profiling of *Eimeria bovis*-infected bovine endothelial host cells. *Vet Res* 41, 70. <https://doi.org/10.1051/vetres/2010041>.
- Tenter, A.M., Heckeroth, A.R., and Weiss, L.M. (2000). *Toxoplasma gondii*: from animals to humans. *Int J Parasitol* 30, 1217–1258. [https://doi.org/10.1016/s0020-7519\(00\)00124-7](https://doi.org/10.1016/s0020-7519(00)00124-7).
- Tomita, T., Yamada, T., Weiss, L.M., and Orlofsky, A. (2009). Externally triggered egress is the major fate of *Toxoplasma gondii* during acute infection. *J Immunol* 183, 6667–6680. <https://doi.org/10.4049/jimmunol.0900516>.

References

- Van Eck, M., Twisk, J., Hoekstra, M., Van Rij, B.T., Van der Lans, C.A.C., Bos, I.S.T., Kruijt, J.K., Kuipers, F., and Van Berkel, T.J.C. (2003). Differential effects of scavenger receptor BI deficiency on lipid metabolism in cells of the arterial wall and in the liver. *J Biol Chem* 278, 23699–23705. <https://doi.org/10.1074/jbc.M211233200>.
- Vielemeyer, O., McIntosh, M.T., Joiner, K.A., and Coppens, I. (2004). Neutral lipid synthesis and storage in the intraerythrocytic stages of *Plasmodium falciparum*. *Mol Biochem Parasitol* 135, 197–209. <https://doi.org/10.1016/j.molbiopara.2003.08.017>.
- Vishnyakova, T.G., Bocharov, A.V., Baranova, I.N., Kurlander, R., Drake, S.K., Chen, Z., Amar, M., Sviridov, D., Vaisman, B., Poliakov, E., et al. (2020). SR-BI mediates neutral lipid sorting from LDL to lipid droplets and facilitates their formation. *PLoS One* 15, e0240659. <https://doi.org/10.1371/journal.pone.0240659>.
- Votýpka, J., Modrý, D., Oborník, M., Šlapeta, J., and Lukeš, J. (2017). Apicomplexa. In *Handbook of the Protists*, J.M. Archibald, A.G.B. Simpson, and C.H. Slamovits, eds. (Cham: Springer International Publishing), pp. 567–624.
- Wang, S.-S., Zhou, C.-X., Elsheikha, H.M., He, J.-J., Zou, F.-C., Zheng, W.-B., Zhu, X.-Q., and Zhao, G.-H. (2022). Temporal transcriptomic changes in long non-coding RNAs and messenger RNAs involved in the host immune and metabolic response during *Toxoplasma gondii* lytic cycle. *Parasit Vectors* 15, 22. <https://doi.org/10.1186/s13071-021-05140-3>.
- Yalaoui, S., Huby, T., Franetich, J.-F., Gego, A., Rametti, A., Moreau, M., Collet, X., Siau, A., van Gemert, G.-J., Sauerwein, R.W., et al. (2008). Scavenger receptor BI boosts hepatocyte permissiveness to *Plasmodium* infection. *Cell Host Microbe* 4, 283–292. <https://doi.org/10.1016/j.chom.2008.07.013>.
- Yan, X., Ji, Y., Liu, X., and Suo, X. (2015). Nitric oxide stimulates early egress of *Toxoplasma gondii* tachyzoites from Human foreskin fibroblast cells. *Parasit Vectors* 8, 420. <https://doi.org/10.1186/s13071-015-1037-5>.
- Yan, X., Han, W., Liu, X., and Suo, X. (2021). Exogenous nitric oxide stimulates early egress of *Eimeria tenella* sporozoites from primary chicken kidney cells in vitro. *Parasite* 28, 11. <https://doi.org/10.1051/parasite/2021007>.

References

- Yang, Q., Zhang, Q., Tang, J., and Feng, W.-H. (2015). Lipid rafts both in cellular membrane and viral envelope are critical for PRRSV efficient infection. *Virology* 484, 170–180. <https://doi.org/10.1016/j.virol.2015.06.005>.
- Yao, Y., Liu, M., Ren, C., Shen, J., and Ji, Y. (2017). Exogenous tumor necrosis factor-alpha could induce egress of *Toxoplasma gondii* from human foreskin fibroblast cells. *Parasite* 24, 45. <https://doi.org/10.1051/parasite/2017051>.
- Zhao, J., Chen, J., Li, M., Chen, M., and Sun, C. (2020). Multifaceted functions of CH25H and 25HC to modulate the lipid metabolism, immune responses, and broadly antiviral activities. *Viruses* 12. <https://doi.org/10.3390/v12070727>.
- Zhou, D.H., Yuan, Z.G., Zhao, F.R., Li, H.L., Zhou, Y., Lin, R.Q., Zou, F.C., Song, H.Q., Xu, M.J., and Zhu, X.Q. (2011). Modulation of mouse macrophage proteome induced by *Toxoplasma gondii* tachyzoites in vivo. *Parasitol Res* 109, 1637–1646. <https://doi.org/10.1007/s00436-011-2435-z>.
- Zhou, X., Zhang, X.-X., Mahmmod, Y.S., Hernandez, J.A., Li, G.-F., Huang, W.-Y., Wang, Y.-P., Zheng, Y.-X., Li, X.-M., and Yuan, Z.-G. (2020). A transcriptome analysis: various reasons of adverse pregnancy outcomes caused by acute *Toxoplasma gondii* infection. *Front Physiol* 11, 115. <https://doi.org/10.3389/fphys.2020.00115>.

7. ACKNOWLEDGMENTS

I would like to extend my deepest gratitude to Prof. Dr. Anja Taubert and Prof. Dr. Carlos Hermosilla for supervising my doctoral thesis and the trust placed in me and my work at the institute of parasitology of the JLU.

Likewise, I would like to pay my special regards to not only to Dr. Liliana Silva, who largely assisted this doctoral thesis, but also to Dr. Ivan Conejeros and Dr. Zahady Velásquez. Overall, this outstanding group of post-doctoral researchers vastly contributed in the development of this doctoral work and my formation as researcher.

Additionally, I would like to thank other doctoral students from the institute: Lisa Segeritz, Lisbeth Rojas, Gabriel Espinosa and Dr. Juan Vélez, with whom I shared a joyful friendship along this challenging years.

I would also like to express my gratitude to Dr. Christin Ritter and Hannah Salecker, the technical assistants of the lab who always supported my daily work over this years.

I am very thankful to Pamela Reyes and Rainer Krause, my parents, who always encouraged me to pursuit my academic development.

Finally, I would like to express my deepest thanks to my loved wife and partner Daniela Grob who accompanies me bringing love and happiness into my live.

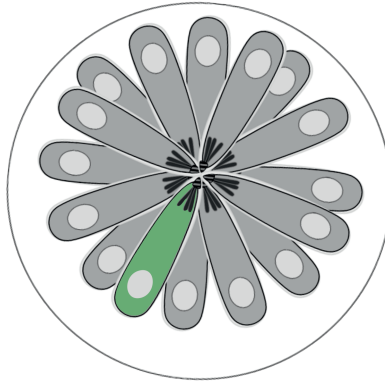
8. DECLARATION

I hereby declare that I have completed the submitted doctoral thesis independently and without any unauthorized outside help and with only those financial forms of support mentioned on this work. All the analyses conducted in this work, followed the principles of good scientific practice, as the stated in the statute of Justus-Liebig University Giessen for ensuring good scientific practices. All the texts that have been quoted verbatim or by analogy from published and non-published writings and all details based on verbal information have been identified as such

9. FUNDING

This study was funded by the Institute of Parasitology, of the Justus-Liebig University Gießen (Germany). Likewise, selected experiments were supported and financed by the German Research Foundation (Deutsche Forschungsgemeinschaft (DFG)); grant No. TA 291/10-1).

Finally, studies and life expenses in Germany were funded by the National Agency for Research and Development (ANID), DOCTORADO BECAS CHILE/2017-72180349.



édition scientifique
VVB LAUFERSWEILER VERLAG

VVB LAUFERSWEILER VERLAG
STAUFENBERGRING 15
D-35396 GIESSEN

Tel: 0641-5599888 Fax: -5599890
redaktion@doktorverlag.de
www.doktorverlag.de

ISBN: 978-3-8359-7082-3



9 78 3 8359 7082 3